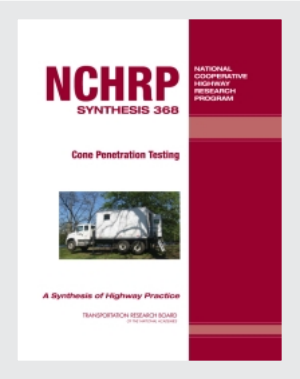

Cone Penetrating Testing

DETAILS

117 pages | | PAPERBACK
ISBN 978-0-309-42134-8 | DOI 10.17226/23143

AUTHORS

NATIONAL COOPERATIVE HIGHWAY RESEARCH PROGRAM

NCHRP SYNTHESIS 368

Cone Penetration Testing

A Synthesis of Highway Practice

CONSULTANT
PAUL W. MAYNE
Georgia Institute of Technology
Atlanta, Georgia

SUBJECT AREAS
Soils, Geology, and Foundations

Research Sponsored by the American Association of State Highway and Transportation Officials
in Cooperation with the Federal Highway Administration

TRANSPORTATION RESEARCH BOARD

WASHINGTON, D.C.
2007
www.TRB.org

NATIONAL COOPERATIVE HIGHWAY RESEARCH PROGRAM

Systematic, well-designed research provides the most effective approach to the solution of many problems facing highway administrators and engineers. Often, highway problems are of local interest and can best be studied by highway departments individually or in cooperation with their state universities and others. However, the accelerating growth of highway transportation develops increasingly complex problems of wide interest to highway authorities. These problems are best studied through a coordinated program of cooperative research.

In recognition of these needs, the highway administrators of the American Association of State Highway and Transportation Officials initiated in 1962 an objective national highway research program employing modern scientific techniques. This program is supported on a continuing basis by funds from participating member states of the Association and it receives the full cooperation and support of the Federal Highway Administration, United States Department of Transportation.

The Transportation Research Board of the National Academies was requested by the Association to administer the research program because of the Board's recognized objectivity and understanding of modern research practices. The Board is uniquely suited for this purpose as it maintains an extensive committee structure from which authorities on any highway transportation subject may be drawn; it possesses avenues of communications and cooperation with federal, state, and local governmental agencies, universities, and industry; its relationship to the National Research Council is an insurance of objectivity; it maintains a full-time research correlation staff of specialists in highway transportation matters to bring the findings of research directly to those who are in a position to use them.

The program is developed on the basis of research needs identified by chief administrators of the highway and transportation departments and by committees of AASHTO. Each year, specific areas of research needs to be included in the program are proposed to the National Research Council and the Board by the American Association of State Highway and Transportation Officials. Research projects to fulfill these needs are defined by the Board, and qualified research agencies are selected from those that have submitted proposals. Administration and surveillance of research contracts are the responsibilities of the National Research Council and the Transportation Research Board.

The needs for highway research are many, and the National Cooperative Highway Research Program can make significant contributions to the solution of highway transportation problems of mutual concern to many responsible groups. The program, however, is intended to complement rather than to substitute for or duplicate other highway research programs.

NOTE: The Transportation Research Board of the National Academies, the National Research Council, the Federal Highway Administration, the American Association of State Highway and Transportation Officials, and the individual states participating in the National Cooperative Highway Research Program do not endorse products or manufacturers. Trade or manufacturers' names appear herein solely because they are considered essential to the object of this report.

NCHRP SYNTHESIS 368

Project 20-5 (Topic 37-14)
ISSN 0547-5570
ISBN 978-0-309-09784-0
Library of Congress Control No. 2007923933

COPYRIGHT PERMISSION

NOTICE

The project that is the subject of this report was a part of the National Cooperative Highway Research Program conducted by the Transportation Research Board with the approval of the Governing Board of the National Research Council. Such approval reflects the Governing Board's judgment that the program concerned is of national importance and appropriate with respect to both the purposes and resources of the National Research Council.

The members of the technical committee selected to monitor this project and to review this report were chosen for recognized scholarly competence and with due consideration for the balance of disciplines appropriate to the project. The opinions and conclusions expressed or implied are those of the research agency that performed the research, and, while they have been accepted as appropriate by the technical committee, they are not necessarily those of the Transportation Research Board, the National Research Council, the American Association of State Highway and Transportation Officials, or the Federal Highway Administration, U.S. Department of Transportation.

Each report is reviewed and accepted for publication by the technical committee according to procedures established and monitored by the Transportation Research Board Executive Committee and the Governing Board of the National Research Council.

Published reports of the

NATIONAL COOPERATIVE HIGHWAY RESEARCH PROGRAM

are available from:

Transportation Research Board
Business Office
500 Fifth Street, NW
Washington, DC 20001

and can be ordered through the Internet at:
http://www.national-academies.org/trb/bookstore

Printed in the United States of America

THE NATIONAL ACADEMIES

Advisers to the Nation on Science, Engineering, and Medicine

The **National Academy of Sciences** is a private, nonprofit, self-perpetuating society of distinguished scholars engaged in scientific and engineering research, dedicated to the furtherance of science and technology and to their use for the general welfare. On the authority of the charter granted to it by the Congress in 1863, the Academy has a mandate that requires it to advise the federal government on scientific and technical matters. Dr. Ralph J. Cicerone is president of the National Academy of Sciences.

The **National Academy of Engineering** was established in 1964, under the charter of the National Academy of Sciences, as a parallel organization of outstanding engineers. It is autonomous in its administration and in the selection of its members, sharing with the National Academy of Sciences the responsibility for advising the federal government. The National Academy of Engineering also sponsors engineering programs aimed at meeting national needs, encourages education and research, and recognizes the superior achievements of engineers. Dr. Charles M. Vest is president of the National Academy of Engineering.

The **Institute of Medicine** was established in 1970 by the National Academy of Sciences to secure the services of eminent members of appropriate professions in the examination of policy matters pertaining to the health of the public. The Institute acts under the responsibility given to the National Academy of Sciences by its congressional charter to be an adviser to the federal government and, on its own initiative, to identify issues of medical care, research, and education. Dr. Harvey V. Fineberg is president of the Institute of Medicine.

The **National Research Council** was organized by the National Academy of Sciences in 1916 to associate the broad community of science and technology with the Academys p urposes of furthering knowledge and advising the federal government. Functioning in accordance with general policies determined by the Academy, the Council has become the principal operating agency of both the National Academy of Sciences and the National Academy of Engineering in providing services to the government, the public, and the scientific and engineering communities. The Council is administered jointly by both the Academies and the Institute of Medicine. Dr. Ralph J. Cicerone and Dr. Charles M. Vest are chair and vice chair, respectively, of the National Research Council.

The **Transportation Research Board** is one of six major divisions of the National Research Council, which serves as an independent adviser to the federal government and others on scientific and technical questions of national importance. The National Research Council is jointly administered by the National Academy of Sciences, the National Academy of Engineering, and the Institute of Medicine. The mission of the Transportation Research Board is to provide leadership in transportation innovation and progress through research and information exchange, conducted within a setting that is objective, interdisciplinary, and multimodal. The Board's varied activities annually engage about 7,000 engineers, scientists, and other transportation researchers and practitioners from the public and private sectors and academia, all of whom contribute their expertise in the public interest. The program is supported by state transportation departments, federal agencies including the component administrations of the U.S. Department of Transportation, and other organizations and individuals interested in the development of transportation. **www.TRB.org**

www.national-academies.org

FOREWORD

By Staff
Transportation
Research Board

Highway administrators, engineers, and researchers often face problems for which information already exists, either in documented form or as undocumented experience and practice. This information may be fragmented, scattered, and unevaluated. As a consequence, full knowledge of what has been learned about a problem may not be brought to bear on its solution. Costly research findings may go unused, valuable experience may be overlooked, and due consideration may not be given to recommended practices for solving or alleviating the problem.

There is information on nearly every subject of concern to highway administrators and engineers. Much of it derives from research or from the work of practitioners faced with problems in their day-to-day work. To provide a systematic means for assembling and evaluating such useful information and to make it available to the entire highway community, the American Association of State Highway and Transportation Officials—through the mechanism of the National Cooperative Highway Research Program—authorized the Transportation Research Board to undertake a continuing study. This study, NCHRP Project 20-5, "Synthesis of Information Related to Highway Problems," searches out and synthesizes useful knowledge from all available sources and prepares concise, documented reports on specific topics. Reports from this endeavor constitute an NCHRP report series, *Synthesis of Highway Practice.*

This synthesis series reports on current knowledge and practice, in a compact format, without the detailed directions usually found in handbooks or design manuals. Each report in the series provides a compendium of the best knowledge available on those measures found to be the most successful in resolving specific problems.

PREFACE

This synthesis reviews the cone penetration testing (CPT) current practices of departments of transportation (DOTs) in the United States and Canada. Information is presented on cone penetrometer equipment options; field testing procedures; CPT data presentation and geostratigraphic profiling; CPT evaluation of soil engineering parameters and properties; CPT for deep foundations, pilings, shallow foundations, and embankments; and CPT use in ground modifications and difficult ground conditions. The report is designed to serve as a resource to states and provinces interested in taking advantage of CPT technology by identifying applications, design procedures, advantages, and limitations for successful implementation.

Information was gathered by a literature review of domestic and international experience, a survey of DOTs in the United States and Canada, and interviews with practitioners.

Paul W. Mayne, Professor, Civil and Environmental Engineering, Georgia Institute of Technology, Atlanta, collected and synthesized the information and wrote the report. The members of the topic panel are acknowledged on the preceding page. This synthesis is an immediately useful document that records the practices that were acceptable within the limitations of the knowledge available at the time of its preparation. As progress in research and practice continues, new knowledge will be added to that now at hand.

CONTENTS

CONE PENETRATION TESTING

SUMMARY

Cone penetration testing (CPT) is a fast and reliable means of conducting highway site investigations for exploring soils and soft ground for support of embankments, retaining walls, pavement subgrades, and bridge foundations. The CPT soundings can be used either as a replacement (in lieu of) or complement to conventional rotary drilling and sampling methods. In CPT, an electronic steel probe is hydraulically pushed to collect continuous readings of point load, friction, and porewater pressures with typical depths up to 30 m (100 ft) or more reached in about 1 to 1½ h. Data are logged directly to a field computer and can be used to evaluate the geostratigraphy, soil types, water table, and engineering parameters of the ground by the geotechnical engineer on-site, thereby offering quick and preliminary conclusions for design. With proper calibration, using full-scale load testing coupled with soil borings and laboratory testing, the CPT results can be used for final design parameters and analysis.

In this NCHRP Synthesis, a review is presented on the current practices followed by departments of transportation (DOTs) in the United States and Canada. A detailed questionnaire on the subject was distributed to 64 DOTs, with 56 total respondents (88%). The survey questions were grouped into six broad categories: (1) use of the cone penetrometer by each agency, (2) maintenance and field operations of the CPT, (3) geostratigraphic profiling by CPT, (4) CPT evaluation of soil engineering parameters and properties, (5) CPT utilization for deep foundations and pilings, and (6) other aspects and applications related to CPT. Of the total number of DOTs responding, approximately 27% use CPT on a regular basis, another 36% only use CPT on one-tenth of their projects, and the remaining 37% do not use CPT at all. Overall, it can be concluded that the technology is currently underutilized and that many DOTs could benefit in adopting this modern device into their site investigation practices; the survey results noted that 64% of the DOTs plan to increase their use of CPT in the future.

In its simplest application, the cone penetrometer offers a quick, expedient, and economical way to profile the subsurface soil layering at a particular site. No drilling, soil samples, or spoils are generated; therefore, CPT is less disruptive from an environmental standpoint. The continuous nature of CPT readings permit clear delineations of various soil strata, their depths, thicknesses, and extent, perhaps better than conventional rotary drilling operations that use a standard drive sampler at 5-ft vertical intervals. Therefore, if it is expected that the subsurface conditions contain critical layers or soft zones that need detection and identification, CPT can locate and highlight these particular features. In the case of piles that must bear in established lower foundation formation soils, CPT is ideal for locating the pile tip elevations for installation operations.

A variety of cone penetrometer systems is available, ranging from small mini-pushing units to very large truck and track vehicles. The electronic penetrometers range in size from small to large probes, with from one to five separate channels of measurements. The penetrometer readings can be as simple as measuring just the axial load over the tip area, giving the cone tip resistance (q_c). A second load cell can provide the resistance over a side area, or sleeve friction (f_s). With both, the electronic friction cone is the normal type penetrometer, termed the cone penetration test. A mechanical-type CPT probe is available for pushing in

very hard and abrasive ground. With the addition of porous filters and transducers, the penetration porewater pressures (u) in saturated soils can be measured, and are thus termed a piezocone penetration test (CPTu). The seismic CTPu contains geophones to permit profiling of shear wave velocity measurements and the resistivity CPTu uses electrodes to obtain readings on the electrical properties of the soil. Details concerning the standard equipment, calibration, field test procedures, and interpretation and presentation of results are discussed in the report. Specialized testing procedures and equipment used to achieve penetration in very dense or cemented ground are also reviewed in this report.

The evaluation of soil type by CPT is indirect and must be inferred from the penetrometer measurements, coupled with a good understanding of the local and regional geology. Therefore, it may be beneficial to cross-calibrate the CPT results with logs from adjacent soil test borings to best utilize the technology in a reliable manner. When necessary, a simple CPT sampler can be deployed for obtaining soil specimens for examination. In addition, video CPT systems are available to allow visual identification of soils and subsurface conditions in real time.

The cone penetrometer is instrumented with load cells to measure point stress and friction during a constant rate of advancement. The results can be interpreted within different theoretical frameworks or by using empirical methods, or both. As the data are logged directly to the computer, additional sensors can be readily incorporated, including porewater pressure, resistivity, inclination, and shear wave velocity, as well as a number of environmental measurements (gamma, pH, salinity, temperature, etc.). The ability of CPT to collect multiple and simultaneous readings with depth is a valuable asset in the screening of subsurface conditions and the evaluation of natural foundation-bearing materials. The recorded data are stored digitally and can be post-processed to interpret a number of geotechnical engineering parameters that relate to soil strength, stiffness, stress state, and permeability. These parameters are needed input in the design and analysis of the stability of embankments and slopes, bearing capacity of shallow and deep foundations, and engineering evaluations concerning displacements, deflections, and settlements of walls, abutments, fills, and foundation systems.

In some circles, the cone penetrometer is considered to be a miniature pile foundation. Thus, the recorded penetrometer data can be used either in a direct CPT method or indirect (or rational) approach for evaluating the point end bearing and side friction resistance of deep foundation systems. Both approaches are discussed in this report, with a particular effort given to describing and outlining some of the newer methods developed for the piezocone and seismic cone. Driven pilings and drilled deep foundations are considered. Methods are also reviewed for the evaluation of bearing capacity and displacements of footings and shallow foundations from CPT results.

From an economical standpoint, CPTs offer cost savings as well as time savings in site investigation. On a commercial testing basis in 2006 dollars, the cost of CPTs is between $20 and $30 per meter ($6 to $9 per foot), compared with soil test borings at between $40 and $80 per meter ($12 to $24 per foot). Post-grouting of CPT holes during closure can add another $10 to $15 per meter ($3 to $4.50 per foot); whereas post-hole closure of the larger size drilled boreholes may add another $15 to $30 per meter ($4.50 to $9.00 per foot).

In earthquake regions, CPT offers several capabilities in the evaluation of seismic ground hazards. First, the sounding can be used to identify loose weak sands and silty sands below the groundwater table that are susceptible to liquefaction. Second, the measurements taken by the CPT can provide an assessment on the amount of soil resistance available to counter shearing during ground shaking. The penetrometer can also be fitted with geophones to allow for the determination of downhole shear wave velocity (V_s) profiles. The V_s data are required for site-specific analyses of ground amplification, particularly in the revised procedures of the International Building Code (IBC 2000/2003).

Ground engineering solutions to soft and/or problematic soils now include a wide range of soil improvement methods, including surcharging, wick drains, dynamic compaction, vibroflotation, and deep soil mixing. Applications of the CPT are particularly useful for quality control during ground modification because they allow a quick contrast in comparing the before and after measured resistances with depth. The CPT also allows for quantification of time effects after completion of improvement.

Because CPTs are economical and expedient, this allows the DOT to deliver more miles of highway and more structures for the same program budget. As shown by the unit costs presented earlier, CPTs offer investigation cost savings if they are used in lieu of some traditional soil test borings; however, CPTs can also have far greater value. In the right settings, CPTs can be used in conjunction with borings to provide a more complete description of the subsurface conditions, thereby reducing uncertainty in design and construction, and thus the need for conservative assumptions and higher construction bid prices to cover risks posed by the uncertainties. As a result, the overall project can benefit owing to a higher degree of reliability and improved overall cost on the design and construction of the highway structure.

On a final note, within the field of geotechnical engineering and site investigation, those who engage in the use of cone penetrometer technology are affectionately known as "coneheads." We therefore encourage the DOT engineer to read this synthesis and learn of the possible advantages and benefits that can be gained by using CPTs on their own transportation projects. With due care and consideration, it is hoped that a growing number of coneheads will emerge from DOTs across the United States.

CHAPTER ONE

INTRODUCTION

Site-specific soil investigations are required for the analysis and design of all highway bridge foundations, embankments, retaining walls, slopes, excavations, and pavements. Toward the optimal design, the state engineer will want to consider safety, reliability, long-term maintenance, and economy in deliberations of various solutions. To collect geotechnical information, most state departments of transportation (DOTs) either maintain their own in-house drill rigs with field crews or else subcontract soil drilling and sampling services from outside consultant companies. Rotary drilling methods have been around for two millenia and are well-established in geotechnical practice as a means to study soil and rock conditions (Broms and Flodin 1988). Although drilling and sampling practices can be adequate, the work is manual and time-consuming, with follow-up laboratory testing often adding two to four weeks for completion of results.

For soil exploration, a modern and expedient approach is offered by cone penetration testing (CPT), which involves pushing an instrumented electronic penetrometer into the soil and recording multiple measurements continuously with depth (e.g., Schmertmann 1978a; Campanella and Robertson 1988; Briaud and Miran 1992). By using ASTM and international standards, three separate measurements of tip resistance (q_c), sleeve friction (f_s), and porewater pressure (u) are obtained with depth, as depicted in Figure 1. Under certain circumstances, the tip and sleeve readings alone can suffice to produce a basic cone sounding that serves well for delineating soil stratigraphy and testing natural sands, sandy fills, and soils with deep water tables. Generally, this is accomplished using an electric cone penetration test (ECPT), with readings taken at 2 cm (0.8 in.) or 5 cm (2.0 in.), although a system for mechanical cone penetration testing (MCPT) is also available that is less prone to damage, but that is advanced slower and provides coarser resolutions using an incremental vertical step of 20-cm (8-in.) intervals. With piezocone penetration testing (CPTu), transducers obtain readings of penetration porewater pressures that are paramount when conditions contain shallow groundwater conditions and fine-grained soils consisting of clays, silts, and sands with fines. The porewater pressures at the shoulder position are required for correcting the measured q_c to the total cone tip resistance, designated q_t. This is especially important in the post-processing phase when determining soil engineering parameters; for example, preconsolidation stress (P_c'), undrained shear strength (s_u), lateral stress ratio (K_0), and pile side friction (f_p). Additional sensors can be provided to increase the numbers and types of measurements taken, with Table 1 providing a quick summary of the various types of CPTs commonly available.

With CPT, results are immediately available on the computer for assessment in real time by the field engineer or geologist. A 10-m (30-ft) sounding can be completed in approximately 15 to 20 min, in comparison with a conventional soil boring that may take between 60 and 90 min. No spoil is generated during the CPT; thus, the method is less disruptive than drilling operations. Therefore, CPTs are especially advantageous when investigating environmentally sensitive areas and/or potentially contaminated sites, because the workers are exposed to a minimal amount of hazardous material. CPTs can be advanced into most soil types, ranging from soft clays and firm silts to dense sands and hard overconsolidated clays, but are not well suited to gravels, cobbles, or hard rock terrain. Soil samples are not normally obtained during routine CPT and therefore may be a disadvantage to those who rely strictly on laboratory testing for specifications and state code requirements. Nevertheless, a large amount of high-quality in situ digital data can be recorded directly by CPT in a relatively short time in the field. These data can subsequently be post-processed to provide quick delineations of the subsurface conditions, including layering, soil types, and geotechnical engineering parameters, as well as both direct and indirect evaluations of foundation systems, including shallow footings, driven pilings, drilled shafts, and ground modification.

A number of difficulties are now recognized with routine drilling practices in obtaining field test values, drive samples, and undisturbed samples (e.g., Schmertmann 1978b; Tanaka and Tanaka 1999). During the advance of the soil boring, the normal practice is to secure small diameter drive samples (termed "split-spoons" or "split-barrel" samples) at 1.5-m (5-ft) vertical intervals, often in general accordance with ASTM D 1586 or AASHTO T-206 procedures for the "Standard Penetration Test" (SPT). The recorded number of blows to drive the sampler 0.3 m (12 in.) is termed the "*N*-value," "blow counts," or SPT resistance. It is well known that this *N*-value can be severely affected by energy inefficiencies in the drop hammer system, as well as additional influences such as borehole diameter, hammer system, sample liner, rod length, and other factors (e.g., Fletcher 1965; Ireland et al. 1970). Thus, these recorded *N*-values require significant corrections to the field measurements before they can be used in engineering analysis (e.g., Robertson et al. 1983; Skempton

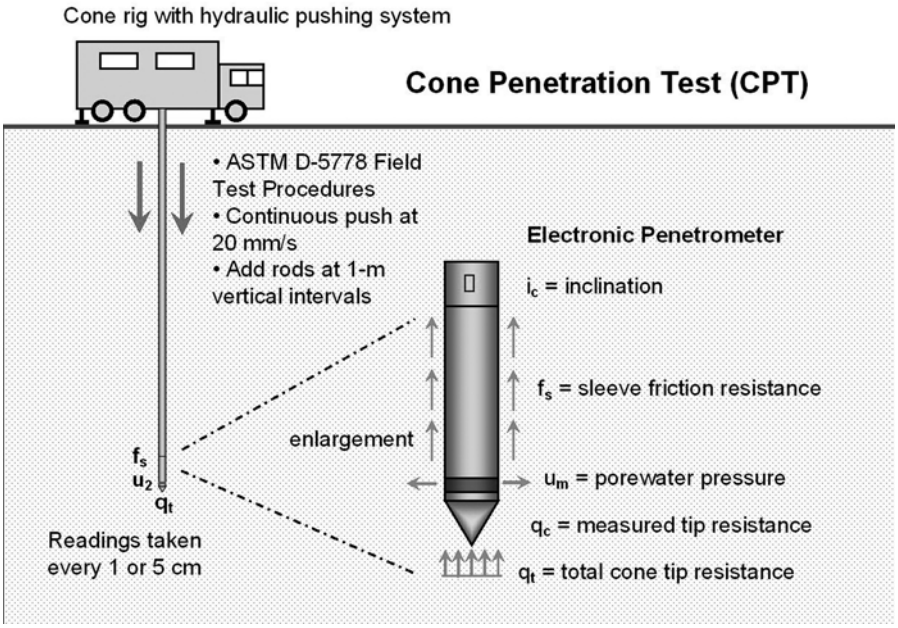

FIGURE 1 Overview of the cone penetration test per ASTM D 5778 procedures.

1986). Moreover, there remains considerable uncertainty in the proper correction of the *N*-values (Kulhawy and Mayne 1990) and the repeatability of SPTs using different equipment and drillers remains an issue (e.g., Anderson et al. 2004).

As a complement to (or in some cases, as a replacement for) soil borings with SPT *N*-values, the cone can provide similar information on the subsurface stratigraphy, soil layers, and consistency. Figure 2 shows a side-by-side comparison of an ECPT point resistance (q_c) profile with a boring log derived from two adjacent boreholes with SPT resistances (*N*-values) in downtown Memphis, Tennessee. The continuous nature of the CPT point resistance is evident in the profiling of the various strata and soil types. The CPT resistance complements the discrete values from the SPTs at the site and helps to better define the interface between layers, thicknesses, and relative consistencies of each stratum.

If geostratification at a site is the primary purpose of the site investigation, then CPT soundings can be readily advanced to detail the strata across the highway alignment. The variations both vertically and laterally can be quickly determined using

TABLE 1
BASIC TYPES OF CONE PENETRATION TESTS AVAILABLE FOR SITE CHARACTERIZATION

Type of CPT	Acronym	Measurements Taken	Applications
Mechanical Cone Penetration Test	MCPT	q_c (or q_c and f_s) on 20-cm intervals. Uses inner and outer rods to convey loads uphole	Stratigraphic profiling, fill control, natural sands, hard ground
Electric Friction Cone	ECPT	q_c and f_s (taken at 1- to 5-cm intervals)	Fill placement, natural sands, soils above the groundwater table
Piezocone Penetration Test	CPTu and PCPT	q_c, f_s, and either face u_1 or shoulder u_2 (taken at 1- to 5-cm intervals)	All soil types. Note: Requires u_2 for correction of q_c to q_t
Piezocone with Dissipation	CPTù	Same as CPTu with timed readings of u_1 or u_2 during decay	Normally conducted to 50% dissipation in silts and clays
Seismic Piezocone Test	SCPTu	Same as CPTu with downhole shear waves (V_s) at 1-m intervals	Provides fundamental soil stiffness with depth: $G_{max} = \rho_t V_s^2$
Resistivity Piezocone Test	RCPTu	Same as CPTu with electrical conductivity or resistivity readings	Detect freshwater–salt water interface. Index to contaminant plumes

Notes: q_c = measured point stress or cone tip resistance, f_s = measured sleeve friction, u = penetration porewater pressure (u_1 at face; u_2 at shoulder), q_t = total cone resistance, V_s = shear wave velocity.

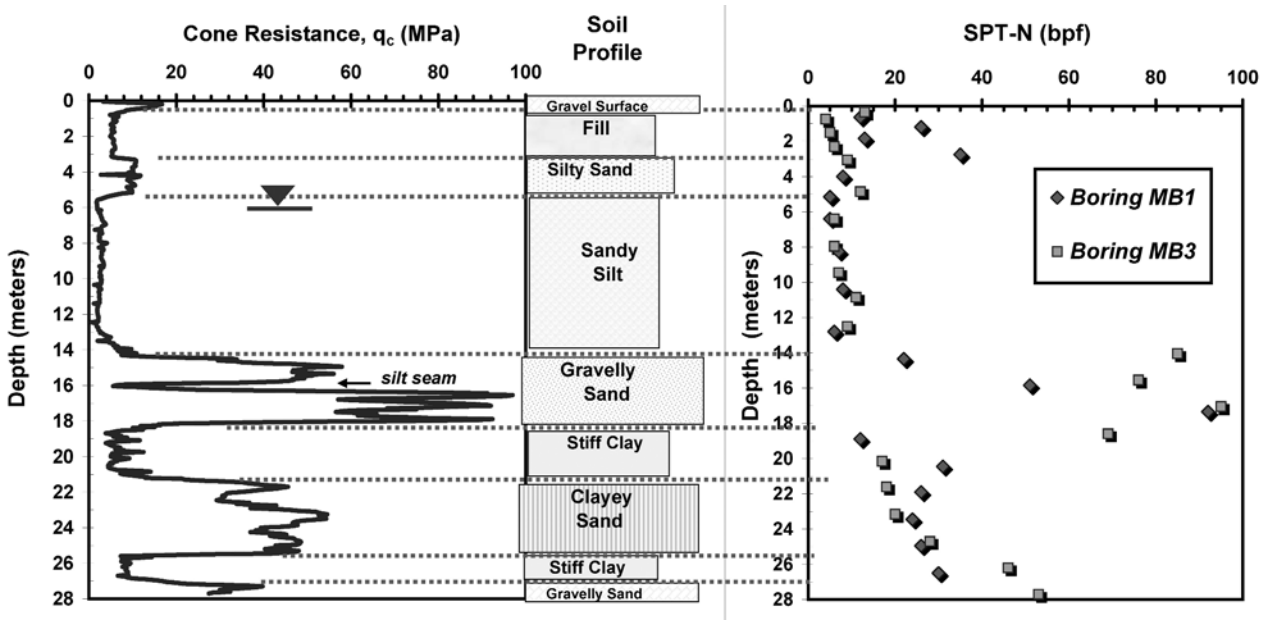

FIGURE 2 Companion profile of CPT cone tip resistance and soil boring log with SPT*N*-values.

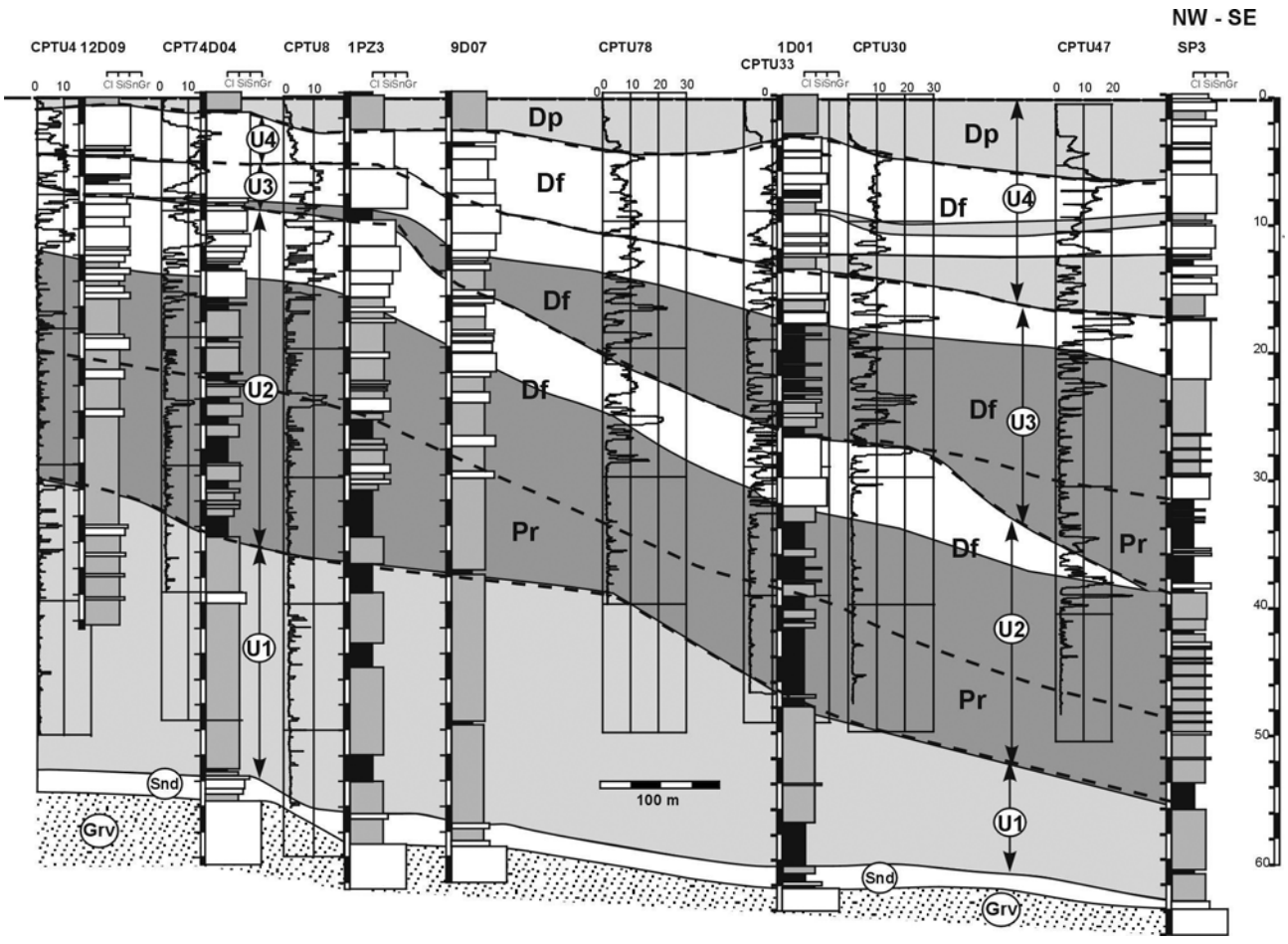

FIGURE 3 Subsurface profile developed from an array of CPT q_c profiles.

the cone tip resistance. Figure 3 is an example subsurface profile developed from CPT q_c profiles. The thicknesses of soft compressible clay and silt layers can be mapped over the region and this information is useful in determining the settlements of embankment fills and shallow foundations, as well as the necessary lengths of driven or drilled piling foundations for the project.

Because soils are very complex and diverse materials within a natural geologic environment, sole reliance on SPT can lead to significant oversimplifications in predicting true soil behavior. Nevertheless, a number of geotechnical firms and highway departments rely on SPTs from soil borings as their primary data source for bridge, wall, and roadway design. One clear advantage of the CPT is its ability to provide three independent and simultaneous measurements. Additional sensors are available to produce up to five direct readings with depth to ascertain a more realistic evaluation of soil behavior.

During routine drilling operations in North America, it is standard practice to obtain "undisturbed samples" using thin-walled (Shelby-type) tubes (e.g., ASTM D 1587 and AASHTO T-207) that will later be used to provide smaller specimens for "high-quality" laboratory testing, such as triaxial shear, one-dimensional consolidation, permeability, direct shear, or resonant column tests. However, it is now well-recognized that "undisturbed samples" are very difficult to obtain with this simple tube sampler, especially when compared with high-quality and more expensive methods, such as the Laval, Sherbrooke, NGI, and JPN samplers (e.g., Tanaka and Tanaka 1999). Methods for correcting laboratory testing for sample disturbance effects include either a consolidation–unloading phase (e.g., Ladd 1991) or reconsolidation phase (DeGroot and Sandven 2004), both of which add to laboratory testing times and more elaborate procedures. In contrast, CPT obtains measurements directly on the soil while still in its natural environs, thus offering a direct assessment of soil behavioral response to loading. Perhaps the best approach is one founded on a combination of quick CPT soundings to scan for weak layers and problematic zones, followed by rotary drilling operations to procure soil samples for examination and laboratory testing.

CHAPTER TWO

SURVEY QUESTIONNAIRE ON CONE PENETRATION TESTING

In many instances, CPT is increasingly being valued as a productive and cost-efficient means of site investigation for highway projects. Because many diverse geologic formations can be found across the North American continent, TRB decided that a synthesis on the state of practice in CPT would be a helpful guide in its upcoming utilization. One purpose of this synthesis was to gather information from all state and provincial DOTs with the objective of defining and sharing common experiences, successes and failures, and value in applying cone penetrometer technology in highway design and construction. Toward this goal, a survey questionnaire was prepared as an initial step in determining the individual practices from highway departments and their consultants. The questionnaire was directed at geotechnical engineers in the 52 state DOTs in the United States and their equivalents at 12 provincial DOTs in Canada. Where pertinent, the state and provincial geotechnical engineers were offered the opportunity to engage responses from selected consultant testing firms to aid in the survey results. Appendix A contains a summary of the findings derived from the responses to the 59 questions posed in the survey. A total of 56 surveys (of 64 sent) were returned; an overall response rate of 88%.

Despite the advantages of CPT, currently 37% of responding state and provincial DOTs do not use any CPT technology whatsoever. Another 36% of the DOTs use CPT only on 10% of their site investigation studies. Fifteen DOTs (or 27% of the respondents) use CPT on a fairly regular basis on their geotechnical projects (see Figure 4). Much of the CPT work is conducted by outside consultants working under contract to the DOT.

The CPT is used to investigate a variety of different geomaterials, but is particularly focused on studies involving soft to firm clays, loose sands, organic soils, and fills. With regard to geotechnical project type, CPT has been used for an assortment of purposes, with the primary applications being bridge design, embankments, and deep foundations (see Figure 5).

Reasons for DOTs not to use the CPT vary considerably across the United States and Canada, as summarized in Figure 6. The most frequently cited obstacle reported was that many geologic settings were apparently too hard and not conducive to successful penetration by standard CPT equipment. Other common reasons for nonutilization included limited accessibility, lack of expertise, and nonfamiliarity with the technology. This synthesis addresses these major issues.

More than two-thirds of the DOTs have not had any unfavorable experiences with the CPT on their projects (see Figure 7). Only 6% of responses indicated difficulties, with another 25% mentioning an occasional problem.

Based on the survey results, it appears that the majority of DOTs are aware of the CPT technology and its availability. Approximately 64% of the respondent DOTs indicated having made plans to increase their use of CPT in coming years for site exploration and geotechnical investigations (see Figure 8).

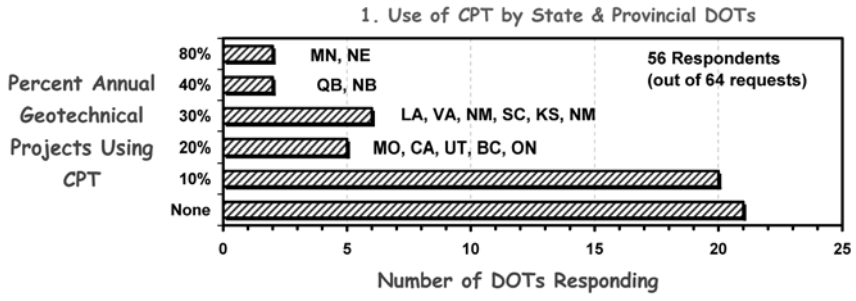

FIGURE 4 Results from survey questionnaire on annual use of CPT by DOTs.

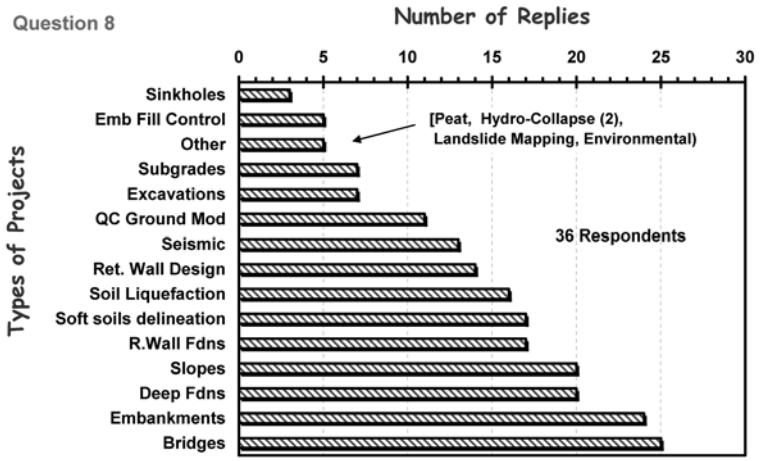

FIGURE 5 Types of geotechnical projects that CPT is used on by state and provincial DOTs.

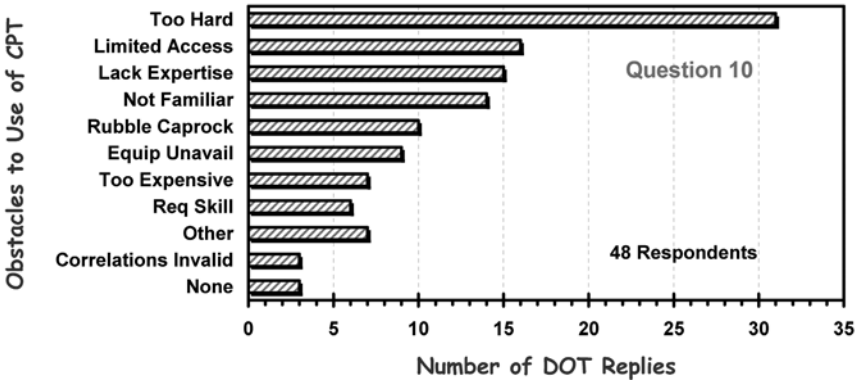

FIGURE 6 Reasons that CPT is not used by state and provincial DOTs.

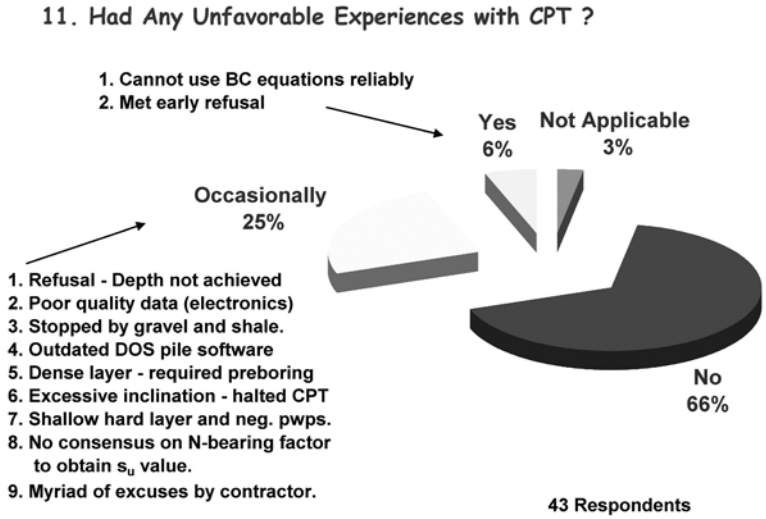

FIGURE 7 Survey results of unfavorable experiences with CPT by DOTs.

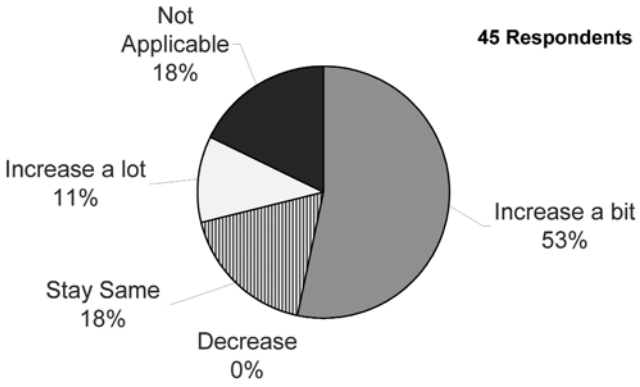

FIGURE 8 Projected use of CPT on future DOT geotechnical projects.

CHAPTER THREE

CONE PENETROMETER EQUIPMENT

HISTORY

Cone penetrometers have been in use for soil exploration since 1932 when the Dutch engineer P. Barentsen used a field cone to measure tip resistances with depth in a 4-m (13.1-ft)-thick fill (Broms and Flodin 1988). Initial cone systems were of the mechanical-type design with two sets of rods. An outer set of steel rods was employed to minimize soil friction and protect an inner stack of rods that transferred tip forces uphole to a pressure gauge read-out at the ground surface. Later, a sleeve was added to provide a secondary measure of vertical loads over a cylindrical surface above the tip (Begemann 1965). A step-wise pushing procedure applied at 20-cm (8-in.) increments permitted successive sets of tip and sleeve readings using the same load cell. Field readings were taken by hand.

Electrical versions were developed circa 1948 by the Delft Soil Mechanics Laboratory, which offered continuous measurements of tip resistance with depth and direct strip chart plotting of the sounding record (Vlasblom 1985). Electrical-type penetrometers with both tip and friction readings were designed as research tools as early as 1949 and became commercially available in the 1960s (deRuiter 1971; Robertson 2001). These solved noted problems associated with poor load readings acquired by mechanical cone systems because of frictional force buildups between the inner and outer sets of rods, primarily the result of rusting and bending. A representative schematic of a standard penetrometer cross section is depicted in Figure 9.

The electrical CPTs are also faster to do than mechanical CPTs because they are conducted at a constant rate of push rather than stepped increments. In the electrical systems, the penetrometer is linked by means of a wired cable through the hollow cone rods to a field computer at the surface for automated data acquisition. An inclinometer was incorporated to detect deviations from verticality and thus offer a warning to the user against excessive slope and/or buckling problems (Van De Graaf and Jekel 1982).

As early as 1962, a research piezocone was being designed for tip and porewater readings by the Delft Soil Mechanics Laboratory (Vlasblom 1985), but was used for exploration in sands. In the 1970s, the advent of piezoprobes showed value in profiling penetration porewater pressures in soft clays and layered soils, particularly those that are highly stratified (Senneset 1974; Battaglio et al. 1981). The merger of the electric cone with the electric piezoprobe was an inevitable design as the hybrid piezocone penetrometer could be used to obtain three independent readings during the same sounding: tip stress, sleeve friction, and porewater pressures (Baligh et al. 1981; Tumay et al. 1981).

Over the past three decades, a number of other sensors or devices have been installed within the penetrometers, including temperature, electrodes, geophones, stress cells, full-displacement pressuremeters, vibrators, radio-isotope detectors for density and water content determination, microphones for monitoring acoustical sounds, and dielectric and permittivity measurements (Jamiolkowski 1995).

More recently, electronic systems have become available that contain the signal conditioning, amplification, and digital output directly within the penetrometer downhole. With digital cone penetrometers, only four wires are needed to transmit the data uphole in series (in lieu of the parallel signals sent by cable). Other developments include a number of wireless CPT systems, as discussed in the next section, and special designs for deployment in the offshore environment (Lunne 2001).

EQUIPMENT

A CPT system includes the following components: (1) an electrical penetrometer, (2) hydraulic pushing system with rods, (3) cable or transmission device, (4) depth recorder, and (5) data acquisition unit. These items are briefly discussed in the following subsections. Additional details on these topics may be found in Robertson and Campanella (1984), Briaud and Miran (1992), and Lunne et al. (1997).

Penetrometers

The standard cone penetrometer consists of a three-channel instrumented steel probe that measures cone tip stress (q_c), sleeve friction (f_s), and penetration porewater pressure (u_m). The front end consists of a 60º apex conical tip that has a small lip approximately 5 mm (0.2 in.) long at the upper portion. The penetrometers are normally available in two standard sizes: (1) a 35.7-mm (1.4-in.) diameter version having a corresponding cross-sectional area, $A_c = 10$ cm^2 and sleeve area, $A_s = 150$ cm^2; and (2) a 44-mm (1.75-in.)

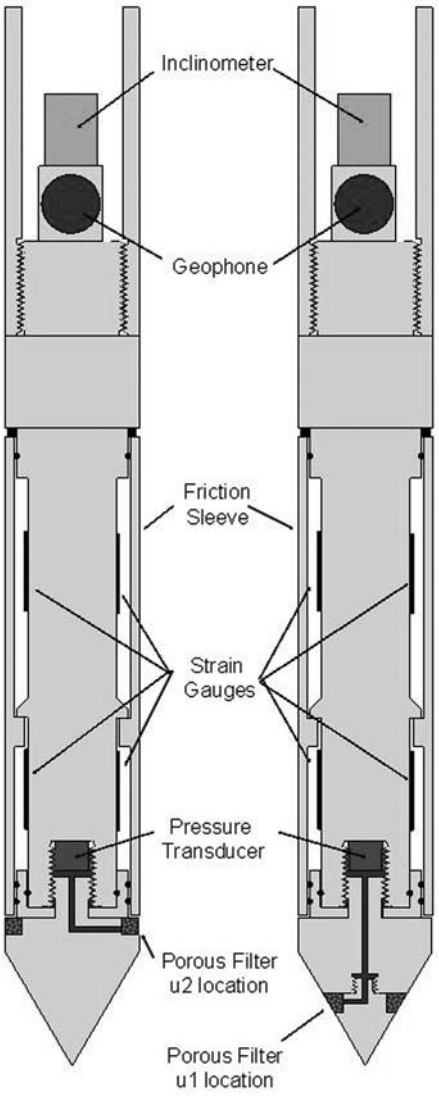

FIGURE 9 Basic internal schematic of an electric cone penetrometer.

diameter version (A_c = 15 cm^2 and A_s = 200 to 300 cm^2). Although the 10-cm^2 size is the original standard size, many commercial firms have found the 15-cm^2 version to be stronger for routine profiling and more easily outfitted with additional sensors in specific needs. As rod sizes are normally 35.7 mm (1.4 in.) in diameter, the 15-cm^2 size cone also tends to open a larger hole and thus reduce side rod friction during pushing. Figure 10 shows the basic styles of penetrometers in routine use and these are patterned after the original Fugro-type designs (de Ruiter 1971).

Depending on the types of soils being tested, the porous filter is usually located either at the apex or mid-face (termed Type 1) or at the shoulder (Type 2) just behind the cone tip, or else positioned behind the sleeve (Type 3). For the proper correction of measured cone tip resistance to total resistance, the Type 2 is required by national and international standards until proven otherwise (Campanella and Robertson 1988).

An internal load cell is used to register the axial force at the front of the penetrometer (F_c). A second load cell is used to record the axial force either along the sleeve (F_s) within a "tension-type cone" design or else located in the back and records the total tip force plus sleeve ($F_c + F_s$). In the latter (termed "subtraction-type cone"), the combined force minus the separately measured front force provides the sleeve force.

State and provincial DOTs that engage in cone penetration work use either commercially manufactured CPT systems, subcontract to firms that use commercial equipment, or maintain an arsenal of their own in-house penetrometers and data acquisition systems.

In special instances, miniature cone penetrometers are available, with reduced cross-sectional sizes of 5 cm^2 and 1 cm^2 discussed in the open literature. These mini-cones have been used in laboratory testing programs, both in calibration chambers and centrifuges, yet also in field applications (e.g., Tumay et al. 1998). Also, large diameter penetrometers have been developed for special projects, including a 33 cm^2 version and a 40 cm^2 model that can be pushed into gravelly soils. Figure 11 shows a selection of penetrometers. Based on the survey results, most DOTs are using 10-cm^2-size penetrometers, with a few deploying the 15 cm^2 type. Several are using advanced cones with seismic, video, or resistivity, whereas only two DOTs are using mini-cones and one DOT is operating a mechanical CPT.

Specifications on the machine tolerances, dimensions, and load cell requirements for electrical CPTs are outlined in ASTM D 5778 and in the international reference test procedure (IRTP 1999). For the older mechanical CPT systems, guidelines per ASTM D 3441 still remain on the books. Most penetrometers are constructed of tool-grade steel, although a few commercial units are available in stainless steel or brass. Periodically, the tip and sleeve elements are replaced as a result of wear or damage. It is common to replace the porewater filter after each sounding with either a disposable plastic ring type or else a reusable sintered metal or ceramic type. The reusable types can be cleaned in an ultrasonics bath.

Penetration Tip and Sleeve Readings

The measured axial force (F_c) divided by the area gives the measured tip resistance, $q_c = F_c/A_c$. This stress must be corrected for porewater pressures acting on unequal tip areas of the cone, especially important in soft to firm to stiff intact clays and silts (Jamiolkowski et al. 1985; Campanella and Robertson 1988; Lunne et al. 1997). The corrected tip stress or total cone tip resistance is designated as q_t, and requires two prerequisites: (1) calibration of the particular penetrometer in a triaxial chamber to determine the net area ratio (a_n);

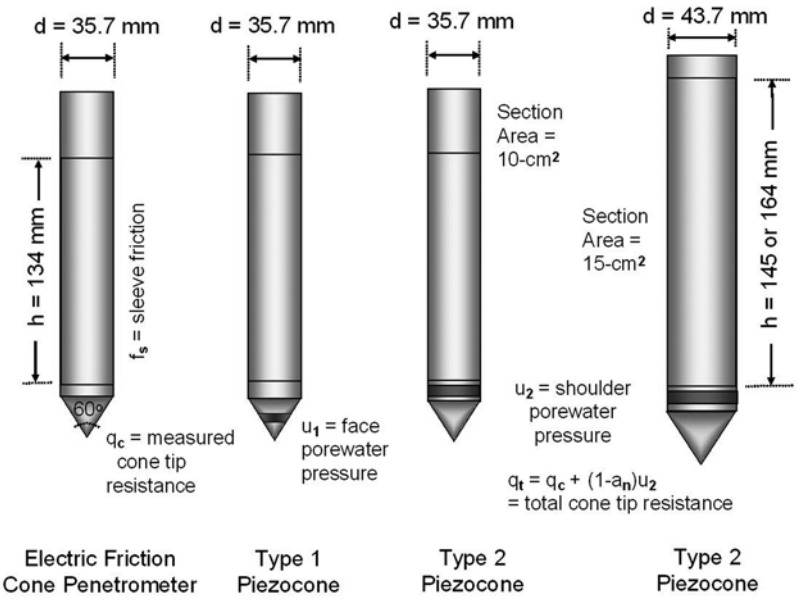

FIGURE 10 Dimensions and measurements taken by standard 10-cm² and 15-cm² penetrometers.

and (2) field porewater pressures to be measured at the shoulder position ($u_b = u_2$), as illustrated in Figure 12. The total cone tip resistance is determined as:

$$q_t = q_c + (1 - a_n)u_2 \quad (1)$$

In clean sands and dense granular soils, the value $q_t \approx q_c$; thus, the correction is not paramount. However, in soft to stiff clayey soils, appreciable porewater pressures are generated and the correction can be very significant, from 20% to 70% in some instances (Lunne et al. 1986; Campanella and Robertson 1988). Perhaps not appreciated is that, even with standard friction-type cones that do not measure porewater pressures, the correction is still needed.

The measured axial force over the sleeve (F_s) is divided by the sleeve area to obtain the sleeve friction, $f_s = F_s/A_s$. However, this too requires a correction; two porewater pressure readings are needed, taken at both the top and bottom ends of the sleeve and therefore, at this time, beyond standard practice and not required by the ASTM nor international standards. Results from the survey indicated that only 48% of DOTs are correcting the measured tip resistances to total tip stress. This is an important finding in that, without the total resistance, the interpretations of soil parameters and application of direct CPT methodologies may not be as reliable as they could be.

An example calibration of a (brand new) cone penetrometer within a pressurized triaxial chamber for all three readings is presented in Figure 13. It can be seen that the porewater transducer provides a one-to-one correspondence with the applied chamber pressures, thus indicating excellent response (best-fit line from regression shown). The uncorrected cone tip resistance (q_c) shows significantly less response, with a corresponding net area ratio, $a_n = 0.58$ for this particular penetrometer. Also shown is the response of the sleeve reading with applied pressure (conceptually, this should show no readings). A friction correction factor ($b_n = 0.014$) can be applied using the guidelines given in the Swedish CPTu standard (e.g., Lunne et al. 1997).

FIGURE 11 Selection of penetrometers from (*left*) van den Berg series, (*center*) Fugro series (left to right: 33-, 15-, 10-, 5-, and 1-cm² sizes), and (*right*) Georgia Tech collection (bottom to top): 5-cm² friction, four 10-cm² piezocones (type 2, type 1, type 2 seismic, dual-piezo-element), and 15-cm² triple-element type.

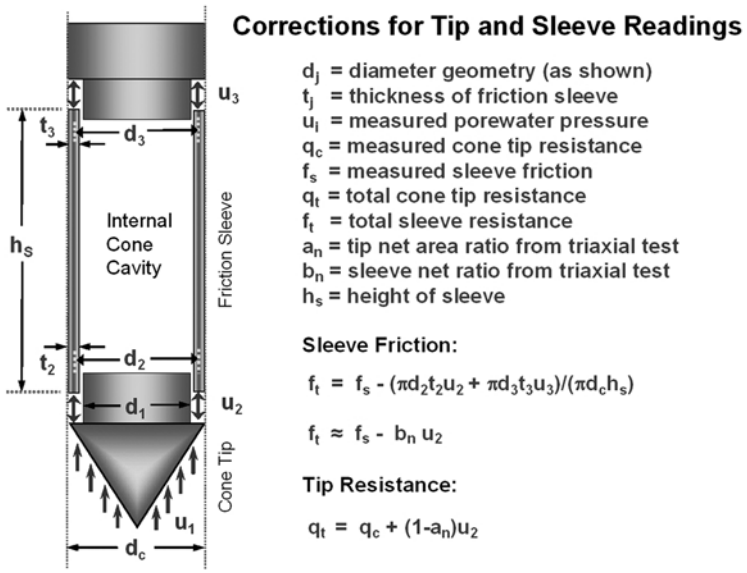

FIGURE 12 Determination of total cone tip resistance and total sleeve friction (Jamiolkowski et al. 1985).

Using the same penetrometer, an illustrative sounding in soft sediments near the city of New Orleans is presented in Figure 14. The soil profile consists of a desiccated crust overlying soft clay and a layer of loose to firm sands to silty sands, with soft silty clays encountered at depths greater than 12 m within the termination depths of 22 m. Here, the raw measured q_c can be compared directly with the corrected total q_t, clearly indicating that the latter is around 35% greater than the uncorrected value. Thus, the importance of using a corrected cone resistance in profiling of soil parameters can be fully appreciated. Also, the effect of a low 12-bit resolution on the data acquisition system results in a stepped reading with depth, rather than a nice smooth profile obtained from a higher 16-bit or 24-bit resolution system.

Penetration Porewater Pressures

The measured porewater pressures (u_m) can be taken at a number of different positions on the penetrometer. Common filter locations include the tip or face (designated u_1) or the shoulder (u_2), and the less common position located behind the sleeve (u_3). Usually, porewater pressures are monitored using a saturated filter element connected through a saturated portal cavity that connects to a pressure transducer housed within the penetrometer. The standard location is the shoulder element (just behind the tip, designated $u_b = u_2$), because of the required correction to total tip stress discussed previously. However, in stiff fissured clays and other geologic formations (e.g., residual soils), zero to negative porewater

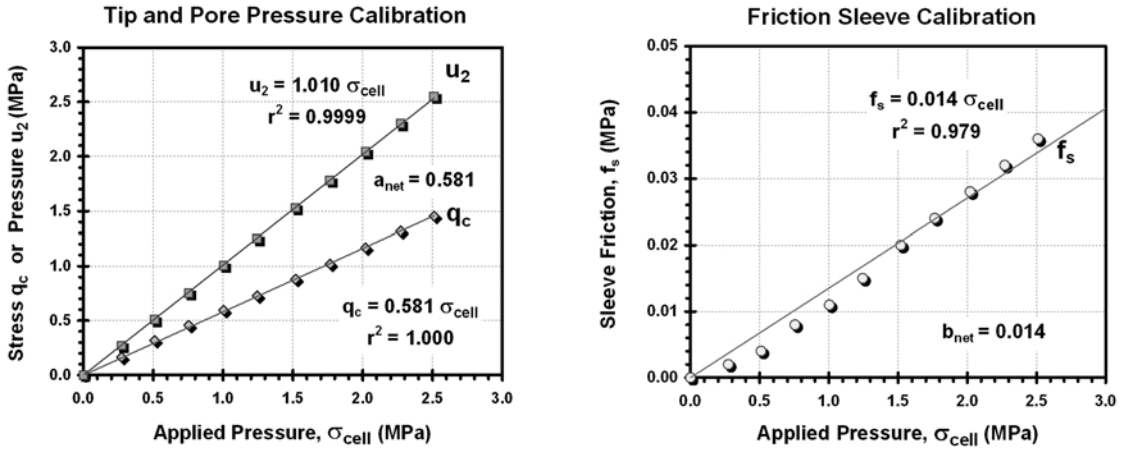

FIGURE 13 Cone calibration results in pressurized triaxial chamber for net area ratio determination.

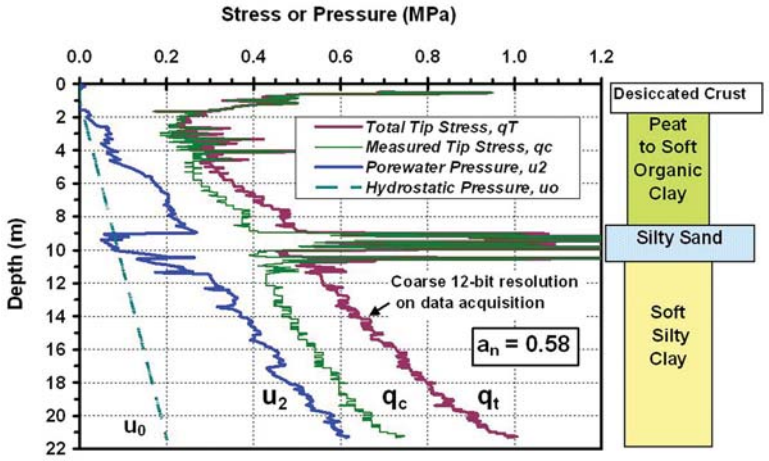

FIGURE 14 Example CPTu sounding showing uncorrected and corrected cone tip resistances.

pressures can be recorded. Therefore, in these cases, superior profiling capability is attained using a face porous element, usually located midface, although some apex versions have been used as well. Most penetrometers measure a single *u*-value, although dual-, triple-, and even quad-element piezocones are also available (e.g., Chen and Mayne 1994).

From the survey, CPTs used on DOT projects generally use a filter element position at the shoulder position (49%), although a good number use a face element (22%), and a fair number employ both u_1 and u_2 readings (11%).

Proper saturation of the filter elements and portal cavities in the penetrometer during assembly is paramount to obtaining good quality penetration porewater pressures. Without due care, the resulting measurements will appear either incorrect or sluggish, not realizing their full magnitude, because of trapped air pockets or gas within the system. Additional remarks on this issue are given in the next chapter.

A series of five CPTus is presented in Figure 15, showing total cone resistance, sleeve friction, and penetration porewater pressure measurements at the shoulder (four soundings) and midface (one sounding). The tests show very good repeatability in the recorded data. The tests were made near the national geotechnical experimentation site at Northwestern University in Evanston, Illinois, where a sandy fill

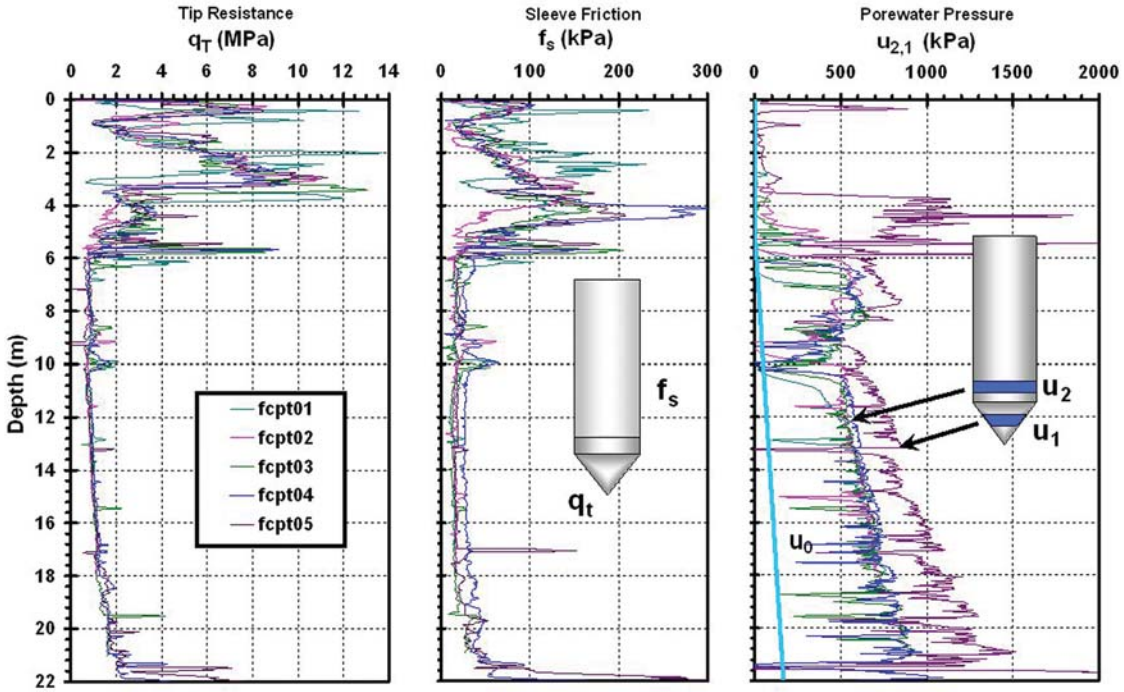

FIGURE 15 Series of piezocone penetration tests at Northwestern University.

layer approximately 4 m thick is underlain by deep deposits of silty clays.

Hydraulic Pushing System

The hydraulic pushing system can consist of a standard drill rig or a dedicated CPT hydraulic system mounted on a truck, track, trailer, all-terrain vehicle, skid arrangement, or portable unit. A full-capacity hydraulic system for CPT work is considered to be on the order of 200 kN (22 tons). A selection of truck-mounted type CPT rigs is shown in Figure 16. For difficult access sites, Figure 17 shows selected track-type and all-terrain rubber-tired vehicles for CPT. The track-mounted systems generally require a second vehicle (tractor trailer) to mobilize the CPT rig, the exception being the special track-truck design shown in Figure 17d.

The dedicated CPT systems push near their centroid of mass and usually rely on deadweight reaction of between 100 to 200 kN (11 to 22 tons) for capacity. A few specialized vehicles have been built with add-on weights to provide up to 350 kN (40 tons) reaction. After being positioned at the desired test location, the rig is usually leveled with hydraulic jacks or "outriggers." There are also many small lightweight CPT systems in the 18 to 50 kN range (2 to 6 tons) that use earth anchoring capabilities to gain capacity. These anchored rigs can obtain significant depths and penetrate rather dense and hard materials, yet are more mobile and portable than the deadweight vehicles (Figure 18).

Typical depths of penetration by CPT rigs depend on the site-specific geologic conditions; however, most commercial systems are set up for up to 30 m (100 ft). In some special cases, onshore CPTs have reached 100 m using direct-push technology from the ground surface. Downhole CPTs can also be conducted step-wise in deep boreholes by alternating off and on with rotary drilling bits, with depths up to 300 m (1,000 ft) or more achievable (e.g., Robertson 1990).

a

b

c

d

FIGURE 16 Selection of truck-mounted cone penetrometer rigs: (*a*) Fugro Geosciences, (*b*) ConeTec Investigations, (*c*) Vertek Type operated by Minnesota DOT, and (*d*) Hogentogler & Company.

a

b

c

d

FIGURE 17 CPT vehicles for difficult access: (*a*) ConeTec track rig, (*b*) remotely operated van den Berg track rig, (*c*) Vertek all-terrain rubber-tired vehicle, and (*d*) Fugro track–truck.

FIGURE 18 Anchored-type CPT rigs: (*left*) GeoProbe Systems, (*center*) Pagani, and (*right*) Hogentogler.

The standard rate of testing is at a constant push of 20 mm/s (0.8 in./s) per ASTM D 5778 and IRTP (1999). The dedicated CPT systems are geared for production testing. In the survey questionnaire, production rates of between 30 m/day to more than 150 m/day (100 to 500 ft/day) were reported by the DOTs, with the majority indicating a typical rate of 60 m/day (200 ft/day). Typical rates of drilling of soil borings by state agencies are between 15 and 30 m/day (50 to 100 ft/day). Therefore, in terms of lineal productivity, CPT is two to five times more efficient than conventional rotary drilling. A disadvantage of the CPT rigs is that their basic abilities include only pushing and pulling the probes. Some limited ability exists for occasional soil sampling, if necessary; however, this is not routine.

The advantages of using standard drill rigs for CPT work include the added capabilities to drill and bore through hard cemented or very dense zones or caprock, if encountered, and then continue the soundings to the desired depths, as well as to obtain soil samples on-site, using the same rig. This reduces costs associated with mobilizing a dedicated CPT truck. Major difficulties with CPTs done using standard drill rigs include: (1) the deadweight reaction is only around 50 kN (5.5 tons); (2) during advancement, rods are pushed from the top, thus an escape slot or special subconnector piece must be provided for the electrical cable, as necessary; (3) during withdrawal, rods must be pulled from the top, thus a subconnector piece must be added and removed for each rod break; and (4) care in manual control of hydraulic pressure must be made to achieve a constant 20 mm/s push rate. In one instance, the DOT damaged the slide base of a CME 850 rig during pushing operation.

Cone Rods

Cone rods consist of 35.7-mm outer diameter hollow steel rods in one-meter lengths with tapered threads. The hydraulic systems of dedicated CPT rigs are usually outfitted with grips (either mechanical- or hydraulic-type) to grasp the sides of the rods during pushing and pulling. If a drill rig is used, a set of standard "A" or "AW" drill rods (or standard cone rods) may be used with a subconnector to convert the metric threads of the penetrometer to the drill rods. A stack of 30 to 40 one-meter-long rods is common (see Figure 19). For hard ground, a larger diameter set of cone rods is also available (d = 44 mm).

A friction reducer is often provided to facilitate pushing operations. The friction reducer is merely an enlarged section of rods (e.g., a ring welded to the outside rod) on the subconnector above the penetrometer that opens the pushed hole to a larger diameter, thereby reducing soil contact on all the upper rods.

Depth Logger

There are several methods to record depth during the advancement of the CPT. Some common systems include depth wheel, displacement transducer [either linear variant displacement transducer (LVDT) or direct current displacement transducer (DCDT)], potentiometer (spooled wire), gear box, ultrasonics sensor, and optical reader. All are available from commercial suppliers and some designs are patented for a particular system. In most cases, a cumulative tracking of each one-meter rod increment is made to determine depth. In other cases, the actual total cable length is monitored. Because each of the channel sensors is technically positioned at slightly different elevations, it is standard practice to correct the readings to a common depth, usually taken at the tip of the penetrometer.

Data Transmission and Cabling

All analog CPT systems and many digital CPT systems use a cable threaded through the rods for transmission of data

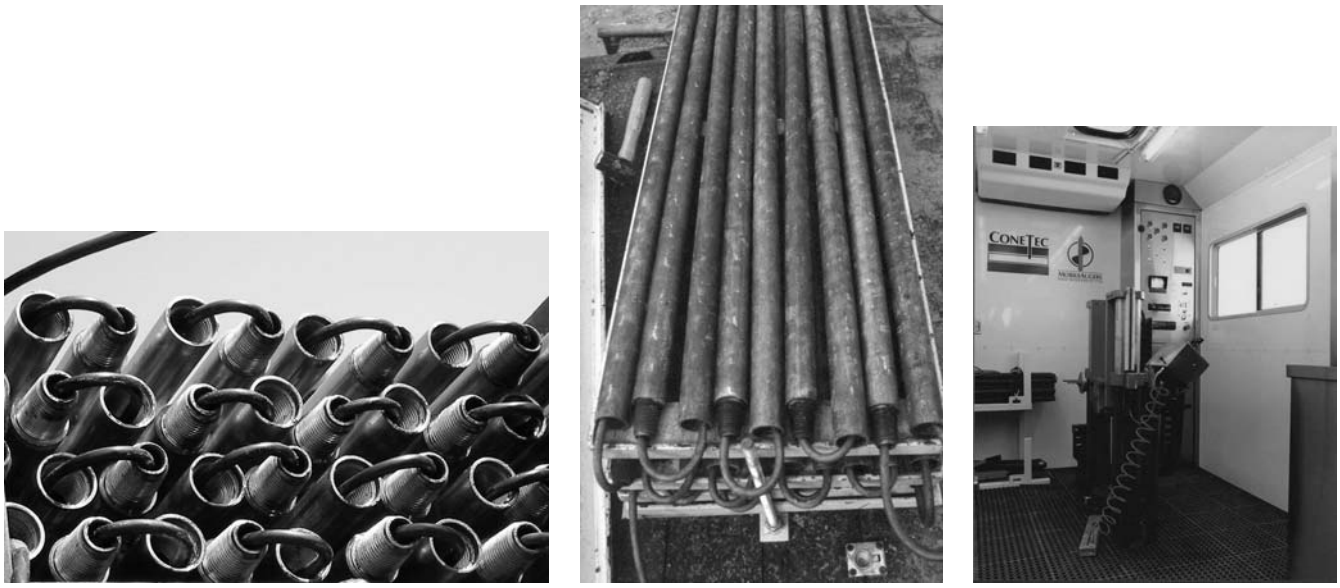

FIGURE 19 Cone rods with threaded electronic cabling and grips with hydraulic rams for pushing.

uphole. The cable is used to provide voltage (or current) to the penetrometer and to transmit data back up to the computer for storage. A power supply is normally used to provide a voltage of between 5 and 20 V, depending on the manufacturer design. In the van den Berg system, in lieu of voltage, electrical current is supplied because the losses over long cable lengths are mitigated. The initial electric CPT systems were analog types that required an external power supply, signal amplifier, and analog–digital converter at the surface. The standard cables were 10-pin type; thus, a maximum of five channels (two wires per channel) could be read. Alternate systems employed 12, 16, 24, and 32 wires; however, at the sacrifice of longevity, because the same outer diameter of the cable had to be maintained to insert it through the hollow center of the cone rods and thus smaller wires internal to the cable were more fragile.

In some of the newest designs, wireless (or cableless) digital CPT systems have been developed. They are particularly favored when CPT is conducted using standard drill rigs and crews (because the cable might easily be damaged) and in offshore site investigations where wireline can deploy the units to great depths. A variety of wireless systems are available based on the following technologies for data transmission or storage: (1) infrared signals conveyed uphole in glass-lined rods; (2) audio-transmitted signals; and (3) data stored in a battery-powered microchip until the penetrometer is retrieved back at the surface. With these infrared and acoustic transmissions, a special receiver is required uphole at the top end of the rods to capture the signals and decode them for digital output.

Data Acquisition Systems

A wide variety of data acquisition systems have been developed for electric CPTs, initially starting with simple pen plotters and analog–digital converters to matrix dot printers, and evolving to fully digital systems with ruggedized notebooks and microchip technologies, with memory within the cone penetrometer itself. An advantage of the older analog systems is that they could be adapted to accommodate any type of commercial cone. The disadvantage of the newer digital systems is that proprietary designs restrict the data coding and channel sequences from the output. Therefore, only a matched set of penetrometer, cable, and data acquisition system can be used.

Geographic Information System and Field Global Positioning System Coordinates

Today, it is quite inexpensive to provide a small hand-held unit that contains a global positioning system (GPS) to give latitude and longitude coordinates. The field record for each CPT sounding should be documented with its GPS location. These coordinates can be entered into a geographic information system (GIS) database for future referencing and archiving of geotechnical information. Currently, the Minnesota DOT (Dasenbrock 2006) and California DOT (Caltrans) (Turner et al. 2006) have both established GIS programs to coordinate and organize statewide sets of soil borings and CPT records.

CHAPTER FOUR

TESTING PROCEDURES AND SOUNDING CLOSURE

In this section, field testing procedures for CPT are reviewed, including calibration, assembly, filter element preparation, baseline readings, pushing, and withdrawal, as well as special testing practices. Procedures for calibrating, maintaining, and preparing the penetrometer and field advancement of CPT are well established through ASTM D 5778, Lunne et al. (1997), International Reference Test Proceedings (1999), and other guidelines. In the retraction of the cone penetrometer and completion of the sounding, however, procedures are quite different and vary across the United States and Canada, depending on hole closure requirements established by the state or province. In many cases, the closure criteria depend on the regional groundwater regime and aquifer characteristics.

CALIBRATION AND MAINTENANCE OF PENETROMETER

The penetrometer requires calibration and maintenance on a regular basis; the frequency of which depends on the amount of use and care taken during storage between soundings. For most CPT operators, it appears that the penetrometers and/or field computers are returned to their respective manufacturers to confirm the equipment is within calibration and tolerances. However, calibrations can be conducted in-house to check for load cell compliance using a compression machine. A sealed and pressurized triaxial apparatus can be used to check for pressure transducer calibrations, as well as the net area ratio (a_n). Full details concerning the calibration of cone and piezocone penetrometers are given elsewhere (e.g., Mulabdić et al. 1990; Chen and Mayne 1994; Lunne et al. 1997).

The tip and sleeve should be replaced if damaged or if excessively worn. For a typical CPT rate of 60 m/day, used 4 days/week, an annual production of 12 000 m/year would likely require tips and sleeves being replaced once to twice per annum. The rate will depend on soils tested, as sands are considerably more abrasive than clays.

FILTER ELEMENTS

The filter elements used for piezocone testing are usually constructed of porous plastic, ceramic, or sintered metal. The plastic versions are common because they are disposable and can be replaced after each sounding to avoid any possible clogging problems particularly those associated with plastic clays. For face elements, a ceramic filter is preferred because it offers better rigidity and is less prone to abrasion when compared with plastic filters. The protocol for environmental soundings recommends that sintered stainless steel filters be used, because polypropylene types are from petroleum-based manufacturer and may cross contaminate readings. Sintered elements are not to be used for face filters however because of smearing problems. The sintered metal and ceramic filters are reusable and can be cleaned using an ultrasonics bath after each sounding.

Saturation of the filter elements should be accomplished using a glycerine bath under vacuum for a period of 24 h. An alternative would be the use of silicone oil as the saturation fluid. It is also possible to use water or a 50–50 mix of glycerine and water; however, those fluids require much more care during cone assemblage. It is normal practice to presaturate 10 to 15 elements overnight for use on the next day's project. The DOT survey indicated that 39% use glycerine, 18% silcone oil, 18% water, and 7% a half–half mix of glycerine and water (Note: 18% responded not applicable).

In the field, the filter elements must be installed so that a continuity of fluid is maintained from the filter face through the ports in the penetrometer and cavity housing the pressure transducer. These ports and cavities must also be fluid-filled at all times. This is best accomplished using a penetrometer having a male plug in the tip section to promote positive fluid displacement when the tip is screwed onto the chassis. The fluid should be 100% glycerine (or silicone oil) that is easily applied using a plastic syringe. Otherwise, if a female plug is provided on the tip unit, the penetrometer must be carefully assembled while submerged in the saturating fluid, usually accomplished with a special cylindrical chamber designed for such purposes. Considerably more effort is expended with this procedure than the aforementioned approach with a positive displacement plug on the tip.

Once assembled, it is common practice to tightly place a prophylactic containing saturation fluid over the front end of the penetrometer. Several rubber bands are used to secure the rubber covering and help maintain the saturated condition. During the initial push into the ground this light rubber membrane will rupture automatically.

In new developments, in lieu of a filter element and saturation procedure, it is possible to use a very thin (0.3 mm)

grease-filled slot to record porewater pressures (Elmgren 1995; Larsson 1995). This avoids problems associated with vacuum presaturation of elements, assembly difficulties in the field, and desaturation of elements in the unsaturated vadose zone, however, at the expense of a more sluggish transducer response and less detailing in the u_m profiling.

BASELINE READINGS

Before each sounding, electronic baselines or "zero readings" of the various channels of the penetrometer are recorded. It is also recommended that a set of baseline readings be secured after the sounding has been completed and the penetrometer withdrawn to the surface. These baselines should be recorded in a field log booklet and checked periodically to forewarn of any mechanical or electronic shifts in their values, as possible damage or calibration errors may occur.

ADVANCING THE PENETROMETER

The standard rate of push for CPT soundings is 20 mm/s, usually applied in one-meter increments (standard cone rod length). With dedicated CPT rigs, the hydraulic system is automatically established to adjust the pressures accordingly to maintain this constant rate. Using a rotary drill rig, however, the driller must be attentive in manually adjusting pressures to seek a rate of approximately 20 mm/s (0.8 in./s). Therefore, in those cases, it would be desirable to measure time as well as depth so that the actual rate can be ascertained.

TESTS AT INTERMITTENT DEPTHS

At each one-meter rod break, there is an opportunity to conduct intermittent testing before the next succession of pushing as the next rod is added. Two common procedures include: (1) dissipation testing, and (2) downhole shear wave velocity measurements.

Porewater Dissipation Tests

Dissipation testing involves the monitoring of porewater pressures as they decay with time. The installation of a full-displacement device such as a cone penetrometer results in the generation of excess porewater pressures (Δu) locally around the axis of perturbation. In clean sands, the Δu will dissipate almost immediately because of the high permeability of sands, whereas in clays and silts of low permeability the measured Δu will require a considerable time to equilibrate. Given sufficient time in all soils, the penetrometer porewater channel will eventually record the ambient hydrostatic condition corresponding to u_0. Thus, the measured porewater pressures (u_m) are a combination of transient and hydrostatic pressures, such that:

$$u_m = \Delta u + u_0 \qquad (2)$$

During the temporary stop for a rod addition at one-meter breaks, the rate at which Δu decays with time can be monitored and used to interpret the coefficient of consolidation and hydraulic conductivity of the soil media. Dissipation readings are normally plotted on log scales; therefore, in clays with low permeability it becomes impractical to wait for full equilibrium that corresponds to $\Delta u = 0$ and $u_m = u_0$. A standard of practice is to record the time to achieve 50% dissipation, designated t_{50}.

Shear Wave Testing

A convenient means to measure the profile of shear wave velocity (V_s) with depth is through the seismic cone penetration test (SCPT). At the one-meter rod breaks, a surface shear wave is generated using a horizontal plank or autoseis unit. The shear wave arrival time can be recorded at the test elevation by incorporating one or more geophones within the penetrometer. The simplest and most common is the use of a single geophone that provides a pseudo-interval downhole V_s (Campanella et al. 1986), as depicted in Figure 20. This approach is sufficient in accuracy as long as the geophone axis is kept parallel to the source alignment (no rotation of rods or cone) and a repeatable shear wave source is generated at each successive one-meter interval.

A more reliable V_s is achieved by true-interval downhole testing; however, this requires two or more geophones at two elevations in the penetrometer [usually 0.5 or 1.0 m vertically apart (1.5 to 3.0 ft)]. Provision of a biaxial arrangement of two geophones at each elevation allows correction for possible cone rod rotation, because the resultant wave can be used ($R_v^2 = x^2 + y^2$). For downhole testing, incorporation of a triaxial geophone with vertical component offers no benefit, because shear waves only have movement in their direction of motion and direction of polarization (only two of three Cartesian coordinate directions). The vertical component could be used in a crosshole test arrangement (e.g., Baldi et al. 1988).

HOLE CLOSURE

After the sounding is completed, a number of possible paths may be followed during or after extraction:

- CPT hole is left open.
- Hole is backfilled using native soils or pea gravel or sand.
- Cavity is grouted during withdrawal using a special "loss tip" or retractable portal.
- After withdrawal, hole is reentered using a separate grouting system.

The need for grouting or sealing of holes is usually established by the state or province, or by local and specific conditions related to the particular project. For instance, for CPTs

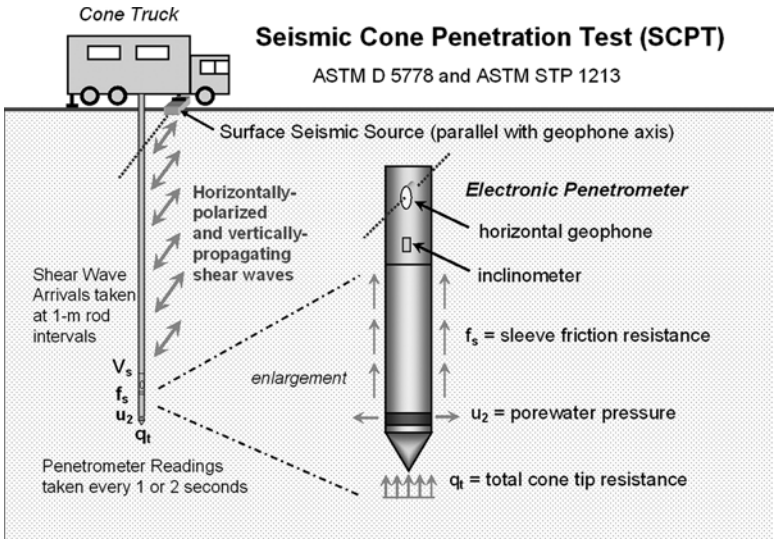

FIGURE 20 Setup and procedure for pseudo-interval seismic cone penetration testing (SCPT).

advanced through asphalt pavements, sealing of the hole would be warranted to prevent water infiltration and/or long-term damage. Most often, the state or province will deem the need or requirement for hole closure by grouting or sealing in specific geologic settings where the groundwater aquifer(s) needs to be protected against vertical cross talk, contamination, or water transmission. The requirement of borehole closure can significantly reduce CPT production rates.

Hole sealing can be accomplished using either a bentonite slurry or a lean grout made from portland cement, gypsum, or a bentonite–cement mix. Pozzolan-based grouts can also be adequate, but they tend to setup more slowly (Lee et al. 1998). The grout or slurry sealants can be placed using surface pour methods, flexible or rigid tremie pipes, or special CPT systems that provide grouting during advancement or during withdrawal, as depicted in Figures 21 and 22. A full discussion of these systems and their advantages and disadvantages is given by Lutenegger and DeGroot (1995) and Lutenegger et al. (1995).

Results of the questionnaire on the subject of CPT hole closure indicated that 43% allow the hole to remain open, 20% backfill with soil, 18% grout during retraction, and 18% grout using a secondary deployment system (e.g., a GeoProbe).

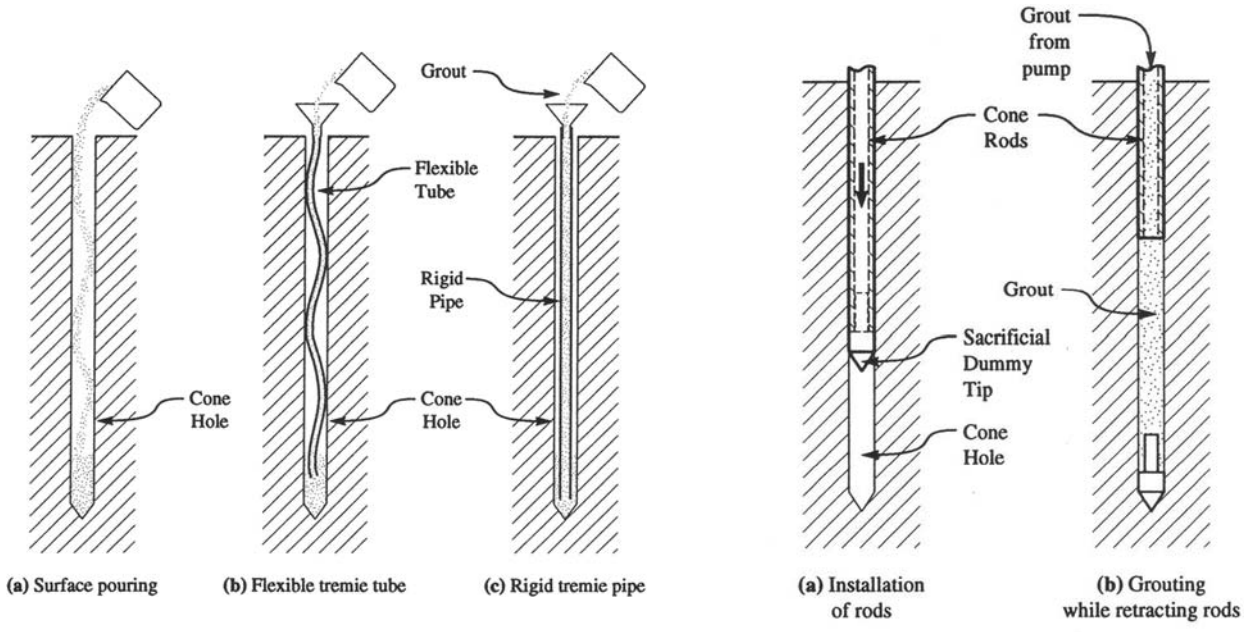

FIGURE 21 Hole closure methods: (*left*) reentry techniques; (*right*) retraction with expendable tip (Lutenegger and DeGroot 1995).

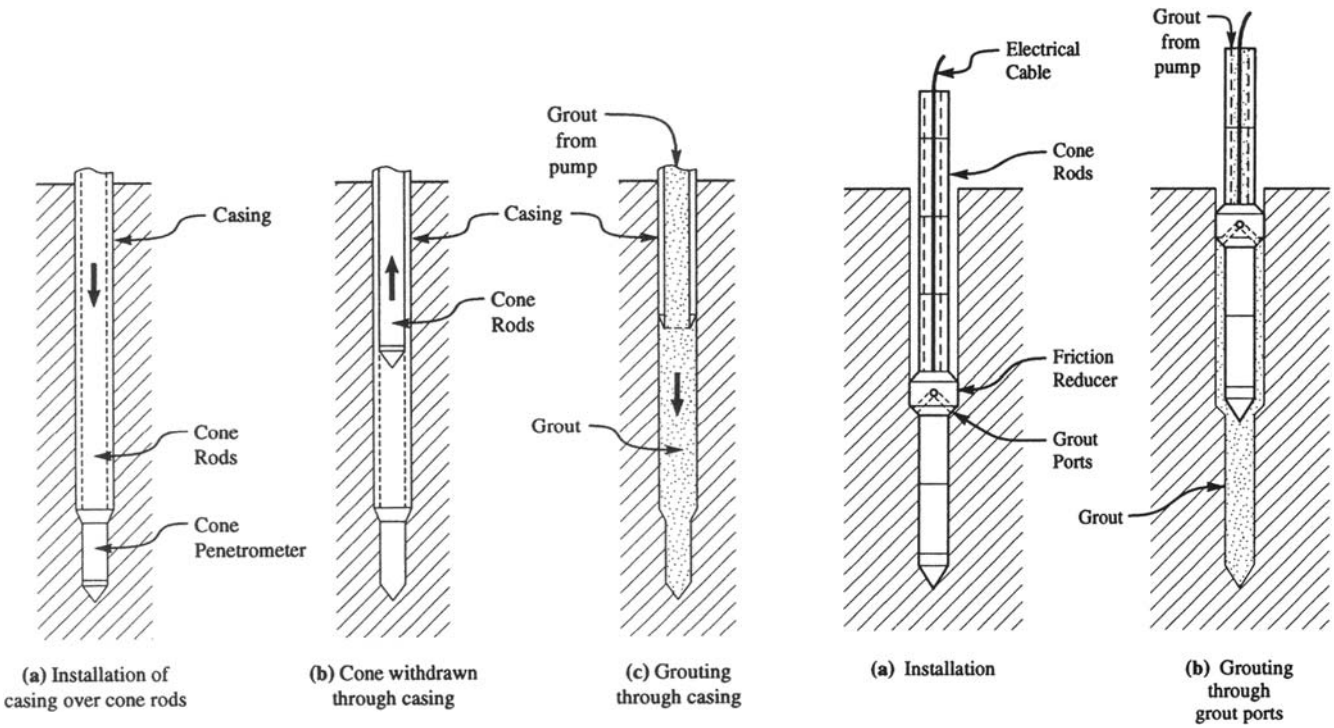

FIGURE 22 Hole closure methods: (*left*) temporary casing; (*right*) grouting through ports in friction reducer (Lutenegger and DeGroot 1995).

CHAPTER FIVE

CONE PENETRATION TESTING DATA PRESENTATION AND GEOSTRATIGRAPHY

In this chapter, the presentation of CPT data for use in detailing subsurface stratigraphic features, soil layering, determination of soil behavioral type, and identification of geomaterials will be presented.

GEOSTRATIGRAPHIC PROFILING

By recording three continuous measurements vertically with depth, the CPT is an excellent tool for profiling strata changes; delineating the interfaces between soil layers; and detecting small lenses, inclusions, and stringers within the ground. The data presentation from a CPT sounding should include the tip, sleeve, and porewater readings plotted with depth in side-by-side graphs, as illustrated by Figure 23. For DOT projects wishing to share CPT information with contractors in bidding documents, perhaps these are the only graphical plots that should be presented, because they represent the raw uninterpreted results.

The total cone tip resistance (q_t) is always preferred over the raw measured value (q_c). For SI units, the depth (z) is presented in meters (m), cone tip stress (q_t) in either kilopascals (1 kPa = 1 kN/m^2) or megapascals (1 MPa = 1000 kN/m^2), and sleeve resistance (f_s) and porewater pressures (u_m) in kPa. For conversion to English units, a simple conversion is: 1 tsf $\approx$ 1 bar = 100 kPa = 0.1 MPa.

If the depth to the water table is known (z_w), it is convenient to show the hydrostatic porewater pressure (u_0) if the groundwater regime is understood to be an unconfined aquifer (no drawdown and no artesian conditions). In that case, the hydrostatic pressure can be calculated from: $u_0 = (z - z_w)\,\gamma_w$, where γ_w = 9.8 kN/m^3 = 62.4 pcf for freshwater; γ_w* = 10.0 kN/m^3 = 64.0 pcf for saltwater. In some CPT presentations, it is common to report the u_m reading in terms of equivalent height of water, calculated as the ratio of the measured porewater pressure divided by the unit weight of water, or $h_w = u_m/\gamma_w$.

SOIL TYPE BY VISUAL INTERPRETATION OF CONE PENETRATION TESTING DATA

Because soil samples are not normally taken during CPT, soil types must be deduced or inferred from the measured readings. In critical cases or uncertain instances, the drilling of an adjacent soil boring with sampling can be warranted to confirm or verify any particular soil classification.

As a general rule of thumb, the magnitudes of CPT measurements fall into the following order: $q_t > f_s$ and $q_t > u_1 > u_2 > u_3$. The measured cone tip stresses in sands are rather high ($q_t > 5$ MPa or 50 tsf), reflecting the prevailing drained strength conditions, whereas measured values in clays are low ($q_t < 5$ MPa or 50 tsf) and indicative of undrained soil response owing to low permeability. Correspondingly, measured porewater pressures depend on the position of the filter element and groundwater level. At test depths above the groundwater table, porewater pressure readings vary with capillarity, moisture, degree of saturation, and other factors and should therefore be considered tentative. Below the water table, for the standard shoulder element, clean saturated sands show penetration porewater pressures often near hydrostatic ($u_2 \approx u_0$), whereas intact clays exhibit values considerably higher than hydrostatic ($u_2 > u_0$). Indeed, the ratio u_2/u_0 increases with clay hardness. For soft intact clays, the ratio may be around $u_2/u_0 \approx 3 \pm$, which increases to about $u_2/u_0 \approx 10 \pm$ for stiff clays, yet as high as 30 or more for very hard clays. However, if the clays are fissured, then zero to negative porewater pressures are observed (e.g., Mayne et al. 1990).

The friction ratio (FR) is defined as the ratio of the sleeve friction to cone tip resistance, designated FR = $R_f = f_s/q_t$, and reported as a percentage. The friction ratio has been used as a simple index to identify soil type. In clean quartz sands to siliceous sands (comparable parts of quartz and feldspar), it is observed that friction ratios are low: $R_f < 1\%$, whereas in clays and clayey silts of low sensitivity, $R_f > 4\%$. However, in soft sensitive to quick clays, the friction ratio can be quite low, approaching zero in many instances.

Returning to Figure 23, a visual examination of the CPTu readings in Steele, Missouri, shows an interpreted soil profile consisting of five basic strata: 0.5 m of sand over desiccated fissured clay silt to 4.5 m, underlain by clean sand to 14 m, soft clay to 24.5 m, ending in a sandy layer.

SOIL BEHAVIORAL CLASSIFICATION

At least 25 different CPT soil classification methods have been developed, including the well-known methods by Begemann (1965), Schmertmann (1978a), and Robertson (1990). Based on the results of the survey, the most popular methods in use by North American DOTs include the

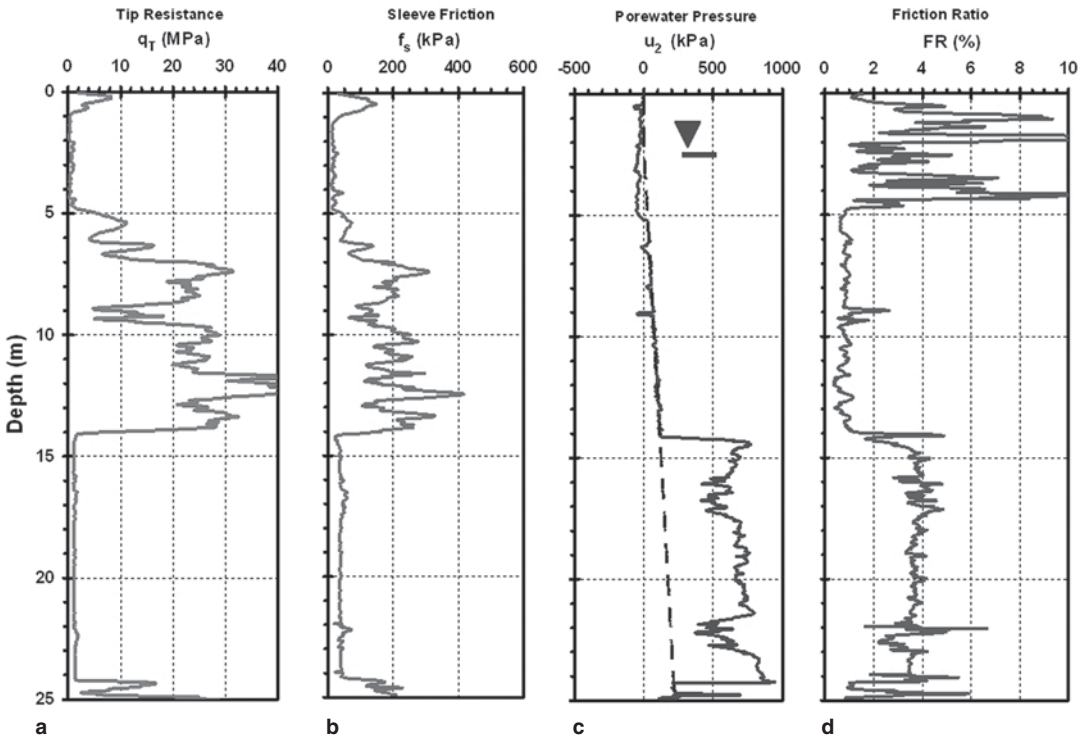

FIGURE 23 Presentation of CPTu results showing (*a*) total cone tip resistance, (*b*) sleeve friction, (*c*) shoulder porewater pressures, and (*d*) friction ratio (FR = $R_f = f_s/q_t$) with depth in Steele, Missouri.

simplified method by Robertson and Campanella (1983) for the electric friction cone, and the charts for all three piezocone readings presented by Robertson et al. (1986) and Robertson (1990).

In the simplified CPT chart method (Robertson and Campanella 1983), the logarithm of cone tip resistance (q_t) is plotted versus FR to delineate five major soil types: sands, silty sands, sandy silts, clayey silts, and clays (see Figure 24).

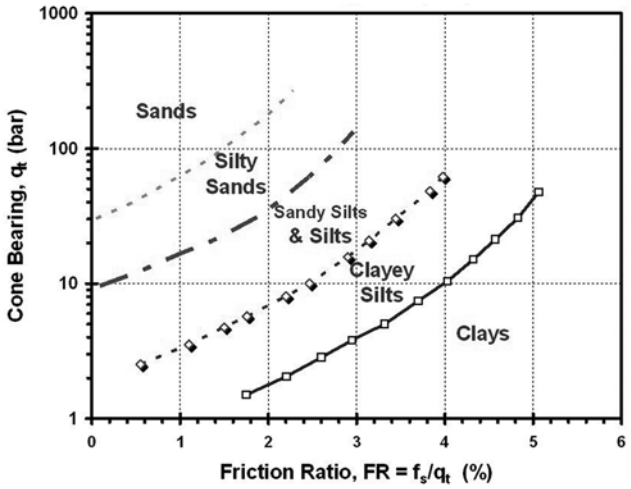

FIGURE 24 Simplified CPT soil type classification chart (after Robertson and Campanella 1983).

The method was expanded to include use of a normalized porewater pressure parameter defined by:

$$B_q = \frac{u_2 - u_0}{q_t - \sigma_{vo}} \tag{3}$$

where σ_{vo} = total vertical overburden stress at the corresponding depth z as the readings. The total overburden at each layer i is obtained from $\sigma_{vo} = \sum(\gamma_{ti}\Delta z_i)$, and effective overburden stress calculated from $\sigma_{vo}' = \sigma_{vo} - u_0$, where u_0 = hydrostatic porewater pressure. Below the groundwater table, as well as for conditions of full capillary rise above the water table, $u_0 = \gamma_w \cdot (z - z_w)$, where z = depth, z_w = depth to groundwater table, and γ_w = unit weight of water. For dry soil above the water table, $u_0 = 0$. Generally, for clean sands, $B_q \approx 0$, whereas in soft to firm intact clays, $B_q \approx 0.6 \pm 0.2$. The soil behavioral type (SBT) represents an apparent response of the soil to cone penetration. The chart in Figure 25 indicates 12 possible SBT zones or soil categories, obtained by plotting log q_t vs. FR with paired sets of log q_t vs. B_q.

The overburden stress and depth influence the measured penetration resistances (Wroth 1988). Therefore, it is more rigorous in the post-processing of CPT data to consider stress normalization schemes for all three of the piezocone readings. In this case, in addition to the aforementioned B_q parameter, it is convenient to define normalized parameters for tip resistance (Q) and friction (F) by:

$$Q = \frac{q_t - \sigma_{vo}}{\sigma_{vo}'} \tag{4}$$

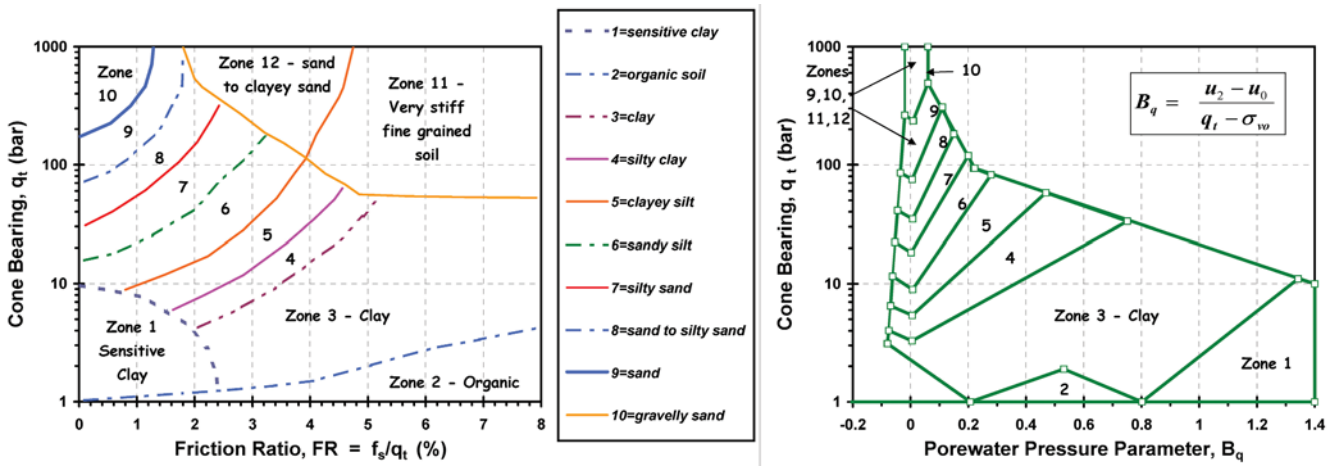

FIGURE 25 CPTu soil behavioral type for layer classification (after Robertson et al. 1986).

$$F = \frac{f_s}{q_t - \sigma_{vo}} \cdot 100 \qquad (5)$$

where $\sigma_{vo}' = \sigma_{vo} - u_0$ = effective vertical overburden stress at the corresponding depth. Using all three normalized parameters (Q, F, and B_q), Robertson (1990) presented a nine-zone SBT chart that may also be found in Lunne et al. (1997). Occasional conflicts arise when using the aforementioned three-part plots, because an SBT may be identified by the Q–F diagram, whereas a different SBT is suggested by the Q–B_q chart.

For general use, Jefferies and Davies (1993) showed that a cone soil classification index ($*I_c$) could be determined from the three normalized CPT parameters (for $B_q < 1$) by:

$$*I_c = \sqrt{\{3 - \log[Q \cdot (1 - B_q)]\}^2 + [1.5 + 1.3 \cdot (\log F)]^2} \qquad (6)$$

The advantage of the calculated $*I_c$ parameter is that it can be used to classify soil types using the general ranges given in Table 2 and easily implemented into a spreadsheet for post-processing results.

Using the SBT approach from Table 1, the CPTu data from Steele, Missouri, is reevaluated in terms of the index I_c to delineate the layering and soil types, as presented in Figure 26. The results are in general agreement with the previously described visual method.

TABLE 2
SOIL BEHAVIOR TYPE OR ZONE NUMBER FROM CPT CLASSIFICATION INDEX, $*I_C$

Soil Classification	Zone No.*	Range of CPT Index $*I_c$ Values
Organic Clay Soils	2	$I_c > 3.22$
Clays	3	$2.82 < I_c < 3.22$
Silt Mixtures	4	$2.54 < I_c < 2.82$
Sand Mixtures	5	$1.90 < I_c < 2.54$
Sands	6	$1.25 < I_c < 1.90$
Gravelly Sands	7	$I_c < 1.25$

After Jefferies and Davies (1993).
*Notes: Zone number per Robertson SBT (1990). Zone 1 is for soft sensitive soils having similar I_c values to Zones 2 or 3, as well as low friction $F < 1\%$.

Alternate CPT stress-normalization procedures have been proposed for the cone readings (e.g., Kulhawy and Mayne 1990; Jamiolkowski et al. 2001). For example, in clean sands, the stress-normalized tip resistance is often presented in the following format:

$$q_{t1} = (q_t/\sigma_{atm})/(\sigma_{vo}'/\sigma_{atm})^{0.5} = q_t/(\sigma_{vo}' \cdot \sigma_{atm})^{0.5} \qquad (7)$$

where σ_{atm} = 1 atm = 1 bar = 100 kPa ≈ 1 tsf ≈ 14.7 psi. Additionally, the normalized side friction can be expressed as $F' = f_s/\sigma_{vo}'$, and normalized penetration porewater pressure given by $U' = \Delta u/\sigma_{vo}'$. The latter offers the simplicity that soil types can be simply evaluated by: $U' < 1$ (sand); $U' > 3$ (clay). A similar relationship based on B_q readings can be adopted: $B_q < 0.1$ (sand); $B_q > 0.3$ (clay). Values in between these limits are indicative either of mixed sand-clay soils or silty materials, or else highly interbedded lenses and layers of clays and sands.

Other alternative and more elaborate stress-normalization procedures for the CPT have been proposed as well (e.g., Olsen and Mitchell 1995; Boulanger and Idriss 2004; Moss et al. 2006), but are beyond full discussion here.

In a recent and novel approach to indirect soil classification by CPT, a probabilistic method of assessing percentages of clay, silt, and sand has been developed by Zhang and Tumay (1999). The method is termed "P-Class" and uses the cone tip resistance and sleeve friction to evaluate probability of soil type. It is fully automated by computer software and available as a free download from the Louisiana Transportation Research Center (LTRC) website (http://www.coe/su.edu/cpt/). Using the same CPT sounding presented in Figures 23 and 26, the P-Class approach has been applied to determine the probability distributions of sand, silt, and clay fractions with depth, as shown in Figure 27 with good results.

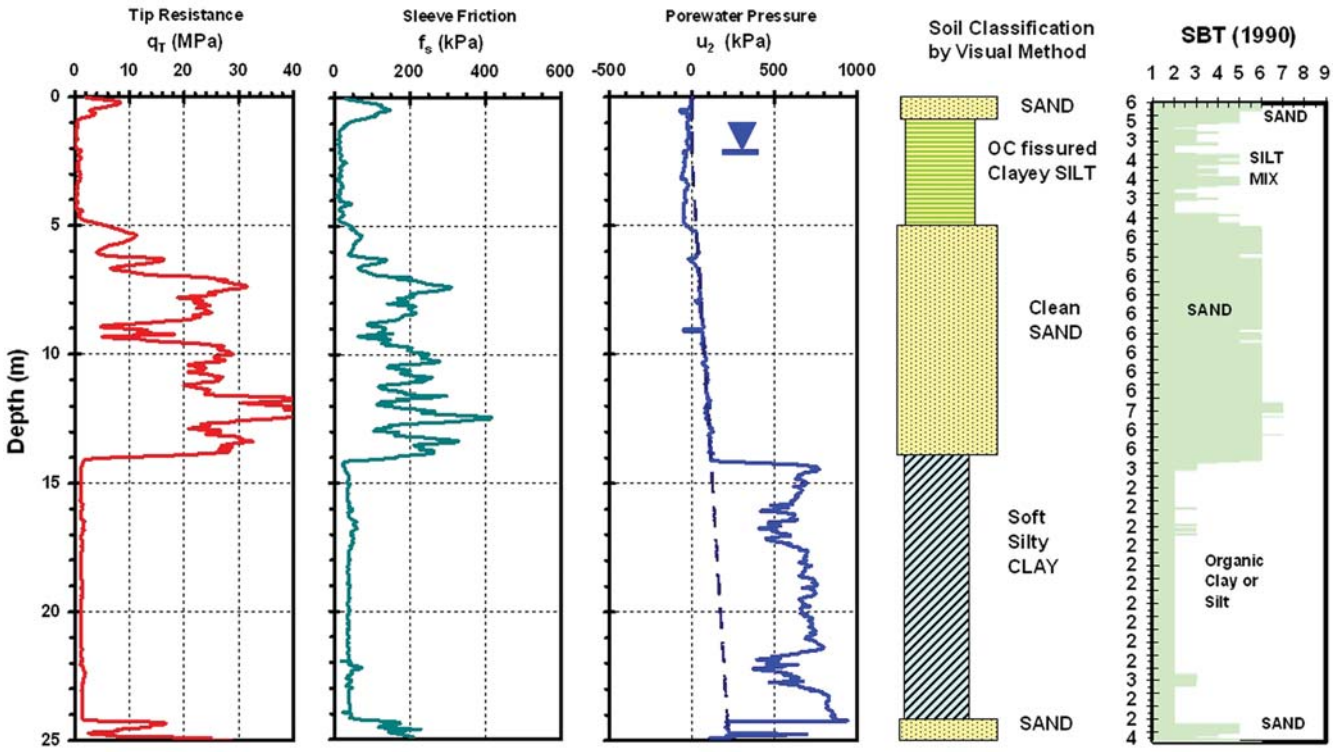

FIGURE 26 CPTu results from Steele, Missouri, evaluated by index I_c for soil behavioral type.

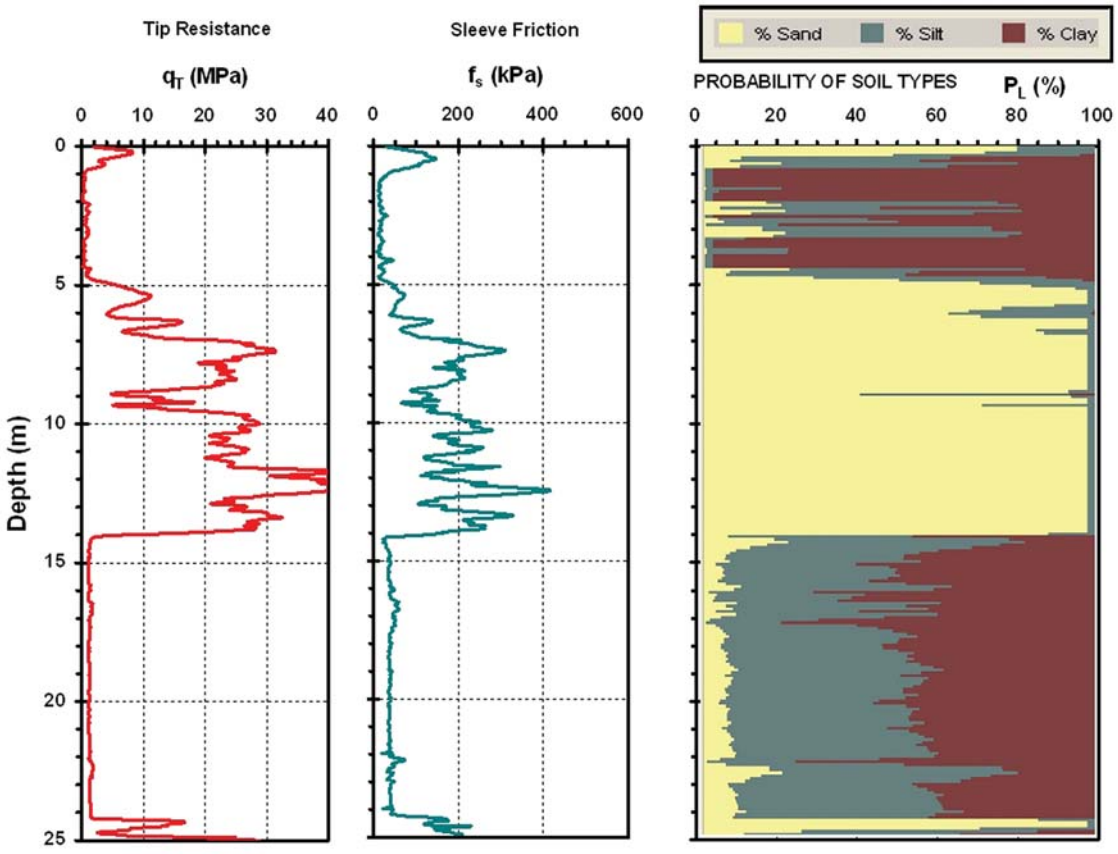

FIGURE 27 Application of probability method for soil type to Missouri CPT sounding.

CHAPTER SIX

SOIL PARAMETER EVALUATIONS

Soils are very complex materials because they can be comprised of a wide and diverse assemblage of different particle sizes, mineralogies, packing arrangements, and fabric. Moreover, they can be created from various geologic origins (marine, lacustrine, glacial, residual, aeolian, deltaic, alluvial, estuarine, fluvial, biochemical, etc.) that have undergone long periods of environmental, seasonal, hydrological, and thermal processes. These facets have imparted complexities of soil behavior that relate to their initial geostatic stress state, natural prestressing, nonlinear stress–strain–strength response, and drainage and flow characteristics, as well as rheological and time–rate effects. As such, a rather large number of different geotechnical parameters have been identified to quantify soil behavior in engineering terms. These include state parameters such as void ratio (e_0), unit weight (γ), porosity (n), relative density (D_R), overconsolidation ratio (OCR), strength parameters (c', ϕ', $c_u = s_u$), stiffness (E', E_u, $G_{\max}$, G', D', K'), compressibility (σ_p', C_r, C_c, C_s), consolidation coefficient (c_{vh}), permeability (k), creep (C_{ae}), subgrade reaction coefficient (k_s), spring constants (k_z), lateral stress parameters (K_A, K_0, K_P), Poisson's ratio (ν', ν_u), dilatancy angle (ψ), strain rate parameters (α), and more.

In this section, the evaluation of select geotechnical parameters from CPT data is addressed, including various post-processing approaches based on theoretical, numerical, analytical, and empirical methods. In the survey results, DOT geotechnical engineers have indicated that CPT results are currently being used to assess several soil parameters that relate to highway design and construction.

Selected relationships utilized in the data reduction of the cone, piezocone, and seismic cone tests are presented in the subsequent subsections. As with conventional practice, soils are grouped into either *clays* or *sands*, in particular referring to "vanilla" clays and "hourglass" sands. That is, the correlations can be expected to apply to "well-behaved" soils of common mineralogies (i.e., kaolin, quartz, feldspar) and typical geologic origins (e.g., marine and alluvial). It can be noted that alternative evaluations of soil properties and parameters are available and that a spreadsheet format best allows for "tuning" and site-specific correlations for particular geologic settings and soil materials. The procedures chosen herein represent a selection of methods based on the author's understanding and experiences in United States and Canadian practices. A number of nontextbook geomaterials can be found throughout North America (e.g., loess, cemented soils, carbonate sands, sensitive structured clays, residual and tropical soils, glacial till, dispersive clays, and collapsible soils) that will undoubtedly not fall within the domain and applicability of these relationships. For those materials, it is suggested that site-specific calibration, testing, and validation be performed by a research institution working with the state DOT. Some guidelines and methods in assessing nontextbook geomaterials are given by Lunne et al. (1996), Coutinho et al. (2004), Schnaid et al. (2004), and Schnaid (2005).

It may be noted that no uniform and consistent methodology currently exists to interpret all necessary soil engineering parameters within a common framework. For specific concerns in the interpretation of CPT data, various parameters have been derived from analyses based in limit equilibrium, plasticity, elasticity, cavity expansion, strain path, stress path, finite elements, discrete elements, finite differences, and dislocation-based theories. At this time, the subsequently noted procedures are based largely on mixed theories tempered with experience and available calibrations with laboratory test results and/or backcalculated values from full-scale load tests and performance monitoring.

SHEAR WAVE VELOCITY

Shear wave velocity (V_s) is a fundamental measurement in all civil engineering solids (steel, concrete, wood, fiberglass, soils, and rocks). V_s can be obtained for all types of geomaterials, including clays, silts, sands, gravels, and fractured and intact rocks, as well as mine tailings and fills. The values of V_s can be readily determined by laboratory tests, including resonant column, ultrasonics, bender elements, torsional shear, and special triaxial apparatuses (Woods 1978) and by a variety of different field geophysical tests, including crosshole, downhole, suspension logging, spectral analysis of surface waves, refraction, and reflection (Campanella 1994).

As noted earlier, the incorporation of one or more geophones within the penetrometer facilitates the conduct of SCPT. This is a version of the downhole geophysics test and may be conducted either by pseudo-interval or true-interval methods, depending on the equipment available, care taken in execution of the test, and degree of reliability needed in the assessed V_s profile. It is best practice to measure the V_s by

direct methods such as the downhole geophysics test and SCPT. However, in some instances, it may be necessary to estimate the V_s profile by means of an empirical correlation if a seismic penetrometer is not available. Also, the correlative relationships may be employed to check on the reasonableness of V_s readings obtained by SCPT and/or identify unusual geomaterials that may fall into the category of unusual or nontextbook type soils (Lunne et al. 1997; Schnaid 2005).

For uncemented, unaged quartzitic sands, Baldi et al. (1989) suggested that V_s may be evaluated from the following relationship:

$$Sands: V_s = 277\ (q_t)^{0.13}\ (\sigma_{vo}')^{0.27} \quad (8)$$

where V_s = shear wave velocity (m/s), q_t = corrected cone tip resistance (MPa), and σ_{vo}' = effective overburden stress (MPa), as shown in Figure 28 (*upper*). For clay soils, Figure 28 (*lower*) shows a generalized interrelationship between shear wave and cone tip resistance for soft to firm to stiff intact clays to fissured clay materials (Mayne and Rix 1995) that determined:

$$Clays: V_s = 1.75\ (q_t)^{0.627} \quad (9)$$

In addition to measured tip resistance (q_t in kPa), the correlative relationship was significantly improved for intact clays if the in-place void ratio (e_0) was also known.

Of particular interest are interpretative methods that accommodate all types of soils. In one approach, an estimate of the in situ V_s can be made from (Hegazy and Mayne 1995):

$$All\ Soils: V_s\ (\text{m/s}) = [10.1 \cdot \log q_t - 11.4]^{1.67}\ [f_s/q_t \cdot 100]^{0.3} \quad (10)$$

where q_t = tip resistance and f_s = sleeve resistance are input in units of kPa. The relationship was derived from a database that included sands, silts, and clays, as well as mixed soil types, and thus is interesting in that it attempts to be global and not a soil-dependent relationship. Another database from well-documented experimental sites in saturated clays, silts, and sands showed that V_s relates directly to the sleeve friction f_s, reported in units of kPa (Mayne 2006b):

$$V_s = 118.8 \log (f_s) + 18.5 \quad (11)$$

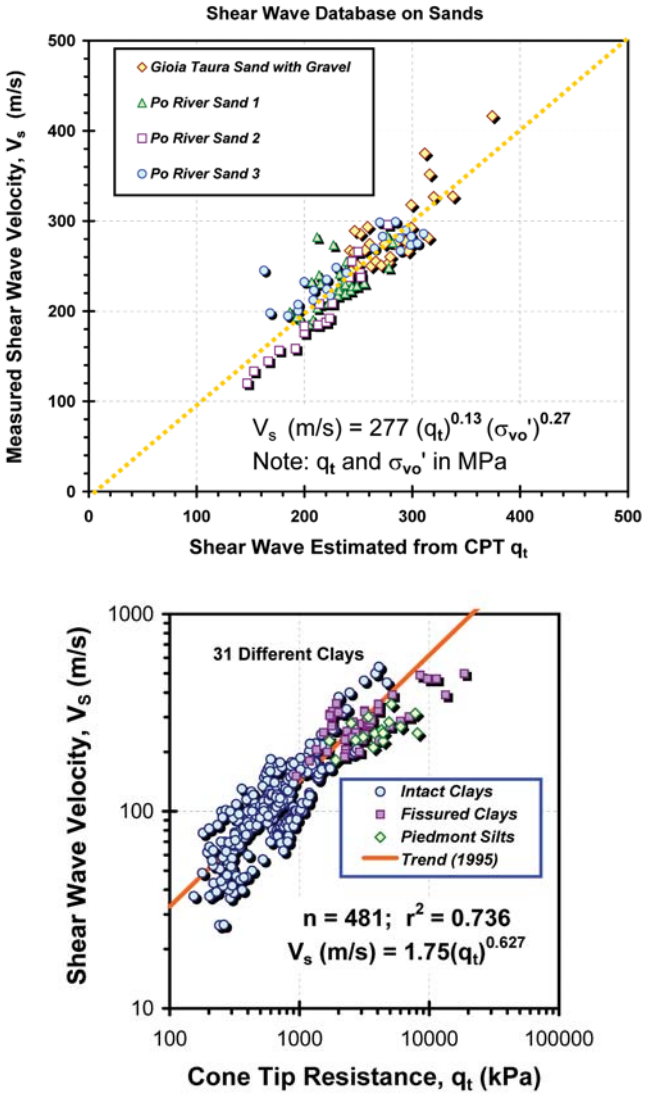

FIGURE 28 Shear wave velocity estimate from CPT data in (*upper*) clean quartz sands (after Baldi et al. 1989), and (*lower*) clay soils (after Mayne and Rix 1995).

UNIT WEIGHT

The saturated unit weight of each of the soil layers is needed in the calculation of overburden stress and in the other calculations. The unit weight is best achieved by obtaining undisturbed, thin-walled tube samples from borings. However, in many soils, undisturbed samples are difficult to obtain, particularly clean sands, cohesionless silts, and gravels. Moreover, during CPT, samples are not routinely obtained; therefore, indirect methods for assessing unit weight are desirable. Based on the survey, nearly 40% of DOTs assume the unit weight (Appendix A, Question 35). Another 15% use an estimate based on the 12-part SBT classification, as discussed by Lunne et al. (1997).

An alternative approach uses results from large-scale calibration chamber tests to evaluate the dry unit weight (γ_d) of sands from normalized cone tip resistance (q_{t1}) given by Eq. 7 (chapter 5). The trend is presented in Figure 29. A regression line is given for uncemented unaged quartz to siliceous sands that has only a rather modest coefficient of determination ($r^2 = 0.488$). Also shown are calibration chamber test data for four different carbonate sands (calcareous type), clearly showing that the relationship

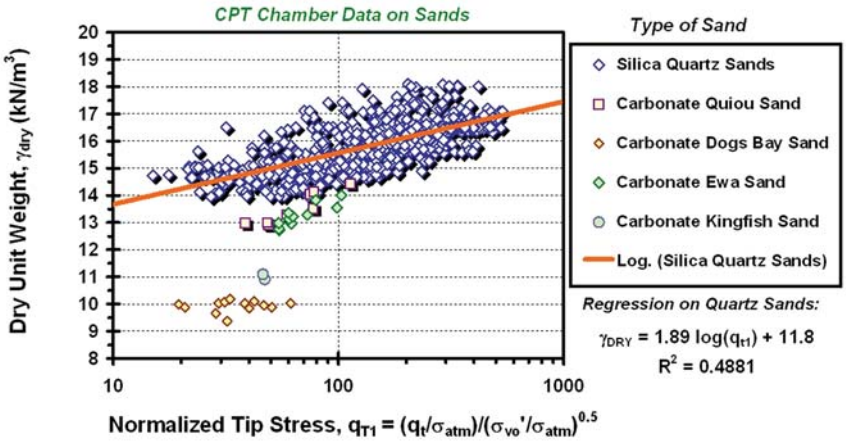

FIGURE 29 Dry unit weight relationship with shear wave velocity and depth.

should be used with caution in sands and that mineralogy and cementation can be important facets of geomaterials.

For saturated soils, the correlation in Figure 30 is based on a large data set of soils, including soft to stiff clays and silts, loose to dense sands and gravels, as well as mixed geomaterials ($n = 727$; $r^2 = 0.808$). For these, the saturated total unit weight depends on both V_s (m/s) and depth z (meters). Also shown for comparative purposes (but not included in the regression) are data from intact rocks whereby a maximum unit weight ($\gamma_{rock} = 26$ kN/m^3) and maximum shear wave velocity ($V_s = 3300$ m/s) can be taken as limiting values. A set of alternate expressions for the dry and saturated unit weights is available in terms of V_s and σ_{vo}' (Mayne 2006b).

By adopting a characteristic specific gravity of solids (G_s), the total unit weight of saturated soils can be directly estimated from CPT f_s (kPa), as presented in Figure 31. In general, the evaluation appears good for soft to stiff clays of marine origin, fissured clays, silts, and a variety of clean quartz sands. Note the effect of specific gravity in affecting the relationship for higher unit weights in the soft freshwater glacial lake clays at the Northwestern University site, as well as the lower unit weights for soft lacustrine clay of Mexico City.

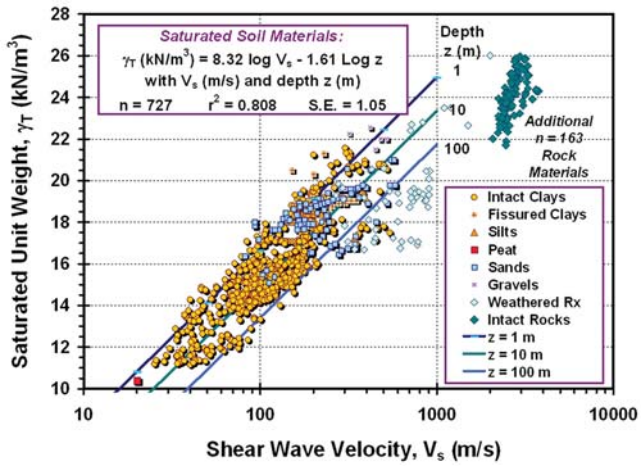

FIGURE 30 Saturated soil unit weight evaluation from shear wave velocity and depth.

POISSON'S RATIO

The value of Poisson's ratio (ν) is normally taken for an isotropic elastic material. Based on recent local strain measurements on samples with special internal high-resolution instrumentation (e.g., Burland 1989; Tatsuoka and Shibuya 1992; Lehane and Cosgrove 2000), the value of drained ν' ranges from 0.1 to 0.2 for all types of geomaterials at working load levels, increasing to larger values as failure states are approached. The value for undrained loading is $\nu_u = 0.5$.

SMALL-STRAIN SHEAR MODULUS

Soils are commonly associated with shearing during loading modes, deformations, and failure, and thus are best represented in terms of their stress–strain–strength behavior in terms of simple shear. The slope of a shear stress (τ) versus shear strain (γ_s) curve is the shear modulus (G). The small-strain shear modulus (termed G_0, or G_{max}), also known as the initial tangent dynamic shear modulus (G_{dyn}), is a fundamental stiffness that relates to the initial state of the soil. This stiffness applies to the initial loading for all stress–strain–strength curves, including static, cyclic, and dynamic types of loading, as well as undrained and drained conditions (Burland 1989; Mayne 2001; Leroueil and Hight 2003). The small-strain shear modulus is calculated from the total soil mass density ($\rho_T = \gamma_T/g$) and shear wave velocity (V_s), where $g = 9.8$ m/s^2 = gravitational acceleration constant:

$$G_{max} = \rho_T V_s^2 \qquad (12)$$

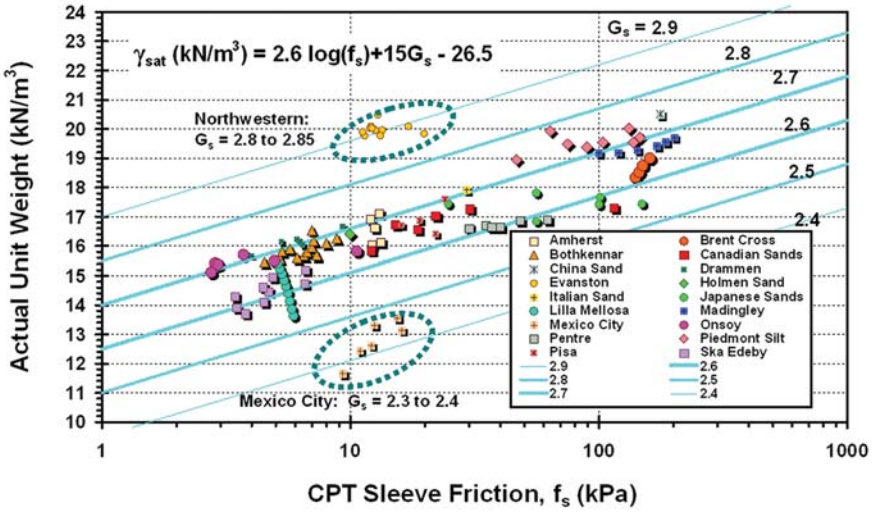

FIGURE 31 Saturated unit weight evaluation from CPT sleeve friction reading and specific gravity of solids.

In lieu of shear modulus, the stiffness can be expressed in terms of an equivalent Young's modulus of soil through elastic theory:

$$E_{max} = 2G_{max}\,(1 + \nu) \tag{13}$$

where $\nu' = 0.2$ applies for drained and $\nu_u = 0.5$ for undrained conditions.

SOIL STIFFNESS

The value of small-strain shear modulus, G_{max} (and corresponding E_{max}), applies strictly to the nondestructive range of strains, where $\gamma_s < 10^{-4}$ as a decimal (or $\gamma_s < 10^{-6}\%$). For loading levels at strains higher than these, modulus reduction curves ($G/G_{max} = G/G_0$) must be implemented. For cyclic loading and dynamic problems in geotechnical engineering, Vucetic and Dobry (1991) present G/G_{max} curves in terms of soil plasticity and shear strain (γ_s). The appropriate value of shear modulus is then obtained from:

$$G = G_{max} \cdot (G/G_{max}) \tag{14}$$

The G/G_{max} curves can be presented in terms of a logarithm of shear strain (γ_s), as discussed by Jardine et al. (1986, 2005a) and Atkinson (2000), or alternatively in terms of mobilized shear stress (τ/τ_{max}), as discussed by Tatsuoka and Shibuya (1992), Fahey and Carter (1993), and LoPresti et al. (1998). The mobilized shear stress is analogous to the reciprocal of the factor of safety ($\tau/\tau_{max} = 1/FS$). In terms of fitting stress-strain data, G/G_{max} versus mobilized stress level (τ/τ_{max}), plots are visually biased toward the intermediate- to large-strain regions of the soil response. In contrast, G/G_{max} versus log γ_s curves tend to accentuate the small- to intermediate-strain range. The ratio (G/G_{max}) is a reduction factor to apply to the maximum shear modulus, depending on current loading conditions.

A selection of modulus reduction curves, represented by the ratio (G/G_{max}), has been collected from monotonic laboratory shear tests performed on an assorted mix of clayey and sandy materials (Mayne 2006b). The results are presented in Figure 32 (*upper*), where $G = \tau/\gamma_s$ = secant shear modulus. These laboratory tests include static torsional shear and special triaxial tests with internal local-strain measurements. An assumed constant value of ν has been applied with the conversion $E = 2G(1 + \nu)$ to permit plotting of E/E_{max} versus q/q_{max}, where $q = (\sigma_1 - \sigma_3)$ = deviator stress. Undrained tests are shown by solid dots and drained tests are indicated by open symbols. In general, the clays were tested under undrained loading (except Pisa), and the sands were tested under drained shearing conditions (except Kentucky clayey sand). Similar trends for the various curves are noted for both undrained and drained tests on both clays and sands.

The nonlinear representation of the stiffness has been a major focus of the recent series of conferences on the common theme: Deformation Characteristics of Geomaterials (e.g., Jardine et al. 2005a). A number of different mathematical expressions can be adopted to produce closed-form stress–strain–strength curves (e.g., LoPresti et al. 1998). One rather simple algorithm involves a modified hyperbola (Fahey and Carter 1993; Fahey 1998) with presented results for modulus reduction (G/G_{max}) versus mobilized stress ($\tau/\tau_{max} = 1/FS$) shown in Figure 32 (*lower*). It can be seen that a limited range of the exponent ($0.2 < g < 0.4$) tends to encompass many of the laboratory torsional shear and triaxial compression data. The modulus reduction can be given by:

$$G/G_{max} = 1 - (\tau/\tau_{max})^g \tag{15}$$

with $g \approx 0.3 \pm 0.1$ for "well-behaved" soils (uncemented, insensitive, not highly structured).

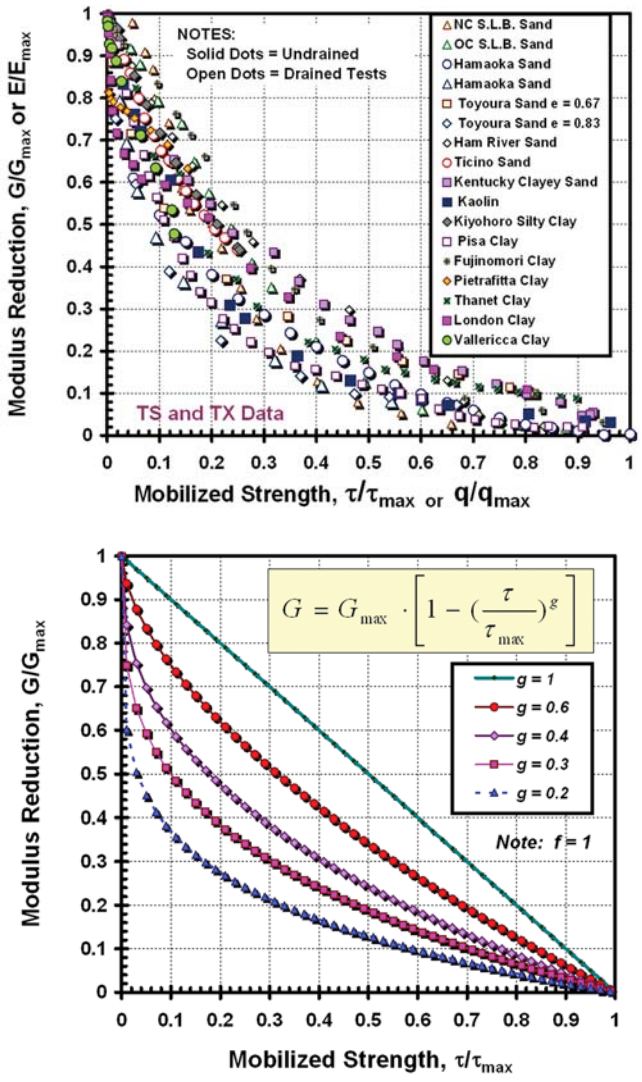

FIGURE 32 Monotonic modulus reduction curves from (*upper*) static torsional and triaxial shear data on clays and sands, and (*lower*) using modified hyperbolic expression proposed by Fahey and Carter (1993).

An equivalent stiffness of soils is also afforded by means of the constrained modulus (D') obtained from one-dimensional consolidation tests. In lieu of e-logσ_v' graphs developed from consolidation tests, the data may be plotted in terms of vertical stress versus vertical strain and the tangent slope is defined as the constrained modulus $D' = \Delta\sigma_v'/\Delta\varepsilon_v$, where $\Delta\varepsilon_v = \Delta e/(1 + e_0)$. From elastic theory, the constrained modulus relates to the equivalent elastic Young's modulus (E') and shear modulus (G') for drained loading conditions:

$$D' = E' \cdot \frac{(1-\nu')}{(1+\nu')(1-2\nu')} = \frac{2G(1-\nu')}{(1-2\nu')} \qquad (16)$$

For foundation settlement analyses, a representative constrained modulus of the supporting soil medium is usually sought. In practice, it has been usual to correlate the modulus D' to a penetration resistance (e.g., Mitchell and Gardner 1975; Schmertmann 1978b; Jamiolkowski et al. 1985). From a collection of diverse geomaterials ranging from sands, silts, intact organic and inorganic clays, and fissured soils (Mayne 2006), Figure 33 (*upper*) shows that a relationship for "well-behaved" soils might take the form:

$$D' \approx \alpha_C' \cdot (q_t - \sigma_{vo}) \qquad (17)$$

with an overall representative value of $\alpha_C' \approx 5$ for soft to firm vanilla clays and normally consolidated (NC) hourglass sands. However, for organic plastic clays of Sweden, a considerably lower $\alpha_C' \approx 1$ to 2 may be appropriate. For cemented (Fucino) clay, a value $\alpha_C' \approx 10$ to 20 may be more appropriate.

With SCPT data, an alternate correlation can be sought between D' and small-strain shear modulus (G_{max}), as presented in Figure 33 (*lower*). In this case, a similar adopted format could be (Burns and Mayne 2002):

$$D' \approx \alpha_G' \cdot G_{max} \qquad (18)$$

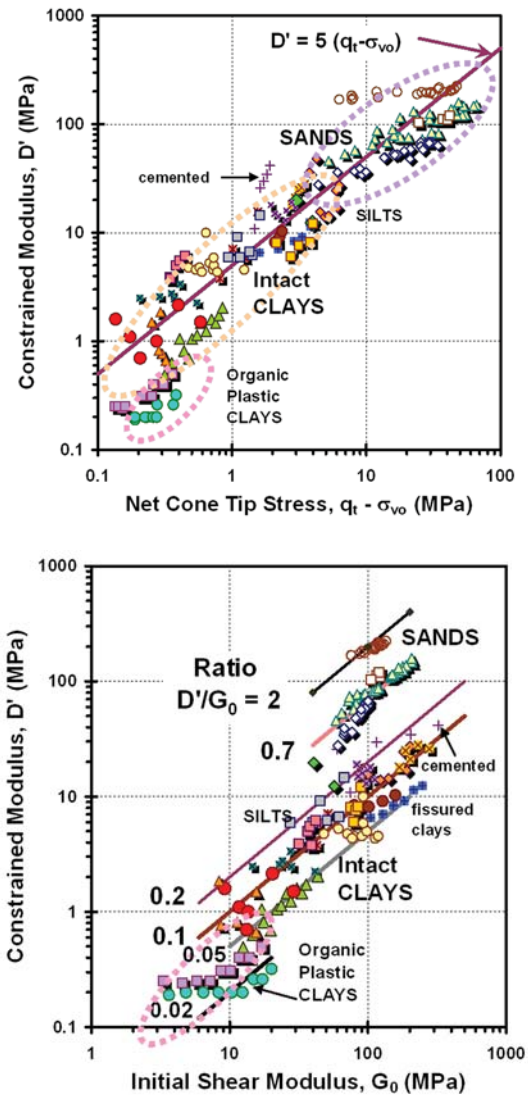

FIGURE 33 Trends between constrained modulus and (*upper*) net cone resistance, and (*lower*) small-strain shear modulus of various and diverse soils.

with assigned values of α_G' ranging from 0.02 for the organic plastic clays up to 2 for overconsolidated quartz sands. In the future, additional studies with multiple regression, artificial neural networks, and numerical modeling may help guide the development of more universally applied global relationships.

STRESS HISTORY

Clays

The stress history of clay soils is classically determined from one-dimensional oedometer tests on high-quality undisturbed samples. The yield point in one-dimensional loading (i.e., consolidation test) denotes the preconsolidation stress (σ_p'), formerly designated σ_{vmax}' or P_c'. In normalized form, the degree of preconsolidation is termed the overconsolidation ratio, OCR = (σ_p'/σ_{vo}'). For intact clays, a first-order estimate of the preconsolidation stress can be obtained from the net cone tip resistance (Mayne 1995; Demers and Leroueil 2002), as shown in Figure 34:

$$\sigma_p' = 0.33\ (q_t - \sigma_{vo}) \tag{19}$$

It can be seen that this expression underestimates values for fissured clays. This is because the macrofabric of cracks and fractures affect the field measurements of the CPT as the blocks of clay are forced away from the axis of penetration. In contrast, any fissures or cracks within the small laboratory oedometric specimens are closed up during constrained compression in one-dimensional loading.

An example of the profiling of preconsolidation stress with depth by cone penetrometer data is illustrated in Figure 35 using results from the national experimental test site at Bothkennar in the United Kingdom (Nash et al. 1992). Extensive geological, laboratory, and in situ field tests have been conducted in the soft clays having thicknesses up to 30 m and a shallow groundwater table of 0.5 to 1.0 m below grade. Using a variety of different sampling techniques, a reference profile of σ_p' has been established from consolidation tests using three laboratory devices at different universities: (1) incremental loading oedometers, (2) constant rate of strain consolidometers, and (3) restricted flow tests. The first-order evaluation from net cone resistance is shown to be in good agreement with the laboratory results.

With piezocone testing, a separate and independent assessment of σ_p' in intact clays can be made from the porewater pressure measurements, as shown in Figure 36. Notably, data for fissured clays lie above the trends. The first-order relationships for intact clays can be expressed as (Chen and Mayne 1996):

$$\textit{Midface Filter Element}: \sigma_p' = 0.40\ (u_1 - u_0) \tag{20}$$

$$\textit{Shoulder Filter Element}: \sigma_p' = 0.53\ (u_2 - u_0) \tag{21}$$

As indicated by Figure 36, a slight additional trend with plasticity index (PI, or I_P) was determined from the database using multiple regression analyses. For Type 1 piezocones, the penetration porewater pressures are positive for all clay consistencies, ranging from soft to hard intact clays to fissured deposits. For Type 2 piezocones, the trend is similar for soft to firm to stiff intact clays; however, for overconsolidated fissured clays the porewater pressures can be negative, thus providing a nonunique relationship.

From a theoretical perspective, the value of preconsolidation stress can also be ascertained from the effective cone tip resistance (Mayne 2005):

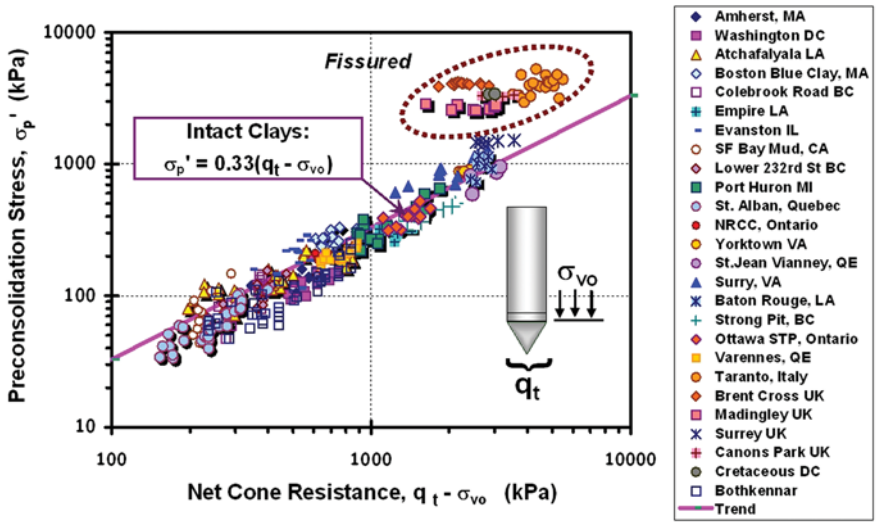

FIGURE 34 First-order relationship for preconsolidation stress from net cone resistance in clays.

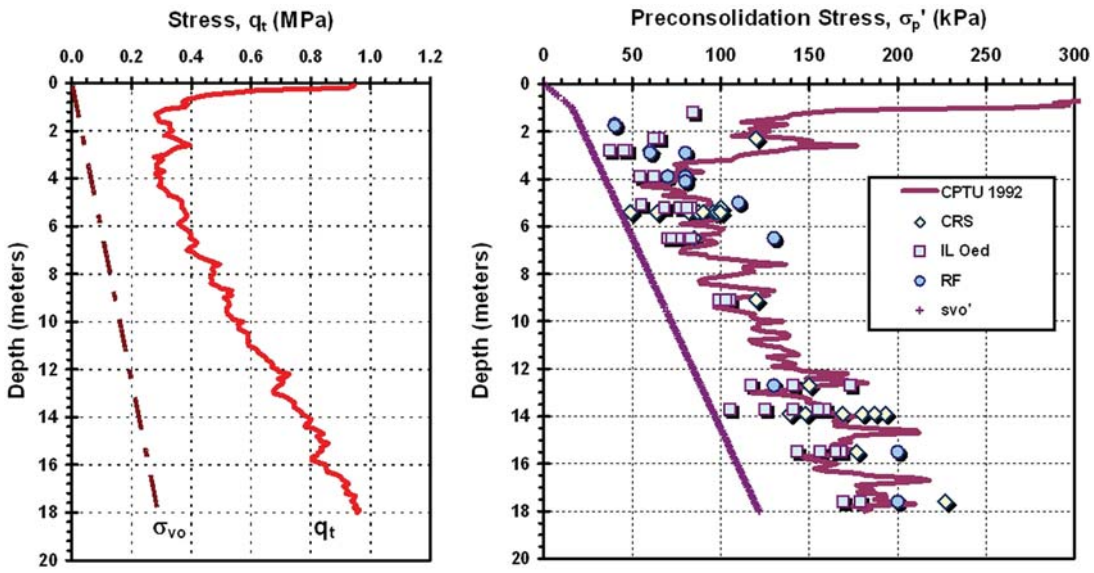

FIGURE 35 Comparison of CPT-based evaluation of preconsolidation stress with laboratory consolidation tests in Bothkennar soft clay (data from Nash et al. 1992). CRS = constant rate of strain; IL Oed = incremental loading oedometer; RF = restrained flow, S_{vo}' (σ_{vo}') = effective vertical (overburden) stress.

$$\textit{Midface Filter Element}: \sigma_p' = 0.75\,(q_t - u_1) \qquad (22)$$

$$\textit{Shoulder Filter Element}: \sigma_p' = 0.60\,(q_t - u_2) \qquad (23)$$

The previous relationships give redundancy to the interpretation of yield stress in clays by means of CPTu data; however, this is interesting as it lends support to the values obtained should they agree. That is, multiple methods give an opportunity to confirm and corroborate the interpreted soil parameters Larsson and Mulabdic (1991). A noted discrepancy offers a reason to investigate why the conflict exists, as well as a caution that additional testing (i.e., oedometer, CRS consolidometer) may be warranted, particularly in unusual soil formations.

For the Bothkennar site, the additional evaluations of stress history using excess porewater pressures (Δu_2) and effective cone resistance ($q_t - u_2$) are presented in terms of the OCR in Figure 37. Again, as with the earlier profiles in Figure 35, good agreement between the laboratory consolidation data and field methods is evident.

Sands

The evaluation of stress history for clean, uncemented, unaged quartz sands is a more challenging assignment for two primary reasons: (1) oedometric e-logσ_v' curves for sands are very flat, thus making detection of a yield stress problematic; and (2) undisturbed sampling of clean quartz to siliceous sands is quite difficult, and though now attainable by new freezing methods, remains very expensive. Therefore, a relationship for obtaining OCR in clean quartz sands has been empirically derived from statistical evaluations on 26 different series of CPT calibration chamber tests (Kulhawy and Mayne 1990; Lunne et al. 1997; Mayne 2001). Chamber tests are very large diameter triaxial specimens having diameters and heights on the order of 0.9 to 1.5 m. Cone penetration is conducted after preparation of the sand sample (dry, moist, saturated) at the desired relative density, effective confining stress levels, and stress history (Jamiolkowski et al. 2001).

For purposes herein, the sands are primarily siliceous (quartz and feldspar) with applied stress histories ranging from NC to overconsolidated states ($1 \le \text{OCR} \le 15$). Multiple regression analyses of the chamber test data ($n = 636$) from anisotropically consolidated sands indicate that the induced OCR is a function of the applied effective vertical stress (σ_{vo}'), effective horizontal stress [$\sigma_{ho}' = (K_0 \cdot \sigma_{vo}')$], and measured cone tip resistance (q_t), as indicated by Figure 38. Here, the OCR is shown normalized by $Q = (qt - \sigma_{vo})/\sigma_{vo}'$. The results can be presented by the following closed-form expression (Mayne 2005):

$$\text{OCR} = \left[\frac{0.192 \cdot \left(q_t / \sigma_{\text{atm}}\right)^{0.22}}{(1 - \sin\phi') \cdot \left(\sigma_{vo}' / \sigma_{\text{atm}}\right)^{0.31}} \right]^{\left(\frac{1}{\sin\phi' - 0.27}\right)} \qquad (24)$$

where ϕ' = effective stress friction angle of the sand, σ_{vo}' = effective overburden stress, and σ_{atm} = a reference stress equal to one atmosphere = 1 bar = 100 kPa ≈ 1 tsf.

From the OCR, the apparent preconsolidation stress of the sand can be calculated from:

$$\sigma_p' = \text{OCR} \cdot \sigma_{vo}' \qquad (25)$$

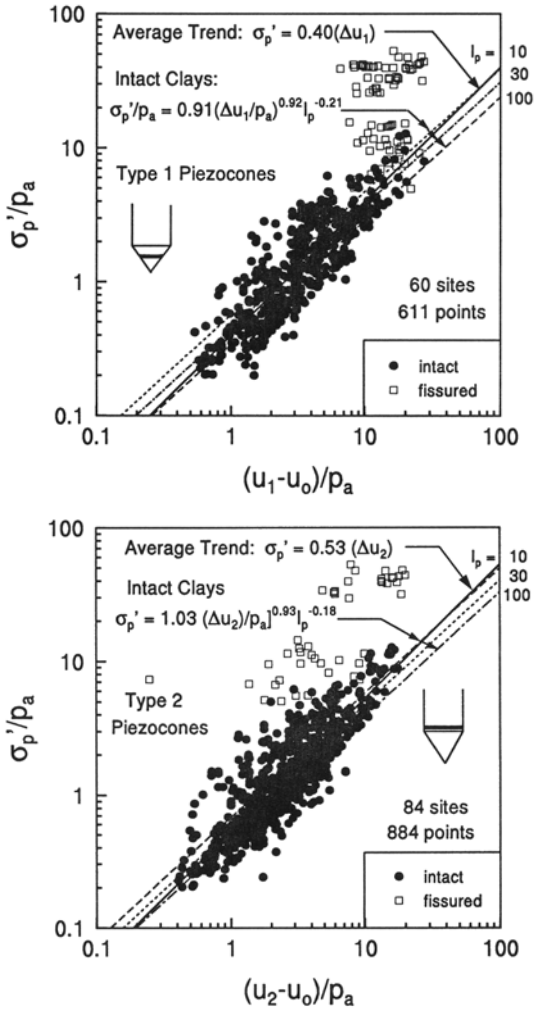

FIGURE 36 First-order trends of preconsolidation stress in clays with excess porewater pressures measured by (*upper*) Type 1 piezocones, and (*lower*) Type 2 piezocones.

An example of the procedure for evaluating stress history from cone tip stress measurements in clean sands is afforded from a quarry site near Stockholm investigated by Dahlberg (1974). The site was comprised of a Holocene deposit of clean, glacial, medium-coarse sand having an initial 24 m thickness overlying bedrock. After the upper 16 m was removed by quarrying operations, a series of in situ testing [SPT, CPT, pressuremeter test (PMT), and screw plate load test] were performed in the remaining 8 m of sand, in addition to special balloon density tests in trenches. The groundwater table was located at the base of the sand just above bedrock. Index parameters of the sand included mean grain size ($0.7 < D_{50} < 1.1$ mm); uniformity coefficient ($2.2 < UC < 3$), mean density $\rho_T = 1.67$ g/cc, and average $D_R \approx 60\%$. Using results from four Borros-type electric CPTs at the site, Figure 39 shows the measured q_t readings and interpreted profiles of OCR and σ_p' in the Stockholm sand. Results of the screw plate load tests were used by Dahlberg (1974) to interpret the preconsolidation stresses in the sand, which are observed to be comparable to the known values from mechanical overburden removal, where the stress history can be determined by calculating the OCR $= (\Delta\sigma_v + \sigma_{vo}')/\sigma_{vo}'$, using the prestress:

$$\Delta\sigma_v = (16 \text{ m})(16.4 \text{ kN/m}^3) = 262 \text{ kPa } (2.72 \text{ tsf})$$

Mixed Soil Types

If seismic cone data are obtained, then the small-strain stiffness may be used together with the overburden stress level to evaluate the effective preconsolidation stress in all soil types (clays, silts, and sands). An original database compiled by Mayne et al. (1998) on a variety of 26 intact clays worldwide has been supplemented with recent data on two cemented clays (Fucino, Italy and Cooper Marl from Charleston, South Carolina) in Figure 40. In addition, data

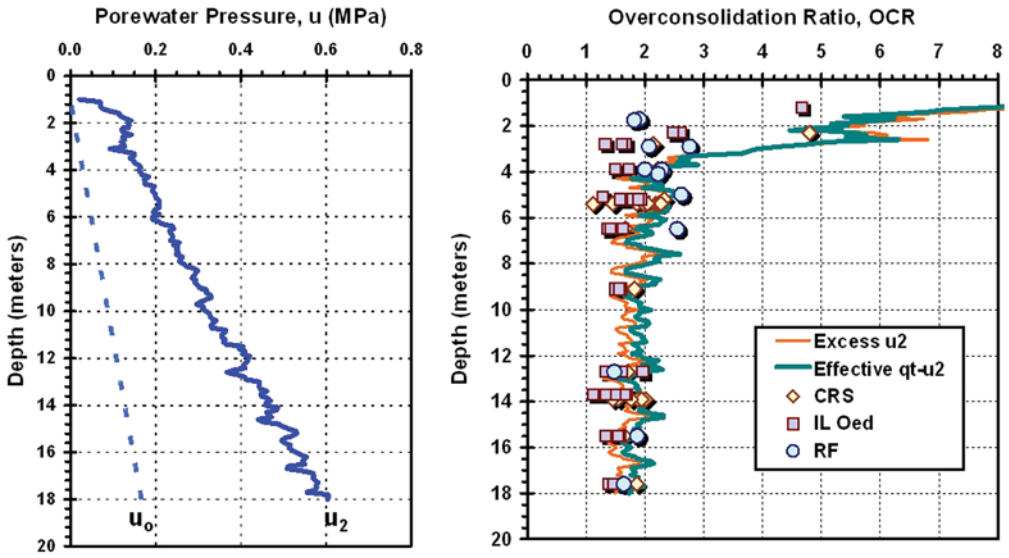

FIGURE 37 Comparison of CPTu-based evaluations of preconsolidation stress with laboratory consolidation tests in Bothkennar soft clay using excess porewater pressures and effective cone resistance (data from Nash et al. 1992). CRS = constant rate of strain, u_2 = porewater pressure, $q_t - u_2$ = effective cone resistance, IL Oed = incremental loading oedometer, RF = restricted flow.

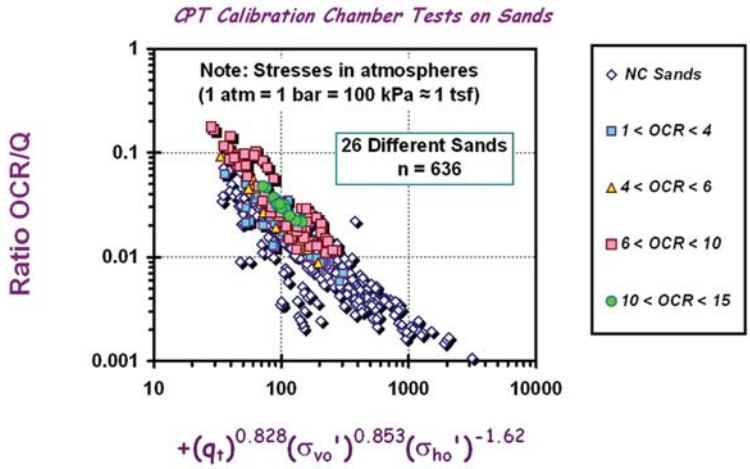

FIGURE 38 Chamber test data showing trend of OCR/*Q* for clean quartz and siliceous sands.

from Po River sand (Ghionna et al. 1995) and Holmen Sand (Lunne et al. 2003), where the stress histories of the granular deposits are well-documented, are also included. Finally, results from Piedmont residual fine sandy silts at the National Geotechnical Test Site (NGES) at Opelika, Alabama, are also considered (Mayne and Brown 2003). The overall relationship for intact geomaterials is shown in Figure 40 and expressed by:

$$\sigma_p' = 0.101\ \sigma_{atm}^{\ 0.102}\ G_0^{\ 0.478}\ \sigma_{vo}'^{\ 0.420} \qquad (26)$$

with a statistical coefficient of determination $r^2 = 0.919$ for intact soils. The approach is evidently not valid for fissured geomaterials. The advantage of this particular approach is that all soil types may be considered in a consistent manner, whereas the separation of soil layers into "clay-like" and "sand-like" often result in mismatched profiles of preconsolidation stress with depth.

EFFECTIVE STRESS STRENGTH

Sands

The strength of soils is controlled by the effective stress frictional envelope, often represented in terms of the Mohr–Coulomb parameters: ϕ' = effective friction angle and c' = effective cohesion intercept. For clean sands, a commonly used CPT interpretation is based on considerations

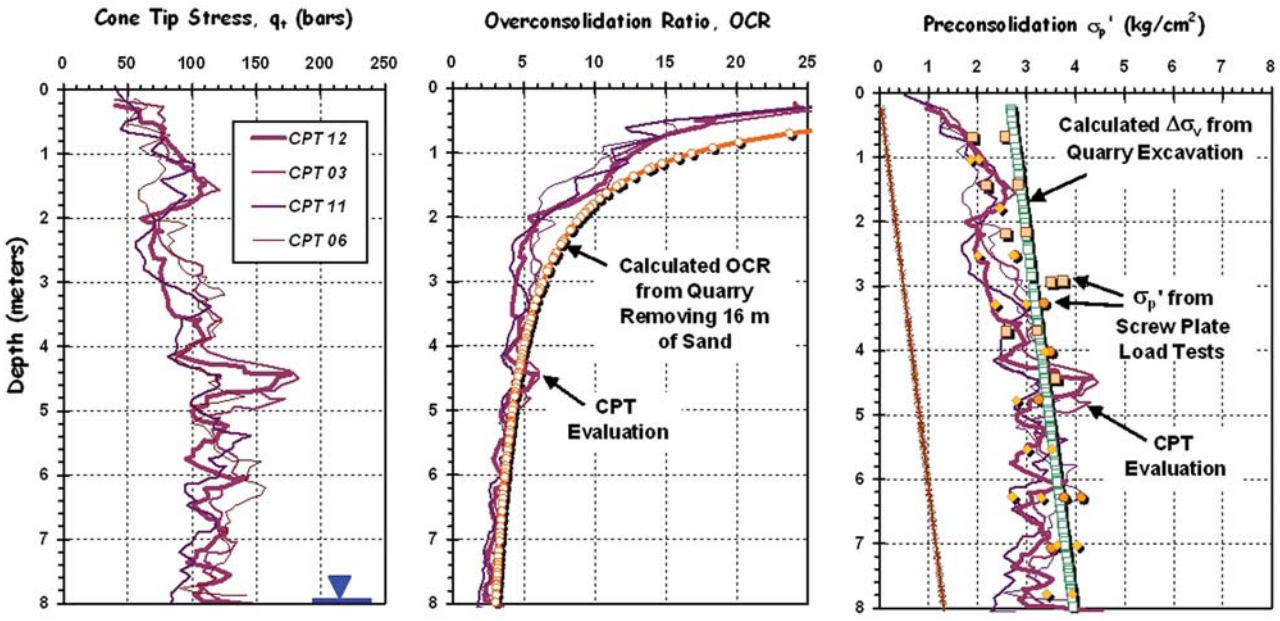

FIGURE 39 Results from Stockholm quarry sand site showing (*left*) cone tip resistances, (*center*) OCR profiles from excavation, and (*right*) preconsolidation stresses (data from Dahlberg 1974).

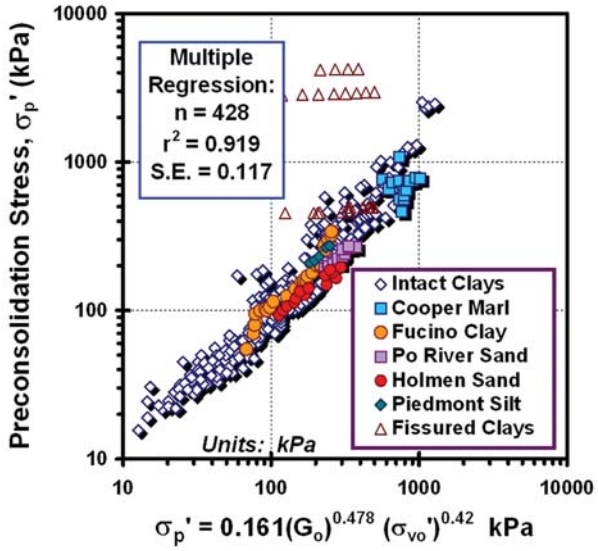

FIGURE 40 Preconsolidation stress evaluation from small-strain shear modulus in soils.

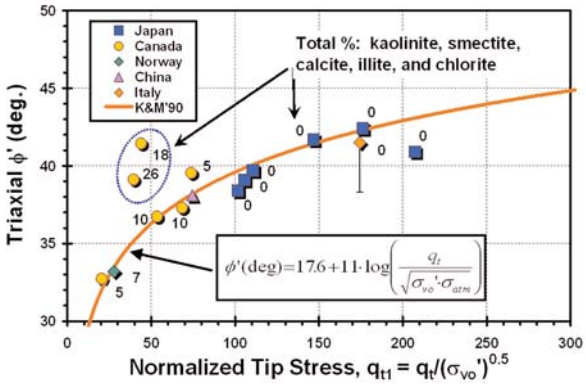

FIGURE 41 Peak triaxial friction angle from undisturbed sands with normalized cone tip resistance.

of an inverted bearing capacity (BC) theory supplemented with CPT calibration chamber data from five sands (Robertson and Campanella 1983). However, the flexible-walled chamber test results were not corrected for boundary size effects. In that approach, the expression for peak friction angle of clean quartz sands is given by the approximation ($c' = 0$):

$$\phi' = \arctan [0.1 + 0.38 \log (q_t/\sigma_{vo}')] \qquad (27)$$

An alternate expression derived from a much larger compilation of a calibration chamber database from 24 sands, where the cone tip stresses were adjusted accordingly for relative size of chamber and cone diameter (*D/d* ratio), was proposed by Kulhawy and Mayne (1990):

$$\phi' = 17.6° + 11.0° \cdot \log (q_{t1}) \qquad (28)$$

where $q_{t1} = (q_t/\sigma_{atm})/(\sigma_{vo}'/\sigma_{atm})^{0.5}$ is a more appropriate form for stress normalization of CPT results in sands (e.g., Jamiolkowski et al. 2001). The relationship for ϕ' with q_{t1} is shown in Figure 41.

Recently, a database was developed on the basis of undisturbed (primarily frozen) samples of 13 sands. These sands were located in Canada (Wride and Robertson 1999, 2000), Japan (Mimura 2003), Norway (Lunne et al. 2003), China (Lee et al. 1999), and Italy (Ghionna and Porcino 2006). In general, the sands can be considered as clean to slightly dirty sands of quartz, feldspar, and/or other rock mineralogy, excepting two of the Canadian sands derived from mining operations that had more unusual constituents of clay and other mineralogies. In terms of grain size distributions, these granular geomaterials include ten fine sands, four medium sands, and one coarse sand (Italy). The sands from Canada were slightly dirty, having fines contents (*FC*) between $5\% < FC < 15\%$, whereas the other sands were all relatively clean with $FC < 4\%$. Mean values of index parameters (with plus and minus one standard deviation) of these sands indicated: specific gravity ($G_s = 2.66 \pm 0.03$), fines content ($FC = 4.36 \pm 4.49$), particle size ($D_{50} = 0.35 \pm 0.23$ mm), and uniformity coefficient ($UC = D_{60}/D_{10} = 2.80 \pm 1.19$). At all sites, results from electric SCPTu were available, except the China site where only CPTu was reported. Each undisturbed sand was tested using a series of either isotropically and/or anisotropically consolidated triaxial shear tests. Additional details are discussed by Mayne (2006a).

The sand database was used to check the validity of the friction angle determinations from in situ CPT tests. The relationship between the triaxial-measured ϕ' of undisturbed (frozen) sands and normalized cone tip resistance is presented in Figure 41. Here, the CPT proves to be an excellent predictor in evaluating the drained strength of the sands. The two outliers from LL and Highmont Dams are mine tailings sands from Logan Lake, British Columbia, that contained high percentages of clay minerals (as noted) and are both underpredicted by the CPT expression.

Mixed Soil Types

An interesting approach by the Norwegian University of Science and Technology (NTNU) is an effective stress limit plasticity solution to obtain the effective stress friction angle for all soil types (Senneset et al. 1988, 1989). In the fully developed version, the NTNU theory allows for the determination of both the effective friction angle (ϕ') and effective cohesion intercept (c') from CPTU data in soils.

For the simple case of Terzaghi-type deep BC (angle of plastification $\beta_P = 0$), and adopting an effective cohesion intercept $c' = 0$, the effective friction angle can be determined from normalized CPT readings $Q = (q_t - \sigma_{vo})/\sigma_{vo}'$ and $B_q = (u_2 - u_0)/(q_t - \sigma_{vo})$ using the chart shown in Figure 42.

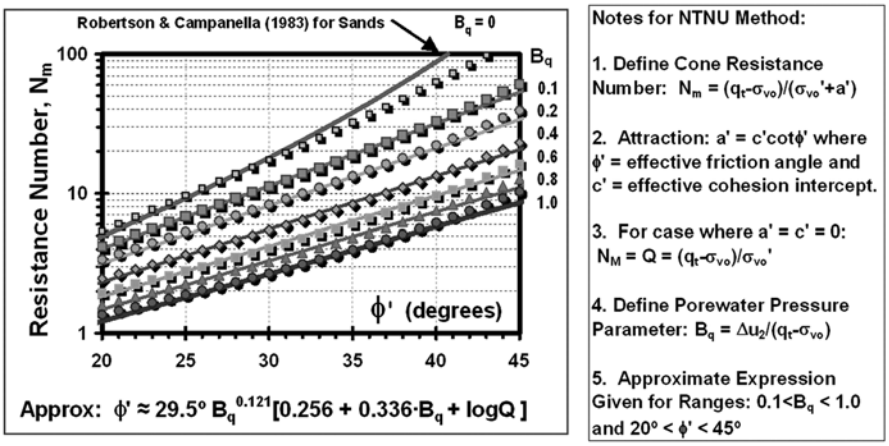

FIGURE 42 Effective stress friction angle for sands, silts, and clays from NTNU method.

An approximate form for a deterministic line-by-line evaluation of $_f'$ for the NTNU method is given by (Mayne and Campanella 2005):

$$\phi'(\text{degrees}) = 29.5° \, B_q^{0.121} \, [0.256 + 0.336 \, B_q + \log Q] \quad (29)$$

that is applicable for $0.1 < B_q < 1.0$ and range: $20° < \phi' < 45°$. For $B_q < 0.1$ corresponding to granular soils, the previous expression for clean sands would apply.

UNDRAINED SHEAR STRENGTH OF CLAYS

For geotechnical applications involving short-term loading of clays and clayey silts, the undrained shear strength ($s_u = c_u$) of the soil (formerly termed c = cohesion) is commonly sought for stability and BC analyses. The classical approach to evaluating s_u from CPT readings is through the net cone resistance:

$$s_u = (q_t - \sigma_{vo})/N_{kt} \quad (30)$$

where N_{kt} is a bearing factor. More papers and research programs have focused on the assessment of relevant value of N_{kT} for an interpretation of s_u than for any other single parameter (e.g., Keaveny and Mitchell 1986; Konrad and Law 1987; Yu and Mitchell 1998), without any consensus reached. This is because, in part, the value of s_u is not unique, but depends on the direction of loading, strain rate, boundary conditions, stress level, sample disturbance effects, and other factors (Ladd 1991). Indeed, a suite of different undrained shear strengths are available for a given clay soil. For the basic laboratory shear modes, there are many available apparatuses, including CIUC, PSC, CK_0UC, direct shear simple (DSS), DS, PSE, CK_0UE, UU, UC, as well as hollow cylinder, true triaxial, and torsional shear (Jamiolkowski et al. 1985; Kulhawy and Mayne 1990). Depending on the particular agency, firm, or institution given responsibility for assessing the appropriate N_{kt}, different test modes will be chosen to benchmark the s_u for the CPT.

In lieu of the classical approach, an alternate and rational approach can be presented that focuses on the assessment of σ_p' from the CPT. The magnitude of preconsolidation stress (σ_p') is uniquely defined as the yield point from the e-logσ_v' plot obtained from a consolidation test. The influence of OCR in governing the undrained shear strength of clays is very well established (e.g., Trak et al. 1980; Leroueil and Hight 2003). Therefore, the OCR profile already evaluated by the CPT results can be used to generate the variation of undrained shear strength with depth in a consistent and rational manner. A three-tiered approach can be recommended based on: (1) critical-state soil mechanics, (2) empirical normalized strength ratio approach, and (3) empirical method at low OCRs, as discussed later. For all cases, a representative mode for general problems of embankment stability, foundation-BC, and slopes and excavations in clays and clayey silts can be taken as that for DSS.

From considerations of critical state soil mechanics (CSSM), this simple shear mode can be expressed in normalized form (Wroth 1984):

$$s_u/\sigma_{vo}'_{\text{DSS}} = \tfrac{1}{2} \sin\phi' \text{OCR}^{\Lambda} \quad (31)$$

where $\Lambda = 1 - C_s/C_c$ = plastic volumetric strain potential, C_s = swelling index, and C_c = virgin compression index of the material. For many clays of low to medium sensitivity, $0.7 \leq \Lambda \leq 0.8$, whereas for sensitive and structured clays, a higher range between $0.9 \leq \Lambda \leq 1.0$ can be observed.

If the compression indices and ϕ' are not known with confidence, a recommended default form based on three decades of experimental laboratory work at the Massachusetts Institute of Technology has been proposed (Jamiolkowski et al. 1985; Ladd 1991; Ladd and DeGroot 2003):

$$s_u/\sigma_{vo}'_{\text{DSS}} = 0.22 \, \text{OCR}^{0.80} \quad (32)$$

which is clearly a subset of the CSSM equation for the case where $\phi' = 26°$ and $\Lambda = 0.80$.

Finally, at low OCRs < 2, the back analyses of failure case records involving corrected vane strengths for embankments,

footings, and excavations, it has been shown that the mobilized undrained shear strength may be taken simply as (Trak et al. 1980; Terzaghi et al. 1996):

$$s_u \approx 0.22\ \sigma_p' \tag{33}$$

which is a subset of both the CSSM and the Massachusetts Institute of Technology approaches.

Available experimental data support the CSSM approach, as shown by Figure 43. For NC clays, the normalized undrained shear strength to effective overburden stress ratio $(s_u/\sigma_{vo}')_{NC}$ increases with effective friction angle. In Figure 44, the larger influence of stress history is shown to dominate the ratio $(s_u/\sigma_{vo}')_{OC}$ for overconsolidated soils. Notably, the CSSM adequately expressed the increase with OCR in terms of a power function.

It is important here to note the exception for fissured clay materials (specifically, London clay from Brent Cross) that have a macrofabric of cracking and preexisting slip surfaces. Fissured soils can exhibit strengths on the order of one-half of the values associated with intact clays. For these cases, fissured clays occurring below the groundwater table can be identified by zero to negative porewater pressures taken at the shoulder position (Type 2); thus, $u_2 \leq 0$ (Lunne et al. 1997). For Type 1 piezocones, zones of fissured clays can be demarcated by a low ratio $u_1/q_t < 0.4$, in comparison with intact clays that exhibit characteristic ratios on the order of $u_1/q_t > 0.7$ (Mayne et al. 1990).

An illustrative example of post-processing CPTs in clays to determine the undrained shear strength variation with depth is shown in Figure 45. This is the national geotechnical experimentation site in soft varved clay at the University of Massachusetts–Amherst (DeGroot and Lutenegger 2003). A series of five CPTs produced the total (corrected) cone tip resistances presented in Figure 45

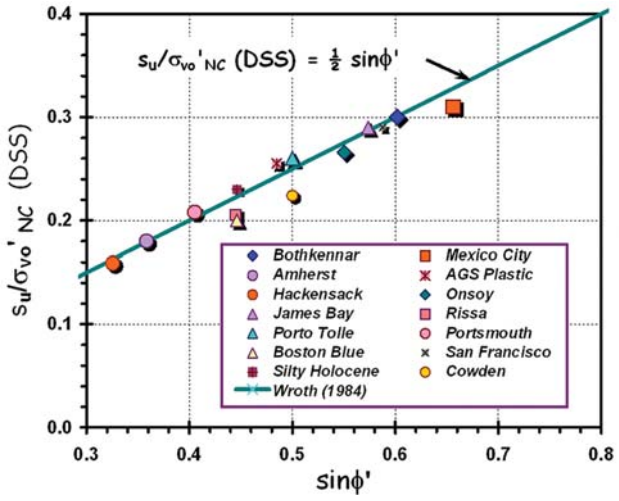

FIGURE 43 Normalized DSS undrained shear strength versus effective friction angle in normally consolidated clays.

(*left*) showing a subsurface profile with 1 m clay fill over a desiccated clay crust to an approximate 4 m depth overlying soft silty clay. The groundwater lies 0.5 to 1 m below grade. The net cone resistances were processed to evaluate σ_p' values as noted in Eq. 19 and produce the overconsolidation ratios shown in Figure 45 (*center*). These were used in turn with an effective $\phi' = 21°$ from Eq. 31 to obtain the profile of undrained shear strengths, as seen in Figure 45 (*right*). The results are in good agreement with the laboratory reference oedometer tests and corresponding DSS strength tests at the site.

On particularly critical projects, it is warranted to perform additional strength testing to confirm and support the CPT interpretations, rather than rely solely on one test method. For instance, reference benchmarking of s_u values can be established using field vane tests with appropriate corrections (e.g., Leroueil and Jamiolkowski 1991) or by laboratory strength testing on high-quality samples (e.g., Ladd and DeGroot 2003).

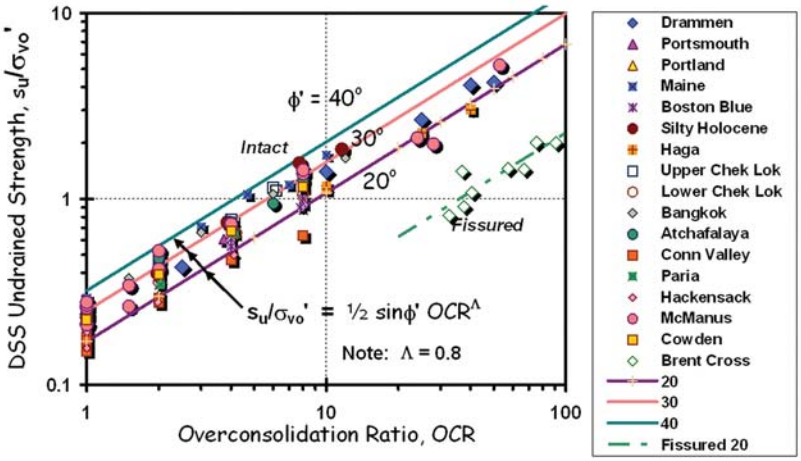

FIGURE 44 Relationship for DSS undrained strength with ϕ', OCR, and degree of fissuring in clays.

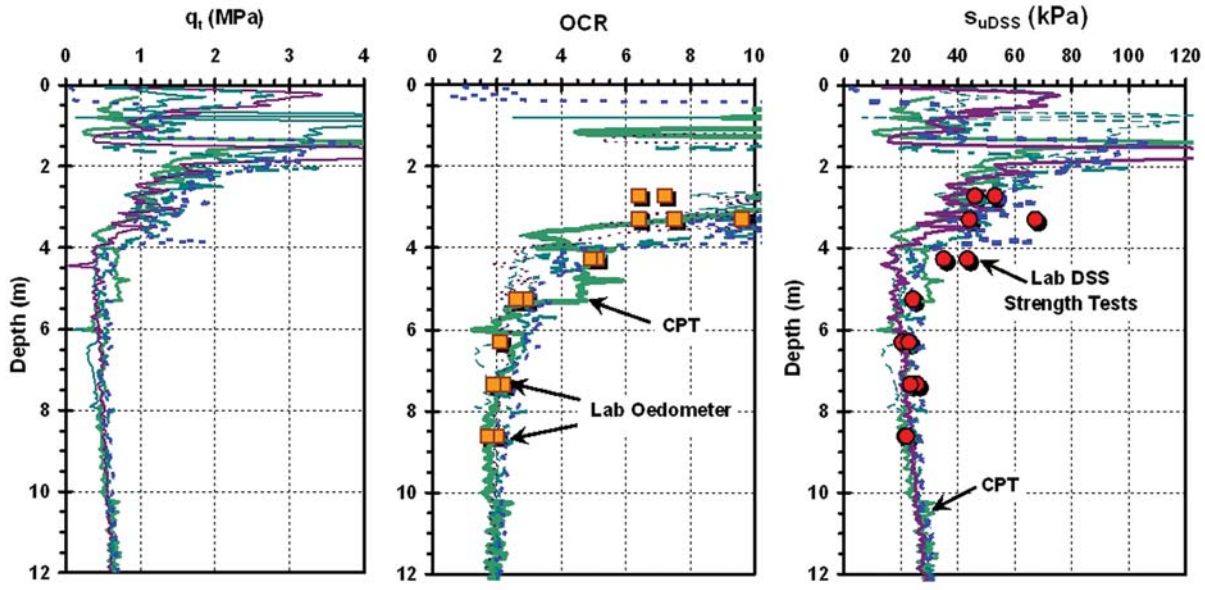

FIGURE 45 Results from Amherst soft clay site showing: (*left*) corrected cone tip resistances, (*center*) over-consolidation ratios, and (*right*) undrained shear strengths (laboratory data from DeGroot and Lutenegger 2003).

SENSITIVITY

In soft clays and silts, the sensitivity (S_t) is considered as an index to problematic construction and field performance difficulties. The reference test for determining S_t is the field vane shear (Chandler 1988), although laboratory testing methods can include the unconfined compression test, miniature vane, and fall cone. With the CPT, the friction sleeve reading can be considered indicative of a remolded undrained shear strength: $f_s \approx s_{ur}$ (e.g., Gorman et al. 1975). Thus, an indicator as to the sensitivity (S_t) of the deposit may be obtained by taking the ratio of peak shear strength to remolded value. Mostly, the value of S_t is sought for soft clays; therefore, using the aforementioned relationship for peak strength at low OCRs (i.e., $s_u \approx 0.22\sigma_p'$) combined with the evaluation of preconsolidation stress from net cone resistance [i.e., $\sigma_p' = 0.33(q_t - \sigma_{vo})$] suggests that (OCRs < 2):

$$S_t \approx 0.073(q_t - \sigma_{vo})/f_s \qquad (34)$$

If a direct and accurate measure of in-place sensitivity is necessary, follow-up testing with the vane shear is prudent.

RELATIVE DENSITY OF CLEAN SANDS

In clean sands with less than 15% fines content, it is common practice to assess the relative density (D_R) by in situ tests. For the CPT, a number of different expressions have been developed from large-scale chamber tests (e.g., Schmertmann 1978a; Robertson and Campanella 1983; Jamiolkowski et al. 1985); however, those correlations did not consider the boundary effects that cause reduced values of q_t measured in flexible walled chambers (e.g., Salgado et al. 1998). A recent reexamination of a large CCT data set by Jamiolkowski et al. (2001), which incorporates a correction factor, has found that a mean relationship in terms of normalized cone tip stress can be expressed by:

$$D_R = 100 \cdot \left[0.268 \cdot \ln\left(\frac{q_t / \sigma_{atm}}{\sqrt{\sigma_{vo}' / \sigma_{atm}}} \right) - 0.675 \right] \qquad (35)$$

and the effects of relative sand compressibility can be considered by reference to Figure 46.

The aforementioned database on undisturbed (frozen) sands also lends an opportunity to assess this revised expression. As seen in Figure 47, the corresponding CPT data on

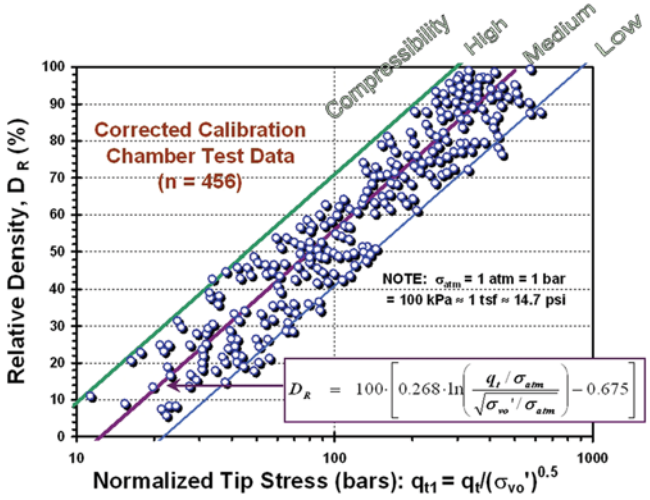

FIGURE 46 Relative density relationship with normalized tip stress and sand compressibility from corrected chamber test results (after Jamiolkowski et al. 2001).

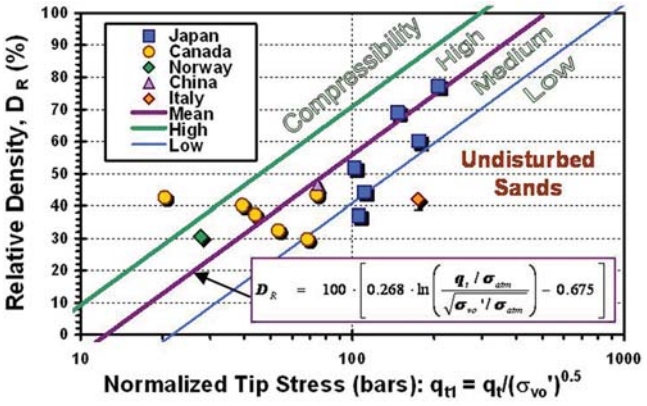

FIGURE 47 Relative density of undisturbed (frozen) quartz sands versus normalized cone tip resistance.

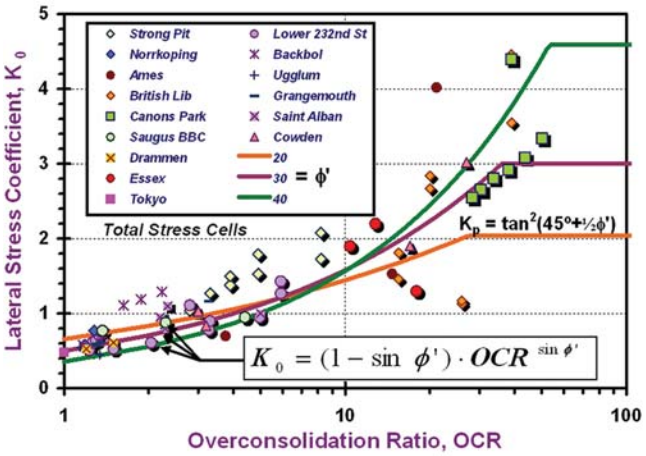

FIGURE 49 Lateral stress coefficient K_0 from total stress cell field measurements versus OCR in clays.

these 15 sands fall generally within the bounds established from the CCT results, with the Canadian sands indicative of high-compressibility materials and the Japanese sands trending on the low-compressibility side.

In sands of carbonate and calcareous composition, the expected trend would follow that for high-compressibility bounds because of particle crushing (Coop and Airey 2003). For this case, a newly created data set from CPT chamber testing on carbonate sands has been compiled, including Quiou Sand (Fioravante et al. 1998), Dogs Bay Sand (Nutt and Houlsby 1991), Ewa Sand (Morioka and Nicholson 2000), and Kingfish Platform (Parkin 1991). These data confirm that carbonate sands would fall at the higher side of trends reported for quartzitic sands because of their higher compressibility, as shown by Figure 48.

GEOSTATIC LATERAL STRESS STATE

The geostatic horizontal stress is represented by the K_0 coefficient, where $K_0 = \sigma_{ho}'/\sigma_{vo}'$. In general, laboratory data on small triaxial specimens and instrumented oedometer tests indicate that the following relationship can be adopted in uncemented sands and well-behaved clays of low to medium sensitivity:

$$K_0 = (1 - \sin\phi') \, \mathrm{OCR}^{\sin\phi'} \tag{36}$$

For structured and cemented soils, higher values of K_0 can be realized, somewhat related to the clay sensitivity (Hamouche et al. 1995). Figure 49 shows field K_0 data from total stress cell (TSC) measurements (or spade cells) in clays that generally agree with the above relationship. Results from self-boring PMTs also give a similar trend between K_0 and OCR for a variety of clay soils (Kulhawy and Mayne 1990).

For clean sands, data from large calibration chamber tests and small laboratory triaxial and oedometer test series show the K_0 – OCR trends in Figure 50. Related to the previous OCR Eq. 24, the derived formulation for the lateral stress

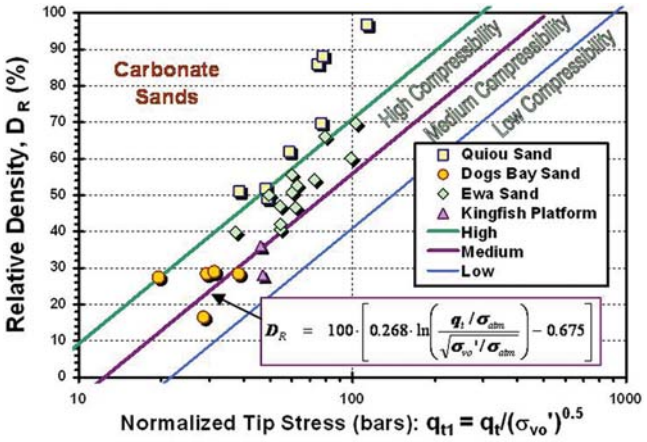

FIGURE 48 Relative density of carbonate sands in terms of normalized cone tip resistances.

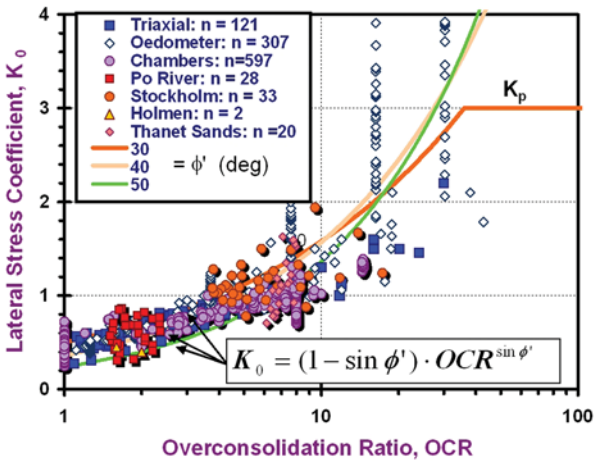

FIGURE 50 Lateral stress coefficient K_0 versus OCR from laboratory tests on sands.

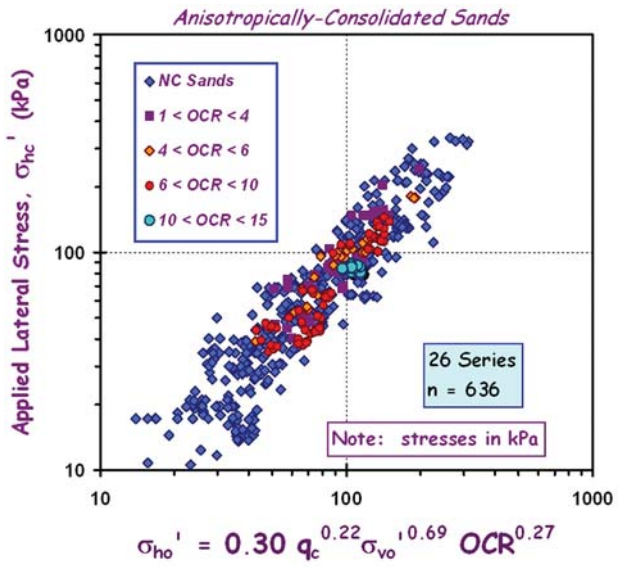

FIGURE 51 Lateral stress evaluation of quartz sands from CPT results in chamber tests.

coefficient from chamber tests is shown in Figure 51 and expressed by:

$$K_0 = 0.192 \cdot \left(q_t / \sigma_{atm} \right)^{0.22} \cdot \left(\sigma_{atm} / \sigma_{vo}' \right)^{0.31} \cdot \left(\mathrm{OCR} \right)^{0.27} \quad (37)$$

A maximum value for K_0 can be set by the passive stress coefficient (K_P), which for a simple Rankine case is given by:

$$K_P = \tan^2 \left(45° + \phi'/2 \right) = \frac{1 + \sin \phi'}{1 - \sin \phi'} \quad (38)$$

The K_p limit is shown in Figures 49 and 50 for the K_0 – OCR relationships for clays and sands, respectively.

Illustration of the approach for K_0 profiling in sands by CPT is afforded from the previous case study of quarried glacial sand near Stockholm (Dahlberg 1974). To utilize Eq. 37 for evaluation of K_0, an a priori relationship between K_0 and OCR must be made; that is, Eq. 36. Samples of the sand were reconstituted in the laboratory at the measured in-place densities and subjected to consolidated drained triaxial shear testing to determine $\phi' = 40°$ (Mitchell and Lunne 1978). Using Eq. 28 provides a comparable evaluation of ϕ' from the four CPTs, as seen in Figure 52. The CPT data together with ϕ' are used in Eq. 24 to obtain the OCR (Figure 39) in either Eqs. 36 or 37 to produce the profiles of K_0. As seen in Figure 52, these are in agreement with the reported field K_0 values determined from lift-off pressures in PMTs performed at the site (Dahlberg 1974).

EFFECTIVE COHESION INTERCEPT

For long-term stability analyses, the effective cohesion intercept (c') is conservatively taken to be zero. The intercept is actually a projection caused by the forced fitting of a straight line (form, $y = mx + b$) to a strength envelope that is actually curved (Singh et al. 1973). Several difficulties are associated with assessing a reputable value of c' to a particular soil, including its dependency on the magnitude of preconsolidation stress (σ_p'), strain rate of loading ($d\varepsilon/dt$), and age of the deposit (t). The projected c' is actually a manifestation of the three-dimensional yield surface that extends above the frictional envelope, as discussed by Hight and Leroueil (2003). For short-term loading conditions, an apparent value of c'

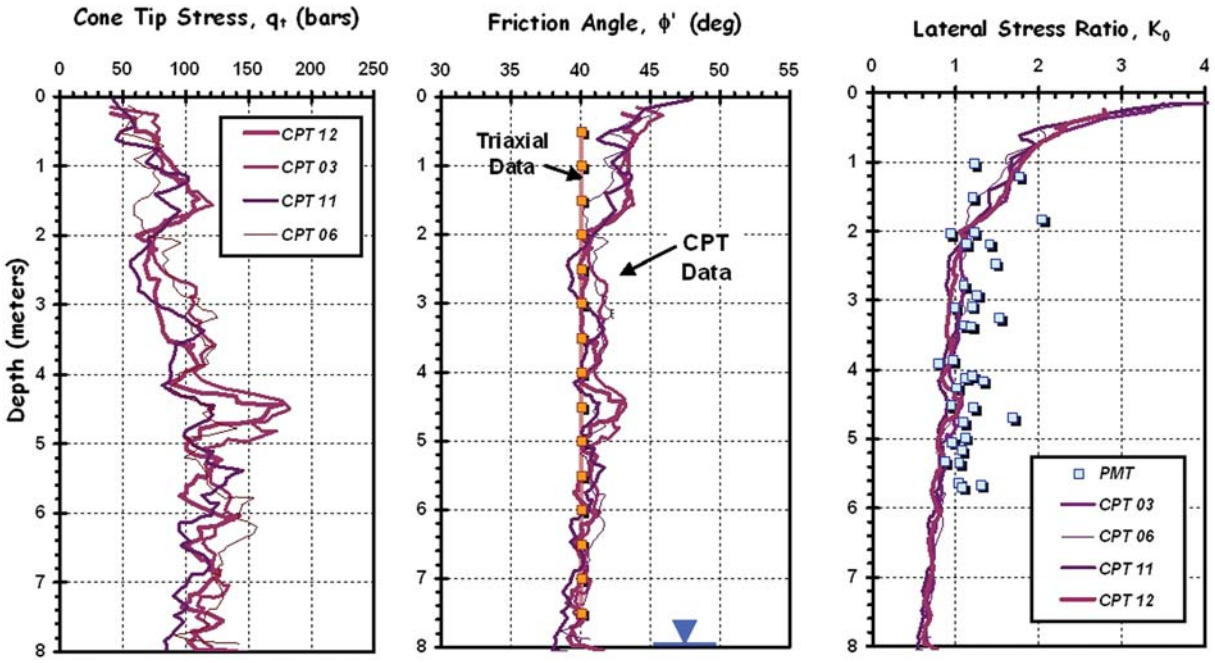

FIGURE 52 CPT post-processing for peak ϕ' and coefficient K_0 in Stockholm sand.

may be assessed from the stress history (Mayne and Stewart 1988; Mesri and Abdel-Ghaffar 1993):

$$c' \approx 0.02\ \sigma_p' \tag{39}$$

COEFFICIENT OF CONSOLIDATION

Porewater pressures generated during cone penetration in fine-grained soils are transient. Once the penetration process is halted, the excess pressures will decay with time and the transducer reading will eventually reach equilibrium corresponding to the hydrostatic value (u_0). The rate of dissipation is governed by the coefficient of consolidation (c_{vh}):

$$c_{vh} = \frac{k \cdot D'}{\gamma_w} \tag{40}$$

where k = coefficient of permeability, D' = constrained modulus, and γ_w = unit weight of water.

For most natural soft marine clays, the horizontal permeability is only around 10% to 20% higher than the vertical value (Mesri 1994; Leroueil and Hight 2003). A summary of the laboratory series of permeability tests on different natural soft clays is given in Figure 53, whereby both standard vertical measurements of hydraulic conductivity (k_v) are compared with horizontal values (k_h) using radial permeameter devices. For varved clays and highly stratified deposits, the ratio of horizontal to vertical permeabilities may range from 3 to 5, and very rarely approaches 10. Guidelines to permeability anisotropy are given in Table 3.

The most popular CPTù method to evaluate c_{vh} in soils at present is the solution from the strain path method (SPM) reported by Houlsby and Teh (1988), although other available

TABLE 3
PERMEABILITY ANISOTROPY IN NATURAL CLAYS

Nature of the Clay	Ratio k_h/k_v
Homogeneous Clays	1 to 1.5
Sedimentary Clays with Discontinuous Lenses and Layers, Well-Developed Macrofabric	2 to 4
Varved Clays and Silts with Continuous Permeable Layers	1.5 to 15

Adapted after Leroueil and Jamiolkowski (1991).
Note: k_h = horizontal hydraulic conductivity; k_v = vertical hydraulic conductivity.

procedures are discussed by Jamiolkowski et al. (1985), Gupta and Davidson (1986), Senneset et al. (1988, 1989), Jamiolkowski (1995), Danzinger et al. (1997), Burns and Mayne (1998, 2002a), and (Abu-Farsakh and Nazzal 2005). For the SPM solution, Teh and Houlsby (1991) provided time factors for a range of porewater pressure dissipations. The degree of excess porewater pressure dissipation can be defined by $U^* = \Delta u/\Delta u_i$, where Δu_i = initial value during penetration. The modified time factor T^* for any particular degree of consolidation is defined by:

$$T^* = \frac{c_{vh} \cdot t}{a^2 \cdot \sqrt{I_R}} \tag{41}$$

where t = corresponding measured time during dissipation and a = probe radius. The SPM solutions relating U^* and T^* for midface u_1 and shoulder u_2 piezo-elements are shown in Figures 54 and 55, respectively. These can be conveniently represented using approximate algorithms as shown, thus offering a means to implement matching data on a spreadsheet.

In terms of calibrating the approach, a fairly comprehensive study between laboratory c_v values and piezocone c_h values in clays and silts was reported by Robertson et al. (1992). Assumptions were made between the ratio of

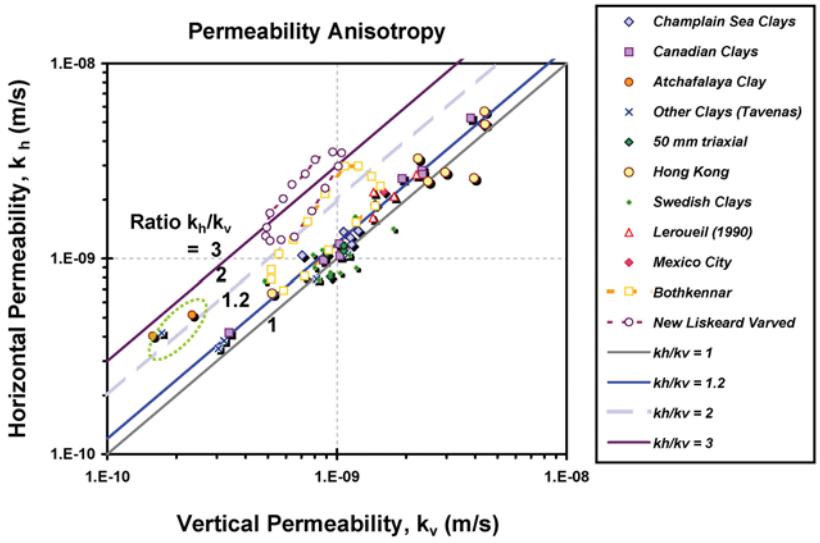

FIGURE 53 Comparison of horizontal and vertical permeabilities on natural clays (after Leroueil et al. 1990).

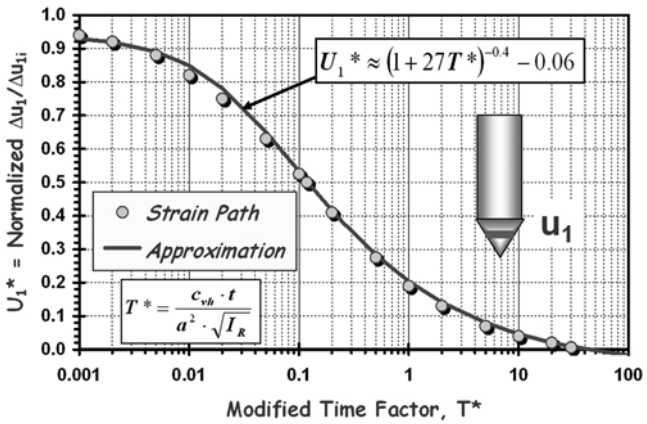

FIGURE 54 Strain path solution for CPTu$_1$ dissipation tests (after Teh and Houlsby 1991).

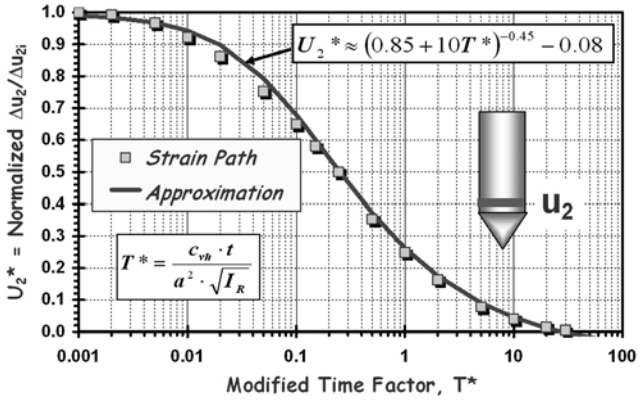

FIGURE 55 Strain path solution for CPTu$_2$ dissipation tests (after Teh and Houlsby 1991).

horizontal to vertical permeability to address possible issues of anisotropy during interpretation. The study compared laboratory-determined results with the SPM solution (Teh and Houlsby 1991) using data from Type 1 piezocones (22 sites) and Type 2 piezocones (23 sites), as well as eight sites where backcalculated field values of c_{vh} were obtained from full-scale loadings.

With the SPM approach in practice, it is common to use only the measured time to reach 50% consolidation, designated t_{50}. An illustrative example of determining t_{50} for a 15-cm^2 Type 2 piezocone dissipation in soft varved clay at the Amherst NGES is shown in Figure 56. At a dissipation test depth of 12.2 m and groundwater located at $z_w = 1$ m, the measured $t_{50} = 9.5$ min.

Using a standard adopted reference at 50% dissipation, the modified time factors are $T_{50}* = 0.118$ for Type 1 midface elements and $T_{50}* = 0.245$ for Type 2 shoulder elements. Then, the calculated coefficient of consolidation is determined from:

$$c_{vh} = \frac{T_{50} * \cdot a_c^{\,2} \cdot \sqrt{I_R}}{t_{50}} \tag{42}$$

where a_c = probe radius and $I_R = G/s_u$ = rigidity index of the soil. For a 15-cm^2 penetrometer, $a_c = 2.2$ cm. Using a value $I_R = 40$ and the measured $t_{50} = 9.5$ min gives $c_{vh} = 0.79$ cm^2/min. The SPM may also be used to fit the entire porewater decay curve, as shown on Figure 56.

If dissipation tests are carried out at select depth intervals during field testing, a fairly optimized data collection is achieved by the SCPTù, because five measurements of soil behavior are captured in that single sounding: q_t, f_s, u_b, t_{50}, and V_s. The results of a (composite) SCPTù in the soft Amherst clays are depicted in Figure 57. Here the results of a seismic cone sounding are augmented with data from a

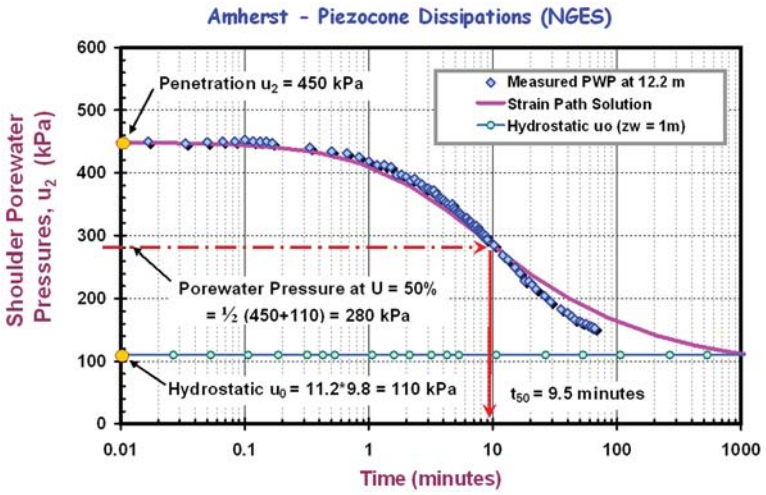

FIGURE 56 Measured dissipation at Amherst NGES and definition of t_{50} at 50% consolidation.

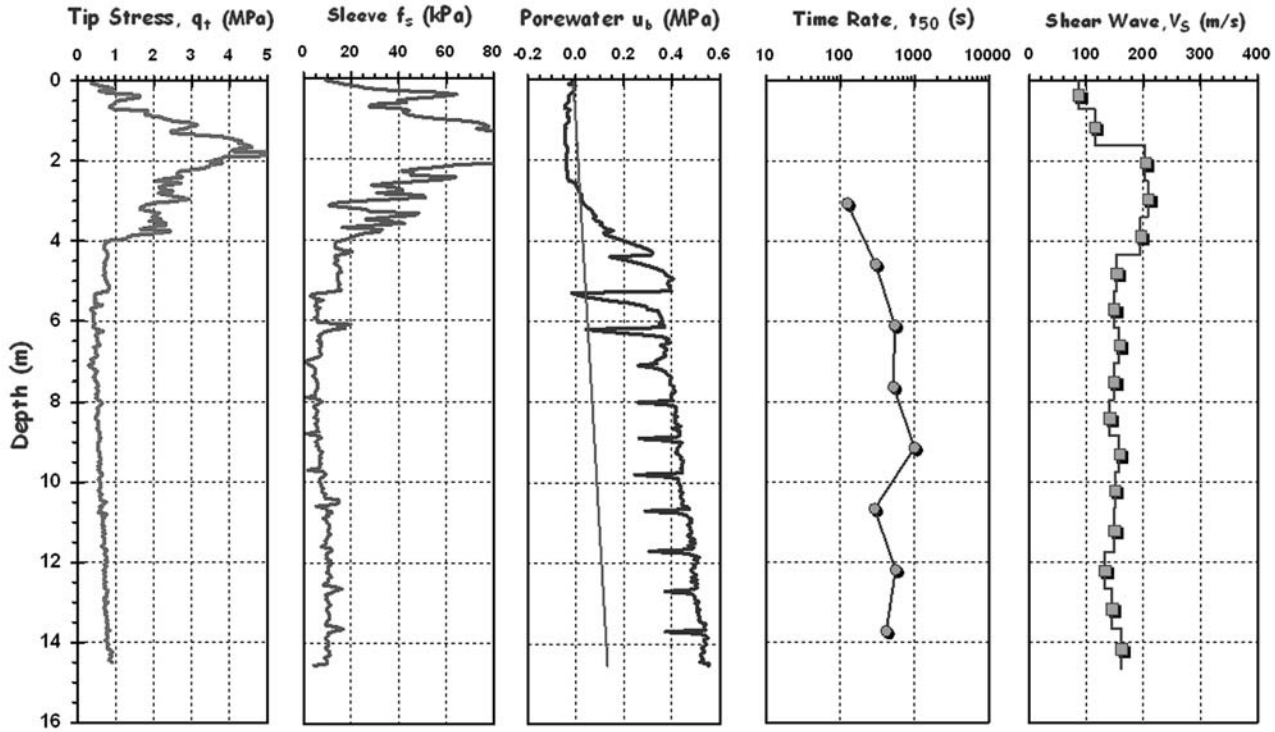

FIGURE 57 Seismic piezocone test with dissipations (termed SCPTù) at the Amherst soft clay test site.

separate series of dissipations conducted by DeGroot and Lutenegger (1994).

RIGIDITY INDEX

The rigidity index (I_R) of soil is defined as the ratio of shear modulus (G) to shear strength (τ_{max}). From considerations of cavity expansion theory and critical-state soil mechanics, the undrained value of rigidity index ($I_R = G/s_u$) in clay and silts can be evaluated directly from the CPTu data (Mayne 2001):

$$I_R = \exp\left[\left(\frac{1.5}{M} + 2.925\right)\left(\frac{q_t - \sigma_{vo}}{q_t - u_2}\right) - 2.925\right] \quad (43)$$

where $M = 6\sin\phi'/(3 - \sin\phi')$. As this is an exponential function, the derived values are particularly sensitive to accurate CPT measurements and therefore require proper saturations for the filter and cone assembly to obtain u_2 readings and correction of measured q_c to total q_t.

If undisturbed samples of the material are available, the rigidity index can be measured in laboratory DSS or triaxial compression tests on undisturbed samples or, alternatively, estimated from expressions based in critical state soil mechanics (Kulhawy and Mayne 1990). An empirical correlation for I_R developed from triaxial test data has been related to clay plasticity index and OCR (Keaveny and Mitchell 1986), as presented in Figure 58.

For sands, the operational rigidity index can be evaluated from the V_s measurement using calibrations based on undisturbed frozen sand specimens (Mayne 2006b).

PERMEABILITY

The permeability may be evaluated by means of the interrelationship with the coefficient of consolidation and constrained modulus (D') such that:

$$k = \frac{c_{vh} \cdot \gamma_w}{D'} \quad (44)$$

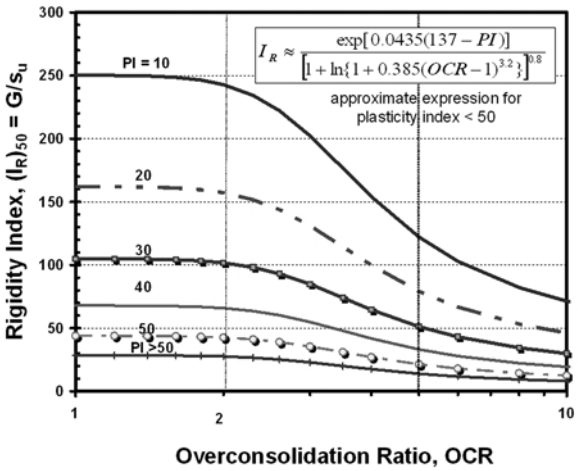

FIGURE 58 Evaluation of rigidity index from plasticity index and OCR (after Keaveny and Mitchell 1986).

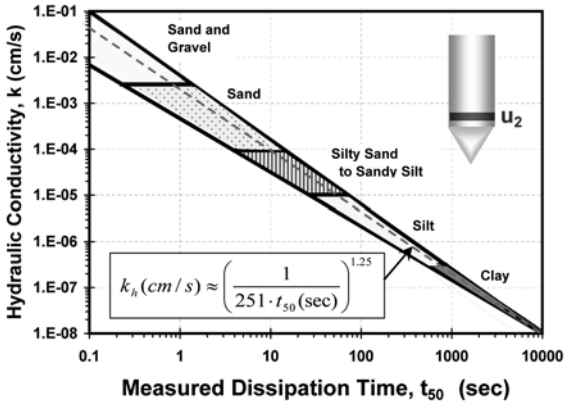

FIGURE 59 Direct evaluation of soil permeability from t_{50} measured in piezo-dissipation tests (after Parez and Fauriel 1988; Leroueil and Jamiolkowski 1991).

For this approach, results from piezo-dissipation testing are used together with an appropriate rigidity index to evaluate c_{vh}, and an estimate of D' is obtained from either of the relationships with net cone resistance or small-strain shear modulus (or both), as discussed previously.

Alternatively, a direct empirical method has been provided by Parez and Fauriel (1988) based on the measured t_{50} value from the dissipation curves, as presented in Figure 59. An approximate expression for the overall mean trend (dashed line) is also shown.

Some additional considerations in the evaluation of piezo-dissipation tests include (1) stress release of rods, and (2) dilatory responses. During the hydraulic push, pressure is placed on the cone rods in the advancing penetration. If a dissipation test is to be performed, then the rod pressure should likely be maintained during the time decay readings, because the release of the rod pressure may cause a stress drop in the initial readings. This is especially evident in Type 1 piezocone dissipation (Campanella and Robertson 1988); however, this can also occur in Type 2 readings conducted in stiff clays and silts.

For Type 1 piezocones, porewater decay with time is always monotonic (decreases with time). For Type 2 piezocone filters in soft to firm soils, a similar monotonic decay is observed. However, during Type 2 dissipation tests in stiff clays and silts, a dilatory response can occur, whereby the measured porewater pressures initally increase after the halt of penetration, climb to a peak value, then decrease with time. Interpretations of piezocone data for dilatory response are discussed by Sully and Campanella (1994) using an empirical approach and by Burns and Mayne (1998, 2002b) within a model based on cavity expansion and critical-state soil mechanics framework. For the latter, a simplified method to address this is presented in Mayne (2001).

OTHER SOIL PARAMETERS

A number of additional soil parameters may be determined from cone penetration results, yet are beyond the scope covered herein. Some guidance toward reference sources that address selected parameter topics is given in Table 4.

ADDITIONAL CONSIDERATIONS: LAYERED SOIL PROFILES

When pushing a cone penetrometer in layered soils, the advancing probe will sense portions of a deeper layer before that stratum is physically reached. For instance, the tip resistance in a uniform clay underlain by sand will register an increase in q_t before the sand layer is actually penetrated. Similarly, a cone advancing through a sand layer underlain by softer clay will start to "feel" the presence of the clay before actually leaving the sand; therefore, the q_t will reduce as the lower clay is approached.

The result is that there will be an apparent false sensing of soil interfaces when CPTs are conducted in layered stratigraphies having large contrasts between different soil types. Efforts to investigate these relative effects have been made using numerical simulations by finite-element analyses

TABLE 4
ADDITIONAL GEOTECHNICAL PARAMETERS DETERMINED BY CPT

Soil Parameter	Reference	Remarks
Attraction, $a' = c' \cot\phi'$	Senneset et al. (1989)	Defined as intercept from plot of net resistance ($q_t - \sigma_{vo}$) vs. effective overburden (σ_{vo}'). Related to c' (below)
California Bearing Ratio	Pamukcu and Fang (1989); Amini (2003)	Relates to pavement design
Effective Cohesion Intercept, c'	Senneset et al. (1988)	Mohr–Coulomb strength parameter. Relates to attraction term above.
Modulus of Subgrade Reaction, k_s	Newcomb and Birgisson (1999)	*NCHRP Synthesis 278*
Resilient Modulus, M_R	Mohammad et al. (2002)	Used in the design of highway pavement sections
State Parameter of Sands, Ψ	Been et al. (1986, 1987, 1988)	Critical state approach for sands
Strain Rate and Partial Saturation	Randolph (2004)	Conduct CPTu twitch testin g" at variable rates of penetration

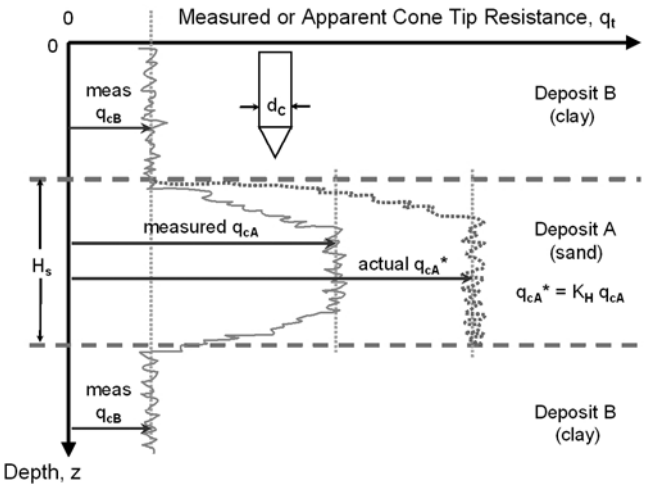

FIGURE 60 Situation of thin-layer effect on measured cone tip resistance (after Robertson and Wride 1998).

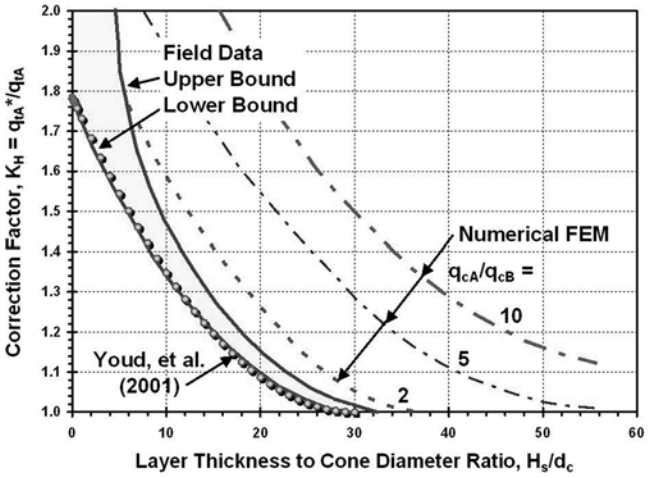

FIGURE 61 Thin-layer correction factor based on numerical (Vreugdenhil et al. 1994) and field CPT data (after Ahmadi and Robertson 2005).

(e.g., Vreugdenhil et al. 1994) and experimentally using miniature CPTs in chamber tests with alternating deposited layers of sand and clay.

In the case of a sand layer that is sandwiched between upper and lower clay layers, Ahmadi and Robertson (2005) discussed the means to correct the apparent measured q_{tA} in the sand to an equivalent q_{tA}* for full thickness layer. The problem is depicted in Figure 60, as per Robertson and Wride (1998). The apparent measured value of cone tip resistance in the middle sandy layer (q_{tA}) is influenced by the value of apparent cone resistance in the clay layers (q_{tB}), the thickness of the sand (H_s), and the diameter of the penetrometer (d_c). Results from numerical simulations and limited field data are presented in Figure 61. A recommended conservative correction is given by the lower bound that can be expressed as:

$$q_{tA}^* = q_{tA}\,\{1 + 0.25\,[0.059(H_s/d_c) - 1.77]^2\} \qquad (45)$$

Of course, it should also be realized that modern electronic piezocone testing involves three or more continuous recordings with depth. Thus, the interface layering can be best ascertained by cross referencing the q_t, f_s, and u_2 readings of the CPTu next to a carefully controlled log from an adjacent soil test boring and evaluated within the context of the available engineering geology understanding of the region.

CHAPTER SEVEN

CONE PENETRATION TESTING FOR SHALLOW FOUNDATIONS AND EMBANKMENTS

CPT is directly suited to evaluating ground response for support of shallow foundations and embankments. According to the results of the study survey (see Figure 5), the top two major uses of CPT by the DOTs include embankment stability and investigations for bridge foundations. In both cases, the CPT is first employed to delineate the subsurface stratigraphy, soil layering, and groundwater regime. Afterwards, the digital data are post-processed to provide numerical values.

This chapter addresses the application of CPT penetration data for (1) calculating the magnitudes of BC and settlements of shallow spread footing foundations, and (2) embankment stability, magnitude of consolidation settlements, and time rate of consolidation.

As noted previously, CPTu offers an excellent means for profiling the subsurface geostratigraphy to delineate soil strata and detect lenses, thin layers, and sand stringers. Figure 62 provides an example of a piezocone record for an Idaho DOT bridge and embankment construction. This sounding was conducted to an extraordinary final penetration depth of 80 m (262 ft) below grade. The exceptional detailing of the silty clay with interbedded sand layers and small stringers is quite evident.

Results from multiple soundings can be combined to form cross-sectional subsurface profiles over the proposed construction area. These are needed to evaluate the thickness and extent of compressible soil layers in calculating the magnitudes of settlements and time duration for completion for embankments and shallow foundation systems. Figure 63 shows a representative cross section derived from four CPT soundings at a test embankment site, clearly indicating the various strata designated A through F with alternating layers of clays, sands, and silts.

SHALLOW FOUNDATIONS

For shallow spread footings, the CPT results can be used in one of two ways to evaluate bearing capacity: (1) rational (or indirect) CPT methods, or (2) direct CPT methods.

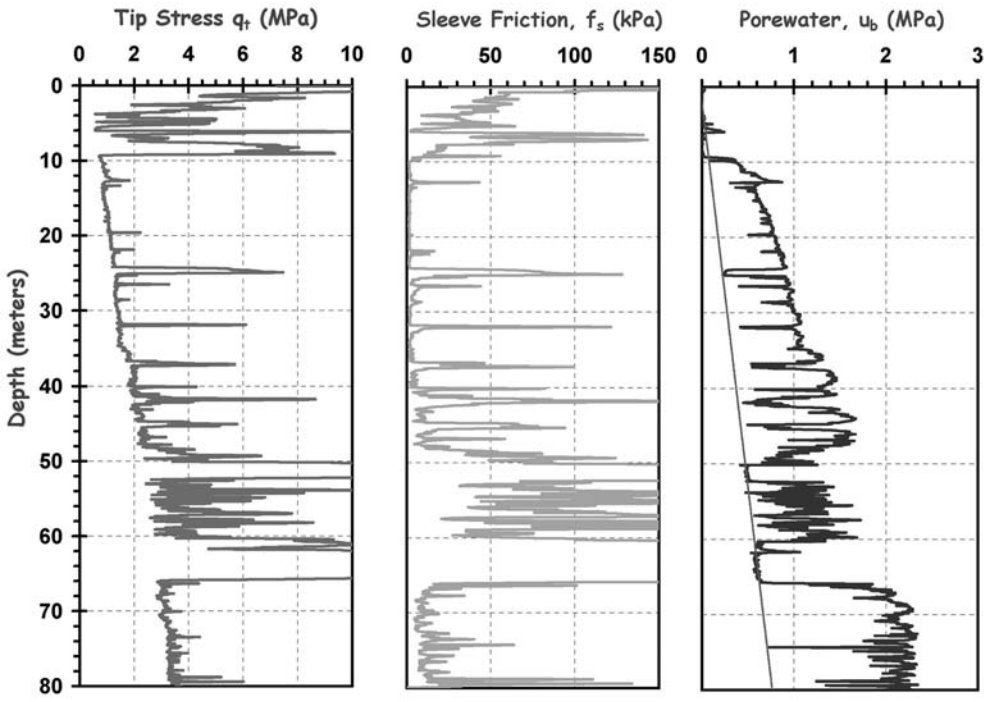

FIGURE 62 Representative piezocone sounding for soil layering detection at Sandpoint, Idaho.

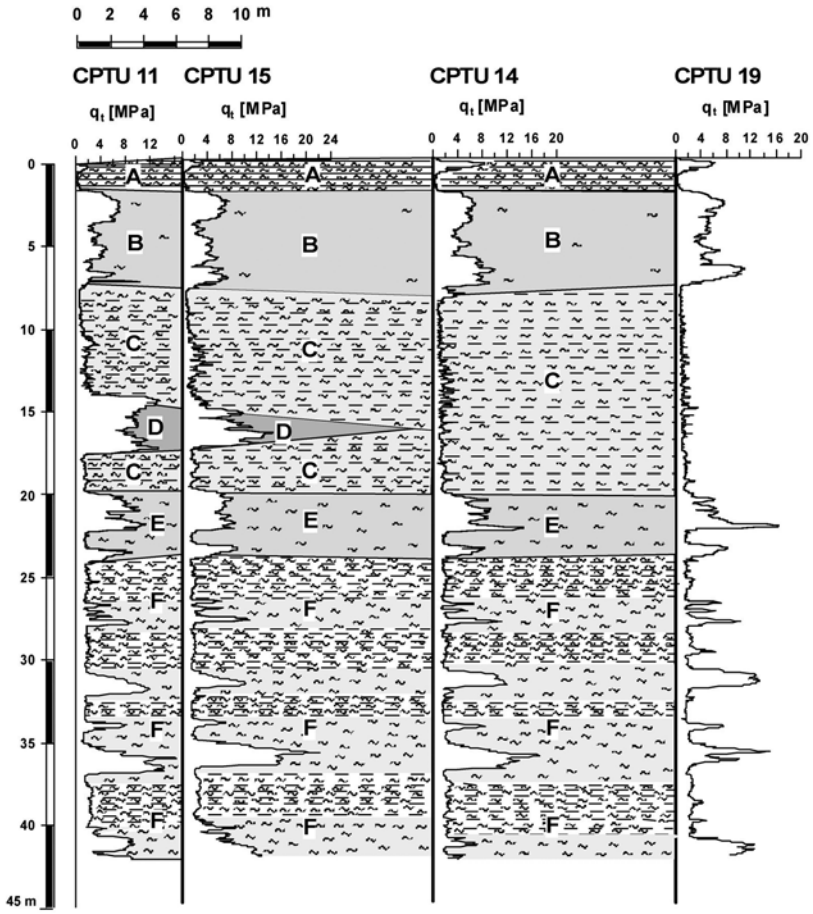

FIGURE 63 Subsurface cross section developed from piezocone soundings at Treporti Embankment (Gottardi and Tonni 2004).

In the rational (indirect) approach, the measured CPT resistances are used to assess soil engineering parameters (c', ϕ', s_u), which are subsequently input into traditional theoretical BC equations. In practice, these BC solutions are based in limit equilibrium analyses, theorems of plasticity, and cavity expansion. Most recently, it has become feasible to use numerical modeling simulations by finite elements (e.g., PLAXIS, CRISP, and SIGMA/W) or finite differences (e.g., FLAC) toward this purpose. The CPT data could be post-processed to provide relevant input parameters for these simulations. For the calculation of foundation settlements, the CPT results are post-processed to provide an equivalent soil modulus for use in elastic continuum theory or an alternate approach using compressibility parameters in an e-logσ_v' framework, also in combination with elastic theory (Bousinessq) to provide calculated stress distributions beneath the surface loaded footing.

In a direct CPT approach, the CPT readings are employed within a methodology that outputs the ultimate bearing capacity directly. The method may be based either on one of the aforementioned theories or else empirically derived from statistical evaluations of field foundation performance.

For both approaches, the allowable bearing stress of the footing (q_{allow}) is obtained by dividing the ultimate bearing capacity (q_{ult}) by an adequate factor of safety (FS): $q_{allow} = q_{ult}/FS$. It is normal geotechnical practice to adopt $FS \geq 3$ for shallow foundations. An alternative to the application of the FS approach is the use of load resistance factored design (LRFD). In simplistic terms, the resistance factor (RF) is used as a reduction term: $q_{allow} = RF \cdot q_{ult}$, where in essence it is the reciprocal of the safety factor, $RF = 1/FS$. However, there are two major improvements offered by LRFD: (1) the RF takes on differing values depending on the quality and source of the data being used in the evaluation, and (2) multiple RF values are utilized on different components of the calculated capacity. For instance, assume that the ultimate stress depends on two calculated components: $q_{ult} = q_x + q_z$. Then, the allowable stress might be ascertained as $q_{allow} = RF_x \cdot q_x + RF_z \cdot q_z$. The assigned RF values are based on risk and reliability indices. Details on the LRFD approach are given by Goble (2000).

Rational or Indirect Cone Penetration Testing Approach for Shallow Foundations

For the rational CPT approach, the limit plasticity BC solution of Vesić (1975) and elastic continuum solutions (Harr

1966; Poulos and Davis 1974) for foundation displacements will be adopted herein.

For BC problems, it is common practice to address short-term loading of clays and silts under the assumption of undrained conditions, whereas drained loading conditions are adopted for sands and gravels. Technically, however, all soils are geological materials and therefore drained loading will eventually apply to clays, silts, sands, and gravels that are very old. The undrained condition will be the critical case for footings situated over soft clays and silts, because of relatively fast rates of loading relative to the low permeability of these soils; therefore, volumetric strains are zero ($\Delta V/V_0 = 0$). However, for overconsolidated materials, either drained or undrained conditions may prove to be the critical case; therefore, both should be checked during analysis. For static loading conditions involving sands, the relatively high permeability allows for drained response ($\Delta u = 0$). In the case of seismic loading of sands, however, it is possible for undrained BC to happen during large earthquakes, especially if liquefaction occurs. In all cases, the drained and undrained BC calculations proceed in the same manner. Drained and undrained cases are considered to be extreme boundary conditions; however, it is plausible that intermediate drainage conditions can arise (i.e., semi-drained, partly undrained).

For undrained loading conditions, the ultimate bearing stress for shallow footings and mats situated on level ground can be calculated as:

$$q_{ult} = {}^*N_c \, s_u \tag{46}$$

where the bearing factor ${}^*N_c = 5.15$ for a strip foundation and ${}^*N_c = 6.14$ for square and circular foundations. The value of undrained shear strength (s_u) is taken as an average from the bearing elevation to a depth equal to one footing width (B = smaller dimension) below the base of the foundation. The simple shear mode (s_{uDSS}) is appropriate and should be calculated using the three-tiered hierarchy, as discussed previously.

For drained BC of shallow foundations where $c' = 0$, the appropriate equation is:

$$q_{ult} = \tfrac{1}{2} B \, {}^*\gamma \, {}^*N_\gamma \tag{47}$$

where the bearing factor ${}^*N_\gamma$ is a function of effective stress friction angle (ϕ') and footing shape (see Figure 64). In the case of rectangular footings, the plan dimensions are length (denoted "c" or "A") and width (denoted "d" or "B"). The appropriate value of soil unit weight (${}^*\gamma$) depends on the depth of the groundwater (z_w) relative to the bearing elevation of the footing. If the foundation has a width B and bears at a depth z_e below grade, then the operational unit weight may be determined as follows:

1. $z_e \le z_w$, then: ${}^*\gamma = \gamma_{sat} - \gamma_w$ = effective unit weight (also, submerged or buoyant unit weight)
2. $z_w \ge (z_e + B)$, then: ${}^*\gamma = \gamma_{total}$, where $\gamma_{total} = \gamma_{dry}$ for sands; yet $\gamma_{total} = \gamma_{sat}$ in clays with capillarity
3. $z_e < z_w < (z_e + B)$, then: ${}^*\gamma = \gamma_{total} - \gamma_w \cdot [1 - (z_w - z_e)/B]$

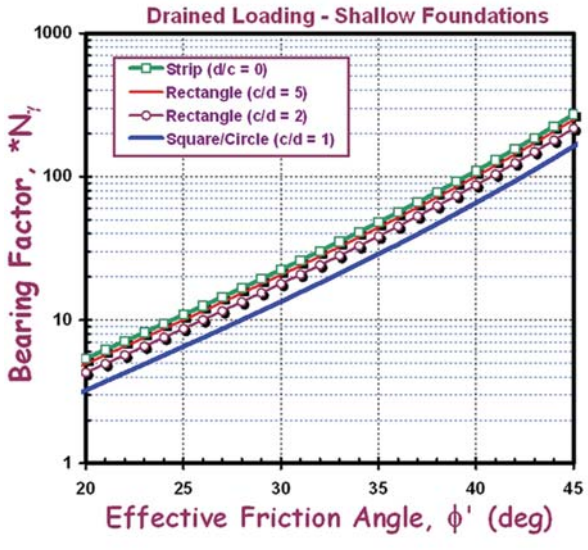

Bearing Factor, *Nγ		
ϕ' (deg)	Strip Footing	Circle or Square
20.0	5.39	3.23
21.0	6.19	3.72
22.0	7.13	4.28
23.0	8.20	4.92
24.0	9.44	5.66
25.0	10.87	6.52
26.0	12.54	7.52
27.0	14.47	8.68
28.0	16.71	10.03
29.0	19.33	11.60
30.0	22.40	13.44
31.0	25.99	15.59
32.0	30.20	18.12
33.0	35.17	21.10
34.0	41.05	24.63
35.0	48.01	28.81
36.0	56.29	33.77
37.0	66.16	39.70
38.0	77.99	46.79
39.0	92.20	55.32
40.0	109.36	65.61
41.0	130.15	78.09

FIGURE 64 Bearing factor for shallow foundations under drained loading (Vesić Solution).

With the appropriate *FS*, the applied stress q is determined and used to evaluate the displacement of the foundation at working loads. For the simple case of a flexible rectangular foundation resting on the surface of a homogenous layer (modulus E constant with depth), which has finite thickness, the elastic continuum solution for the centerpoint displacement (s_c) is:

$$s_c = \frac{q \cdot d \cdot I_H \cdot (1 - v^2)}{E_s} \tag{48}$$

where the equivalent elastic modulus and Poisson's ratio are appropriately taken for either undrained conditions (immediate distortion) or drained settlements (owing to primary consolidation). That is, the use is synonymous with the e-logσ_v' approach within the context of recompression settlements owing to the close interrelationship of D' and E', plus the standard utilization of elastic theory for calculating stress distributions (Fellenius 1996, updated 2002). Displacement influence factors for various distortions of rectangles of length "*c*" and width "*d*" are given by Harr (1966) and shown in Figure 65 for a compressible layer of thickness "*h*." Also, an approximate solution using a spreadsheet integration of the Boussinesq equation is also given by the method described by Mayne and Poulos (1999), with excellent agreement.

Additional variables that can be considered in the evaluation of displacements beneath shallow footings and mats include: (1) soil modulus increase with depth (i.e., "Gibson Soil"), (2) foundation rigidity, (3) embedment, and (4) approximate nonlinear soil stiffness with load level. In a simplified approach, Mayne and Poulos (1999) showed that the first three of these factors could be expressed by:

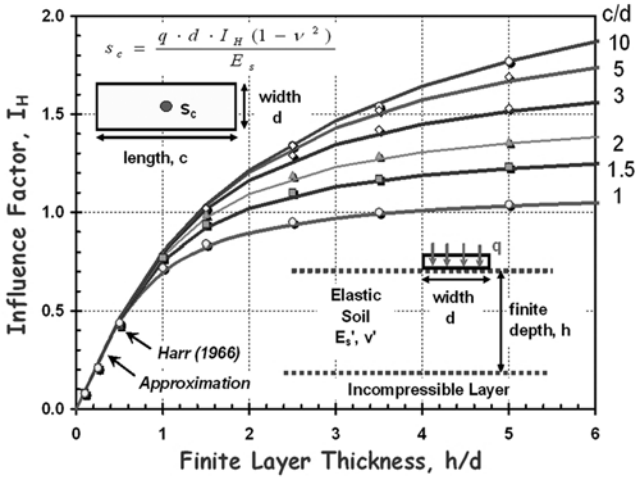

FIGURE 65 Displacement influence factors for flexible rectangular surface loading over finite layer.

$$s_c = \frac{q \cdot d_e \cdot I_{GH} \cdot I_F \cdot I_E \cdot (1 - v^2)}{E_{so}} \tag{49}$$

where d_e = diameter of an equivalent circular foundation in plan area [$A_F = c \cdot d = \pi(0.5d_e)^2$], the factor I_{GH} = displacement influence factor, I_F = modifier for relative foundation flexibility, I_E = modifier for foundation embedment, and E_{so} = soil modulus at the bearing elevation of the foundation base. Relevant terms are defined in Table 5 with the elastic displacement influence factor for homogeneous to Gibson-type soil shown in Figure 66.

The analysis can proceed as an equivalent elastic analysis using an appropriate modulus (e.g., $D' = E'$ from Figure 33) or an approximate nonlinear approach can be taken by adopting

TABLE 5
TERMS FOR CIRCULAR SHALLOW FOUNDATION DISPLACEMENT CALCULATIONS

Term or Factor	Equation	Remarks/Notes
Soil Modulus, E_s	$E_s = E_{so} + k_E \cdot d$	E_{so} = modulus at footing bearing elevation, $k_E = \Delta E_s/\Delta z$ = rate parameter, d = equivalent diameter, and Homogeneous case: $k_E = 0$
Normalized Gibson Rate	$\beta_G = E_{so}/ k_E \cdot d$	Homogeneous case: $\beta_G \rightarrow \infty$
Elastic Displacement Factor	$I_{GH} \approx \frac{1}{[\frac{0.56}{\beta_G^{0.8}}] + [\frac{0.235}{(h/d)} + 1]^2}$	For finite homogeneous to Gibson-type soils where h = thickness of compressible layer
Foundation Rigidity Modifier	$I_F \approx \frac{\pi}{4} + \frac{1}{4.6 + 10K_F}$	K_F = footing rigidity factor $K_F = (\frac{E_{FDN}}{E_{s(av)}}) \cdot (\frac{t}{a})^3$, E_{FDN} = foundation modulus, t = thickness of foundation, a = ½, and d = footing radius
Foundation Embedment Modifier	$I_E \approx 1 - \frac{1}{3.5\exp(1.22\nu - 0.4)(1.6 + d/z_e)}$	z_e = depth of embedment

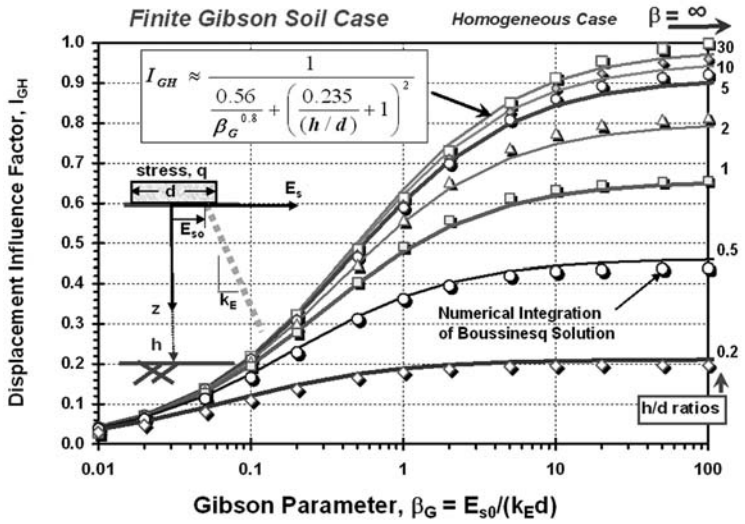

FIGURE 66 Displacement influence factor for finite homogeneous to Gibson-type soil for shallow circular footings and mat foundations.

the modified hyperbolic algorithm for modulus reduction with level of loading, as described previously (see Figure 32). Here, the magnitude of mobilized shear stress (τ/τ_{max}) can be evaluated as the level of applied loading to ultimate stress from the BC calculations, which is equal to the reciprocal to the calculated factor of safety: $q/q_{ult} = 1/FS$. Combining this aspect into the generalized equation gives:

$$s_c = \frac{q \cdot d_e \cdot I_{GH} \cdot I_F \cdot I_E \cdot (1-\nu^2)}{E_{max} \cdot [1-(q/q_{ult})^g]} \tag{50}$$

where the exponent g may be assumed to be on the order of 0.3 ± 0.1 for uncemented sands and fine-grained silts and clays of low to medium sensitivity. This approach has been used successfully in the prediction of footings on sands (e.g., Fahey et al. 1994; Mayne 1994) and clays (e.g., Mayne 2003).

Direct Cone Penetrating Testing Approaches for Shallow Foundations

The CPT point resistance is a measure of the ultimate strength of the soil medium. Therefore, by means of empirical methodologies and/or experimental studies, a direct relationship between the measured CPT q_t and foundation BC (q_{ult}) has been sought (e.g., Sanglerat 1972; Frank and Magnan 1995; Lunne and Keaveny 1995; Eslami 2006). Here, two methods will be presented: one each for sands and clays.

For shallow footings on sands, Schmertmann (1978a) presents a direct relationship between q_{ult} and q_t (shown in Figure 67) as long as the following conditions are met relative to foundation embedment depth (z_e) and size (B):

- When $B > 0.9$ m (3 ft), embedment $z_e \geq 1.2$ m (4 ft).
- When $B \leq 0.9$ m (3 ft), then embedment $z_e \geq 0.45$ m + $\frac{1}{2}$ B [or $z_e \geq 1.5' + \frac{1}{2}$ B (ft)].

For the range of measured cone tip resistances $20 \leq q_t \leq 160$ tsf, the ultimate BC stresses can be approximated by:

$$\textit{Square footings}: \quad q_{ult} = 0.55\ \sigma_{atm}\ (q_t/\sigma_{atm})^{0.785} \tag{51}$$

$$\textit{Strip footings}: \quad q_{ult} = 0.36\ \sigma_{atm}\ (q_t/\sigma_{atm})^{0.785} \tag{52}$$

where σ_{atm} = reference stress equal to one atmosphere (1 atm = 100 kPa ≈ 1 tsf).

For shallow footings on clays, Tand et al. (1986) defined a parameter R_k as follows:

$$R_k = \frac{q_{ult} - \sigma_{vo}}{q_t - \sigma_{vo}} \tag{53}$$

which is obtained from Figure 68. The term R_k depends on the embedment ratio (H_e/B), where H_e = depth of embedment and B = foundation width, as well as whether the clay is intact (upper curve) or fissured (lower curve).

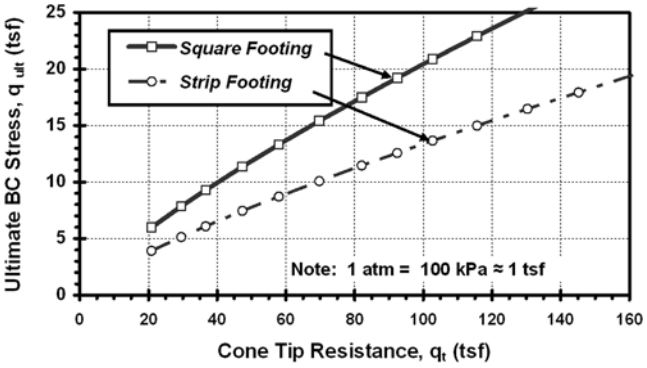

FIGURE 67 Direct relationship for ultimate bearing stress and CPT measured tip stress in sands (after Schmertmann 1978a).

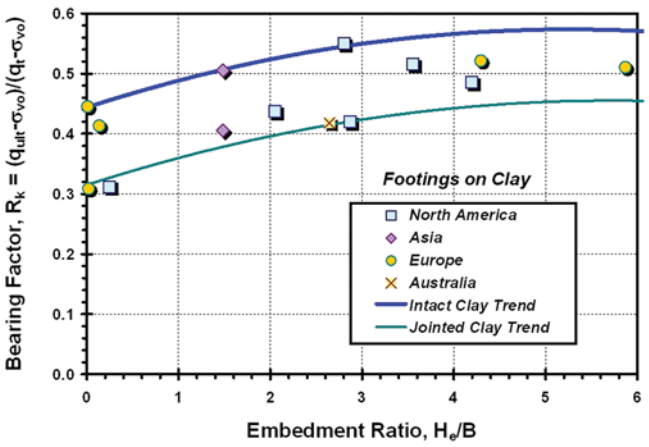

FIGURE 68 Direct CPT method for determination of ultimate bearing stresses on clay (Tand et al. 1986).

Rearranging, the BC for shallow foundations on clay becomes:

$$q_{\text{ult}} = \sigma_{vo} + R_k \cdot (q_t - \sigma_{vo}) \tag{54}$$

For the direct assessment of footing settlements at working loads by CPT, a number of methods have been proposed (e.g., Meyerhof 1965; Schmertmann 1970; Lunne and Keaveny 1995). Many of these approaches are a form of the elastic theory solution described earlier where the CPT resistance is used to provide a direct evaluation of modulus through:

$$D' \approx E' = \alpha\, q_t \tag{55}$$

or alternate form: $D' \approx \alpha_c\,(q_t - \sigma_{vo})$, as discussed previously. Notably, since q_t is actually a measure of strength, the use of the same measurement for estimating stiffness has noted a wide range in α values from as low as 0.4 for organic clays (Frank and Magnan 1995), $1 < \alpha < 10$ for clays and sands (Mitchell and Gardner 1975), to $\alpha = 40+$ for OC sands at low relative densities (Kulhawy and Mayne 1990). The use of $G_{\max}$ to obtain a relevant stiffness may therefore be more justifiable (e.g., Fahey et al. 1994).

Footing Case Study

A case study can be presented to show the approximate nonlinear load-displacement-capacity response from Eq. 50. Results are taken from the load test program involving large square footings on sand as reported by Briaud and Gibbens (1994). The large north footing ($B = 3$ m) can be used with data from SCPT conducted by the Louisiana Transportation Research Center, as reported by Tumay (1997) and presented in Figure 69. The site is located at Texas A&M University and underlain by clean sands to about 5 to 6 m, whereby the sands become slightly silty and clayey with depth. The groundwater table lies about 5.5 m deep. Results from the seismic cone testing indicate a representative mean value of cone tip resistance q_c (ave) = 7.2 MPa (72 tsf) and mean shear wave velocity V_s (ave) at approximately 250 m/s.

The calculation procedure is detailed in Figure 70. Using the direct Schmertmann CPT approach from Eq. 51, the ultimate bearing stress is calculated as $q_{\text{ult}} = 1.6$ MPa (16.6 tsf). Alternatively, the CPT data can be post-processed to determine an effective stress friction angle $\phi' = 40.1°$, which determines $q_{\text{ult}} = 1.7$ MPa (17.7 tsf) from Vesic BC solution from Eq. 47. The initial stiffness $E_{\max}$ is obtained from the shear wave velocity measurements and can be used in Eq. 50 to generate the curve in Figure 70. Good agreement is shown in comparison to the measured load-displacement response of the footing.

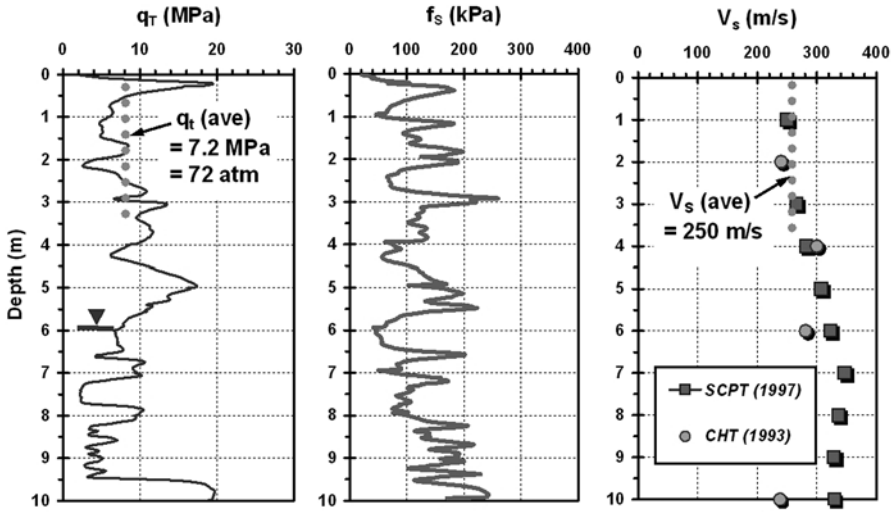

FIGURE 69 Results from seismic cone tests at Texas A&M experimental test site.

Texas A&M NGES - Sand Site - North Footing Load Test

INPUT PARAMETERS

Footing Width, B =	3	m
q_c (average) =	72	atm
V_s (average) =	250	m/s
Poisson's ratio, v' =	0.2	
Dry Unit Weight γ_d =	17.1	kN/m^3
Mass Density, ρ_T =	1.74	g/cc
$G_{max} = \rho_t V_s^2$ =	109	MPa
$E_{max} = 2G_{max}(1+\nu')$ =	262	MPa
$q_{ult} = 0.55\ (q_c)^{0.785}$ =	15.79	atm
$Q_{ult} = q_{ult} B^2$ =	14211	kN
Footing Area, A_f =	9	m^2
Equivalent d_e =	3.39	m
Influence I_{GH} =	1.00	
Flex Factor, I_F =	0.79	
Embed Factor, I_E =	0.99	
Influence, I_{GHFE} =	0.78	

q/q_{ult}	E/E_{max}	q (kPa)	Q (kN)	s (mm)
0.00	1.000	0	0.0	0.0
0.10	0.499	152	1.4	2.9
0.20	0.383	303	2.7	7.6
0.30	0.303	455	4.1	14.5
0.35	0.270	531	4.8	18.9
0.40	0.240	606	5.5	24.3
0.45	0.213	682	6.1	30.9
0.50	0.188	758	6.8	39.0
0.55	0.164	834	7.5	49.0
0.60	0.142	909	8.2	61.8
0.65	0.121	985	8.9	78.4
0.70	0.101	1061	9.5	100.9
0.75	0.083	1137	10.2	132.7
0.80	0.065	1213	10.9	180.7
0.85	0.048	1288	11.6	261.3
0.90	0.031	1364	12.3	423.1

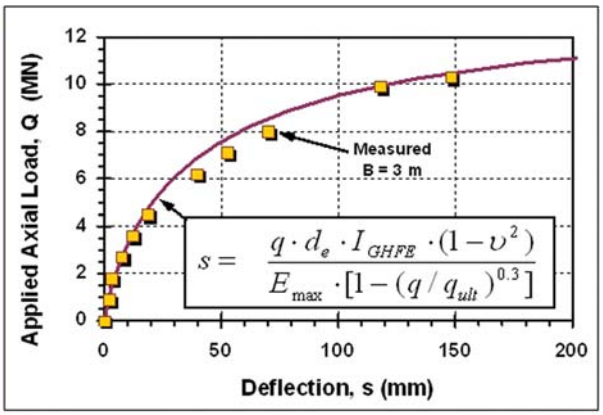

FIGURE 70 Calculated and measured response of large 3-m square footing at Texas A&M University sand site.

EMBANKMENT STABILITY AND SETTLEMENTS

In geotechnical practice, stability analyses of embankments are handled by limit equilibrium analyses, usually by trial and error search routines within computer software codes, such as UTEXAS4, GeoSlope, STABL, and others. Settlements resulting from the primary consolidation of the underlying soft ground are calculated using one-dimensional consolidation theory to evaluate both their magnitudes and time rate behavior. The key advantages of using CPTu for embankment settlement calculations include: (1) the ability to obtain a continuous profile of OCR in soft ground, and (2) in situ assessment of c_{vh} from dissipation testing.

Displacements Beneath Embankments

For embankments on soft ground it is common practice to use elastic theory to calculate the magnitudes of undrained distortion (immediate displacements), as detailed by Foott and Ladd (1981). These displacements are determined in the same manner as described previously for shallow footings, but apply displacement influence factors that account for the side slopes and height of the embankment. The stiffness is assessed in terms of an undrained soil modulus (E_u) and corresponding $\nu_u = 0.5$.

The calculation of consolidation settlements can proceed in a similar manner using elastic theory with the appropriate displacement influence factors (Poulos and Davis 1974) and a drained stiffness (E') and drained Poisson's ratio (ν'), provided that the applied embankment stresses do not exceed the natural preconsolidation stresses: $\sigma_{vo}' + \Delta\sigma_v' < \sigma_p'$. At the centerpoint of the embankment, the total vertical displacements for undrained distortion and drained primary consolidation settlements, plus additional displacements resulting from long-term creep, are then given by:

[undrained distortion] [drained settlements] [secondary compression]

$$s_c = \frac{q \cdot d \cdot I_H' \cdot (1-v_u^2)}{E_u} + \frac{q \cdot d \cdot I_H' \cdot (1-\nu'^2)}{E'} + s_{creep} \quad (56)$$

The calculation of long-term displacements caused by creep can be assessed from:

$$s_{creep} = \frac{C_{\alpha e}}{(1+e_o)} \cdot \Delta z \cdot \log(t) \quad (57)$$

where Δz = thickness of layer undergoing creep, t = time, and $C_{\alpha e}$ = coefficient of secondary consolidation. Extensive lab testing on various soils has shown the ratio of $C_{\alpha e}/C_c$ is constant for a given NC soil (Mesri 1994; Leroueil and Hight 2003), including $C_{\alpha e}/C_c = 0.025 \pm 0.01$ for sands, $C_{\alpha e}/C_c = 0.04 \pm 0.01$ for inorganic clays and silts, and up to $C_{\alpha e}/C_c = 0.06 \pm 0.01$ for organic materials. The same constant also applies to that soil in overconsolidated states, but uses the recompression index in the ratio; that is, $C_{\alpha e}/C_r = 0.04$ for inorganic clays.

In the case of embankment loadings where the imposed earth loadings exceed the preconsolidation stresses, either the special method described by Schmertmann (1986) can be used, or else the conventional calculations for one-dimensional consolidation owing to primary settlements:

Drained settlements:

$$s_c = \frac{C_r}{(1+e_o)} \cdot \Delta z \cdot \log(\text{OCR}) + \frac{C_c}{(1+e_p)} \cdot \Delta z \cdot \log(\sigma_{vf}'/\sigma_p') \quad (58)$$

The CPTu is particularly suited to the in situ and continuous profiling of the effective preconsolidation stress (σ_p') and corresponding OCRs with depth, thus aiding in a more definitive calculation of settlements. In contrast, determining OCRs from oedometer and/or consolidometer testing are rather restricted, as only discrete points are obtained in limited numbers because of high costs in sampling, time, and laboratory

testing budgets. In addition, sample disturbance effects tend to lower and flatten the e-logσ_v' curves and imply yield values that are lower than true in situ σ_p' profiles (Davie et al. 1994).

Embankment Stability

Stability analyses of embankments include: (1) the evaluation of the soft ground conditions beneath large fills, and (2) the constructed embankment itself, with adequate side slopes and use of suitable soil fill materials. For the underlying natural soft ground, the CPTu can provide the profile of preconsolidation stress that controls the undrained shear strength for the stability analysis:

$$s_{u\text{DSS}} \approx 0.22\ \sigma_p' \tag{59}$$

that applies for OCRs < 2, as described previously.

For control of constructed fills, the CPTu can be used as a measure of quality control and quality assurance. This is perhaps advantageous when large fills are made using the hydraulic fill process (e.g., Yilmaz and Horsnell 1986).

Time Rate Behavior

Large areal fills and embankments constructed over soft ground may require long times for completion of primary consolidation, ranging from months to tens of years, depending on the thickness of the consolidating layer, coefficient of consolidation, and available drainage paths. Results from CPTu soundings can provide information on layer thickness, presence of lower sand drainage layers, and the detection of sand lenses or stringers that may promote consolidation. Dissipation testing by CPTù helps assess c_{vh} needed in the one-dimensional rate of consolidation analysis, as well as the calculated spacing of vertical wick drains, sand drains, or stone columns that may be required by the geotechnical engineer to expedite the consolidation process.

The time for completion of one-dimensional consolidation for a doubly drained soil layer (top and bottom) can be estimated from:

$$t = T_v\, h_p^2/c_v \tag{60}$$

where $T_v \approx 1.2$ = time factor (assuming 96% consolidation is essentially "complete") from one-dimensional vertical consolidation and h_p = drainage path length (= one-half layer thickness for double drainage). Time factors for other percentage degrees of consolidation are given by Holtz and Kovacs (1981) with approximations cited as:

$$U < 60\%: \quad T_v \approx 0.785(U\%/100)^2 \tag{61a}$$

$$U \geq 60\%: \quad T_v \approx 1.781 - 0.933 \log(100 - U\%) \tag{61b}$$

CHAPTER EIGHT

APPLICATIONS TO PILINGS AND DEEP FOUNDATIONS

In one viewpoint, the cone penetrometer can be considered as a mini-pile foundation, whereby the measured point stress and measured sleeve resistance correspond to the pile end bearing and component of side friction. Therefore, the analysis of pile foundations can be accomplished using classical soil mechanics principles (i.e., by means of "indirect CPT" assessments of s_u, K_0, tanϕ', α factor, and β factor), or by "direct CPT" methods, whereby the measured readings are scaled up for evaluation of full-size pilings. The two concepts are depicted in Figure 71. A review of various methods is summarized here, particularly noting newly available approaches that have recently been developed. Emphasis is on the axial pile response (compression and tension modes); however, mention of lateral and moment loading will also be made.

From those DOTs responding to the questionnaire summary, approximately 68% use the results for axial pile capacity determinations (see Figure 72). The DOTs employ various direct CPT methods (28%), indirect methods (11%), and both methods (29%). Additional details on the methodologies used are given in Appendix A.

The axial compression capacity of deep foundations is derived from a combination of side resistance and end bearing (Poulos and Davis 1980). For axial uplift or tension loading, the analysis may consider only the side resistance component. For undrained loading, the side resistance in compression and uplift will generally be of the same magnitude. For drained loading, numerical and analytical studies supplemented by experimental results have shown that the magnitude of unit side resistance in tension is from 70% to 90% of that in compression loading (DeNicola and Randolph 1993) primarily as a result of a Poisson effect. Calculation procedures given subsequently refer to compression-type loading.

The summation of the unit side resistances acting along the perimetric area of the sides of the pile shaft provides the total shaft capacity (Q_s). The unit side resistance (f_p) of driven piles and drilled and bored shafts can be calculated using the in situ CPT results by either direct methods or rational (indirect) approaches, or both. Likewise, the unit end-bearing resistance (q_b) of driven pilings or drilled piers can be evaluated by direct or indirect methods to obtain the capacity at the toe or base (Q_b). The total axial capacity is obtained as shown in Figure 71.

Prior reviews on selected available direct and indirect approaches for evaluating axial pile capacity from CPT results are given by Robertson et al. (1988) and Poulos [(1989), including the well-known alpha methods for clays and beta methods for sands (e.g., Vesić 1977; Poulos and Davis 1980; O'Neill and Reese 1999)]. Although the basic concepts remain, many of the early studies were based on data obtained with mechanical or electrical friction-type penetrometers. The more recent utilization of piezocones, with three separate readings with depth, offers improved correlations for both rational and direct CPT analyses. One reason for these improvements is that the measured cone tip resistance is corrected for porewater pressures acting behind the tip, as detailed previously (Lunne et al. 1997). A second benefit relates to methodologies based on two or three readings (q_t, f_s, and/or u_2) to obtain axial capacities, as opposed to the older methods, many of which were based solely on q_c. Third, improved interpretation procedures for soil engineering parameters from CPTu have been introduced (Mayne 2005; Schnaid 2005). Finally, with two decades of use of the SCPTu, it has now become possible to provide an evaluation of the entire load-displacement-capacity curve for axial pile foundations.

RATIONAL OR INDIRECT CONE PENETRATION TESTING METHOD FOR AXIAL PILE CAPACITY

With the rational CPT method, the in-situ test data are used first to calculate soil parameters and properties, followed by engineering analyses of unit side resistance (f_p) and end-bearing resistance (q_b) within a theoretical framework. Commonly, total stress analyses (alpha method) are used in clays and effective stress approaches (beta method) applied to sands (Poulos 1989). However, the beta method has shown usefulness and reliability for all soil types (i.e., clays, silts, sands, and gravels). In a generalized beta method for different pile types and methods of pile installation, the unit pile side resistance is calculated (Kulhawy et al. 1983):

$$f_p = C_M \, C_K \, K_0 \, \sigma_{vo}' \, \tan\phi' \tag{62}$$

where C_M = modifier term for soil-structure interaction (pile material type), and C_K = modifier term for installation, as shown in Table 6. The relevant values for evaluating the lateral stress coefficient (K_0) and frictional characteristics (ϕ') for the soil layers from the CPT have been discussed in previous sections.

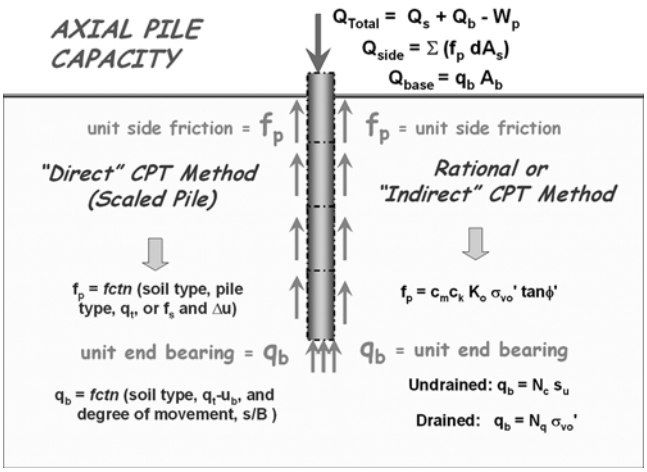

FIGURE 71 Direct CPT versus rational (or indirect) method for evaluating axial pile capacity.

The unit end bearing ($q_b = q_{ult}$) can be calculated from theoretical solutions for $*N_q$ based in limit plasticity or cavity expansion (e.g., Vesić 1977). The limit plasticity solution for undrained loading is given as:

$$\textit{Undrained}: q_b = *N_c \cdot s_u \tag{63}$$

where $*N_c = 9.33$ for circular or square foundations and s_u is the representative undrained shear strength beneath the foundation base from depth $z = L$ to depth $z = L + d$. For drained loading, q_b is a function of ϕ' and presented in Figure 73. For very large diameter piles in sands, especially drilled shaft foundations, the theoretical end-bearing resistance will not be realized within tolerable displacements. This is because the full mobilization of base resistance requires the toe/tip to undergo considerable movements on the order of $s \approx B$ for complete development of these resistances. Thus, reduction factors have been recommended for large-diameter drilled shafts and piles that result in only 5% to 15% of the calculated capacities that can be utilized under normal acceptable movements (e.g., Ghionna et al. 1993; Fioravante et al. 1995; Lee and Salgado 1999, 2003). As such, a practical value for end-bearing resistance at working loads is:

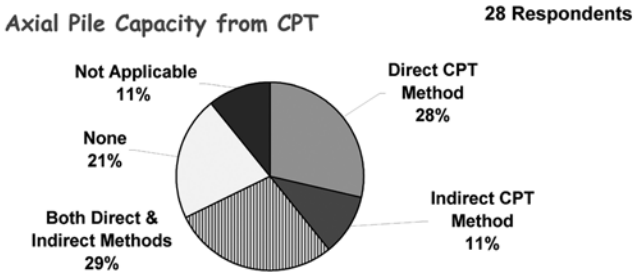

FIGURE 72 Survey results on DOT use of CPT for axial pile foundation design.

$$\textit{Operational drained}: \quad q_b = 0.1\, N_q \cdot \sigma_{vo}' \tag{64}$$

The total axial compression capacity ($Q_{total} = Q_{ult}$) of the deep foundation is calculated from:

$$Q_{ult} = Q_s + Q_b - WE = \Sigma\, (f_{pi}\, \pi\, d\, \Delta z_i) + q_b\, A_b - W \tag{65}$$

where Q_s = side capacity, Q_b = base capacity, W = weight of the pile, f_{pi} = unit side resistance at each soil layer, and A_b = base/toe area of the pile tip.

DIRECT CONE PENETRATION TESTING METHODS FOR AXIAL PILE CAPACITY

Several direct CPT procedures will be reviewed in this section, including the Laboratoire Central des Ponts et Chaussées (LCPC), Norwegian Geotechnical Institute–Building Research Establishment (NGI–BRE), Politecnico di Torino, Unicone, and Takesue methods.

Laboratoire Central des Ponts et Chaussées Method for Driven and Drilled Piles

For the CPT direct methods, the well-known LCPC was based on results from 197 pile load tests (Bustamante and Gianeselli 1982). The approach offers versatility in the variety and types of different deep foundation systems and geomaterials that can be accommodated, including driven, bored, jacked, high-pressure grouted, augered, and screwed piles. Table 7 lists the

TABLE 6
MODIFIER TERMS FOR PILE MATERIAL TYPE (C_M) AND INSTALLATION EFFECTS (C_K)

Pile Installation Effects Modifier C_K	Jetted pile	C_K = 0.5 to 0.6
	Drilled and bored piles	C_K = 0.9 to 1.0
	Low-displacement driven piles (e.g., H-piles; open-ended pipe)	C_K = 1.0 to 1.1
	High-displacement driven piles (e.g., closed-ended pipe; precast)	C_K = 1.1 to 1.2
Pile Material Effects Modifier C_M	Soil/rough concrete (drilled shafts)	C_M = 1.0
	Soil/smooth concrete (precast)	C_M = 0.9
	Soil/timber (wood pilings)	C_M = 0.8
	Soil/rough steel (normal H- and pipe pilings)	C_M = 0.7
	Soil/smooth steel (cone penetrometer)	C_M = 0.6
	Soil/stainless steel (flat dilatometer)	C_M = 0.5

Adapted after Kulhawy et al. 1983.

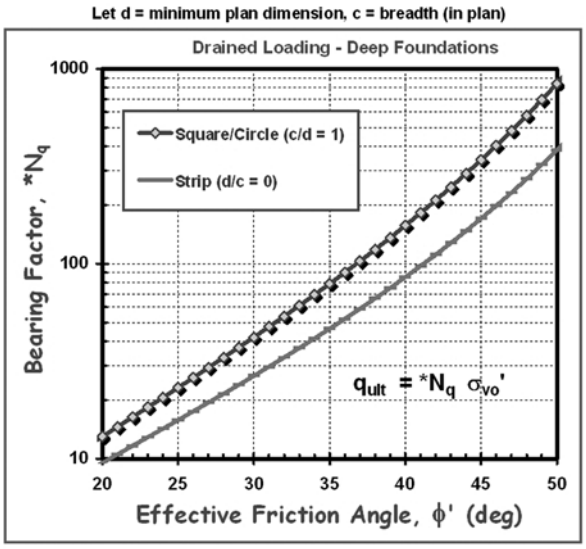

Bearing Factor, $^*N_q$		
ϕ' (deg)	Strip Footing	Circle or Square
20.0	9.53	12.99
21.0	10.54	14.58
22.0	11.65	16.36
23.0	12.89	18.36
24.0	14.27	20.62
25.0	15.80	23.17
26.0	17.51	26.05
27.0	19.41	29.31
28.0	21.55	33.00
29.0	23.94	37.21
30.0	26.63	42.01
31.0	29.67	47.49
32.0	33.09	53.77
33.0	36.98	60.99
34.0	41.40	69.32
35.0	46.43	78.94
36.0	52.19	90.11
37.0	58.81	103.12
38.0	66.43	118.32
39.0	75.24	136.17
40.0	85.48	157.20

FIGURE 73 End-bearing resistance from limit plasticity solution (after Vesić 1977).

various pile categories. The LCPC method has a primary reliance on q_c for evaluating f_p along the pile sides and for q_b beneath the pile toe. Specifically, the end bearing is determined from:

$$\textit{LCPC unit end bearing}: \quad q_b = k_c \cdot q_c \tag{66}$$

The reduction factor k_c is obtained from the pile type and ground conditions, and averages 0.35 ± 0.2. Full details for obtaining f_p and q_b are given in Bustamente and Gianeselli (1982). For piles in soils, Table 8 provides the k_c factors using a simplified LCPC approach (Frank and Magnan 1995; Bustamente and Frank 1997). Summary graphical approaches for unit side friction (f_p) by the LCPC method are provided by Poulos (1989) and are presented in Figures 74 and 75, respectively, for clays and sands. Additional details on the appropriate design values and the specific averaging procedures to obtain a characteristic q_c beneath the pile tip, particularly for layered soil profiles, are discussed by Lunne et al. (1997).

Norwegian Geotechnical Institute–Building Research Establishment Method for Driven Piles in Clay

An empirical approach for driven piles in clay has been developed jointly by the NGI, Oslo, and BRE, London. Using the total cone resistance, Almeida et al. (1996) related the driven pile side resistance in clays to total cone tip stress. In an updated form given by Powell et al. (2001), the side friction is obtained from:

$$\textit{Clays}: \quad f_p = \frac{q_t - \sigma_{vo}}{10.5 + 13.3 \log Q} \tag{67}$$

where Q = normalized cone tip resistance. The unit end bearing (q_b) is determined from:

TABLE 7
VARIOUS PILE CATEGORIES FOR LCPC DIRECT CPT METHOD

Pile Category	Type of Pile
IA	Plain bored piles, mud bored piles, hollow auger bored piles, case screwed piles, Type I micropiles, piers, barrettes
IB	Cased bored piles, driven cast piles
IIA	Driven precast piles, prestressed tubular piles, jacked concrete piles
IIB	Driven steel piles, jacked steel piles
IIIA	Driven grouted piles, driven rammed piles
IIIB	High pressure grouted piles (d > 0.25 m), Type II micropiles

TABLE 8
BASE BEARING CAPACITY FACTORS k_c FOR LCPC DIRECT CPT METHOD

Soil Type	Nondisplacement Pile	Displacement Type Pile
Clay and/or Silt	0.40	0.55
Sand and/or Gravel	0.15	0.50

Simplified approach by Frank and Magnan (1995); Bustamante and Frank (1997).

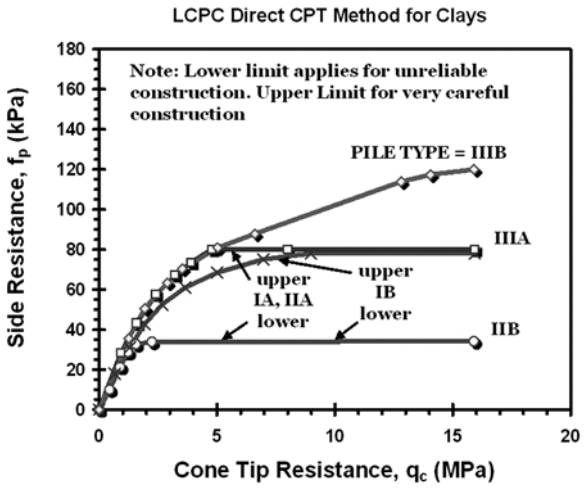

FIGURE 74 LCPC method for pile side resistance evaluation from CPT in clays (based on Bustamante and Gianeselli 1982; adapted from Poulos 1989).

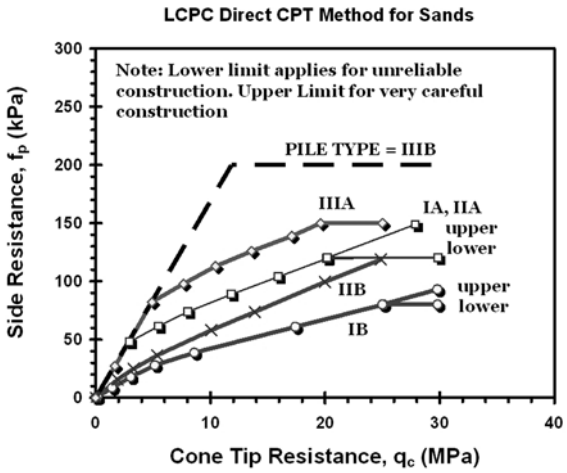

FIGURE 75 LCPC method for pile side resistance evaluation from CPT in sands (based on Bustamante and Gianeselli 1982; adapted from Poulos 1989).

$$Clays: \quad q_b = \frac{q_t - \sigma_{vo}}{k_2} \tag{68}$$

where $k_2 = N_{kt}/9$ and a value of $N_{kt} = 15$ is often appropriate for piles in soft to firm intact clays where DSS mode controls the bearing mechanism. However, in fissured to hard clays, N_{kt} may be as high as 25 to 35 (Powell and Quarterman 1988). Direct backfigured values of k_2 were reported to range from 1.5 to 3.4 for just three piles in intact clays (Almeida et al. 1996).

Politecnico di Torino Method for Drilled Shafts in Sand

A direct CPT method for drilled shafts in sands has been developed by the Politecnico di Torino, Italy. For clean quartzitic uncemented NC sands, the side resistance of drilled shafts may be estimated from the CPT resistance (Fioravante et al. 1995), where an average trend can be represented by:

$$Sands: \quad f_p\,(\text{MPa}) \approx \left(\frac{q_t\,(\text{MPa})}{274} \right)^{0.75} \tag{69}$$

The unit end bearing depends on the actual movement of the base, yet can be taken as approximately 10% of the cone resistance: $q_b \approx 0.10 q_t$ (e.g., Ghionna et al. 1993). In this regard, an improved relationship has been developed by Lee and Salgado (1999) based on numerical analyses. Neglecting the minor effects of sand relative density, an average relationship can be expressed by:

$$Sands: \quad q_b \approx \frac{q_t}{1.90 + \dfrac{0.62}{(s/d)}} \tag{70}$$

where s = pile base deflection and d = pile base diameter. A nominal value of $s/d = 0.10$ is often taken for a relative capacity, thereby giving $q_b \approx 0.12 q_t$ and in general agreement with the aforementioned. An updating of this approach is presented by Jamiolkowski (2003).

Unicone Method for Driven and Bored Piles

A generalized direct CPTu method for sands, silts, and clays has been proposed by Eslami and Fellenius (1997, 2006) based on 106 load tests from both driven and bored piling foundations. The method uses all three piezocone readings (q_t, f_s, and u_2). In this Unicone approach, the soils are classified into one of five SBT zones according to their effective cone resistance ($q_E = q_t - u_2$) and sleeve friction (f_s) according to Figure 76.

For each layer, the unit side resistance is obtained from:

$$f_p = C_{se} \cdot q_E \tag{71}$$

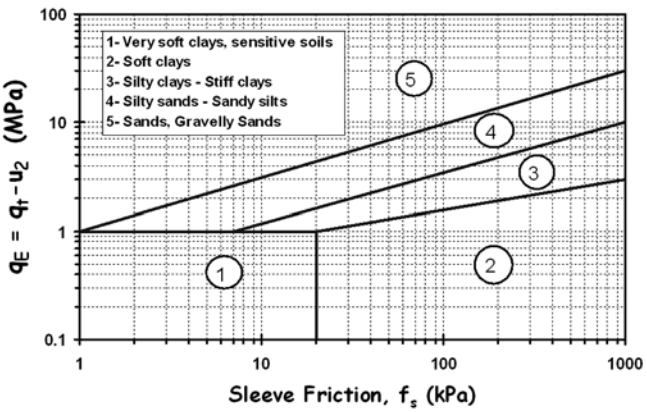

FIGURE 76 Unicone chart to determine zone number and soil type (after Eslami and Fellenius 1997).

TABLE 9
UNICONE METHOD FOR SOIL TYPE, ZONE, AND ASSIGNED SIDE FRICTION COEFFICIENT

Zone No.	Soil Type	Side Factor, C_{se}
1	Soft sensitive soils	0.08
2	Soft clay and silt	0.05
3	Stiff clay and silt	0.025
4	Silty sandy mixtures	0.01
5	Sands	0.004

where C_{se} = the side correlation coefficient obtained from Table 9. The unit end-bearing resistance can be obtained from the effective cone tip resistance beneath the pile toe:

$$q_b = C_{te} \cdot (q_t - u_b) \tag{72}$$

where C_{te} = toe correlation coefficient, generally taken equal to 1. If the CPT record indicates high spikes and variability in the effective cone resistance profile, Eslami and Fellenius (1997) recommend the use of a geometric mean for averaging readings, rather than the more common arithmetic mean. The geometric mean is given by:

$$q_E \text{ (ave)} = [q_{E1} \cdot q_{E2} \cdot q_{E3} \cdot \cdots \cdot q_{E1}]^{(1/n)} \tag{73}$$

where n = number of data.

Takesue Method for Driven and Drilled Piles

In the method of Takesue et al. (1998), the unit pile side resistance (f_p) is estimated from the measured CPT f_s, which is scaled up or down depending on the magnitude of the measured CPT excess porewater pressures (Δu_2), as presented in Figure 77. The data used to derive the correlation were obtained from both bored and driven pile foundations in clays, sands, and mixed ground conditions. As such, the method has been shown to work well in the nontextbook sandy silts to silty fine sandy soils of the Atlantic Piedmont residuum (e.g., Mayne and Elhakim 2003) that typically show negative CPTu porewater pressure during penetration. From Figure 77, the scaling factors are divided into two porewater pressures regimes at $\Delta u_2 = 300$ kPa, with a maximum $\Delta u_2 < 1200$ kPa.

The Takesue method does not specifically indicate a means for evaluating unit end bearing of piles; therefore, either the aforementioned NGI–BRE, LCPC, Torino, or Unicone methods could be used for that purpose.

OTHER DIRECT CONE PENETRATION TESTING METHODS FOR AXIAL CAPACITY

A number of new direct CPT methods for driven piles in sands have emerged recently from work funded by the offshore oil industry, including: (1) Imperial College Pile (ICP) Method (Jardine et al. 2005); (2) UWA Procedure (Lehane et al. 2005); (3) NGI Method (Clausen et al. 2005); and (4) Fugro Method (Kolk et al. 2005).

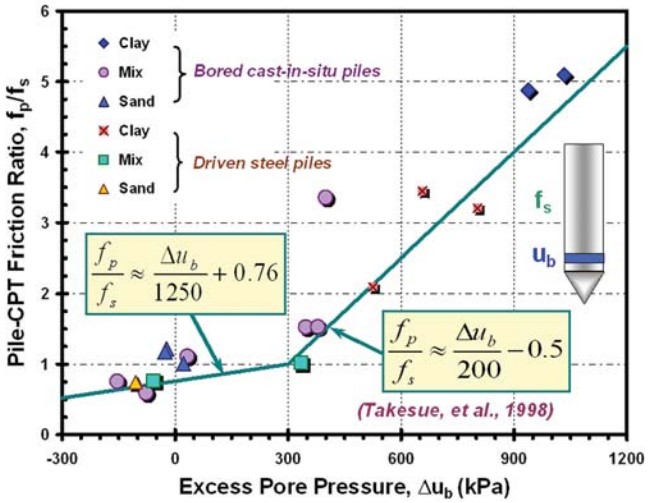

FIGURE 77 Direct CPTu method for evaluating side friction of bored and driven piles in different soils (after Takesue et al. 1998).

For evaluating driven piles in clay from CPT data, new interpretative approaches include: (1) ICP method (Jardine et al. 2005), and (2) the NGI Method (Karlsrud et al. 2005).

Caution should be exercised when using any calculated pile capacity method without proper checking and validation. On critical projects, verification by full-scale load tests and/or calibration at well-established experimental test sites may be warranted by the particular DOT.

FOUNDATION DISPLACEMENTS

The load-displacement behavior of deep foundations subjected to loading may be analyzed using empirical, analytical, and/or numerical methods. In all cases, data input on the soil parameters and geostratigraphy must be supplied. Elastic continuum theory is one popular method that is also consistent with the analysis of shallow foundation systems, as discussed in the next section.

Elastic Continuum Solutions

Elastic continuum theory provides a convenient means for representing the load-displacement response of pile foundations under axial loading, as well as lateral loading and moments (Poulos and Davis 1980). An approximate closed-form solution has been developed that can account for axial piles either floating or end-bearing, situated in homogeneous or Gibson-type soils, as well as accommodate pile compressibility effects and belled pier situations (Randolph and Wroth 1978, 1979; Fleming et al. 1992). For a pile of diameter d and length L residing within an elastic medium, the top displacement (w_t) is given by:

$$w_t = \frac{Q_t \cdot I_\rho}{d \cdot E_s} \tag{74}$$

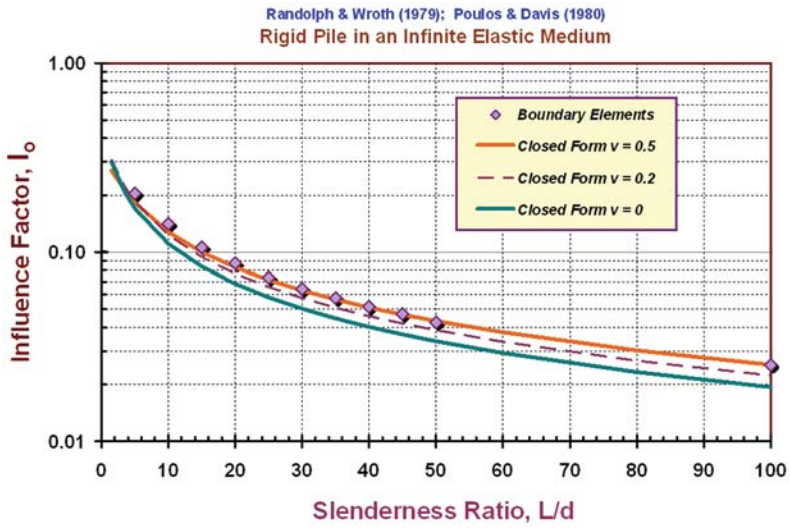

FIGURE 78 Displacement influence factors for rigid pile in homogeneous soil.

where Q_t = applied axial load and I_ρ = displacement influence factor. For the simple case of a rigid pile embedded in a homogeneous soil:

$$I_\rho = \frac{1}{\frac{1}{1-\upsilon^2} + \frac{\pi}{(1+\upsilon)} \cdot \frac{(L/d)}{\ln[5(L/d)(1-\upsilon)]}} \tag{75}$$

where Figure 78 shows that the classic boundary element solution (Poulos and Davis 1980) agrees well with the approximate closed-form approach.

By the closed-form solution, the percentage of total load at the top (Q_t), which is transferred to the toe or base (Q_b), is given by:

$$\frac{Q_b}{Q_t} = \frac{I_\rho}{1-\upsilon^2} \tag{76}$$

For the more generalized case involving friction- to end-bearing type shafts and homogeneous to Gibson soil profiles with E_s either constant or increasing with depth, and pile compressibility effect, the specific solutions for I_ρ and percentage load transfer to the tip or toe (Q_b/Q_t) are given elsewhere (Randolph and Wroth 1978, 1979; Fleming et al. 1992; O'Neill and Reese 1999; Mayne and Schneider 2001).

Approximate Nonlinear Pile Load Displacements

The stiffness of soils is highly nonlinear at all levels of loading. The most fundamental stiffness is that measured at small strains (Burland 1989), as it represents the beginning of all stress-strain curves at the initial state. The small-strain modulus (E_{max}) combined with the aforementioned modified hyperbola (exponent $g = 0.3 \pm 0.1$) for modulus reduction allows for an approximate nonlinear load-displacement-capacity representation of the form:

$$w_t = \frac{Q_t \cdot I_\rho}{d \cdot E_{max} \cdot [1-(Q_t/Q_{tu})^g]} \tag{77}$$

With the utilization of SCPTs, the advantage here is that the CPT resistances (q_t, f_s, and u_2) are employed to determine the ultimate axial pile capacity (Q_{tu}) and the downhole shear wave velocity (V_s) is used to determine the initial stiffness (E_{max}). The ratio of applied axial load to the calculated axial capacity represents the reciprocal of the current factor of safety: $(Q_t/Q_{tult}) = 1/FS$. The overall concept of this procedure is depicted in Figure 79, whereby all four readings of the SCPTu are used in evaluating the response of the deep foundation under axial compression loading.

Illustrative Example

An application of the methodology will be shown for a drilled shaft foundation constructed at the NGES near Opelika, Alabama. The facility is operated for the Alabama DOT. The natural soils consist of residuum of the Atlantic Piedmont geologic province, comprised of fine sandy silts and silty fine sands derived from the in-place weathering of the underlying parent gneiss and schist bedrock. A representative SCPTU from the site is presented in Figure 80 (Mayne and Brown 2003).

A dry cased-type installation was used to form the drilled shaft foundation with a diameter of 0.914 m (3.0 ft) and embedment length L = 11 m (36 ft). The shaft was load tested in axial compression and results are reported by Brown (2002). Using the Takesue et al. (1998) method for side resistance, the CPT-measured f_s is reduced to an oper-

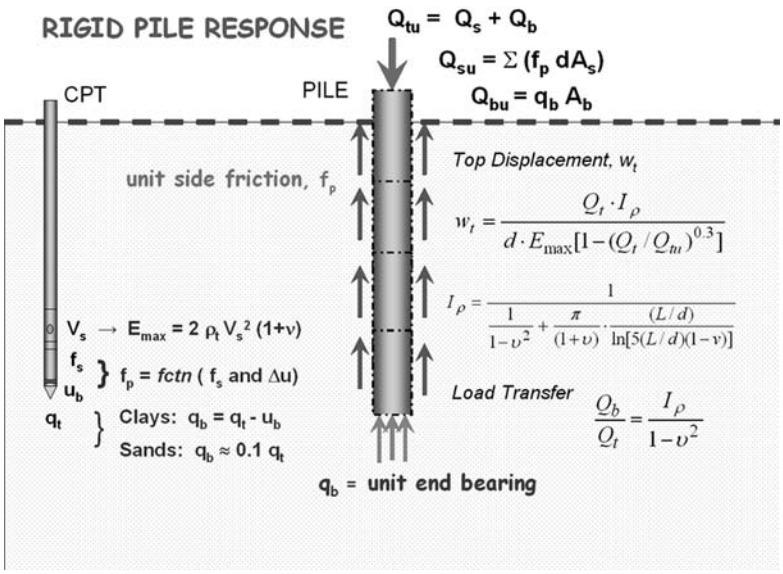

FIGURE 79 Concept of using SCPTu for evaluating an approximate nonlinear axial pile response.

ational pile side friction of f_p = 96 kPa (1 tsf) because of the CPTu-measured negative Δu throughout most of the profile. With the pile side area A_s = 31.6 m^2 (340 ft^2), the total side capacity is Q_s = 3032 kN (340 tons). Because these soils drain relatively rapidly, an equivalent sand method is considered applicable. Therefore, the end bearing resistance is taken as 10% of the measured cone tip stress beneath the foundation base (average q_t = 3380 kPa = 35 tsf). With a base area A_b = 0.66 m^2 (7.1 ft^2), the total end bearing capacity is Q_b = 223 kN (25 tons). This gives a total axial compression capacity: $Q_t = Q_s = Q_b$ = 3255 kN (365 tons).

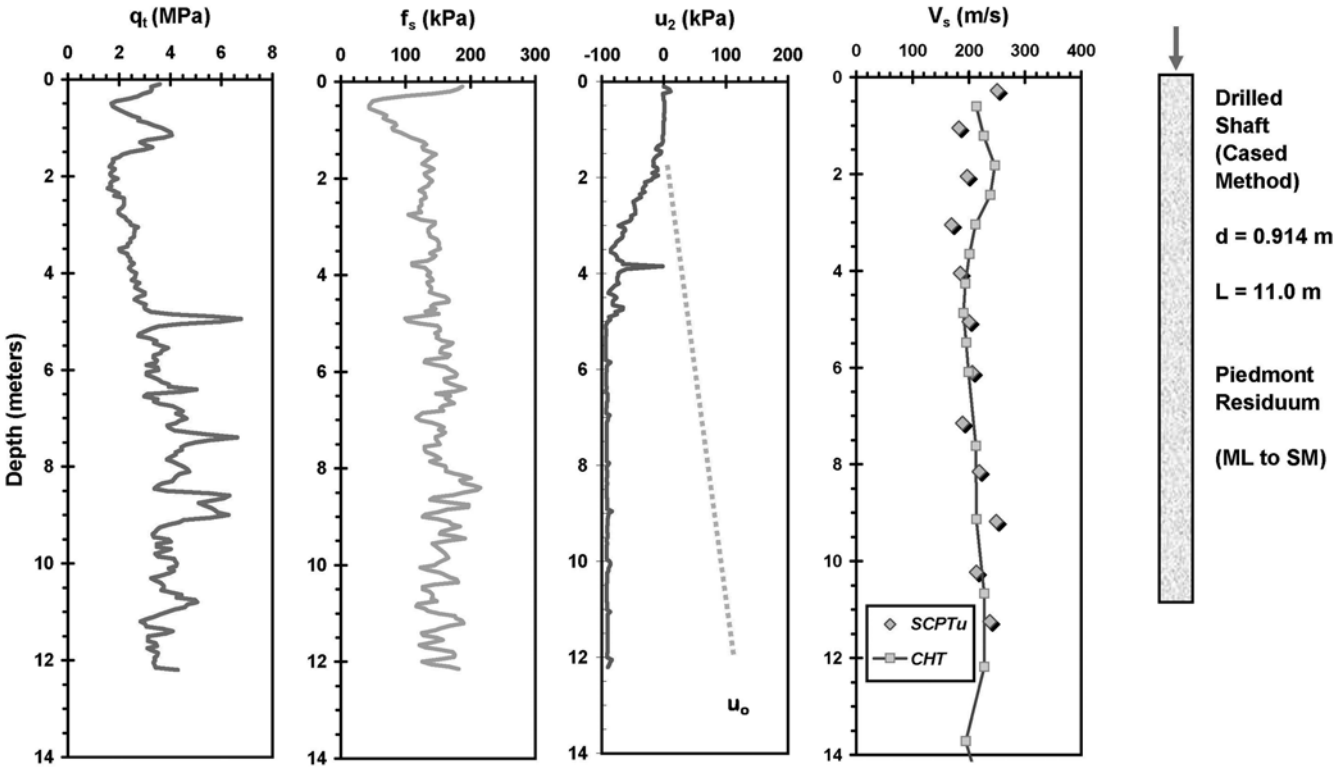

FIGURE 80 Representative SCPTU in Piedmont residuum at the NGES, Opelika, Alabama.

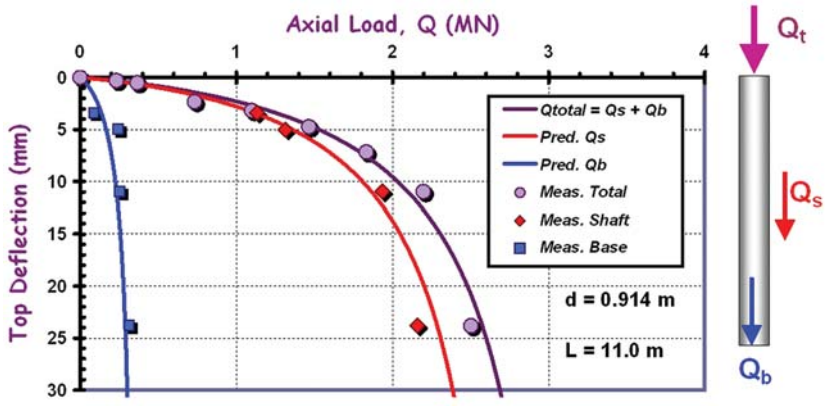

FIGURE 81 Measured and SCPTu-predicted axial response of Opelika drilled shaft.

Adopting a homogenous case for the modulus variation with depth, a representative shear wave velocity of V_s = 216 m/s (708 ft/s) with a corresponding total mass density ρ_T = 1.7 g/cc and drained ν' = 0.2 gives an initial small-strain stiffness of E_{max} = 190 MPa (1979 tsf). Results of the equivalent elastic continuum method with the modulus reduction scheme (g = 0.3) is presented in Figure 81. It can be seen that the overall axial load-displacement response is in excellent agreement with the measured top-down shaft response. The elastic continuum solution appropriately proportions the amounts of load transfer carried by the sides and base components. In addition, the modified hyperbola nicely fits the observed nonlinear response of the deep foundation.

CHAPTER NINE

CONE PENETRATION TESTING USE IN GROUND MODIFICATION

During ground modification works, the soil is changed in its condition, consistency, and/or properties from its initial state. In situ testing by CPT allows quantification of the level and degree of quality control and effectiveness of the site improvement program. The quality assurance can be checked by simple and direct comparisons between the original CPT measurements and results taken following site improvement. Alternatively, with its strong theoretical basis and documented calibrations with laboratory test data, the CPT can be used to provide engineering parameters for reevaluation of the completed works and modified ground conditions. Selected applications of ground modification techniques that have benefited from CPT verification programs for these purposes are addressed in this chapter. Table 10 lists a number of different site improvement techniques and representative reference sources for additional details on the results.

An important aspect of quality control testing is to realize that time effects may occur after implementation of the site improvement program. Therefore, it may be necessary to conduct a series of CPTu soundings at various times after the ground modification has been applied to properly quantify the degree of effectiveness and to fully appreciate the benefits of the improvement program (Mitchell 1986).

An example of the use of CPTs to detail the depth and degree of improvement following dynamic compaction at a resort development near San Juan is shown in Figure 82. At this site, dynamic compaction was carried out using a 15-ton weight dropped repeatedly from 18 m height. The cone tip and sleeve resistances both show improvement occurring to depths of 7 m (22 ft) below grade, whereas the porewater measurements and friction ratio show little change.

The average cone tip resistance following site improvement by dynamic compaction depends on the applied energy intensity over the project site area. This energy intensity (U_E) can be calculated as the sum of the energy per drop (W·H), times number of drops per grid (n), divided by the area of the area treated:

$$U_E = \Sigma\,(n \cdot W \cdot H)/s^2 \tag{78}$$

where s = spacing per grid, W = weight of falling mass, and H = drop height. For sands, Figure 83 shows the observed trend between final average q_t within the depth of improvement versus the applied U_E for a number of deep dynamic compaction projects.

TABLE 10
SELECTED GROUND MODIFICATION METHODS AND RELEVANCE OF CPT FOR QUALITY ASSURANCE AND QUALITY CONTROL

Ground Modification Method	Reference Source	Use of CPT
Blast Densification	Mitchell (1986)	Quantify time increases with q_t
Compaction of Trench Backfill	Islam and Hashmi (1995)	Determine relative compaction
Compact Natural Sands by Rollers	Alperstein (2001)	CPTs to quantify improvement
Compaction Grouting	Chun et al. (2003)	CPTUs for check on remediation of foundation settlements
Controlled Modulus Columns	Plomteux et al. (2004)	CPTs for initial investigation; columns too hard for CPTs after cement grouting
Deep Soil Mixing	Puppala and Porhaba (2004); Puppala et al. (2004)	Quality assurance and verification
Dynamic Compaction	Ghosh (1995)	Quality control by CPT
	Huang et al. (1998)	CPT for quality assurance
GeoPiers (rammed aggregate piers)	Lillis et al. (2004)	Piers in clay at NGES–Amherst
Jet Grouting	Collotta et al. (2004)	CPTs initially; too hard for CPTs after cement grouting
Stone Columns	Durgunoglu et al. (1995)	Quality control
	Chen and Bailey (2004)	Lessons in sands and silts
	Shenthan et al. (2006)	CPT before and after installation
Surcharging	Schneider and Mayne (2000)	Measure degree of improvement
Vibro-Compaction	Mitchell and Solymar (1984)	Measure CPT increases with time
	Alperstein (2001)	Verify sand condition by CPT
Vibro-Replacement	Howie et al. (2000)	SCPTU for degree of change
Wick Drains	Lutenegger et al. (1988)	Evaluate c_{vh} from dissipations

NGES = National Geotechnical Experimentation Site.

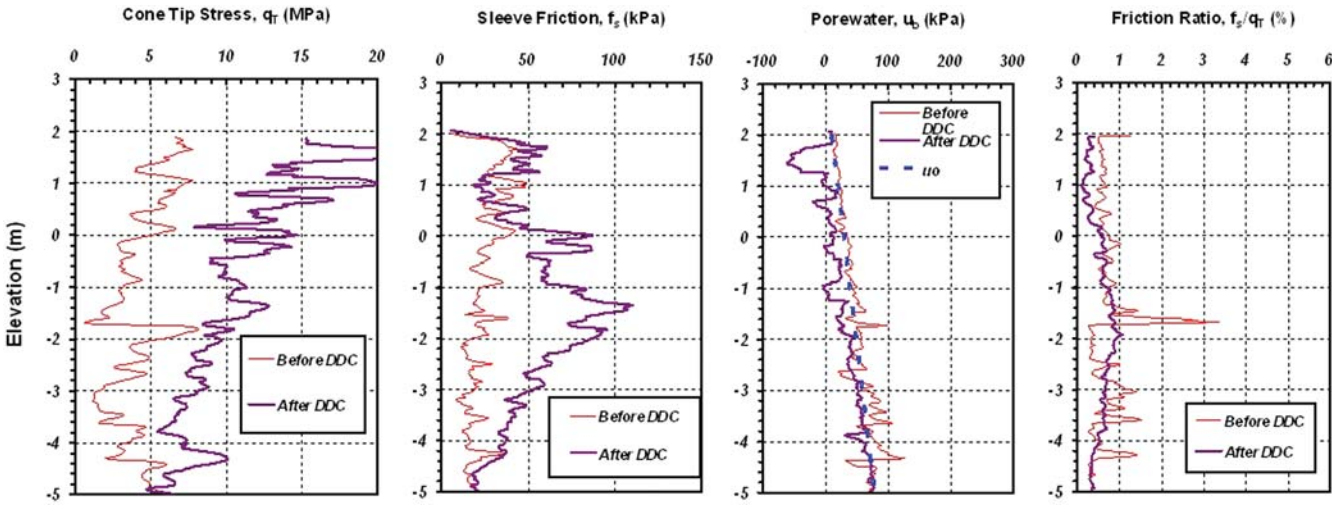

FIGURE 82 CPT results before and after dynamic compaction near San Juan, Puerto Rico.

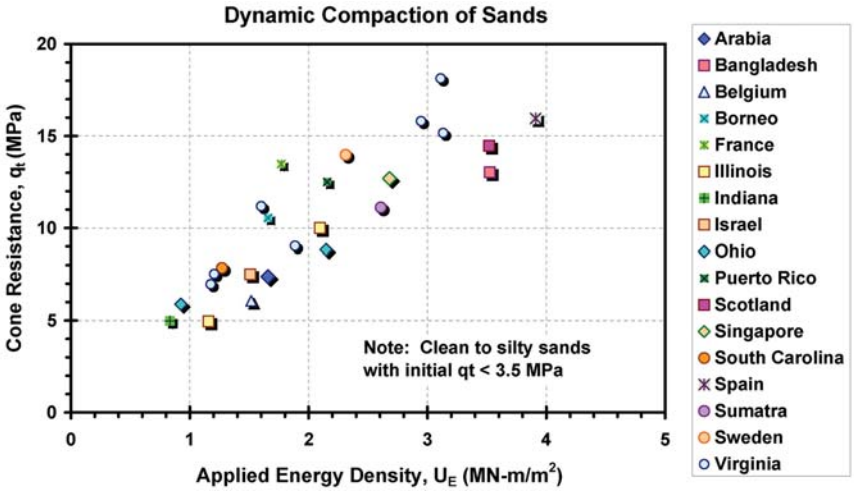

FIGURE 83 Measured cone tip stress in sands following ground improvement by dynamic compaction.

CHAPTER TEN

SEISMIC GROUND HAZARDS

For seismicity issues, the utilization of cone penetrometer technology, particularly the seismic piezocone, is described with reference to the following topics: (1) determination of soil stratigraphy and identification of potentially liquefiable soils, (2) collection of shear wave velocities for use in either *International Building Code* (IBC 2000) class or site-specific ground-shaking analyses, (3) deterministic and probabilistic means to assess soil liquefaction potential by stress-normalized cone tip resistance (q_{t1}), (4) deterministic and probabilistic means to assess soil liquefaction potential by stress-normalized shear wave velocity (V_{s1}), as well as (5) post-cyclic undrained strength of sands for stability considerations.

An attractive feature of the SCPTU is the ability to use the data directly in assessing the site-specific ground amplification of the soil column and evaluation of soil liquefaction potential in seismic regions. The small-strain stiffness ($G_0 = G_{max}$) is required input for determining the level of ground shaking by means of SHAKE, DEEPSOIL, RASCALS, DESRA, or other computer codes available for site amplification. Their output includes an evaluation of the applied ratio of cyclic shear stress normalized to effective overburden stress, termed the cyclic stress ratio: CSR = τ_{cyc}/σ_{vo}'. The amount of soil resistance available to counter the effects of liquefaction is represented by either the stress-normalized cone tip resistance (q_{t1}) or alternatively expressed by the stress-normalized shear wave velocity (V_{s1}). These can be compared with the cyclic resistance ratio (CRR) curves for natural sands to silty sands to assess the tendency or risk of liquefaction. The CRR line demarcates two regions corresponding to liquefaction-prone versus liquefaction-resistant. A clear advantage of the SCPTU is its ability to identify possible loose silty to clean sand layers within the subsurface profile and then provide the required measured values at the site (G_{max}, q_{t1}, and V_{s1}) for analysis, all from the same sounding. The procedure is illustrated in Figure 84.

IDENTIFICATION OF LIQUEFACTION PRONE SOILS

Soils that are prone or susceptible to liquefaction during large seismic events include loose young (i.e., Holocene) clean to silty sands below the groundwater table (Youd et al. 2001). The use of the aforementioned classification charts for SBT for the CPTu can be used to identify and delineate the sand and silty sand layers in the soil profile (e.g., Robertson 1990).

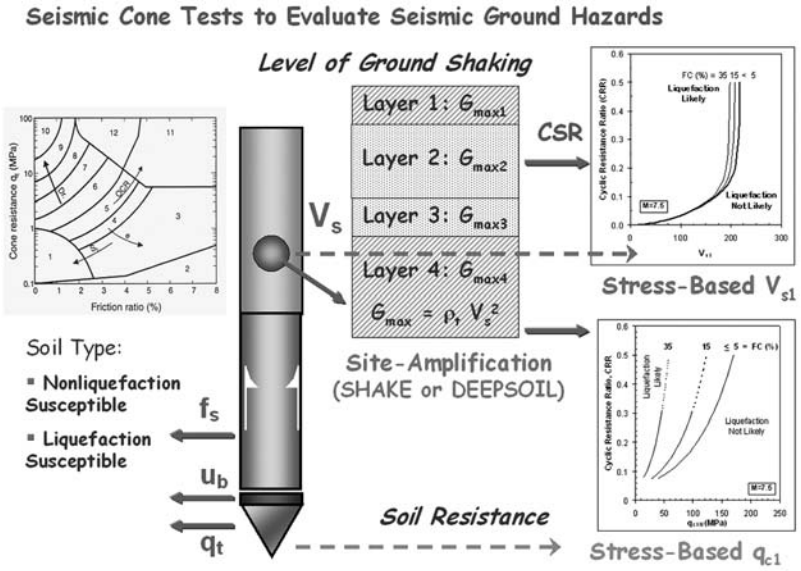

FIGURE 84 Use of seismic cone penetrometer for evaluating site-specific soil liquefaction concerns.

DETERMINE LEVEL OF GROUND SHAKING

In liquefaction analyses, the level of ground shaking from seismic loading is expressed in terms of the CSR. The CSR can be estimated using seismic ground hazard maps published by the U.S. Geological Survey, state geological agencies, the IBC, or the National Earthquake Hazard Research Program, or alternatively evaluated more properly using site-specific G_{max} data within commercial codes (e.g., RASCALS, SHAKE, EduSHAKE, SHAKE2000, or DEEPSOIL). Using the conventional simplified procedures, the CSR is expressed as (Seed and Idriss 1971):

$$\text{CSR} = \frac{\tau_{ave}}{\sigma'_{vo}} = 0.65\left(\frac{a_{max}}{g}\right)\left(\frac{\sigma_{vo}}{\sigma'_{vo}}\right)r_d \qquad (79)$$

where τ_{ave} is the average equivalent uniform shear stress generated by the earthquake (assumed to be 65% of the maximum induced stress), a_{max} is the peak ground acceleration, g = the gravitational acceleration constant (g = 9.8 m/s^2 = 32 ft/s^2), σ_{vo} and σ_{vo}' are the total and effective vertical stresses, respectively, and r_d is a stress reduction coefficient that accounts for the flexibility of the model soil column ($0.5 \leq r_d \leq 1.0$). By using the recommendations of the National Center for Earthquake Engineering workshop on soil liquefaction (Youd et al. 2001), r_d can be obtained with depth z (meters) as follows:

For depth $z \leq 9.15$ m: $r_d = (131 - z)/131$ (80a)

For 9.15 m $\leq z \leq$ 23 m: $r_d = (44 - z)/37$ (80b)

For 23 m $\leq z \leq$ 30 m: $r_d = (93 - z)/125$ (80c)

For $z >$ 30 m: $r_d = 0.50$ (80d)

The value of a_{max} is taken from the appropriate design events for a given project (i.e., the 2%, 5%, or 10% probability earthquake for a certain period of time, the maximum credible event for a known fault located a certain distance from the site, or a code-based response spectrum).

The CRR is the threshold for liquefaction and used to compare the available soil resistance with level of ground shaking represented by the CSR. Therefore, if the CSR value is higher than the CRR, the soil has a high likelihood of liquefaction. It the CSR falls beneath the CRR, the likelihood of liquefaction is small. The CRR can be expressed using conventional deterministic approaches that give a binary decision (liquefaction or no liquefaction), or alternatively, in terms of probabilistic curves of increasing risks of liquefaction.

Deterministic approaches include procedures based on stress-normalized tip resistance (e.g., Stark and Olson 1995; Robertson and Wride 1998; Youd et al. 2001) and/or stress-normalized shear wave velocity (e.g., Andrus and Stokoe 2000; Youd et al. 2001). For the CPT-based method shown in Figure 85 (*upper*), the cone tip resistance is normalized as a function of the effective stress (actual normalization criteria depends on the CPT soil classification) and is designated q_{c1N}. For clean quartz sands:

$$q_{c1N} = \frac{(q_t / \sigma_{atm})}{(q_{vo}' / \sigma_{atm})^{0.5}} = \frac{q_t}{\sqrt{\sigma_{vo}' \cdot \sigma_{atm}}} \qquad (81)$$

where atmospheric pressure is used to make the form dimensionless (note: 1 atm = 1 bar = 100 kPa). For silty sands, the stress-normalized cone tip resistance is modified to the adjusted tip resistance, designated $(q_{c1N})_{cs}$, which is its equivalent clean sand value, by the relationship:

$$(q_{c1N})_{cs} = k_c \cdot q_{c1N} \qquad (82)$$

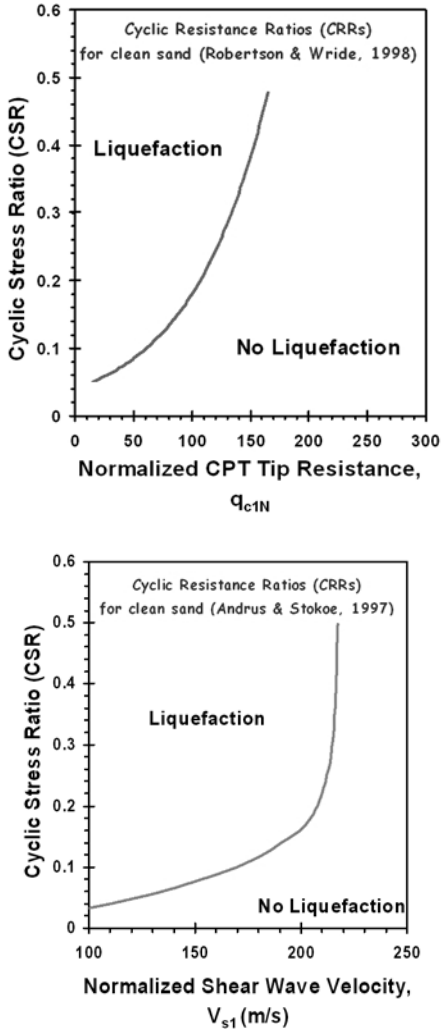

FIGURE 85 Deterministic approaches for liquefaction analysis of clean sand based on (*upper*) normalized cone tip resistance (after Robertson and Wride 1998) and (*lower*) normalized shear wave velocity (after Andrus and Stokoe 2000).

TABLE 11
CPT CLASSIFICATION INDEX I_C FOR SAND LIQUEFACTION EVALUATION

Soil Classification	Zone No.*	Range of CPT Index I_c Values
Organic Clay Soils	2	$I_c > 3.60$
Clays	3	$2.95 < I_c < 3.60$
Silt Mixtures	4	$2.60 < I_c < 2.95$
Sand Mixtures	5	$2.05 < I_c < 2.60$
Sands	6	$1.31 < I_c < 2.05$
Gravelly Sands	7	$I_c < 1.31$

After Robertson and Wride (1998).
*Note: Zone number per Robertson SBT (1990).

where K_c is the correction factor for the apparent fines content and is empirically calculated from a modified CPT soil classification index, I_c. Here, the index is redefined by Robertson and Wride (1998) using only CPT Q and F data because porewater pressures are often near hydrostatic for loose to firm clean sands (thus both Δu and $B_q \approx 0$) (see Table 11). The modified CPT soil type index is:

$$I_c = \sqrt{[3.47 - \log Q]^2 + [1.22 + \log F]^2} \quad (83)$$

Specifically, K_c is evaluated from:

For $I_c \leq 1.64$: $K_c = 1.0$ (84a)

For $I_c > 1.64$:
$$K_c = -0.403 I_c^4 + 5.581 I_c^3 - 21.63 I_c^2 + 33.75 I_c - 17.88 \quad (84b)$$

This requires iteration as the value of Q is adjusted to q_{c1N} for stress normalization if $I_c < 2.6$ (see Robertson and Wride 1998). The level of ground motion (CSR) and the adjusted tip resistance $(q_{c1N})_{cs}$ are compared with the CRR to determine whether liquefaction will or will not occur. For clean sand, the CRR is calculated by the following equation for an earthquake moment magnitude of 7.5 (Youd et al. 2001; Robertson and Wride 1998):

If $50 \leq (q_{c1N})_{cs} < 160$ $\quad \mathrm{CRR}_{7.5} = 93\left[\dfrac{(q_{c1N})_{cs}}{1000}\right]^3 + 0.08$ (85a)

If $(q_{c1N})_{cs} < 50$ $\quad \mathrm{CRR}_{7.5} = 0.833\left[\dfrac{(q_{c1N})_{cs}}{1000}\right] + 0.05$ (85b)

For liquefaction evaluation based on shear wave velocity, a deterministic chart procedure is shown in Figure 85 (*lower*) using the stress-normalized shear wave velocity that is designated V_{s1} and determined as:

$$V_{s1} = \frac{V_s}{(\sigma_{vo}'/\sigma_{atm})^{0.25}} \quad (86)$$

where V_s is in meters/second. The CRR for an earthquake moment magnitude of 7.5 is found in Andrus and Stokoe (2000) and Youd et al. (2001):

$$\mathrm{CRR}_{7.5} = a\left(V_{s1}/100\right)^2 + b\left[1/\left(V_{s1c} - V_{s1}\right) - 1/V_{s1c}\right] \quad (87)$$

where $a = 0.03$ and $b = 0.9$ are fitting parameters and V_{s1c} is an asymptote related to fines contents (FC):

$V_{s1c} = 220$ m/s for $FC \leq 5\%$;

$V_{s1c} = 210$ m/s for $FC = 20\%$; and

$V_{s1c} = 200$ m/s for $FC \geq 35\%$.

A calculated factor of safety (F_s) can be defined as F_s = CRR/CSR for a particular earthquake magnitude and set of data. In more recent evaluations, CRR curves of different probabilities of occurrence have been developed from mapping functions (Chen and Juang 2000; Juang and Jiang 2000) to relate the safety factor F_s to the liquefaction probability P_L. Based on a database of 225 CPT-based cases reported by Juang and Jiang (2000) for q_{c1N} probability curves:

$$P_L = 1\Big/\left[1 + \left(F_s/1.0\right)^{3.34}\right] \quad (88)$$

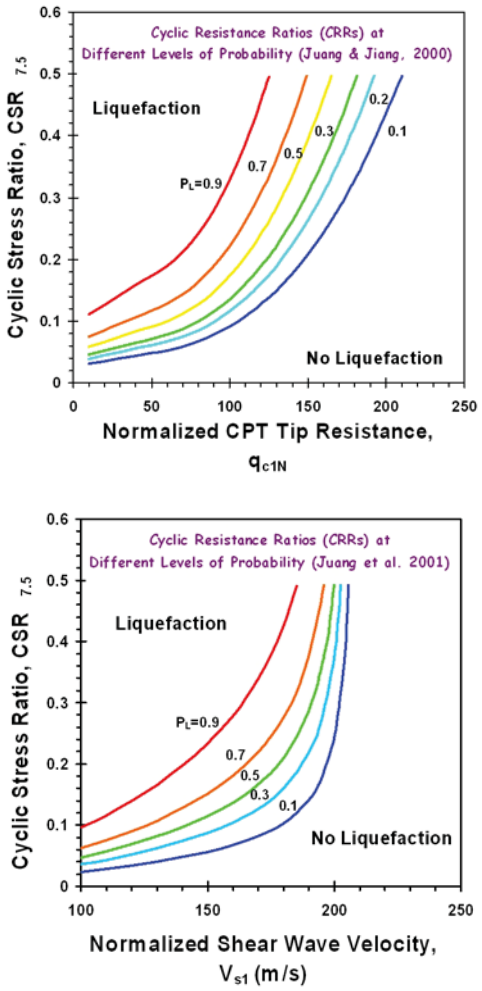

FIGURE 86 Probabilistic cyclic resistance ratios (CRRs) for clean sands based on (*upper*) normalized cone tip resistance and (*lower*) normalized shear wave velocity (after Juang and Jiang 2000).

For the normalized shear wave velocity (V_{s1}), there is a similar mapping function (Juang et al. 2001):

$$P_L = 1 \Big/ \left[1 + \left(F_s / 0.72 \right)^{3.1} \right] \tag{89}$$

Separate CRR curves corresponding to different probabilities of liquefaction ranging from 10% to 90% using q_{c1N} and V_{s1} are presented in Figures 86 (*upper*) and 86 (*lower*), respectively.

Alternate methods of post-processing CPT data to obtain probabilistic assessments of soil liquefaction potential have been recently proposed by Moss et al. (2003, 2006). These include special stress-normalization procedures for the CPT resistances and have been specifically developed to better address the reliability of seismic ground hazards in sands having various percentage fines contents.

CHAPTER ELEVEN

MISCELLANEOUS USES OF CONE PENETRATION TESTING AND SPECIALIZED CONE PENETRATION TESTING EQUIPMENT

This section discusses a variety of other applications for CPT, including slope stability investigations and landslide forensics, pavement investigations, sinkholes, and environmental investigations.

In certain circumstances, cone penetrometer technology has been employed to assist in delineating and detecting anomalous conditions or unusual features in the ground. Because traditional drilling and sampling is intermittent at say 5-ft-depth increments (1.5 m), the continuous nature of CPT helps provide detailed logging with three or more channels. Although downhole probes (e.g., geophysical tools or video cameras) can be lowered down a predrilled borehole, the process often requires casing of the hole and is much more destructive than CPT invasion (i.e., an augured 8-in. or 200-mm-diameter hole versus a 1.4-in. or 36-mm pushed-place hole). A listing of select special applications by CPT is presented in Table 12, with a cited reference source given should additional details be desired.

CPT has enjoyed particular use on geo-environmental site investigations because the test produces no samples, no cuttings, and no spoil, thereby minimizing the generation of above-ground cleanup in sensitive areas and contaminated ground. Of well-known acclaim, the conductivity cone is commercially available from manufacturers and CPT service firms as an expedient means to map contaminant plumes and detect the presence of underground pollutants (Campanella and Weemees 1990). Resistivity (ohm-meter) is the reciprocal of electrical conductivity; therefore, the device is also referred to as the resistivity cone (see Figure 87). The electrodes are provided as an array of either four axial rings at set vertical spacings or with a button array (positioned diametrically). The special membrane interface probe offers a single button electrode for an index determination of in situ resistivity penetration and gas sampling. An example resistivity piezocone sounding ($RCPTu_1$) from downtown Memphis, Tennessee, is presented in Figure 88. Electrical conductivity can be used to identify soil types. It is also employed in coastal areas to distinguish the upper freshwater table from the lower salt water regime.

Whereas resistivity induces a direct current electrical current into the ground, a similar approach can be provided using alternating current and thus established to obtain dielectric measurements (permittivity). These dielectric readings can be interpreted to provide direct real-time profiles of volumetric water content. For portions of the sounding that extend below the groundwater table, the gravimetric water content can be mapped. Figure 87 (*center*) shows a special dielectric CPT penetrometer developed for this purpose (Shinn et al. 1998).

New developments in sensors and testing procedures for CPT have been introduced to enhance the capabilities of direct-push technologies. Selected instruments and innovations are listed in Table 13. Illustrative examples of these CPT technologies include the use of cableless systems to transmit or store data, as shown in Figure 89, including: (*left*) memocone and (*right*) audio-signal cone. Another cableless system utilizes special glass-lined rods to allow transmission by infrared signals. These systems are advantageous in the following situations: (1) when conducting CPTu with drill rigs where the crew is not sensitive to working with electronic cables, (2) offshore deployment, and (3) wireline systems and deep soundings. In the case of the memocone, the data are stored downhole until the penetrometer is retrieved back at the ground surface and the readings of time t, q_t, f_s, and u_2 are matched with the depth logger readings of time t and depth z. In the audio-signal cone, the data are transmitted by sound waves up through the center of the rods in real time and a special microphone used to capture the sounds that are digitally decoded for the data logger. A similar approach is used for infrared signals.

With standard analog systems, the basic logging was restricted to depth (z), cone tip stress (q_t), sleeve friction (f_s), porewater pressures (u), and inclination (i), often because the electronic cable was of the 10-pin type (10 wires). Although 12-, 16-, 24-, and even 32-pin wires have been available, they are fragile with short lives because of the restrictive inner diameter of the cone rods that the cable must be threaded through. A few analog systems could circumvent the 10-wire limitations by either forgoing the inclinometer or friction readings. The multi-piezo-elements shown in Figure 90 are all analog penetrometers that allow simultaneous porewater pressure readings. In other novel analog systems, wiring is shared during different portions of testing (such as the Fugro true-interval seismic cone).

TABLE 12
SPECIAL APPLICATIONS OF CONE PENETROMETER TECHNOLOGY

CPT Application	Reference Source
Environmental Site Investigation and Detection of Soil Contamination	Campanella and Weemees (1990) Auxt and Wright (1995) Bratton and Timian (1995) Campanella et al. (1998) Lambson and Jacobs (1995) Lightner and Purdy (1995) Mlynarek et al. (1995) Pluimgraaff et al. (1995) Robertson et al. (1998) Shinn and Bratton (1995)
Landslide Forensics and Slope Stability	Collotta et al. (1989) Leroueil et al. (1995) Romani et al. (1995) Hight and Leroueil (2003)
Pavement Investigations	Badu-Tweneboah et al. (1988) Newcomb and Birgisson (1999)
Sinkhole Detection in Limestone Terrain	Foshee and Bixler (1994)

Most recently, electronic digital cones can now process the readings downhole and the data can be transmitted uphole in series (rather than parallel with analog). Thus, the restriction on the numbers of simultaneous channels has been lifted. Figure 91 (*left*) shows a multi-friction sleeve penetrometer that uses several sleeves of different roughness and textures to quantify soil-pile interface response (DeJong and Frost 2002).

Other developments include vibrocone penetrometers [Figure 91 (*center*)] for site-specific evaluation of soil liquefaction potential (without the use of empirical CRR curves) and T-bar testing [Figure 91 (*right*)] for defining shear strengths of very soft clays and silts (Long and Gudjonsson 2004). The T-bar is actually a penetrometer with a larger 100 cm^2 hammerhead that replaces the

FIGURE 87 Electrical conductivity measurements: (*left*) Fugro conductivity cones, (*center*) Vertek Dielectric and Hogentogler resistivity cones, and (*right*) Diametric (Button) Electrode Array for Resisitivity.

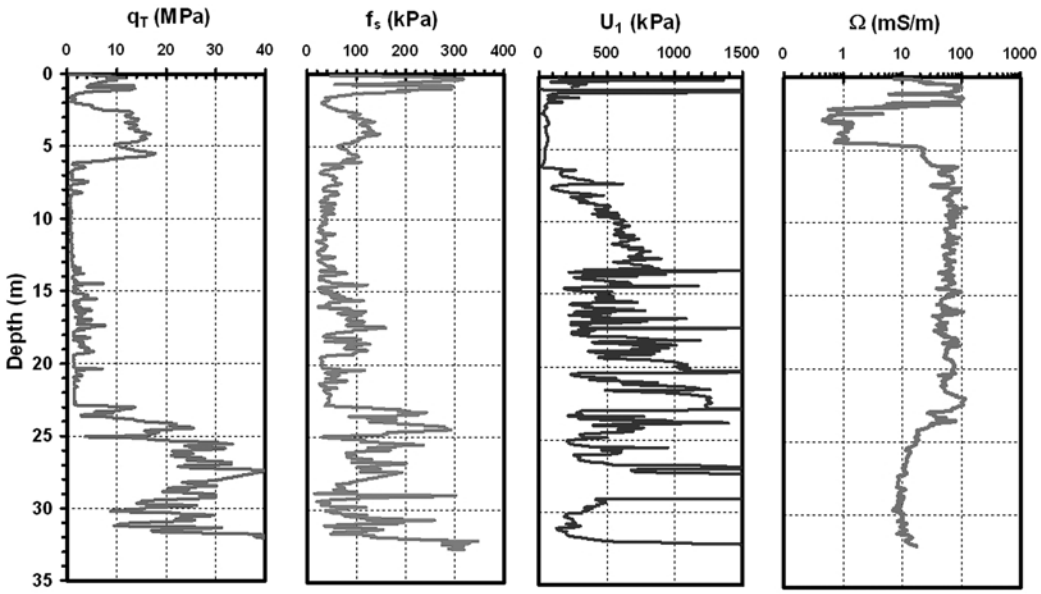

FIGURE 88 Example of conductivity piezocone test at Mud Island, Memphis, Tennessee.

TABLE 13
SPECIALIZED SENSORS OR MODIFICATIONS TO CONE PENETROMETER TECHNOLOGY

Specialized CPT System	Reference Source	Notes/Remarks
Acoustic Emission CPT	Houlsby and Ruck (1998)	Indicator of soil type
	Menge and Van Impe (1995)	Delineate soil type and lenses
AutoSeis Generator	Casey and Mayne (2002)	Portable remote shear wave source
CPT Soil Sampler	Lunne et al. (1997)	Obtains soil sample when needed
Dielectric CPT*	Shinn et al. (1998)	Maps volumetric water contents
Horizontal CPT	Broere and Van Tol (2001)	Towards tunnel investigations
Lateral Stress Cone	Takesue and Isano (2001)	Measures total horizontal stress
	Campanella et al. (1990)	Total lateral stress during penetration
Multi-Element Piezocones	Juran and Tumay (1989)	Dual-element piezocone
	Skomedal and Bayne (1988)	Triple-element piezocone
	Danzinger et al. (1997)	Quad-element piezocone
Multi-Friction Sleeve Penetrometer	DeJong and Frost (2002)	Four friction sleeves of different roughness for pile interface studies
	Hebeler et al. (2004)	
Radio-Isotope CPT	Shrivastava and Mimura (1998)	Measures density and water content in real time
	Dasari et al. (2006)	
T-Bar Penetrometer	Randolph (2004)	Penetrometer with 100 cm^2 head to increase load cell resolution in soft soils
	Lunne et al. (2005)	
Temperature	Kurfurst and Woeller (1988)	Measures thermal changes
Vibro-Piezocone	McGillivray et al. (2000)	Evaluate site-specific soil liquefaction
	Bonita et al. (2000)	Vibration to locally cause liquefaction
Vision Cone Penetrometer (VisCPT)	Hryciw et al. (1998)	Real-time videocam of soil profile
	Hryciw and Shin (2004)	Detection of thin layers and lenses

*Also termed "soil moisture probe."

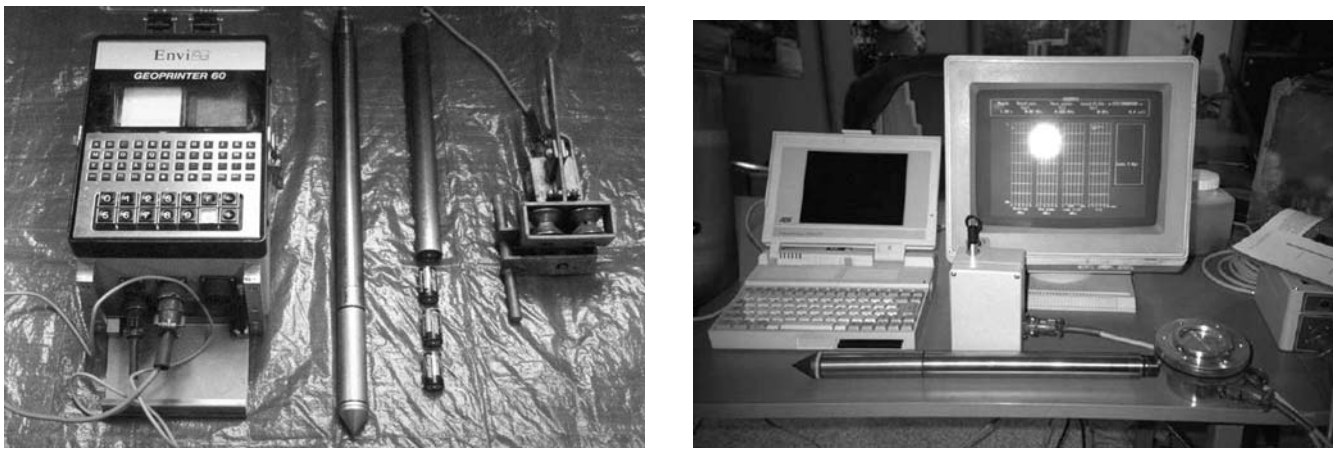

FIGURE 89 Cableless CPT systems: (*left*) Memocone (ENVI) and (*right*) audio-signal unit (Geotech AB).

FIGURE 90 Multi-piezo-element penetrometers: (*left*) dual-element type with midface and shoulder filters (van den Berg type), (*center*) Fugro triple-element cone, and (*right*) quad element (Oxford University).

FIGURE 91 CPT modifications: (*left*) multi-friction sleeve penetrometer, (*center*) vibro-piezocone, (*right*) T-bar.

standard 10 cm^2 cone tip to increase resolution on the force gauge. If soil samples are deemed absolutely critical, then special CPT samplers have been developed that can obtain a disturbed pushed sample from specified depth (Figure 92).

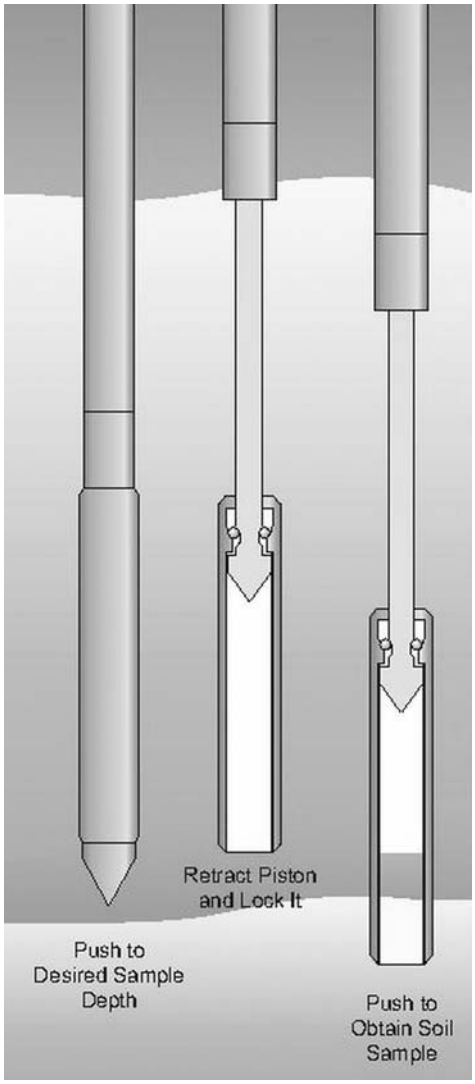

FIGURE 92 CPT sampling devices for necessary retrieval of soil samples.

In lieu of sampling, several vision or video cone systems have been built that allow a real-time digital camera viewing of the soils by means of a small window port (Figure 93). The VisCPT has been used with digital image analysis processing to better define soil type and particle characterization, as well as show clear evidence of soil contamination.

For seismic cone testing, automatic seismic sources have been constructed to produce repeatable transient shear waves that can be detected by the geophone(s). When the SCPT was devised, the recording of analog wavelet signals required the paired matching of left and right strikes to define the first crossover point that was used in the pseudo-interval downhole procedure (Campanella et al. 1986). With the advent of autoseis units, the downhole testing offers a quicker field testing time and only left (or right) series of strikes are needed because computers can easily post-process the consecutive waveforms and match them using cross-correlation. A selection of autoseis sources is shown in Figure 94, including portable electric, pneumatic, and electro-mechanical units. Heavy-duty hydraulic units for generating deep (60 m) waves are also available that are mounted to the truck belly (Figure 95).

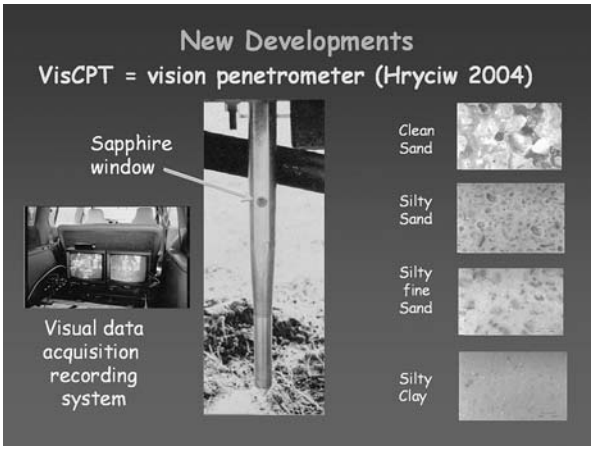

FIGURE 93 Vision penetrometer system for real-time videocam soil viewing (after Hryciw and Shin 2004).

FIGURE 94 Autoseis units for surface shear wave generation during seismic cone testing.

FIGURE 95 Rig with mounted hydraulic autoseis unit for deep downhole testing.

CHAPTER TWELVE

CONE PENETRATION TESTING MODIFICATIONS FOR DIFFICULT GROUND CONDITIONS

Some obstacles to advancing CPTs in certain geologic formations and working in problematic soils are discussed in this chapter, with brief overviews given regarding novel approaches to solving these situations and special systems developed to cope with such difficulties. A common response to the DOT survey question regarding the limited use of CPT in exploration in their state indicated that the ground conditions were often too hard for penetration or that a dense impenetrable shallow layer prohibited advance of the CPT. Toward this purpose, a section is devoted herein to describing special systems that have been developed toward overcoming cone penetration in hard ground.

REMOTE ACCESS CONE PENETRATION TESTS

For remote access CPTs, innovations include the construction of special deployment vehicles for cone penetrometer technology, particularly in urban areas; small limited access locations; and remote arctic weather, as shown by the selections presented in Figure 96. In areas of high water table, special deployment of CPTs can be accomplished by airboats, barges, and/or swamp buggy (Figure 97).

Of particular interest is the completely automated PROD (portable remotely operated drill) that was developed for offshore use with capabilities to drill, sample, push CPTs, vane shear testing, and obtain rock coring to depths of up to 100 m (330 ft) below mudline (Randolph et al. 2005). Several PROD components are shown in Figure 98.

CONE PENETRATION TESTS IN HARD GROUND

From the survey questionnaire (Appendix A, Question 55), one of the biggest obstacles to the use of CPTs by the DOTs is that the ground is too hard for static penetration, as shown by Figure 99. The second highest reported obstacle was the presence of gravels or stones. In this section, available means to overcome these obstacles are discussed.

Various creative and novel means of deploying CPTs have been designed to achieve depths of penetration in very dense sands, weak rocks (chalks, mudstones, tuff), and transitional zones of residuum to saprolite, as well as cemented layers and caprocks. An excellent overview on conducting CPTs in very hard soils and weak rocks is provided by Peuchen (1998), based in large part on the long experience of the Dutch, and efforts advanced in the offshore site exploration industry. With the proper techniques, electric cone tip stresses of more than 100 MPa (1000 atms) and mechanical CPT resistances up to 150 MPa (1500 atms) have been recorded. Table 14 provides a general overview on methods developed to overcome CPT in hard ground.

For increased penetration in dense ground, large deadweight vehicles on the order of 180 kN (20 tons) are available, having considerable more pushing reaction compared with drill rigs. Trucks with weights as high as 360 kN (40 tons) have been built to facilitate CPTs in very dense sands and gravels [Figure 100 (*left*)] for routine application at the Hanford nuclear site in Washington State (Bratton 2000). These vehicles are too heavy to meet roadway load requirements at full capacity; therefore, they are mobilized to the site at acceptable weight limits (say 180 kN) and the additional 180 kN deadweight are added at the testing location.

Another means to increase the reaction capacity is to employ earth anchors. The anchors can be installed with variable size plates and depths of 1, 2, or 3 m, depending on local conditions [Figure 100 (*right*)]. Anchoring permits small lightweight CPT rigs (60 kN) to achieve depths of 30 to 40 m and successful penetration in fairly dense sands ($N > 30$ bpf).

An illustrative example of a CPTu conducted in hard saprolite and partially weathered rock of the Piedmont in north Atlanta is shown in Figure 101 (Finke and Mayne 1999). The very high resistances measured by the SPT *N*-values in an adjacent soil boring clearly shows the dense ground conditions. Nevertheless, the piezocone sounding was successfully advanced into these hard residual soils. Note the characteristic negative porewater pressures in the Piedmont upon reaching the groundwater table.

When cemented layers, caprock, or hard concretions are encountered in the profile, the CPT sounding can be halted and the penetrometer can be withdrawn. Then, a rotary drill rig can be set up and used to bore through the cemented zone. The prebored hole can be filled with a backfilled sand or pea gravel and the CPT sounding can be resumed. The backfill helps to stabilize the cone rods and prevent buckling. On completion, the results of part A of the sounding can be


FIGURE 96 Special CPT deployment systems: (*left*) single personnel track vehicle (Sweden), (*center*) cherry-picker for urban access (New Zealand), and (*right*) portable unit for arctic work (Canada).

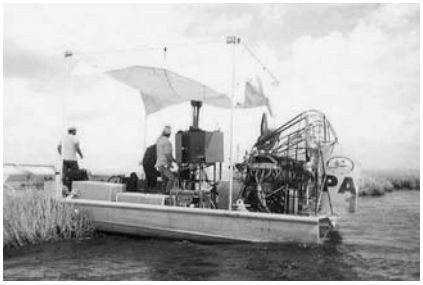

FIGURE 97 Special CPT deployment by (*left*) airboat, (*center*) barge, and (*right*) New Orleans marsh buggy.



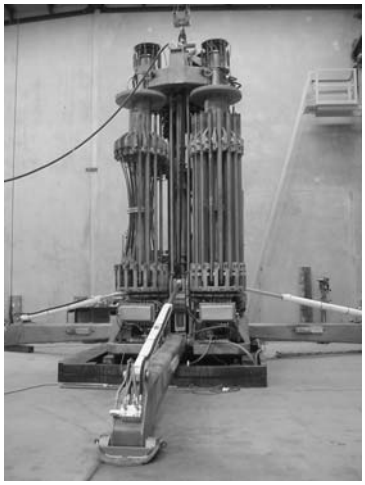

FIGURE 98 Components of portable remotely operated drill (PROD): (*left*) 3000-m-long umbilical cable, (*center*) remote control panel and data acquisition, (*right*) CPT and rotary drill platform.

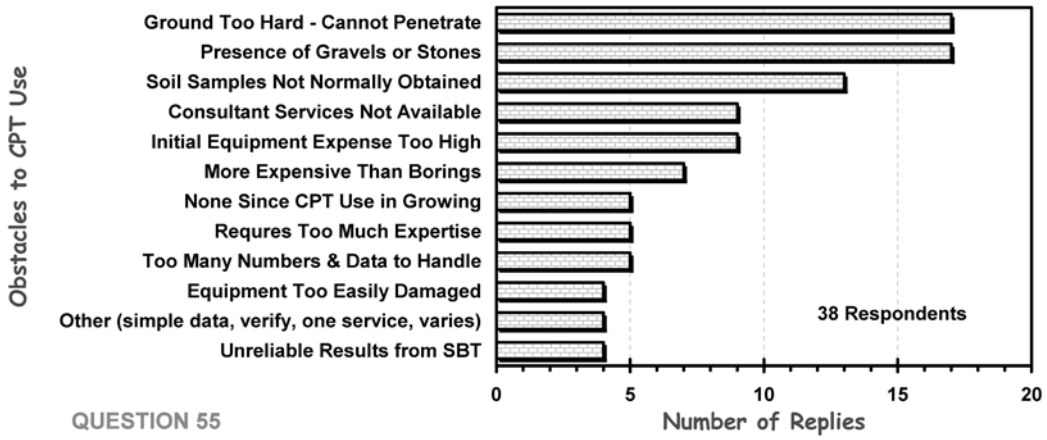

FIGURE 99 Questionnaire responses concerning major obstacles to use of CPT.

added to part B of the sounding to produce a complete depth profile. Although this is somewhat unattractive to routine production type CPTs, it does help obtain the desired results, which include electronic readings of tip stress, sleeve friction, porewater pressures, and shear wave velocities. If the geologic conditions of the region normally encounter an embedded hard cemented layer, perhaps the CPT user would wish to obtain a combine rig (as shown in Figure 102) that has capabilities of both static CPT push and rotary drilling operations.

The ROTAP tool is specially designed to advance CPTs through hard cemented zones (Sterckx and Van Calster 1995). Initially, the CPT is advanced in a normal procedure

TABLE 14
SPECIAL TECHNIQUES FOR INCREASED SUCCESS OF CONE PENETRATION IN HARD GEOMATERIALS

Advancing Technique	Reference	Comments/Remarks
Heavy 20-Ton Deadweight CPT Trucks and Track Rigs	Mayne et al. (1995)	Increased weight reaction over standard drill rig
Friction Reducer	van de Graaf and Schenk (1988)	Effective in frictional soils, but not so in very dense sands
Cycling of Rods (up and down)	Shinn (1995, personal communication)	Local encounter in thin hard zones of soil
Large diameter penetrometer (i.e., 44-mm cone; 36-mm rods)	van de Graaf and Schenk (1988)	Works like friction reducer
Guide Casing: Double Set of Rods; Standard 36-mm Rods Supported Inside Larger 44-mm Rods; Prevents Buckling	Peuchen (1988)	Works well in situations involving soft soils with dense soils at depth
Drill Out (downhole CPTs)	NNI (1996)	Alternate between drilling and pushing
Mud Injection	Van Staveren (1995)	Needs pump system for bentonitic slurry
Earth Anchors	Pagani Geotechnical Equipment Geoprobe Systems	Increases capacity for reaction
Static–Dynamic Penetrometer	Sanglerat et al. (1995)	Switches from static mode to dynamic mode when needed
Downhole Thrust System	Zuidberg (1974)	Single push stroke usually limited to 2 m or 3 m
Very Heavy 30- and 40-Ton Rigs	Bratton (2000)	After large 20-ton rig arrives at site, added mass for reaction
ROTAP—Outer Coring Bit	Sterkx and Van Calster (1995)	Special drilling capabilities through cemented zones
CPTWD	Sacchetto et al. (2004)	Cone penetration test while drilling
Sonic CPT	Bratton (2000)	Use of a vibrator to facilitate penetration through gravels and hard zones
EAPS	Farrington (2000); Shinn and Haas (2004); Farrington and Shinn (2006)	Wireline systems for enhanced access penetrometer system

Adapted and modified after Peuchen 1998.
NNI = Nederlands Normalisatie Institute; CPTWD = cone penetration test while drilling; EAPS = enhanced access penetrometer system.

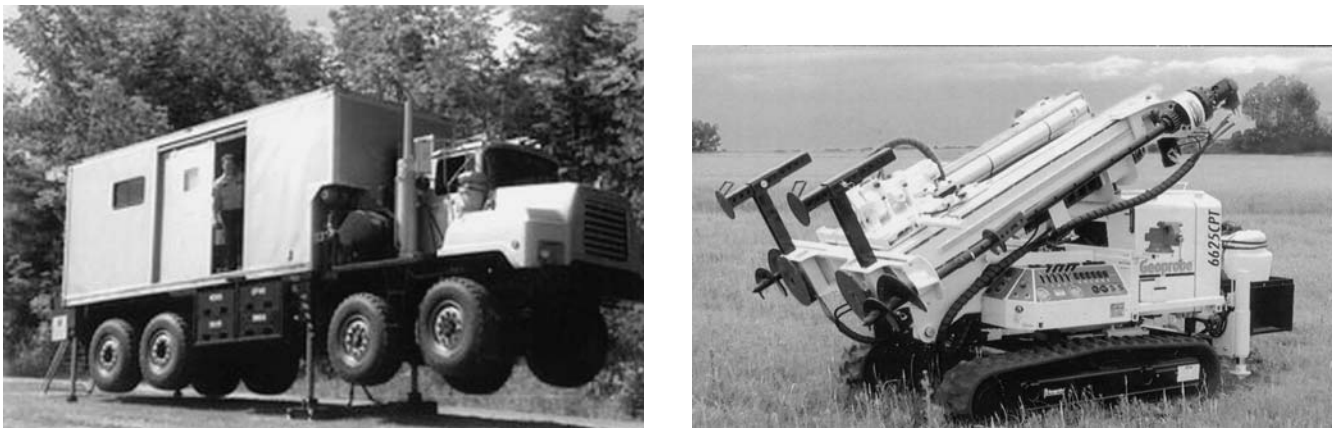

FIGURE 100 CPT vehicles for hard ground including: (*left*) 40-ton truck, (*right*) anchored track rig.

until the hard caprock or concretion is encountered. Then the penetrometer is removed and the ROTating AParatus (i.e., ROTAP) is installed and used to drill through the hard zone. Once through the desired hard layer, the penetrometer is reinstalled to continue the sounding.

A special series of Ateliers Mobiles d'Ausultation par Pénétration des Sols (Mobile Soil Testing Unit by Penetration) static–dynamic penetrometer systems has been developed for testing a range of soft soils to very hard and dense geomaterials with reported q_c up to 140 MPa (1400 tsf) and depths up to 100 m (Sanglerat et al. 1995). A heavy-duty van den Berg track truck is used for the hydraulic pushing. The sounding has three distinct phases: (1) static electric CPT push, (2) static mechanical CPT push, and (3) dynamic mechanical CPT. The test begins as a standard CPT with either a 44- or 50-cm^2 electrical penetrometer (q_c and f_s) pushed at 20 mm/s until hard static refusal is met at 30 MPa (300 tsf). The sounding is resumed using a 12-cm^2 mechanical cone in static push mode until 120 MPa (1200 tsf) is reached. To penetrate very dense sands, gravels, rocks, and other obstacles, a special dynamic fast-action hydraulic hammer is used to advance the cone and, if conditions permit, resume again with the static push phase. Example results of static–dynamic penetration in dense sandstone are shown in Figure 103 with all three phases of testing shown.

A sonic CPT system is detailed by Bratton (2000), whereby a vibrator can be intervened when the soil resistance becomes too great for normal static CPT pushing. The sonic vibrator is installed in the CPT truck and uses two twin 25-hp hydraulic motors with eccentric masses at the top of

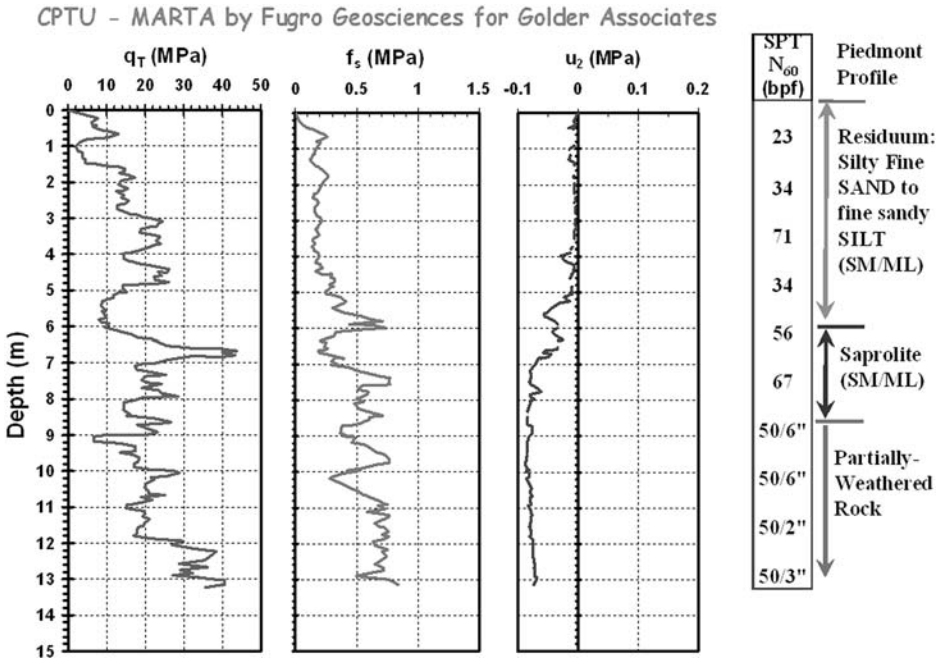

FIGURE 101 Piezocone advanced into very hard partially weathered gneiss.

FIGURE 102 Combine rig with both CPT hydraulic rams and drilling capabilities.

the rods. The vibrations are in the range of 25 to 125 Hz and used to facilitate CPT penetration through dense sands and gravels. Figure 104 shows the sonic CPT unit within an ARA truck.

A special wireline-based system that combines CPT with drilling capabilities has been termed CPTWD (cone penetration test while drilling) and is detailed by Sacchetto et al. (2004). A special modified wireline-type core barrel has been developed to house the cone penetrometer. An Envi-type memocone penetrometer is used to store the CPTu data downhole in a memory chip. The system also employs MWD (measurements while drilling) during simultaneous operation of the CPT; therefore, two sets of penetration readings are obtained, including piezocone measurements (q_t, f_s, and u_2), as well as the MWD readings of penetration rate, torque, and fluid pressure. When hard impenetrable layers are encountered (too hard for CPT), then the sounding advances strictly on the basis of wireline coring techniques with MWD data still obtained. Figure 105 shows the basic CPTWD scheme, equipment, and a full set of results of six measurements from a site near Parma, Italy.

An enhanced access penetrometer system (EAPS) is presented by Shinn and Haas (2004) and Farrington and Shinn (2006). This is based on a wireline system (Farrington 2000) and offers a means to interrupt the CPT steady-state rate of penetration and utilize downhole wireline coring intermittently and advance soundings through very dense or cemented zones or dense or hard geomaterials. The EAPS also has the ability to take soil samples as needed. Some aspects are illustrated in Figure 106.

Comparative studies of the EAPS deployment and normal direct-push technology for CPTs have been made by Applied Research Associates. Figure 107 shows four sets of superimposed piezocone soundings at a test site with two CPTUs produced by the EAPS downhole wireline method (Nos. 2A and 2B) and two CPTUs per normal push methods (Nos. 2C and 2D), with very good agreement seen for all cases.

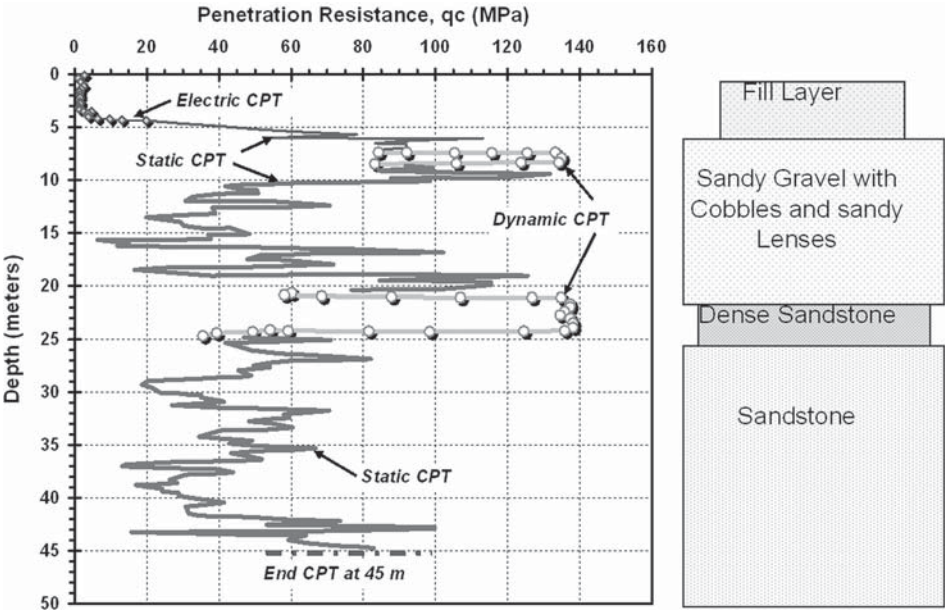

FIGURE 103 AMAP static–dynamic penetration system in dense sandstone (after Sanglerat et al. 1999).

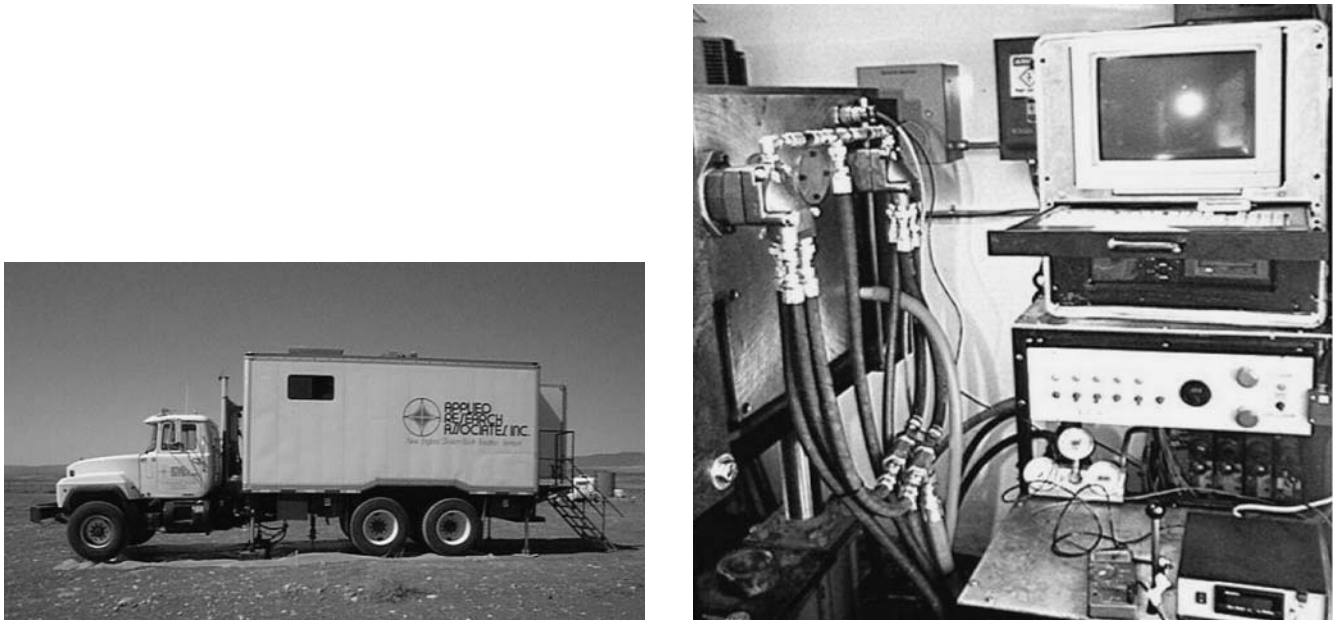

FIGURE 104 Sonic CPT system with (*left*) deadweight truck, and (*right*) sonic vibrator unit.

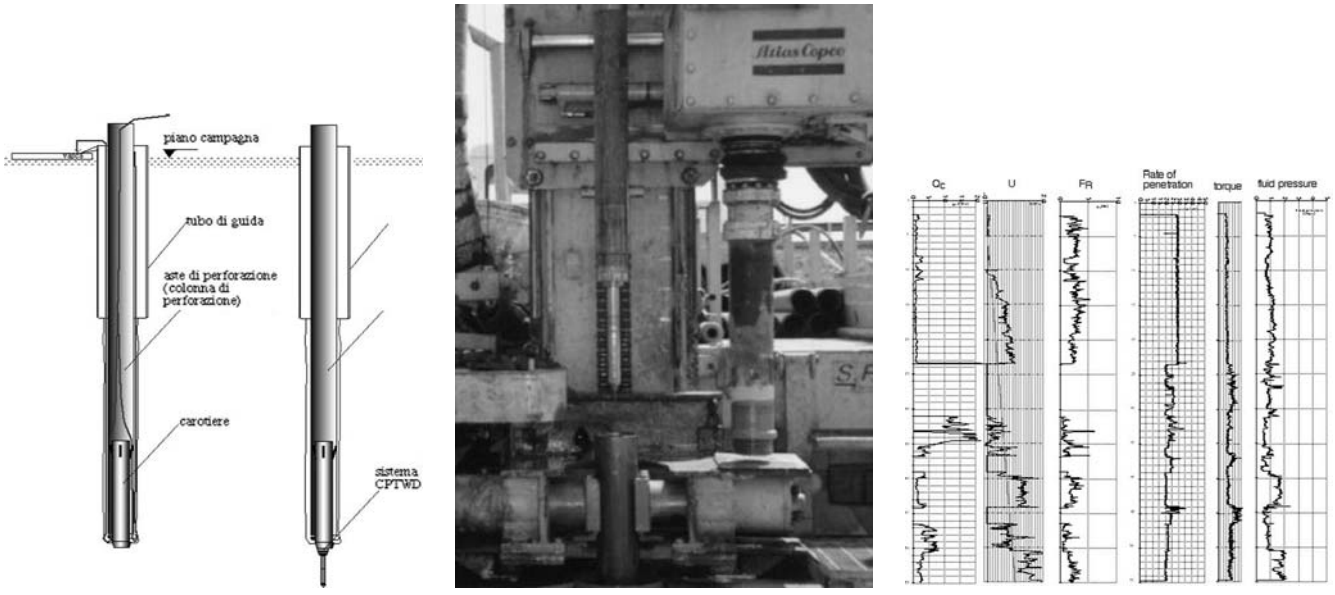

FIGURE 105 CPTWD wireline-based system (Sacchetto et al. 2004).

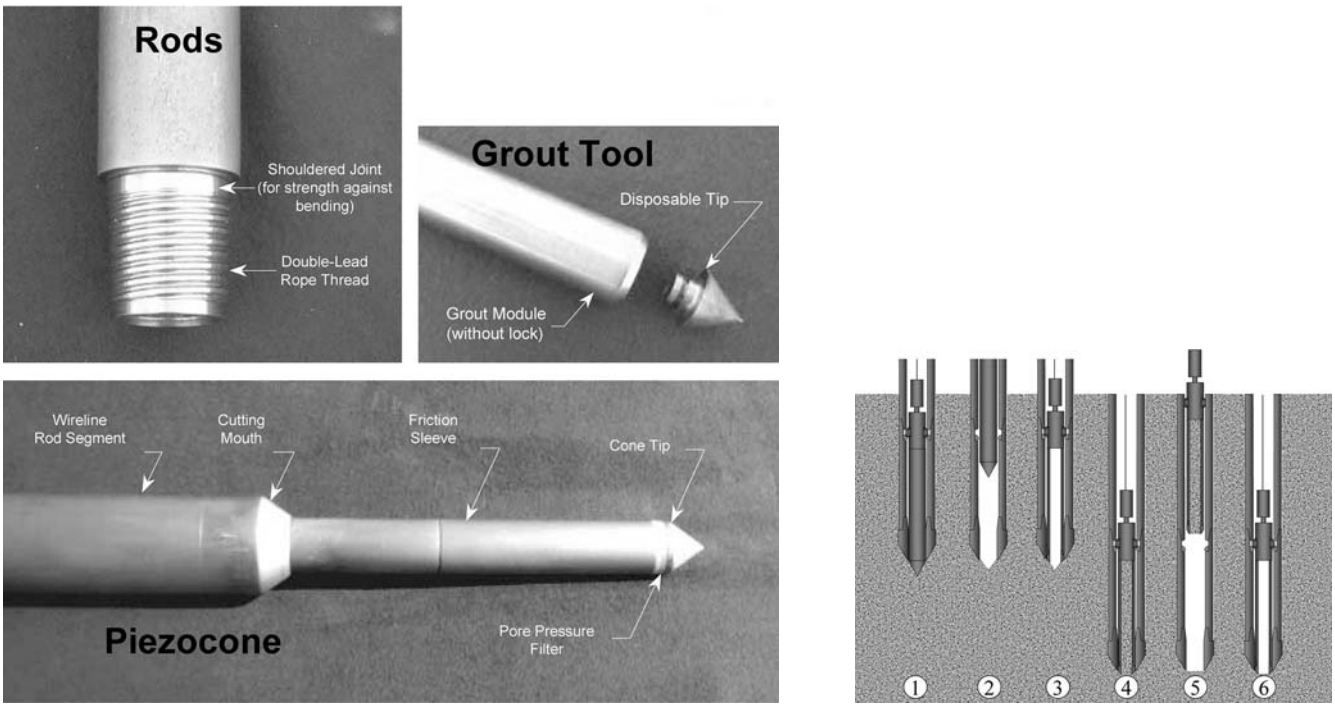

FIGURE 106 Enhanced access penetration system (EAPS) for penetration of hard geomaterials (after Farrington 2000).

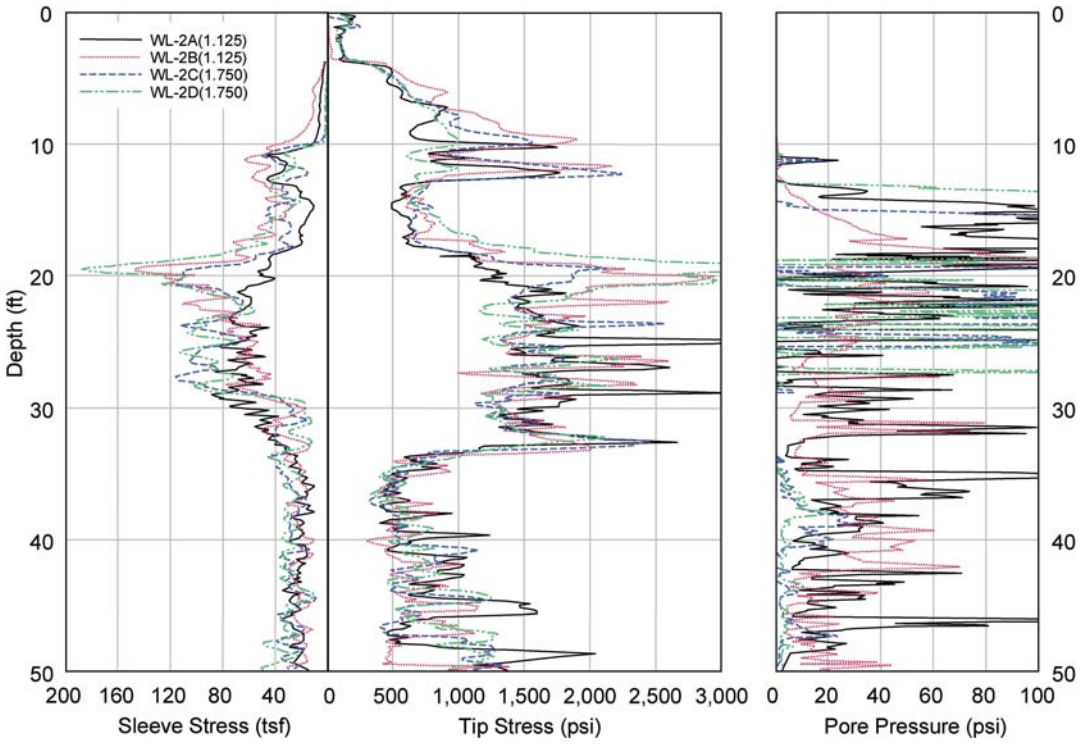

FIGURE 107 Comparison of CPTUs from standard push and EAPS wireline deployed systems (Farrington 2000).

FIGURE 108 Jackup rigs for nearshore CPT deployment: (*left*) SeaCore, and (*right*) The Explorer.

FIGURE 109 Vessels for offshore CPTs: (*left*) Markab, Australia; (*right*) Bucentaur, Brasil (Courtesy: Fugro Geosciences).

NEARSHORE AND OFFSHORE DEPLOYMENT

On some highway projects, the highway alignment crosses over a body of water, particularly bridges over rivers or streams or waterway canals. The CPTs can be mobilized to conduct soundings from floating barges. In swampy coastal areas with shallow water, movable pontoons are used that are floated empty to their location, then filled with water to prepare a working platform for the CPT truck or rig. In nearshore environments, highways may follow the coastal shoreline or connect small islands and land masses. In these cases, the use of a jackup rig may be warranted. Figure 108 shows two jackup-type platforms in use for drilling, sampling, and CPT works. If water depths are greater than 15 m, then a special CPT ship can be deployed to conduct offshore site investigations (Figure 109).

CHAPTER THIRTEEN

CONCLUSIONS AND RECOMMENDED FUTURE RESEARCH

Cone penetration technology can assist the geotechnical highway engineer in the collection of site-specific soils information in a cost-effective, quick, and reliable manner. From a practical standpoint, the cone penetration test (CPT) soundings obtain continuous logging of the soil layers and stratigraphy. In many cases, the CPT outperforms the normal and conventional rotary drilling and sampling operations in the field and the associated laboratory testing that can take weeks to produce results. However, the two methods can be complementary, with the CPT providing immediate profiling of the subsurface conditions and follow-up confirmation and select verification by the boring, sampling, and lab testing program.

A questionnaire was distributed to the 52 U.S. and 12 Canadian departments of transportation (DOTs) to survey the state of the practice in highway site investigations relevant to use of the CPT. With a total of 56 DOTs responding, 63% indicated that they were using the CPT on their projects to some degree; the remaining 37% of the respondents indicated no use of the CPT whatsoever in their state or province. Therefore, the CPT appears to be underutilized at present for highway projects in the United States and Canada. On a positive note, 64% of the respondent DOTs did foresee an increase in the probable use of this technology on future highway projects.

CPT capabilities include the direct assessments on the geostratigraphy, with detailed demarcation on the numbers, depths, and thicknesses of soil layers; presence of interbedded lenses; groundwater table(s); and relative hardness of the various strata in the subsurface environment. These soundings are recorded and stored digitally and thus can be quickly manipulated to create cross sections and subsurface profiles of the general ground conditions. The digital data can also be post-processed to provide evaluations on geotechnical parameters related to soil strength, stiffness, stress history, and flow characteristics.

The basic electric cone penetrometer obtains readings of tip stress (q_c) and sleeve friction (f_s) at 1- to 5-cm vertical intervals. At a constant rate of penetration of 2 cm/s, the test can be completed to 30 m depth in only 1 to 2 h. In hard abrasive ground, a mechanical CPT system obtains similar information, but at a coarser 20-cm depth interval. The piezocone collects a third reading of penetration porewater pressures (u) that is particularly useful for the following conditions: (1) saturated soils below the groundwater table, (2) correction of tip resistances in clays and silts (q_t), and (3) conducting piezo-dissipation tests to evaluate soil permeability and coefficient of consolidation. Moreover, seismic piezocone testing with dissipation phases (SCPTù) is a particularly attractive in situ test for modern day highway projects, because it offers up to five independent readings on soil behavioral response within a single sounding, including cone tip stress (q_t), sleeve friction (f_s), penetration porewater pressure (u), time rate of dissipation (t_{50}), and downhole shear wave velocity (V_s). This provides an optimal means for data collection and parameter identification.

Those DOTs using the CPT have found value in its ability to post-process the multiple readings in assessing questions related to the design and performance of embankments, slopes, ground improvement studies, and the analysis of shallow and deep foundations. The digital CPT data can be post-processed to provide input soil parameters for empirical, analytical, and/or numerical simulations of geotechnical problems. The data also lend themselves to use in direct CPT methods that output solutions for foundation capacity and displacement calculations.

The most common obstacles to CPT use include the presence of very hard ground, cemented layers, or dense geomaterials, thereby preventing penetration. A review of 15 available methods to tackle hard ground conditions is presented to aid DOTs in selecting an approach or suite of techniques to overcome these problems.

On large and critical DOT projects, the integrated approach to geotechnical characterization will require a combination of geophysics, drilling and sampling, in situ soundings, laboratory testing, and engineering analyses (Figure 110). The wide diversity and complexities of natural geomaterials makes for a challenging task because of their many geologic origins, ages, constituents, grain size, mineralogies, fabrics, and environmental histories. Therefore, parameter values interpreted from the CPT may need verification with other means, such as alternate in situ tests (e.g., vane), laboratory testing (e.g., triaxial shear and consolidation), and/or full-scale load tests (e.g., O-cell).

The growth of cone penetrometer technology is guaranteed in future site characterization and geotechnical investigations because of its direct tie to computerization for data

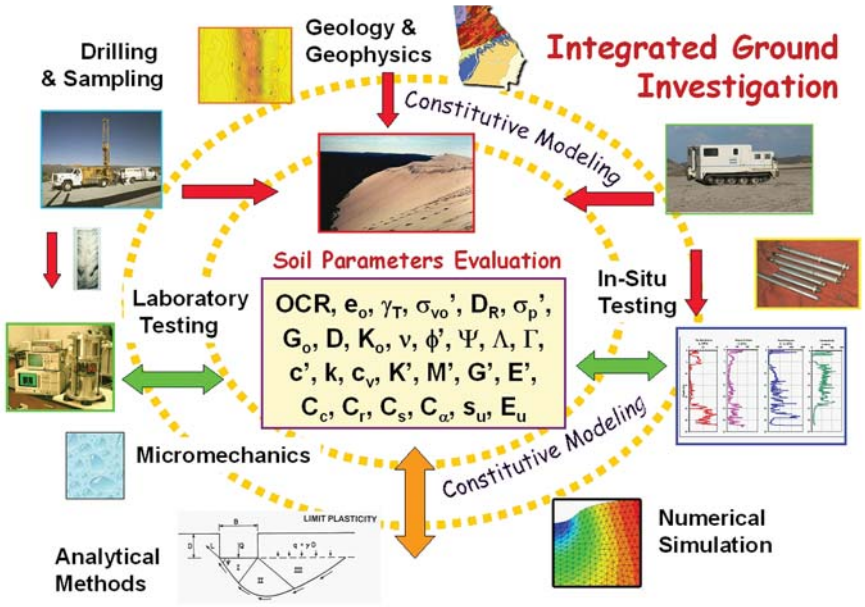

FIGURE 110 Integrated approach to site investigation and evaluation of geotechnical parameters.

acquisition and post-processing of digital data records. Today, as soon as the sounding is completed on-site, the data can be conveyed through wireless telecom transmission back to the DOT geotechnical engineer in the office. Real-time decisions can be made by senior project engineers or the chief engineer. Instant feedback by text messaging or a simple cell phone call back to the CPT crew and field engineer can request a piezo-dissipation test immediately or advance the sounding deeper than originally specified. As the data are available immediately, the post-processing of soil engineering parameters can commence "on-the-fly," with assessments of undrained shear strength (s_u), preconsolidation stress (σ_p'), and axial pile capacity (Q_u) produced on-the-spot as the engineer observes the CPT sounding being advanced.

From the survey results, it was determined that the needs of the DOT community include improved software capabilities for handling and post-processing the large amounts of CPT data that are generated (Figure 111), as well as new directions of research and applications of CPT (Figure 112). It is likely that some of these developers will introduce new software that may address the issues of CPT interpretation in nontextbook-type geomaterials such as peats, residual soils, saprolites, collapsible soils, silts, and intermediate geomaterials.

In the case of several of the research needs listed in survey question 56, several of these topics have been initially addressed by universities (e.g., continuous V_s and VisCPT) and manufacturers (e.g., static-dynamic CPT); however, they either have not yet been fully developed for practice or else not been made known to the DOTs for implementation. Needs related to pavement investigations appear to show an excellent area for CPT growth and use, especially because the readings can be effectively scaled down to shallow depths using miniature-size probes and sensors. With regard to the top priority (continuous soil sampling correlations with the CPT), this is now very possible and perhaps best achieved by local site calibrations in a particular geologic region using side-by-side comparisons of CPTu soundings with geoprobe samples. Both devices are now readily available across the United States and Canada.

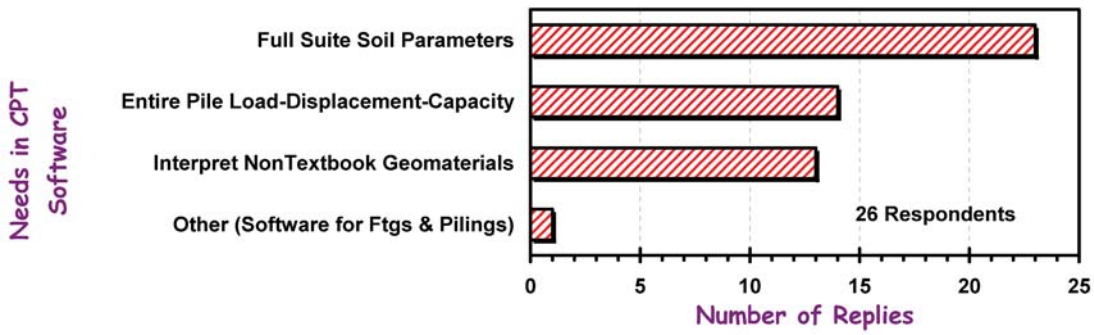

FIGURE 111 DOT survey results indicating CPT software needs.

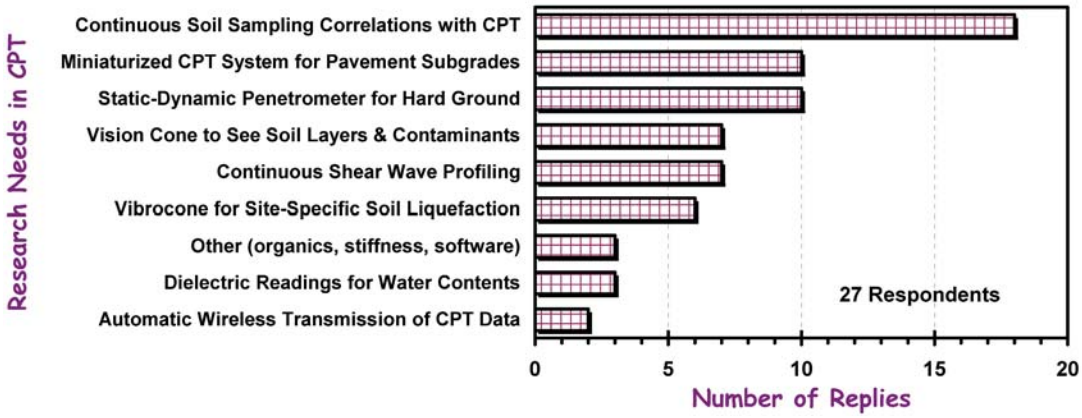

FIGURE 112 Research needs in cone penetrometer technology identified by DOT survey.

The newest electronic models of penetrometers in production collect the data directly in digital format, thus allowing as many channels as possible. It may soon become possible to take as many as ten readings continuously with depth, including q_t, f_s, u_1, u_2, u_3, V_s, dielectric (ζ), resistivity (Ω), lateral stress (σ_h), and pH. Developmental research with laboratory experiments, chamber testing, centrifuge modeling, and numerical simulations with advanced constitutive soil modeling will permit a more reliable and defensible interpretative framework for evaluation of the varied and complex soil parameters needed for design.

The importance and applicability of the shear wave velocity (V_s) in providing the fundamental soil stiffness ($G_{max} = \rho_T V_s^2$) has been shown herein with examples applied to both full-scale shallow and deep foundation systems, as well as discussed for use in obtaining saturated soil unit weights and application for evaluating seismic ground hazards. The methodology has been used to provide approximate nonlinear stress-strain-strength curves for both sands and clays, and therefore could be used as such for any and all depths. The importance of G_{max} in pavements is also fundamental and can be integrally related to the more common resilient modulus (M_R) for proper analyses.

Means of making continuous V_s measurements toward improving the state of the practice in collecting V_s by seismic cone testing are underway. Figure 113 shows results from the

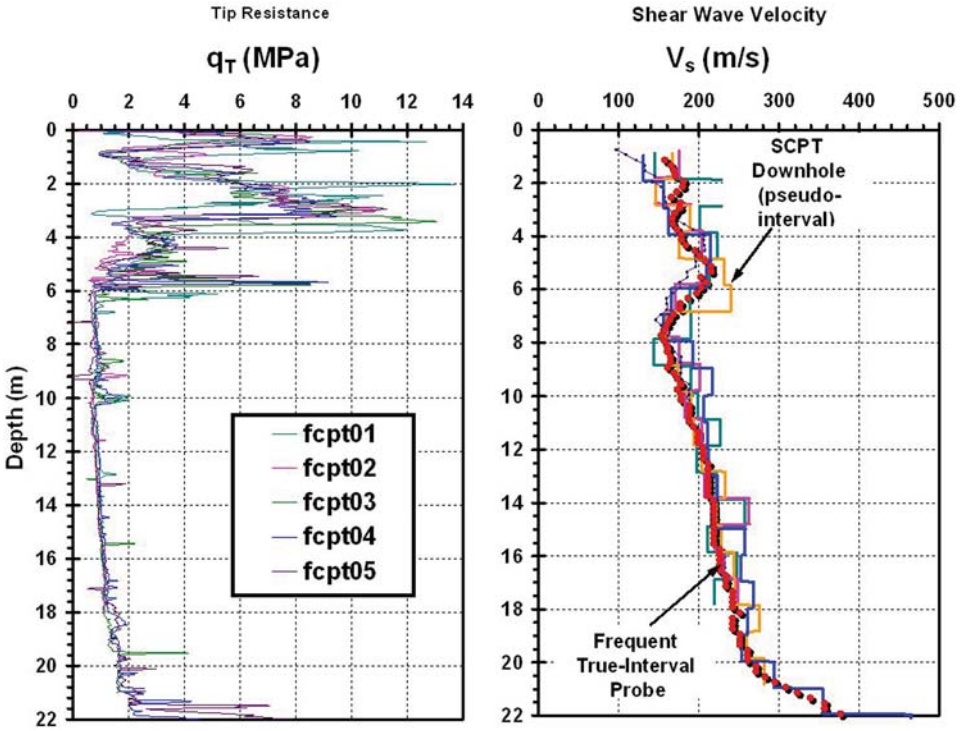

FIGURE 113 Results of special close-interval shear wave profiling at Northwestern University campus, Evanston, Illinois.

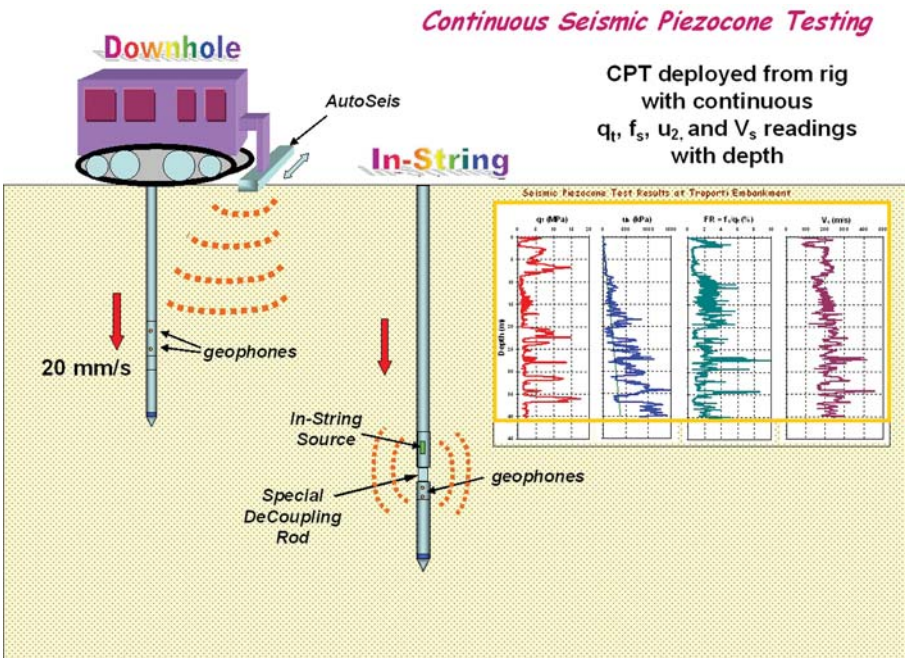

FIGURE 114 Concepts for continuous SCPTu by downhole and in-string arrays.

national test site at Northwestern University using a special probe to capture V_s measurements at close frequency intervals (i.e., every 20 cm). In addition, five standard series of SCPTu soundings were advanced, with the tip, sleeve, and porewater readings reported earlier in Figure 15 in chapter three. The results from the special frequent-interval downhole testing are seen to be "well-behaved" and much finer resolution and profiling of V_s than the standard coarser 1-m intervals.

An improvement to the SCPTu would be the capability for continuous shear wave measurements without the current practice of stopping every 1 m to conduct a standard downhole test. In this regard, the geophones reside at all times within the penetrometer, and it is merely that the practice continues to promulgate the original concept of oscillating between continuous CPT for the tip, sleeve, and porewater readings, then switch to a downhole geophysics test for shear wave determination. Alternative means to improve the SCPTu include use of a repeating autoseis positioned at the surface with continuous downhole wavelets captured during the penetrometer advancement or an in-string source-receiver unit that would "talk" to each other at a set distance and provide continuous P- and S-wave readings with depth. Both concepts are depicted in Figure 114.

REFERENCES

Abu-Farsakh, M.Y. and M.D. Nazzal, "Reliability of Piezocone Penetration Test Methods for Estimating the Coefficient of Consolidation of Cohesive Soils," *Transportation Research Record 1913*, Transportation Research Board, National Research Council, Washington, D.C., 2005, pp. 62–76.

Ahmadki, M.M. and P.K. Robertson, "Thin Layer Effects on the CPT *qc* Measurement," *Canadian Geotechnical Journal*, Vol. 42, Sep. 2005, pp. 1302–1317.

Almeida, M.S.S., F.A.B. Danziger, and T. Lunne, "Use of the Piezocone Test to Predict the Axial Capacity of Driven and Jacked Piles in Clay," *Canadian Geotechnical Journal,* Vol. 33, No. 1, 1996, pp. 33–41.

Alperstein, R., "Surface and Deep Vibratory Compaction of Sand," *Foundations and Ground Improvement* (GSP No. 113), American Society of Civil Engineers, Reston, Va., 2001, pp. 46–60.

Amini, F., "Potential Applications of Dynamic and Static Cone Penetrometers in MDOT Pavement Design and Construction," Report FHWA/MS-DOT-RD-03-162, Jackson State University, Jackson, Miss., Sep. 30, 2003, 31 pp.

Anderson, J.B., F.C. Townsend, and E. Horta, "A Brief Study on the Repeatability of In-Situ Tests at the Florida Department of Transportation Deep Foundations Research Site in Orlando, Florida," *Geotechnical & Geophysical Site Characterization*, Vol. 2 (ISC-2, Porto, Portugal), Millpress, Rotterdam, The Netherlands, 2004, pp. 1597–1604.

Andrus, R.D. and K.H. Stokoe, II, "Liquefaction Resistance of Soils Based on Shear Wave Velocity," *Journal of Geotechnical and Geoenvironmental Engineering*, Vol. 126, No. 11, 2000, pp. 1015–1026.

Atkinson, J.H., "Nonlinear Soil Stiffness in Routine Design," *Geotechnique*, Vol. 50, No. 5, 2000, pp. 485–508.

Auxt, J.A. and D. Wright, "Environmental Site Characterization in the US Using the Cone Penetrometer," *Proceedings, International Symposium on Cone Penetration Testing*, Vol. 2, Swedish Geotechnical Society Report 3:95, Oct. 4–5, 1995, Linköping, Sweden, pp. 387–392.

Badu-Tweneboah, K., D. Bloomquist, B.E. Ruth, and W.G. Miley, "CPT and DMT Testing of Highway Pavements in Florida," *Penetration Testing 1988*, Vol. 2, Balkema, Rotterdam, The Netherlands, 1988, pp. 627–633.

Baldi, G., D. Bruzzi, S. Superbo, M. Battaglio, and M. Jamiolkowski, "Seismic Cone in Po River Sand," *Penetration Testing 1988*, Vol. 2 (Proc. ISOPT-1, Orlando, Fla.), Balkema, Rotterdam, The Netherlands, 1988, pp. 643–650.

Baldi, G., R. Bellotti, V.N. Ghionna, M. Jamiolkowski, and D.C.F. LoPresti, "Modulus of Sands from CPTs and DMTs," *Proceedings, 12th International Conference on Soil Mechanics and Foundation Engineering*, Vol. 1, Rio de Janeiro, Brazil, 1989, Balkema, Rotterdam, The Netherlands, pp. 165–170.

Baligh, M.M., A.S. Azzouz, A.Z.E. Wissa, R.T. Martin, and M.J. Morrison, "The Piezocone Penetrometer," *Cone Penetration Testing and Experience* (Proc. ASCE National Convention, St. Louis, Mo.), 1981, pp. 247–263.

Battaglio, M., M. Jamiolkowski, R. Lancellotta, and R. Maniscalco, "Piezometer Probe Test in Cohesive Deposits," *Cone Penetration Testing and Experience* (Proc., ASCE National Convention, St. Louis, Mo.), 1981, pp. 264–302.

Been, K., J.H.A. Crooks, D.E. Becker, and M.G. Jefferies, "The Cone Penetration Test in Sands: State Parameter," *Geotechnique*, Vol. 36, No. 2, 1986, pp. 239–249.

Been, K., B.E. Lingnau, J.H.A. Crooks, and B. Leach, "Cone Penetration Test Calibration for Erksak Beaufort Sea Sand," *Canadian Geotechnical Journal*, Vol. 24, No. 4, 1987, pp. 601–610.

Been, K., J.H.A. Crooks, and M.G. Jefferies, "Interpretation of Material State from the CPT in Sands and Clays," *Penetration Testing in the UK*, Thomas Telford, London, United Kingdom, 1988, pp. 215–218.

Begemann, H.K., "The Friction Jacket Cone as an Aide in Determining the Soil Profile," *Proceedings, 6th International Conference on Soil Mechanics and Foundation Engineering*, Vol. 1, Montreal, QC, Canada, 1965, pp. 17–20.

Bonita, J.A., J.K. Mitchell, and T.L. Brandon, "In-Situ Liquefaction Evaluation Using a Vibrating Penetrometer," *Soil Dynamics and Liquefaction 2000* (GSP 107), American Society of Civil Engineers, Reston, Va., 2000, pp. 181–205.

Boulanger, R.W. and I.M. Idriss, "State Normalization of Penetration Resistance and the Effect of Overburden Stress on Liquefaction Resistance," *Proceedings, 11th Conference on Soil Dynamics and Earthquake Engineering*, Berkeley, Calif., 2004, pp. 484–491.

Bratton, W.L., "Cone Penetrometer: An Enabling Technology for Characterization and Monitoring Systems," *Proceedings, Advanced Vadose Zone Characterization Workshop*, Jan. 19, 2000, Applied Research Associates, Royalton, Vt. [Online]. Available: vadose.pnl.gov/.

Bratton, J.L. and D.A. Timian, "Environmental Site Applications of the CPT," *Proceedings, International Symposium on Cone Penetration Testing*, Vol. 2, Swedish Geotechnical Society Report 3:95, Oct. 4–5, 1995, Linköping, Sweden, pp. 429–434.

Briaud, J.-L. and J. Miran, *The Cone Penetrometer Test*, Report FHWA-SA-91-043, Federal Highway Administration, Washington, D.C., Feb. 1992, 161 pp.

Briaud, J.-L. and R.M. Gibbens, *Predicted and Measured Behavior of Five Spread Footings on Sand*, GSP No. 41, American Society of Civil Engineers, Reston, Va., 1994, 256 pp.

Broere, W. and A.F. Van Tol, "Horizontal Cone Penetration Testing in Sand," *Proceedings, International Conference on In-Situ Measurement of Soil Properties and Case Histories*, Bali, Indonesia, May 21–24, 2001, pp. 649–654.

Broms, B.B. and N. Flodin, "History of Soil Penetration Testing," *Proceedings of the First International Symposium on Penetration Testing*, Vol. 1, Orlando, Fla. (*Penetration Testing 1988*), Balkema, Rotterdam, The Netherlands, Mar. 20–24, 1988, pp. 157–220.

Brown, D.A., "Effect of Construction on Axial Capacity of Drilled Foundations in Piedmont Silts," *Journal of Geotechnical and Geoenvironmental Engineering*, Vol. 128, No. 12, 2002, pp. 967–973.

Brown, S.F., "Thirty-Sixth Rankine Lecture: Soil Mechanics in Pavement Engineering," *Geotechnique,* Vol. 46, No. 3, Sep. 1996, pp. 381–426.

Burland, J.B., "Small Is Beautiful: The Stiffness of Soils at Small Strains," *Canadian Geotechnical Journal*, Vol. 26, No. 4, 1989, pp. 499–516.

Burns, S.E. and P.W. Mayne, "Monotonic and Dilatory Pore Pressure Decay During Piezocone Tests," *Canadian Geotechnical Journal*, Vol. 35, No. 6, 1998, pp. 1063–1073.

Burns, S.E. and P.W. Mayne, "Analytical Cavity Expansion-Critical State Model for Piezocone Dissipation in Fine-Grained Soils," *Soils and Foundations*, Vol. 42, No. 2, 2002a, pp. 131–137.

Burns, S.E. and P.W. Mayne, "Interpretation of Seismic Piezocone Results for the Evaluation of Hydraulic Conductivity in Clays," *Geotechnical Testing Journal*, Vol. 25, No. 3, 2002b, pp. 333–340.

Bustamante, M. and L. Gianeselli, "Pile Bearing Capacity Prediction by Means of Static Penetrometer," *Proceedings, European Symposium on Penetration Testing*, Vol. 2, Amsterdam, The Netherlands, 1982, pp. 493–500.

Bustamante, M. and R. Frank, "Design of Axially Loaded Piles—French Practice," *Design of Axially Loaded Piles—European Practice* (Proc. ERTC3, Brussels, Belguim), Balkema, Rotterdam, The Netherlands, 1997, pp. 161–175.

Campanella, R.G., "Field Methods for Dynamic Geotechnical Testing," *Dynamic Geotechnical Testing II* (Special Tech Publication 1213), American Society for Testing and Materials, West Conshohocken, Pa., 1994, pp. 3–23.

Campanella, R.G., P.K. Robertson, and D. Gillespie, "Seismic Cone Penetration Test," *Use of In-Situ Tests in Geotechnical Engineering* (GSP 6), American Society of Civil Engineers, Reston, Va., 1986, pp. 116–130.

Campanella, R.G. and P.K. Robertson, "Current Status of the Piezocone Test," *Proceedings of the First International Symposium on Penetration Testing*, Vol. 1, Orlando, Fla. (*Penetration Testing 1988*), Balkema, Rotterdam, The Netherlands, Mar. 20–24, 1988, pp. 93–116.

Campanella, R.G., J.P. Sully, J.W. Greig, and G. Jolly, "Research and Development of a Lateral Stress Piezocone," *Transportation Research Record 1278*, Transportation Research Board, National Research Council, Washington, D.C., 1990, pp. 215–224.

Campanella, R.G. and I. Weemees, "Development and Use of an Electrical Resistivity Cone for Groundwater Contaminant Studies," *Canadian Geotechnical Journal*, Vol. 27, No. 5, 1990, pp. 557–567.

Campanella, R.G., H. Kristiansen, C. Daniel, and M.P. Davies, "Site Characterization of Soil Deposits Using Recent Advances in Piezocone Technology," *Geotechnical Site Characterization*, Vol. 2 (Proc. ISC-1, Atlanta, Ga.), Balkema, Rotterdam, The Netherlands, 1998, pp. 995–1000.

Casey, T.J. and P.W. Mayne, "Development of an Electrically Driven Automatic Downhole Seismic Source," *Soil Dynamics and Earthquake Engineering,* Vol. 22, 2002, pp. 951–957.

Chandler, R.J., "The In-Situ Measurement of the Undrained Shear Strength of Clays Using the Field Vane," *Vane Shear Strength Testing in Soils: Field and Lab Studies*, ASTM STP 1014, American Society for Testing and Materials, West Conshohocken, Pa., 1988, pp. 13–44.

Chen, B.S.-Y. and P.W. Mayne, *Profiling the Overconsolidation Ratio of Clays by Piezocone Tests*, Report No. GIT-CEEGEO-94-1 to National Science Foundation by Geosystems Engineering Group, Georgia Institute of Technology, Atlanta, 1994, 280 pp. [Online]. Available: http://www.ce.gatech.edu/~geosys/Faculty/Mayne/papers/index.html.

Chen, B.S.-Y. and P.W. Mayne, "Statistical Relationships Between Piezocone Measurements and Stress History of Clays," *Canadian Geotechnical Journal*, Vol. 33, No. 3, 1996, pp. 488–498.

Chen, B.S.-Y. and M.J. Bailey, "Lessons Learned from a Stone Column Test Program in Glacial Deposits," *Geo-Support 2004* (GSP 124), American Society of Civil Engineers, Reston, Va., 2004, pp. 508–519.

Chen, C.J. and C.H. Juang, "Calibration of SPT- and CPT-Based Liquefaction Evaluation Methods," *Innovations and Applications in Geotechnical Site Characterization* (GSP 97), American Society of Civil Engineers, Reston, Va., 2000, pp. 49–64.

Chun, B.S., Y.H. Yeoh, Y.K. Joung, and M. Sagong, "A Case Study on the Reduction of Settlement Causing by Compaction Grouting System," *Deformation Characteristics of Geomaterials*, Vol. 2 (Proc. Lyon, France), Swets and Zeitlinger, Lisse, The Netherlands, 2003, pp. 1411–1416.

Clausen, C.J.F., P.M. Aas, and K. Karlsrud, "Bearing Capacity of Driven Piles in Sand: The NGI Approach," *Frontiers in Offshore Geotechnics* (Proc. ISFOG, Perth, Australia), Taylor & Francis Group, London, United Kingdom, 2005, pp. 677–681.

Collota, T., R. Cantoni, and P.C. Moretti, "Italian Motorway System: Experiences with In-Situ Tests and Inclinometers for Urgent Remedial Works," *Transportation Research Record 1235*, Transportation Research Board, National Research Council, Washington, D.C., 1989, pp. 55–59.

Collotta, T., A. Frediani, and V. Manassero, "Features and Results of a Jet-Grouting Trial Field in Very Soft Peaty Soils," *GeoSupport 2004* (GSP 124), American Society of Civil Engineers, Reston, Va., 2004, pp. 887–901.

Coop, M.R. and D.W. Airey, "Carbonate Sands," *Characterization and Engineering Properties of Natural Soils*, Vol. 2 (Proc. Singapore), Swets and Zeitlinger, Lisse, The Netherlands, 2003, pp. 1049–1086.

Coutinho, R.Q., J.B. de Souza Neto, and K.C. de Arruda Dourado, "General Report: Characterization of Non-Textbook Geomaterials," *Geotechnical & Geophysical Site Characterization*, Vol. 2 (Proc. ISC-2, Porto, Portugal), Millpress, Rotterdam, The Netherlands, 2004, pp. 1233–1257.

Dahlberg, R., "Penetration, Pressuremeter, and Screw-Plate Tests in a Preloaded Natural Sand Deposit," *Proceedings of the European Symposium on Penetration Testing*, Vol. 2.2, Stockholm, Sweden, 1974, pp. 68–87.

Danzinger, F.A.B., M.S.S. Almeida, and G.C. Sills, "The Significance of Strain Path Analysis in Interpretation of Piezocone Dissipation Data," *Geotechnique*, Vol. 47, No. 5, 1997, pp. 901–914.

Dasari, G.R., M. Karthikeyan, T. Tan, M. Mimura, and K.K. Phoon, "In-Situ Evaluation of Radioisotope Cone Penetrometers in Clays," *Geotechnical Testing Journal*, Vol. 29, No. 1, 2006, pp. 45–53.

Dasenbrock, D.D., "Minnesota DOT's On-Line Geo-Spatial Borehole/Sounding Database Development," *Proceedings, GeoCongress 2006* (Atlanta, Ga.), 2006, pp. 1–6.

Davie, J.R., H. Senapathy, and W. Murphy, "Settlement Predictions Using Piezocone," *Vertical and Horizontal Deformations of Foundations and Embankments*, Vol. 1 (GSP 40), American Society of Civil Engineers, Reston, Va., 1994, pp. 818–829.

DeBeer, E.E., E. Goelen, W.J. Heynen, and K. Joustra, "Cone Penetration Test: International Reference Test Procedure," *Penetration Testing 1988*, Vol. 1 (Proc. ISOPT-1, Orlando, Fla.), Balkema, Rotterdam, The Netherlands, 1988, pp. 27–52.

DeGroot, D.J. and A.J. Lutenegger, "A Comparison Between Field and Laboratory Measurements of Hydraulic Conductivity in a Varved Clay," *Hydraulic Conductivity and Waste Contaminant Transport in Soil*, ASTM STP 1142, American Society for Testing and Materials, West Conshohocken, Pa., 1994, pp. 300–317.

DeGroot, D.J. and A.J. Lutenegger, "Geology and Engineering Properties of Connecticut Valley Varved Clay," *Characterization and Engineering Properties of Natural Soils*, Vol. 1, Swets and Zeitlinger, Lisse, The Netherlands, 2003, pp. 695–724.

DeGroot, D.J. and R. Sandven, "General Report: Laboratory and Field Comparisons," *Geotechnical & Geophysical Site Characterization*, Vol. 2 (ISC-2, Porto, Portugal), Millpress, Rotterdam, The Netherlands, 2004, pp. 1775–1789.

DeJong, J.T. and J.D. Frost, "A Multi-Friction Sleeve Attachment for the Cone Penetrometer," *Geotechnical Testing Journal*, Vol. 25, No. 2, 2002, pp. 111–127.

Demers, D. and S. Leroueil, "Evaluation of Preconsolidation Pressure and the Overconsolidation Ratio from Piezocone Tests of Clay Deposits in Quebec," *Canadian Geotechnical Journal*, Vol. 39, No. 1, 2002, pp. 174–192.

DeNicola, A. and M.F. Randolph, "Tensile and Compressive Shaft Capacity of Piles in Sand," *Journal of Geotechnical Engineering*, Vol. 119, No. 12, 1993, pp. 1952–1973.

deRuiter, J., "Electric Penetrometer for Site Investigations," *Journal of the Soil Mechanics and Foundations Division*, Vol. 97, No. SM2, 1971, pp. 457–472.

deRuiter, J., "Current Penetrometer Practice," *Cone Penetration Testing and Experience* (Proc. ASCE National Convention, St. Louis, Mo.), American Society of Civil Engineers, Reston, Va., 1981, pp. 1–48.

deRuiter, J., "The Static Cone Penetration Test," *Proceedings of the Second European Symposium on Penetration Testing*, Vol. 2 (Amsterdam), May 24–27, 1982, Balkema, Rotterdam, The Netherlands, pp. 389–405.

Durgunoğlu, H.T., H.F. Kulaç, O. Nur, S. Ikiz, O. Akbal, and C.G. Olgun, "A Case Study of Determination of Soil Improvement Realization Using CPT," *Proceedings, International Symposium on Cone Penetration Testing*, Vol. 2, Swedish Geotechnical Society Report 3:95, Oct. 4–5, 1995, Linköping, Sweden, pp. 441–446.

Elmgren, K., "Slot-Type Pore Pressure CPTu Filters," *Proceedings, International Symposium on Cone Penetration Testing*, Vol. 2, Swedish Geotechnical Society Report 3:95, Oct. 4–5, 1995, Linköping, The Netherlands, pp. 9–12.

Eslami, A., "Bearing Capacity of Shallow and Deep Foundations from CPT Resistance," *Proceedings, GeoCongress* (Atlanta, Ga.), American Society of Civil Engineers, Reston, Va., Feb. 26–Mar. 1, 2006, 6 pp.

Eslami, A. and B.H. Fellenius, "Pile Capacity by Direct CPT and CPTu Methods Applied to 102 Case Histories," *Canadian Geotechnical Journal*, Vol. 34, No. 6, 1997, pp. 880–898.

Fahey, M., "Deformation and In-Situ Stress Measurement," *Geotechnical Site Characterization*, Vol. 1 (Proc. ISC-1, Atlanta, Ga.), 1998, Balkema, Rotterdam, The Netherlands, pp. 49–68.

Fahey, M. and J.P. Carter, "A Finite Element Study of the Pressuremeter in Sand Using a Nonlinear Elastic Plastic Model," *Canadian Geotechnical Journal*, Vol. 30, No. 2, 1993, pp. 348–362.

Fahey, M., P.K. Robertson, and A.A. Soliman, "Towards a Rational Method of Predicting Settlements of Spread Footings on Sand," *Vertical and Horizontal Deformations of Foundations and Embankments*, Vol. 1, GSP 40, American Society of Civil Engineers, Reston, Va., 1994, pp. 598–611.

Farrington, S.P., "Development of a Wireline CPT System for Multiple Tool Usage," *Proceedings, Industry Partnerships for Environmental Science and Technology*, Oct. 17–19, 2000, 40 pp.

Farrington, S.P. and J.D. Shinn, "Hybrid Penetration for Geotechnical Site Investigation," *Proceedings, GeoCongress 2006*, Atlanta, Ga., 5 pp.

Fellenius, B.H., *Basics of Foundation Design*, BiTech Publishers, Richmond, BC, Canada, 1996, 134 pp. [Online]. Available: www.geoforum.com [2002].

Finke, K.A. and P.W. Mayne, "Piezocone Response in Piedmont Residual Geomaterials," *Behavioral Characteristics of Residual Soil* (GSP 92), American Society of Civil Engineers, Reston, Va., 1999, pp. 1–11.

Fioravante, V., et al. (1995) "Load Carrying Capacity of Large Diameter Bored Piles in Sand and Gravel," *Proceedings, 10th Asian Regional Conference on Soil Mechanics and Foundation Engineering*, Beijing, China, 1995.

Fioravante, V., M. Jamiolkowski, V.N. Ghionna, and S. Pedroni, "Stiffness of Carbonatic Quiou Sand from CPT," *Geotechnical Site Characterization*, Vol. 2, Balkema, Rotterdam, The Netherlands, 1998, pp. 1039–1049.

Fletcher, G.F.A., "Standard Penetration Test: Its Uses and Abuses," *Journal of the Soil Mechanics and Foundations Division*, Vol. 91, No. SM4, July 1965, pp. 67–75.

Foshee, J. and B. Bixler, "Cover Subsidence Sinkhole Evaluation of State Road 434, Longwood, Florida," *Journal of Geotechnical Engineering*, Vol. 120, No. 11, 1994, pp. 2026–2040.

Frank, R. and J.-P. Magnan, "Cone Penetration Testing in France: National Report," *Proceedings, International Symposium on Cone Penetration Testing*, Vol. 3, Swedish Geotechnical Society Report 3:95, Oct. 4–5, 1995, Linköping, Sweden, pp. 147–156.

Ghionna, V.N. and D. Porcino, "Liquefaction Resistance of Undisturbed and Reconstituted Samples of a Natural Coarse Sand from Undrained Cyclic Triaxial Tests," *Journal of Geotechnical and Geoenvironmental Engineering*, Vol. 132, No. 2, 2006, pp. 194–202.

Ghosh, N., "Correlation of In-Situ Tests for the Evaluation of Design Parameters," *Proceedings, International Symposium on Cone Penetration Testing*, Vol. 2, Swedish Geotechnical Society Report 3:95, Oct. 4–5, 1995, Linköping, Sweden, pp. 461–466.

Goble, G., *NCHRP Synthesis of Highway Practice 276: Geotechnical Related Development and Implementation of Load and Resistance Factor Design* (*LRFD*) *Methods*, Transportation Research Board, National Research Council, Washington, D.C., 1999, 69 pp.

Gorman, C.T., V.P. Drnevich, and T.C. Hopkins, "Measurement of In-Situ Shear Strength," *In-Situ Measurement of Soil Properties*, Vol. II, American Society of Civil Engineers, Reston, Va., 1975, pp. 139–140.

Gottardi, G. and L. Tonni, "Use of Piezocone Tests to Characterize the Silty Soils of the Venetian Lagoon at Treporti Test Site," *Geotechnical and Geophysical Site Characterization*, Vol. 2, Millpress, Rotterdam, The Netherlands, 2004, pp. 1643–1650.

Gupta, R.C. and J.L. Davidson, "Piezoprobe Determined Coefficient of Consolidation," *Soils & Foundations*, Vol. 26, No. 3, 1986, pp. 12–22.

Gwizdala, K. and A. Tejchman, "Pile Settlement Analysis Using CPT and Load-Transfer Functions t-z and q-z," *Proceedings, International Symposium on Cone Penetration Testing*, Vol. 2, Swedish Geotechnical Society Report 3:95, Oct. 4–5, 1995, Linköping, Sweden, pp. 473–478.

Hamouche, K.K., S. Leroueil, M. Roy, and A.J. Lutenegger, "In-Situ Evaluation of K_0 in Eastern Canada Clays," *Canadian Geotechnical Journal*, Vol. 32, No. 4, 1995, pp. 677–688.

Harr, M.E., *Foundations of Theoretical Soil Mechanics*, McGraw–Hill Publishing, New York, N.Y., 1966.

Hebeler, G.L., J.D. Frost, and J.D. Shinn, "A Framework for Using Textured Friction Sleeves at Sites Traditionally Problematic for CPT," *Geotechnical and Geophysical Site Characterization*, Vol. 1 (Proc. ISC-2, Porto, Portugal), Millpress, Rotterdam, The Netherlands, 2004, pp. 693–699.

Hegazy, Y.A. and P.W. Mayne, "Statistical Correlations Between V_s and CPT Data for Different Soil Types," *Proceedings, Symposium on Cone Penetration Testing*, Vol. 2, Swedish Geotechnical Society, Linköping, Sweden, 1995, pp. 173–178.

Hight, D. and S. Leroueil, "Characterization of Soils for Engineering Purposes," *Characterization and Engineering Properties of Natural Soils*, Vol. 1, Swets and Zeitlinger, Lisse, The Netherlands, 2003, pp. 255–360.

Holtz, R.D. and W.D. Kovacs, *An Introduction to Geotechnical Engineering*, Prentice–Hall, Inc., Englewood Cliffs, N.J., 1981, 733 pp.

Houlsby, G.T. and C.I. Teh, "Analysis of the Piezocone in Clay," *Penetration Testing 1988*, Vol. 2, Balkema, Rotterdam, The Netherlands, 1988, pp. 777–783.

Houlsby, G.T. and B.M. Ruck, "Interpretations of Signals from an Acoustic Cone Penetrometer," *Geotechnical Site Characterization*, Vol. 2 (Proc. ISC-1, Atlanta, Ga.), Balkema, Rotterdam, The Netherlands, 1998, pp. 1075–1080.

Howie, J.A., C. Daniel, A.A. Asalemi, and R.G. Campanella, "Combinations of In-Situ Tests for Control of Ground Modification in Silts and Sands," *Innovations and Applications in Geotechnical Site Characterization* (GSP 97), American Society of Civil Engineers, Reston, Va., 2000, pp. 181–198.

Hryciw, R.D., A.M. Ghalib, and S.A. Raschke, "In-Situ Soil Characterization Using Vision Cone Penetrometer," *Geotechnical Site Characterization*, Vol. 2 (Proc. ISC-1, Atlanta, Ga.), Balkema, Rotterdam, The Netherlands, 1998, pp. 1081–1086.

Hryciw, R.D. and S. Shin, "Thin Layer and Interface Characterization by VisCPT," *Geotechnical and Geophysical Site Characterization*, Vol. 1 (Proc. ISC-2, Porto, Portugal), Millpress, Rotterdam, The Netherlands, 2004, pp. 701–706.

Huang, A.B., J.W. Chang, D. Chen, and C.C. Yeh, "Site Characterization of a Dynamically Compacted Silty Sand," *Geotechnical Site Characterization*, Vol. 2 (Proc. ISC-1, Atlanta, Ga.), Balkema, Rotterdam, The Netherlands, 1998, pp. 1253–1258.

International Building Code, ICC IBC-2000, International Code Council, Washington, D.C., 2000.

Ireland, H.O., O. Moretto, and M. Vargas, "The Dynamic Penetration Test: A Standard That Is Not Standardized," *Geotechnique*, Vol. 20, No. 2, June 1970, pp. 185–192.

Islam, M.S. and Q.S.E. Hashmi, "Evaluation of Trench Backfill Compaction Using CPT," *Proceedings, International Symposium on Cone Penetration Testing*, Vol. 2, Swedish Geotechnical Society Report 3:95, Oct. 4–5, 1995, Linköping, Sweden, pp. 485–494.

Jamiolkowski, M., "Opening Address: CPT'95," *Proceedings, International Symposium on Cone Penetration Testing*, Vol. 1, Swedish Geotechnical Society Report 3:95, Oct. 4–5, 1995, Linköping, Sweden, pp. 7–15.

Jamiolkowski, M., "Soil Parameters Relevant to Bored Pile Design from Laboratory and In-Situ Tests," *Deep Foundations on Bored and Auger Piles*, Millpress, Rotterdam, The Netherlands, 2003, pp. 83–100.

Jamiolkowski, M., C.C. Ladd, J.T. Germaine, and R. Lancellotta, "New Developments in Field and Lab Testing of Soils," *Proceedings, 11th International Conference on Soil Mechanics and Foundation Engineering*, Vol. 1, San Francisco, Calif., Aug. 12–16, 1985, pp. 57–154.

Jamiolkowski, M., D.C.F. LoPresti, and M. Manassero, "Evaluation of Relative Density and Shear Strength of Sands from Cone Penetration Test and Flat Dilatometer Test," *Soil Behavior and Soft Ground Construction* (GSP 119), American Society of Civil Engineers, Reston, Va., 2001, pp. 201–238.

Jardine, R.J., D.M. Potts, A.B. Fourie, and J.B. Burland, "Studies of the Influence of Non-Linear Stress-Strain Characteristics in Soil-Structure Interaction," *Geotechnique*, Vol. 36, No. 3, 1986, pp. 377–396.

Jardine, R.J., J.R. Standing, and N. Kovacevic, "Lessons Learned From Full Scale Observations and the Practical Application of Advanced Testing and Modeling," *Deformation Characteristics of Geomaterials*, Vol. 2, Taylor & Francis Group, London, United Kingdom, 2005a, pp. 201–245.

Jardine, R.J., F. Chow, R. Overy, and J. Standing, *ICP Design Methods for Driven Piles in Sands and Clays,* Thomas Telford Ltd., London, United Kingdom, 2005b, 105 pp.

Jefferies, M.G. and M.P. Davies, "Use of CPTu to Estimate Equivalent SPT N60," *Geotechnical Testing Journal*, Vol. 16, No. 4, Dec. 1993, pp. 458–468.

Juang, C.H. and T. Jiang, "Assessing Probabilistic Methods for Liquefaction Potential Evaluation," *Soil Dynamics and Liquefaction* (GSP 107), American Society of Civil Engineers, Reston, Va., 2000, pp. 148–162.

Juang, C.H., C.J. Chen, and T. Jiang, "Probabilistic Framework for Liquefaction Potential by Shear Wave Velocity," *Journal of Geotechnical and Geoenvironmental Engineering,* Vol. 127, No. 8, 2001, pp. 670–678.

Juran, I. and M.T. Tumay, "Soil Stratification Using the Dual-Element Pore-Pressure Piezocone Test," *Transportation Research Record 1235*, Transportation Research Board, National Research Council, Washington, D.C., 1989, pp. 68–78.

Karlsrud, K., C.J.F. Clausen, and P.M. Aas, "Bearing Capacity of Driven Piles in Clay: The NGI Approach," *Frontiers in Offshore Geotechnics* (Proc. ISFOG, Perth, Australia), Taylor & Francis Group, London, United Kingdom, 2005, pp. 775–782.

Keaveny, J.M. and J.K. Mitchell, "Strength of Fine-Grained Soils Using the Piezocone," *Use of In-Situ Tests in Geotechnical Engineering* (GSP 6), American Society of Civil Engineers, Reston, Va., 1986, pp. 668–699.

Kolk, H.J., A.E. Baaijens, and M. Senders, "Design Criteria for Pipe Piles in Silica Sands," *Frontiers in Offshore Geotechnics* (Proc. ISFOG, Perth, Australia), Taylor & Francis Group, London, United Kingdom, 2005, pp. 711–716.

Konrad, J.-M. and K.T. Law, "Undrained Shear Strength from Piezocone Tests," *Canadian Geotechnical Journal*, Vol. 24, No. 3, 1987, pp. 392–405.

Kulhawy, F.H., C.H. Trautmann, J.F. Beech, T.D. O'Rourke, and W. McGuire, *Transmission Line Structure Foundations for Uplift-Compression Loading*, Report EL-2870, Electric Power Research Institute, Palo Alto, Calif., 1983, 412 pp.

Kulhawy, F.H. and P.W. Mayne, *Manual on Estimating Soil Properties for Foundation Design*, Report EPRI EL-6800, Electric Power Research Institute, Palo Alto, Calif., 1990, 306 pp.

Ladd, C.C., "Stability Evaluation During Staged Construction," The 22nd Terzaghi Lecture, *Journal of Geotechnical Engineering*, Vol. 117, No. 4, 1991, pp. 540–615.

Ladd, C.C. and D.J. DeGroot, "Recommended Practice for Soft Ground Site Characterization," *Soil & Rock America 2003* (Proc. 12th Pan American Conf., Massachusetts Institute of Technology, Boston), Verlag Glückauf, Essen, Germany, 2003, pp. 3–57.

Lambson, M. and P. Jacobs, "The Use of the Laser Induced Fluorescence Cone for Environmental Investigations," *Proceedings, International Symposium on Cone Penetration Testing*, Vol. 2, Swedish Geotechnical Society Report 3:95, Oct. 4–5, 1995, Linköping, Sweden, pp. 29–34.

Larsson, R., "Use of a Thin Slot as Filter in Piezocone Tests," *Proceedings, International Symposium on Cone Penetration Testing*, Vol. 2, Swedish Geotechnical Society Report 3:95, Oct. 4–5, 1995, Linköping, Sweden, pp. 35–40.

Lee, J.H. and R. Salgado, "Determination of Pile Base Resistance in Sands," *Journal of Geotechnical and Geoenvironmental Engineering*, Vol. 125, No. 8, 1999, pp. 673–683.

Lee, L.T., P.G. Malone, and G.E. Robitaille, "Grouting on Retraction of Cone Penetrometer," *Geotechnical Site Characterization*, Vol. 1 (Proc. ISC-1, Atlanta, Ga.), Balkema, Rotterdam, The Netherlands, 1998, pp. 641–643.

Lehane, B. and E. Cosgrove, "Applying Triaxial Compression Stiffness Data to Settlement Prediction of Shallow Foundations," *Geotechnical Engineering,* Vol. 142, Oct. 2000, pp. 191–200.

Lehane, B.M., J.A. Schneider, and X. Xu, *A Review of Design Methods for Offshore Driven Piles in Siliceous*

Sand, Report GEO: 05358, University of Western Australia, Perth, Sep. 2005, 105 pp.

Leroueil, S., G. Bouclin, F. Tavenas, L. Beregeron, and P. LaRochelle, "Permeability Anisotropy of Natural Clays as a Function of Strain," *Canadian Geotechnical Journal,* Vol. 27, No. 5, Oct. 1990, pp. 568–579.

Leroueil, S. and M. Jamiolkowski, "Exploration of Soft Soil and Determination of Design Parameters," *Proceedings, GeoCoast'91*, Yokohama, Japan, Vol. 2, Port and Harbour Research Institute, Hasaki, Japan, 1991, pp. 969–998.

Leroueil, S., G. Martel, D. Demers, D. Virely, and P. LaRochelle, "Practical Use of the Piezocone in Eastern Canada," *Proceedings, International Symposium on Cone Penetration Testing*, Vol. 2, Swedish Geotechnical Society Report 3:95, Oct. 4–5, 1995, Linköping, Sweden, pp. 515–522.

Leroueil, S. and D. Hight, "Behavior and Properties of Natural Soils and Soft Rocks," C*haracterization and Engineering Properties of Natural Soils*, Vol. 1, Swets and Zeitlinger, Lisse, The Netherlands, 2003, pp. 29–254.

Lightner, E.M. and C.B. Purdy, "Cone Penetrometer Development and Testing for Environmental Applications," *Proceedings, International Symposium on Cone Penetration Testing*, Vol. 2, Swedish Geotechnical Society Report 3:95, Oct. 4–5, 1995, Linköping, Sweden, pp. 41–48.

Lillis, C., A.J. Lutenegger, and M. Adams, "Compression and Uplift of Rammed Aggregate Piers in Clay," *GeoSupport 2004* (GSP 124), American Society of Civil Engineers, Reston, Va., 2004, pp. 497–507.

Long, M. and G.T. Gudjonsson, "T-Bar Testing in Irish Soils," *Geotechnical and Geophysical Site Characterization*, Vol. 1 (Proc. ISC-2, Porto, Portugal), Millpress, Rotterdam, The Netherlands, 2004, pp. 719–726.

LoPresti, D.C.F., O. Pallara, V. Fioravante, and M. Jamiolkowski, "Assessment of Quasi-Linear Models for Sands," *Pre-Failure Deformation Behavior of Geomaterials*, Thomas Telford Ltd., London, United Kingdom, 1998, pp. 363–372.

Lunne, T., "In-Situ Testing in Offshore Geotechnical Investigations," *Proceedings, International Conference on In-Situ Measurement of Soil Properties and Case Histories*, Bali, Indonesia, 2001, pp. 61–81.

Lunne, T., T. Eidsmoen, D. Gillespie, and J.D. Howland, "Laboratory and Field Evaluation of Cone Penetrometers," *Use of In-Situ Tests in Geotechnical Engineering* (GSP 6), American Society of Civil Engineers, Reston, Va., 1986, pp. 714–729.

Lunne, T. and J. Keaveny, "Technical Report on Solution of Practical Problems Using CPT," *Proceedings, International Symposium on Cone Penetration Testing*, Vol. 3, Swedish Geotechnical Society Report 3:95, Oct. 4–5, 1995, Linköping, Sweden, pp. 119–138.

Lunne, T., J.J.M. Powell, and P.K. Robertson, "Use of Piezocone Tests in Non-Textbook Materials," *Advances in Site Investigation Practice*, Thomas Telford Ltd., London, United Kingdom, 1996, pp. 438–451.

Lunne, T., P.K. Robertson, and J.J.M. Powell, *Cone Penetration Testing in Geotechnical Practice*, Blackie Academic, EF Spon/Routledge Publishers, New York, N.Y., 1997, 312 pp.

Lunne, T., M. Long, and C.F. Forsberg, "Characterization and Engineering Properties of Holmen, Drammen Sand," *Characterisation and Engineering Properties of Natural Soils*, Vol. 2 (Proc. Singapore), Swets and Zeitlinger, Lisse, The Netherlands, 2003, pp. 1121–1148.

Lutenegger, A.J., M.G. Kabir, and S.R. Saye, "Use of Penetration Tests to Predict Wick Drain Performance in Soft Clay," *Penetration Testing 1988*, Vol. 2, Balkema, Rotterdam, The Netherlands, 1988, pp. 843–848.

Lutenegger, A.J. and D.J. DeGroot, "Techniques for Sealing Cone Penetrometer Holes," *Canadian Geotechnical Journal*, Vol. 32, No. 5, 1995, pp. 880–891.

Lutenegger, A.J., D.J. DeGroot, C. Mirza, and M. Bozozuk, *NCHRP Report 378: Recommended Guidelines for Sealing Geotechnical Exploratory Holes*, Transportation Research Board, National Research Council, Washington, D.C., 1995, 52 pp.

Mayne, P.W., "CPT-Based Prediction of Footing Response," *Measured and Predicted Behavior of Five Spread Footings on Sand* (GSP 41), American Society of Civil Engineers, Reston, Va., 1994, pp. 214–218.

Mayne, P.W., "Stress-Strain-Strength-Flow Parameters from Enhanced In-Situ Tests," *Proceedings, International Conference on In-Situ Measurement of Soil Properties and Case Histories*, Bali, Indonesia, 2001, pp. 27–48.

Mayne, P.W., "Class-A Footing Response Prediction from Seismic Cone Tests," *Deformation Characteristics of Geomaterials*, Vol. 1 (Proc. IS-Lyon, France), Swets and Zeitlinger, Lisse, The Netherlands, 2003, pp. 883–888.

Mayne, P.W., "Integrated Ground Behavior: In-Situ and Lab Tests," *Deformation Characteristics of Geomaterials*, Vol. 2 (Proc. Lyon, France), Taylor & Francis, London, United Kingdom, 2005, pp. 155–177.

Mayne, P.W., "In-Situ Test Calibrations for Evaluating Soil Parameters," Overview Paper, *Characterization and Engineering Properties of Natural Soils II* (Proc. Singapore Workshop), Taylor & Francis Group, London, United Kingdom, 2006a.

Mayne, P.W., "The 2nd James K. Mitchell Lecture: Undisturbed Sand Strength from Seismic Cone Tests," *Geomechanics and Geoengineering*, Vol. 1, No. 4, 2006b, pp. 239–247.

Mayne, P.W. and H.E. Stewart, "Pore Pressure Response of K_0 Consolidated Clays," *Journal of Geotechnical Engineering*, Vol. 114, No. 11, 1988, pp. 1340–1346.

Mayne, P.W., F.H. Kulhawy, and J.N. Kay, "Observations on the Development of Porewater Pressures During Piezocone Testing in Clays," *Canadian Geotechnical Journal*, Vol. 27, No. 4, 1990, pp. 418–428.

Mayne, P.W., J.K. Mitchell, J.A. Auxt, and R. Yilmaz, "U.S. National Report on CPT," *Proceedings, International Symposium on Cone Penetration Testing*, Vol. 1, Swedish

Geotechnical Society Report 3:95, Linköping, Sweden, Oct. 4–5, 1995, pp. 263–276.

Mayne, P.W. and G.J. Rix, "Correlations Between Shear Wave Velocity and Cone Tip Resistance in Clays," *Soils & Foundations*, Vol. 35, No. 2, 1995, pp. 107–110.

Mayne, P.W., P.K. Robertson, and T. Lunne, "Clay Stress History Evaluated from Seismic Piezocone Tests," *Geotechnical Site Characterization*, Vol. 2, Balkema, Rotterdam, The Netherlands, 1998, pp. 1113–1118.

Mayne, P.W. and H.G. Poulos, "Approximate Displacement Influence Factors for Elastic Shallow Foundations," *Journal of Geotechnical and Geoenvironmental Engineering*, Vol. 125, No. 6, 1999, pp. 453–460.

Mayne, P.W. and J.A. Schneider, "Evaluating Axial Drilled Shaft Response by Seismic Cone," *Foundations & Ground Improvement,* GSP 113, American Society of Civil Engineers, Reston, Va., 2001, pp. 655–669.

Mayne, P.W. and A. Elhakim, "Axial Pile Response Evaluation by Geophysical Piezocone Tests," *Proceedings, Ninth International Conference on Piling and Deep Foundations*, Nice, France, June 3–5, 2002, pp. 543–550.

Mayne, P.W. and D.A. Brown, "Site Characterization of Piedmont Residuum of North America," *Characterization and Engineering Properties of Natural Soils*, Vol. 2, Swets and Zeitlinger, Lisse, The Netherlands, 2003, pp. 1323–1339.

Mayne, P.W. and Campanella, R.G., "Versatile Site Characterization by Seismic Piezocone," *Proceedings, 16th International Conference on Soil Mechanics and Geotechnical Engineering*, Vol. 2 (Osaka), Millpress, Rotterdam, The Netherlands, 2005, pp. 721–724.

McGillivray, A.V., T. Casey, P.W. Mayne, and J.A. Schneider, "An Electro-Vibrocone for Site-Specific Evaluation of Soil Liquefaction Potential," *Innovations and Applications in Geotechnical Site Characterization* (GSP 97), American Society of Civil Engineers, Reston, Va., 2000, pp. 106–117.

Menge, P. and W. Van Impe, "The Application of Acoustic Emission Testing with Penetration Testing," *Proceedings, International Symposium on Cone Penetration Testing*, Vol. 2, Swedish Geotechnical Society Report 3:95, Oct. 4–5, 1995, Linköping, Sweden, pp. 49–54.

Mesri, G., "Settlement of Embankments on Soft Clays," *Vertical and Horizontal Deformations of Foundations and Embankments*, Vol. 1 (GSP 40), American Society of Civil Engineers, Reston, Va., 1994, pp. 8–56.

Mesri, G. and M. Abdel-Ghaffar, "Cohesion Intercept in Effective Stress Stability Analysis," *Journal of Geotechnical Engineering*, Vol. 119, No. 8, 1993, pp. 1229–1249.

Meyerhof, G.G., "Shallow Foundations," *Journal of the Soil Mechanics and Foundations Division*, Vol. 91, No. SM2, Mar. 1965, pp. 21–31.

Meyerhof, G.G., "Bearing Capacity and Settlement of Pile Foundations," *Journal of the Geotechnical Engineering Division*, Vol. 102, No. GT3, Mar. 1976, pp. 197–228.

Mimura, M., "Characteristics of Some Japanese Natural Sands—Data from Undisturbed Frozen Samples," *Characterisation and Engineering Properties of Natural Soils*, Vol. 2 (Proc. Singapore), Swets and Zeitlinger, Lisse, The Netherlands, 2003, pp. 1149–1168.

Mimura, M., T. Shibata, A.K. Shrivastava, and M. Nobuyama, "Performance of RI Cone Penetrometers in Sand Deposit," *Proceedings, International Symposium on Cone Penetration Testing*, Vol. 2, Swedish Geotechnical Society Report 3:95, Oct. 4–5, 1995, Linköping, Sweden, pp. 55–60.

Mitchell, J.K., "Ground Improvement Evaluation by In-Situ Tests," *Use of In-Situ Tests in Geotechnical Engineering* (GSP 6), American Society of Civil Engineers, Reston, Va., 1986, pp. 221–236.

Mitchell, J.K. and W.S. Gardner, "In-Situ Measurement of Volume Change Characteristics," *In-Situ Measurement of Soil Properties*, Vol. II (Proc. Raleigh, N.C. Conference), American Society of Civil Engineers, Reston, Va., 1975, pp. 279–345.

Mitchell, J.K. and T. Lunne, "Cone Resistance as a Measure of Sand Strength," *Journal of Geotechnical Engineering*, Vol. 104 (GT7), 1978, pp. 995–1012.

Mitchell, J.K. and Z.V. Solymar, "Time-Dependent Strength Gain in Freshly Deposited or Densified Sand," *Journal of Geotechnical Engineering*, Vol. 110, No. 11, 1984, pp. 1559–1576.

Mlynarek, Z., E. Welling, and W. Tschuschke, "Conductivity Piezocone Penetration Test for Evaluation of Soil Contamination," *Proceedings, International Symposium on Cone Penetration Testing*, Vol. 2, Swedish Geotechnical Society Report 3:95, Oct. 4–5, 1995, Linköping, Sweden, pp. 233–237.

Mohammad, L.N., H.H. Titi, and A. Herath, "Effect of Moisture Content and Dry Unit Weight on the Resilient Modulus of Subgrade Soils Predicted by Cone Penetration Test," Report FHWA/LA.00/355, Louisiana Transportation Research Center, Baton Rouge, June 2002, 86 pp.

Morioka, B.T. and P.G. Nicholson, "Evaluation of Liquefaction Potential of Calcareous Sand," *Proceedings, Tenth International Offshore and Polar Engineering Conference*, Seattle, Wash., May 28–June 2, 2000, pp. 494–500.

Moss, R.E.S., R.B. Seed, R.E. Kayen, J.P. Stewart, and A. Der Kiureghian, "CPT-Based Probabilistic Assessment of Seismic Soil Liquefaction Initiation," Report No. PEER-2003/xx, Pacific Earthquake Engineering Research, Berkeley, Calif., Sep. 2003, 70 pp.

Moss, R.E.S., R.B. Seed, and R.S. Olsen, "Normalizing the CPT for Overburden Stress," *Journal of Geotechnical and Geoenvironmental Engineering*, Vol. 132, No. 3, 2006, pp. 378–387.

Moss, R.E.S., R.B. Seed, R.E. Kayen, J.P. Stewart, A. Der Kiureghian, and K.O. Cetin, "CPT-Based Probabilistic and Deterministic Assessment of In-Situ Seismic Soil Liquefaction Potential," *Journal of Geotechnical and Geoenvironmental Engineering*, Vol. 132, No. 8, Aug. 2006, pp. 1032–1051.

Mulabdić, M., S. Eskilson, and R. Larsson, "Calibration of Piezocones for Investigations in Soft Soils and Demands for Accuracy of the Equipment," *Report Varia 270*, Swedish Geotechnical Institute, Linköping, Sweden, 1990, 62 pp.

Nash, D.F.T., J.J.M. Powell and I.M. Lloyd, "Initial Investigation of the Soft Clay Test Site at Bothkennar," *Geotechnique*, Vol. 42, No. 2, June 1992, pp. 163–183.

Nederlands Normalisatie Institute (NNI), "Geotechnics: Determination of the Cone Resistance and Sleeve Friction of Soil. Electric Cone Penetration Test," *Dutch Standard NEN 5140*, Delft, The Netherlands, 1996.

Newcomb, D.E. and B. Birgisson, *NCHRP Synthesis of Highway Practice 278: Measuring In Situ Mechanical Properties of Pavement Subgrade Soils*, Transportation Research Board, National Research Council, Washington, D.C., 1999, 73 pp.

Nutt, N.R.F. and G.T. Houlsby, "Calibration Tests on the Cone Pressuremeter in Carbonate Sand," *Calibration Chamber Testing*, Elsevier, New York, N.Y., 1991, pp. 265–276.

Olsen, R.S. and J.K. Mitchell, "CPT Stress Normalization and Prediction of Soil Classification," *Proceedings, International Symposium on Cone Penetration Testing*, Vol. 2, Swedish Geotechnical Society, Linköping, Sweden, 1995, pp. 257–262.

O'Neill, M.W. and L.C. Reese, *Drilled Shafts: Construction Procedures & Design Methods*, Vols. I and II, Publication FHWA-IF-99-025, U.S. Department of Transportation, ADSC, International Association of Foundation Drilling, Dallas, Tex., 1999, 758 pp.

Pamukcu, S. and H.Y. Fang, "Development of a Chart for Preliminary Assessments in Pavement Design Using Some In-Situ Soil Parameters," *Transportation Research Record 1235*, Transportation Research Board, National Research Council, Washington, D.C., 1989, pp. 38–44.

Parez, L. and R. Faureil, "Le Piézocone. Améliorations Apportées á la Reconnaissance de Sols," *Revue Française de Géotech*, Vol. 44, 1988, pp. 13–27.

Parkin, A.K., "Chamber Testing of Piles in Calcareous Sand and Silt," *Calibration Chamber Testing*, Elsevier, New York, N.Y., 1991, pp. 289–302.

Peuchen, J., "Commercial CPT Profiling in Soft Rocks and Hard Soils," *Geotechnical Site Characterization*, Vol. 2, (Proc. ISC-1, Atlanta, Ga.), Balkema, Rotterdam, The Netherlands, 1998, pp. 1131–1137.

Plomteux, C., A. Porhaba, and C. Spaulding, "CMC Foundation System for Embankment Support," *GeoSupport 2004* (GSP 124), American Society of Civil Engineers, Reston, Va., 2004, pp. 980–992.

Pluimgraaff, D., W.L. Bratton, and M. Hilhorst, "CPT Sensor for Bio-Characterization of Contaminated Sites," *Proceedings, International Symposium on Cone Penetration Testing*, Vol. 2, Swedish Geotechnical Society Report 3:95, Oct. 4–5, 1995, Linköping, Sweden, pp. 569–576.

Poulos, H.G., "Pile Behavior: Theory and Applications" (Rankine Lecture), *Geotechnique*, Vol. 39, No. 3, 1989, pp. 363–415.

Poulos, H.G. and E.H. Davis, *Elastic Solutions for Soil and Rock Mechanics*, John Wiley & Sons, New York, N.Y., 1974, 441 pp.

Poulos, H.G. and E.H. Davis, *Pile Foundation Analysis and Design*, John Wiley & Sons, New York, N.Y., 1980, 397 pp.

Powell, J.J.M. and R.S.T. Quarterman, "The Interpretation of Cone Penetration Tests in Clays with Particular Reference to Rate Effects," *Penetration Testing 1988*, Vol. 2, (Orlando, Fla.), Balkema, Rotterdam, The Netherlands, 1988, pp. 903–909.

Powell, J.J.M., T. Lunne, and R. Frank, "Semi-Empirical Design for Axial Pile Capacity in Clays," *Proceedings, 15th International Conference on Soil Mechanics and Geotechnical Engineering*, Vol. 2, (Istanbul, Turkey), Balkema, Rotterdam, The Netherlands, 2001, pp. 991–994.

Puppala, A.J. and A. Porhaba, "International Perspectives on Quality Assessment of Deep Mixing," *GeoSupport 2004* (GSP 124), American Society of Civil Engineers, Reston, Va., 2004, pp. 826–837.

Puppala, A.J., V. Bhadriarju, and A. Porhaba, "In-Situ Methods and Their Quality Assessments in Ground Improvement Projects," *Geotechnical and Geophysical Site Characterization*, Vol. 2 (Proc. ISC-2 Porto, Portugal), Millpress, Rotterdam, The Netherlands, 2004, pp. 1185–1190.

Randolph, M.F., "Characterization of Soft Sediments for Offshore Applications," *Geotechnical and Geophysical Site Characterization*, Vol. 1 (Proc. ISC-2, Porto, Portugal), Millpress, Rotterdam, The Netherlands, 2004, pp. 209–232.

Randolph, M.F. and C.P. Wroth, "Analysis of Deformation of Vertically-Loaded Piles," *Journal of the Geotechnical Engineering Division*, Vol. 104, No. GT12, 1978, pp. 1465–1488.

Randolph, M.F. and C.P. Wroth, "A Simple Approach to Pile Design and the Evaluation of Pile Tests," *Behavior of Deep Foundations*, STP 670, American Society for Testing and Materials, West Conshohocken, Pa., 1979, pp. 484–499.

Randolph, M.F., M. Cassidy, S. Gourvenec, and C. Erbrich, "Challenges of Offshore Geotechnical Engineering," *Proceedings, 16th International Conference on Soil Mechanics and Geotechnical Engineering*, Vol. 1, Osaka, Japan, Sep. 12–16, 2005, pp. 123–176.

Robertson, P.K., "Soil Classification Using the Cone Penetration Test," *Canadian Geotechnical Journal*, Vol. 27, No. 1, 1990, pp. 151–158.

Robertson, P.K., "Sixty Years of the CPT—How Far Have We Come?" *Proceedings, International Conference on In-Situ Measurement of Soil Properties and Case Histories*, Bali, Indonesia, May 21–24, 2001, pp. 1– 16.

Robertson, P.K. and R.G. Campanella, "Interpretation of Cone Penetration Tests: Sands," *Canadian Geotechnical Journal*, Vol. 20, No. 4, 1983, pp. 719–733.

Robertson, P.K., R.G. Campanella, and A. Wightman, "SPT–CPT Correlations," *Journal of the Geotechnical Engineering* Division, Vol. 108, No. GT 11, 1983, pp. 1449–1459.

Robertson, P.K. and R.G. Campanella, *Guidelines for Use and Interpretation of the Electronic Cone Penetration Test*, Hogentogler & Company, Inc., Gaithersburg, Md., 1984, 154 pp.

Robertson, P.K., R.G. Campanella, D. Gillespie, and J. Greig, "Use of Piezometer Cone Data," *Use of In-Situ Tests in Geotechnical Engineering* (GSP 6), American Society of Civil Engineers, Reston, Va., 1986, pp. 1263–1280.

Robertson, P.K., R.G. Campanella, M.P. Davies, and A. Sy, "Axial Capacity of Driven Piles in Deltaic Soils Using CPT," *Penetration Testing 1988*, Vol. 2, Balkema, Rotterdam, The Netherlands, 1988, pp. 919–928.

Robertson, P.K., J.P. Sully, D.J. Woeller, T. Lunne, J.J.M. Powell, and D.G. Gillespie, "Estimating Coefficient of Consolidation from Piezocone Tests," *Canadian Geotechnical Journal*, Vol. 39, No. 4, 1992, pp. 539–550.

Robertson, P.K., T. Lunne, and J.J.M. Powell, "GeoEnvironmental Applications of Penetration Testing," *Geotechnical Site Characterization*, Vol. 1 (Proc. ISC-1, Atlanta, Ga.), Balkema, Rotterdam, The Netherlands, 1998, pp. 35–48.

Robertson, P.K. and C.E. Wride, "Evaluating Cyclic Liquefaction Potential Using the Cone Penetration Test," *Canadian Geotechnical Journal*, Vol. 35, No. 3, 1998, pp. 442–459.

Robertson, P.K., et al., "The CANLEX Project: Summary & Conclusions," *Canadian Geotechnical Journal*, Vol. 37, No. 3, 2000, pp. 563–591.

Romani, F., R.M. Beard, and P.E. Mooney, "Some CPT Applications for Foundation and Landslide Studies in Southern California," *Penetration Testing 1988*, Vol. 2, Balkema, Rotterdam, The Netherlands, 1988, pp. 929–932.

Sacchetto, M., A. Trevisan, K. Elmgren, and K. Melander, "Cone Penetration Test While Drilling," *Geotechnical and Geophysical Site Characterization*, Vol. 1 (Proc. ISC-2, Porto, Portugal), Millpress, Rotterdam, The Netherlands, 2004, pp. 787–794.

Salgado, R., J.K. Mitchell, and M. Jamiolkowski, "Calibration Chamber Size Effects on Penetration Resistance in Sand," *Journal of Geotechnical and Geoenvironmental Engineering*, Vol. 124, No. 9, 1998, pp. 878–888.

Sanglerat, G., *The Penetrometer and Soil Exploration*, Elsevier Publishing Company, Amsterdam, The Netherlands, 1972, 488 pp.

Sanglerat, G., M. Petit-Maire, F. Bardot, and P. Savasta, "Additional Results of the AMAP Sols Static-Dynamic Penetrometer," *Proceedings, International Symposium on Cone Penetration Testing*, Vol. 2, Swedish Geotechnical Society Report 3:95, Oct. 4–5, 1995, Linköping, Sweden, pp. 85–91.

Sanglerat, G., M. Petit-Maire, F. Bardot, and P. Savasta, "Static Penetration in Dense Gravel, Sandstone, and Hard Claystone," *Revue Française de Géotechnique*, No. 97, 1999, pp. 43–54.

Schmertmann, J.H., "Static Cone to Compute Static Settlement over Sand," *Journal of the Soil Mechanics and Foundations Division,* Vol. 96, No. SM3, 1970, pp. 1011–1043.

Schmertmann, J.H., *Guidelines for Cone Penetration Test: Performance and Design*, Report FHWA-TS-78-209, Federal Highway Administration, Washington, D.C., 1978a, 146 pp.

Schmertmann, J.H., "Use the SPT to Measure Soil Properties?" *Dynamic Geotechnical Testing*, Special Technical Publication No. 654, American Society for Testing and Materials, West Conshohocken, Pa., 1978b, pp. 341–355.

Schmertmann, J.H., "Dilatometer to Compute Foundation Settlements," *Use of In-Situ Tests in Geotechnical Engineering* (GSP 6), American Society of Civil Engineers, Reston, Va., 1986, pp. 303–321.

Schnaid, F., "Geocharacterization and Engineering Properties of Natural Soils by In-Situ Tests," *Proceedings, 16th International Conference on Soil Mechanics and Geotechnical Engineering*, Vol. 1 (Osaka, Japan), Sep. 12–16, 2005, Millpress, Rotterdam, The Netherlands, pp. 3–45.

Schnaid, F., B.M. Lehane, and M. Fahey, "In-Situ Test Characterization of Unusual Geomaterials," *Geotechnical and Geophysical Site Characterization*, Vol. 1 (Proc. ISC-2, Porto, Portugal), Millpress, Rotterdam, The Netherlands, 2004, pp. 49–74.

Schneider, J.A. and P.W. Mayne, "Ground Improvement Assessment Using SCPTUs and Crosshole Data," *Innovations and Applications in Geotechnical Site Characterization* (GSP 97), American Society of Civil Engineers, Reston, Va., 2000, pp. 169–180.

Seed, H.B. and I.M. Idriss, "Simplified Procedure for Evaluating Soil Liquefaction Potential," *Journal of the Soil Mechanics and Foundations Division,* Vol. 97, No. SM 9, 1971, pp. 1249–1273.

Senneset, K., "Penetration Testing in Norway," *Proceedings of the European Symposium on Penetration Testing*, Vol. 1, Swedish Geotechnical Society, Stockholm, Sweden, June 5–7, 1974, pp. 85–95.

Senneset, K., R. Sandven, T. Lunne, T. By, and T. Amundsen, "Piezocone Tests in Silty Soils," *Penetration Testing 1988*, Vol. 2, Balkema, Rotterdam, The Netherlands, 1988, pp. 955–974.

Senneset, K., R. Sandven, and N. Janbu, "Evaluation of Soil Parameters from Piezocone Tests," *Transportation Research Record 1235*, Transportation Research Board, National Research Council, Washington, D.C, 1989, pp. 24–37.

Shenthan, T., S. Tehvanayagam, and G.R. Martin, "Numerical Simulation of Soil Densification Using Vibro-Stone Columns," *Proceedings, GeoCongress* (Atlanta), American Society of Civil Engineers, Reston, Va., 2006, 6 pp.

Shinn, J.D. and W.L. Bratton, "Innovations with CPT for Environmental Site Characterization," *Proceedings, International Symposium on Cone Penetration Testing*, Vol. 2, Swedish Geotechnical Society Report 3:95, Oct. 4–5, 1995, Linköping, Sweden, pp. 93–98.

Shinn, J.D., D.A. Timian, R.M. Morey, and R.L. Hull, "Development of a CPT Probe to Determine Volumetric Soil Moisture Content," *Geotechnical Site Characterization*, Vol. 1 (Proc. ISC-1, Atlanta, Ga.), Balkema, Rotterdam, The Netherlands, 1998, pp. 595–599.

Shinn, J.D. and J.W. Haas, "Enhanced Access Penetration System: A Direct Push System for Difficult Site Conditions," *Geotechnical and Geophysical Site Characterization*, Vol. 1 (Proc. ISC-2, Porto, Portugal), Millpress, Rotterdam, The Netherlands, 2004, pp. 795–800.

Shrivastava, A.K. and M. Mimura, "Radio-Isotope Cone Penetrometers and the Assessment of Foundation Improvement," *Geotechnical Site Characterization*, Vol. 1 (Proc. ISC-1, Atlanta, Ga.), Balkema, Rotterdam, The Netherlands, 1998, pp. 601–606.

Singh, R., D.J. Henkel, and D.A. Sangrey, "Shear and K_0 Swelling of Overconsolidated Clay," *Proceedings, 8th International Conference on Soil Mechanics and Foundation Engineering*, Vol. 1.2, Moscow, Russia, 1973, pp. 367–376.

Skempton, A.W., "Standard Penetration Test Procedures and the Effects in Sands of Overburden Stress, Relative Density, Particle Size, Ageing, and Overconsolidation," *Geotechnique*, Vol. 36, No. 3, 1986, pp. 425–447.

Skomedal, E. and J.M. Bayne, "Interpretation of Pore Pressure Measurements from Advanced Cone Penetration Testing," *Penetration Testing in the UK*, Thomas Telford, London, United Kingdom, 1988, pp. 279–283.

Stark, T.D. and S.M. Olson, "Liquefaction Resistance Using CPT and Field Case Histories," *Journal of Geotechnical Engineering,* Vol. 121, No. 12, 1995, pp. 859–869.

Sterckx, K. and P. Van Calster, "The ROTAP: A Useful Tool for the Execution of CPT," *Proceedings, International Symposium on Cone Penetration Testing*, Vol. 2, Swedish Geotechnical Society Report 3:95, Oct. 4–5, 1995, Linköping, Sweden, pp. 105–110.

Sully, J.P. and R.G. Campanella, "Evaluation of Field CPTU Dissipation Data in Overconsolidated Fine-Grained Soils," *Proceedings, 13th International Conference on Soil Mechanics and Foundation Engineering*, Vol. 1, New Delhi, India, 1994, pp. 201–204.

Takesue, K. and T. Isano, "Development and Application of a Lateral Stress Cone," *Proceedings, International Conference on In-Situ Measurements of Soil Properties and Case Histories*, Bali, Indonesia, May 21–24, 2001, pp. 623–629.

Tanaka, H. and M. Tanaka, "Key Factors Governing Sample Quality," *Characterization of Soft Marine Clays*, T. Tsuchida and A. Nakase, Eds., A.A. Balkema, Rotterdam, The Netherlands, 1999, pp. 57–81.

Tand, K.E., E.G. Funegard, and J.-L. Briaud, "Bearing Capacity of Footings on Clays: CPT Method," *Use of In-Situ Tests in Geotechnical Engineering* (GSP No. 6), American Society of Civil Engineers, Reston, Va., 1986, pp. 1017–1033.

Tatsuoka, F. and S. Shibuya, *Deformation Characteristics of Soils and Rocks from Field and Laboratory Tests*, Report of the Institute of Industrial Science, University of Tokyo, Japan, Vol. 37, No. 1, 1992, 136 pp.

Teh, C.I. and G.T. Houlsby, "An Analytical Study of the Cone Penetration Test in Clay," *Geotechnique*, Vol. 41, No. 1, 1991, pp. 17–34.

Terzaghi, K., R. Peck, and G. Mesri, *Soil Mechanics in Engineering Practice*, 3rd ed., John Wiley & Sons, New York, N.Y., 1996.

Test Method for Performing Electronic Friction Cone and Piezocone Penetration Testing of Soils, ASTM D 5778, Vol. 04.08, American Society for Testing and Materials, West Conshohocken, Pa., 2000.

Test Method for Performing Mechanical Cone Penetrometer Testing of Soils, ASTM D 3441, Vol. 04.08, American Society for Testing and Materials, West Conshohocken, Pa., 2000.

Trak, B., P. LaRochelle, F. Tavenas, S. Leroueil, and M. Roy, "A New Approach to the Stability Analysis of Embankments on Sensitive Clays," *Canadian Geotechnical Journal*, Vol. 17, No. 4, 1980, pp. 526–544.

Tumay, M.T., "In-Situ Testing at the National Geotechnical Experimentation Sites (Phase II)," Final Report, FHWA Contract No. DTFH61-97-P-00161, Louisiana Transportation Research Center, Baton Rouge, Feb. 1997, 300 pp.

Tumay, M.T., R.L. Boggess, and Y. Acar, "Subsurface Investigations with Piezocone Penetrometers," *Cone Penetration Testing and Experience* (Proceedings ASCE National Convention, St. Louis, Mo.), 1981, pp. 325–342.

Tumay, M.T., P.U. Kurup, and R.L. Boggess, "A Continuous Intrusion Electronic Miniature CPT," *Geotechnical Site Characterization*, Vol. 2, Balkema, Rotterdam, The Netherlands, 1998, pp. 1183–1188.

Turner, L.L., C. Hannenian, and S. Mahnke, "Geotechnical Data Management Initiatives at Caltrans," *Proceedings, GeoCongress* (Atlanta, Ga.), 2006, pp. 1–5.

Van De Graaf, H.C. and J.W.A. Jekel, "New Guidelines for the Use of Inclinometer with the CPT," *Penetration Testing*, Vol. 2 (Proc. ESOPT-1, Amsterdam, The Netherlands), Balkema, Rotterdam, The Netherlands, 1982, pp. 581–584.

Van De Graaf, H.C. and P. Schenk, "The Performance of Deep CPTs," *Penetration Testing 1988*, Vol. 2 (Proc. ISOPT-1, Orlando, Fla.), Balkema, Rotterdam, The Netherlands, 1988, pp. 1027–1034.

Vesić, A.S., "Expansion of Cavities in Infinite Soil Mass," *Journal of the Soil Mechanics and Foundations Division*, Vol. 98, No. SM3, 1972, pp. 265–290.

Vesić, A.S, "Bearing Capacity of Shallow Foundations," Chapter 3, In *Foundation Engineering Handbook*, Van Nostrand Reinhold, New York, N.Y., 1975, pp. 121–147.

Vesić, A.S., *NCHRP Synthesis of Highway Practice 42: Design of Pile Foundations,* Transportation Research Board, National Research Council, Washington, D.C., 1977, 68 pp.

Vlasblom, A., *The Electrical Penetrometer: A Historical Account of Its Development*, LGM Mededelingen Report No. 92, Delft Soil Mechanics Laboratory, The Netherlands, Dec. 1985, 51 pp.

Vreugdenhil, R., R. Davis, and J. Berrill, "Interpretation of Cone Penetration Results in Multilayered Soils," *International Journal of Numerical and Analytical Methods in Geomechanics*, Vol. 18, 1994, pp. 585–599.

Vucetic, M. and R. Dobry, "Effect of Soil Plasticity on Cyclic Response," *Journal of Geotechnical Engineering*, Vol. 117, No. 1, Jan. 1991, pp. 89–107.

Woods, R.D., "Measurement of Dynamic Soil Properties," *Earthquake Engineering and Soil Dynamics*, Vol. 1 (Proc. ASCE Conference, Pasadena, Calif.), American Society of Civil Engineers, Reston, Va., 1978, pp. 91–178.

Wride, C.E. and P.K. Robertson, *CANLEX: The Canadian Liquefaction Experiment: Data Review Report* (Five Volumes), BiTech Publishers Ltd., Richmond, BC, Canada, 1999, 1,081 pp.

Wroth, C.P., "The Interpretation of In-Situ Soil Tests," *Geotechnique*, Vol. 34, No. 4, Dec. 1984, pp. 449–489.

Wroth, C.P., "Penetration Testing: A More Rigorous Approach to Interpretation," *Penetration Testing 1988*, Vol. 1 (Proc. ISOPT-1, Orlando, Fla.), Balkema, Rotterdam, The Netherlands, 1988, pp. 303–311.

Yilmaz, R. and M.R. Horsnell, "The Use of Cone Penetrometer Testing to Investigate Sand Fill Subsidence Beneath Highways," *Use of In-Situ Tests in Geotechnical Engineering* (GSP No. 6), American Society of Civil Engineers, Reston, Va., 1986, pp. 1178–1188.

Youd, T.L., et al., "Liquefaction Resistance of Soils: Summary Report from the 1996 NCEER and 1998 NCEER/NSF Workshops on Evaluation of Liquefaction Resistance of Soils," *Journal of Geotechnical and Geoenvironmental Engineering*, Vol. 127, No. 10, 2001, pp. 817–833.

Zhang, Z. and M.T. Tumay, "Statistical to Fuzzy Approach Toward CPT Soil Classification," *Journal of Geotechnical and Geoenvironmental Engineering*, Vol. 125, No. 3, 1999, pp. 179–186.

Zuidberg, H., "Use of Static Cone Penetrometer Testing in the North Sea," *Proceedings of the European Symposium on Penetration Testing* (ESOPT), Vol. 2.2, Stockholm, Sweden, 1974, pp. 433–436.

ABBREVIATIONS AND ACRONYMS

BRE = Building Research Establishment (United Kingdom)
CCT = calibration chamber tests
CPT = cone penetration test
CPTu = piezocone test (cone penetration test with porewater pressures)
CPTù = piezocone test with dissipation readings with time
CPTWD = Cone Penetration Test While Drilling
CRR = cyclic resistance ratio
CSR = cyclic stress ratio = τ_{cyc}/σ_{vo}'
CSSM = critical state soil mechanics
DCDT = direct current displacement transducer
DHT = downhole test (geophysics)
DSS = direct simple shear test
EAPS = Enhanced Access Penetrometer System
ECPT = Electric Cone Penetration Test
GIS = geographic information system
GPS = global positioning system
IRPT = International Reference Procedure Test
LCPC = Laboratoire Central des Ponts et Chaussées
LRFD = Load Resistance Factored Design
LVDT = Linear variant displacement transducer
MCPT = Mechanical Cone Penetration Test
MIT = Massachusetts Institute of Technology
MWD = Measurements While Drilling
NGES = National Geotechnical Experimentation Site
NGI = Norwegian Geotechnical Institute, Oslo
NTNU = Norwegian University of Science & Technology, Trondheim
OCR = overconsolidation ratio = σ_p'/σ_{vo}'
PMT = pressuremeter test
RCPT = resistitivity cone penetration test
SBT = soil behavioral type (used in soil classification by CPT)
SCPT = seimic cone penetration test
SPT = standard penetration test
TSC = total stress cells (spade cells)

GLOSSARY OF SYMBOLS

This section lists the common symbols used in the synthesis.

a' = effective soil attraction = c' cotϕ'
a_c = radius of cone penetrometer (also designated a)
a_{max} = PGA = maximum (horizontal) ground acceleration (during an earthquake)
a_n = net area ratio (see ASTM D 5778)
c = length of rectangular foundation
c' = effective cohesion intercept
c_u = s_u = undrained shear strength
c_v = coefficient of consolidation
c_{vh} = coefficient of (vertical and horizontal) consolidation
d = diameter of pile foundation
d = width of rectangular foundation
d_c = diameter of cone penetrometer = $2a_c$
d_e = equivalent diameter
e = void ratio
e_0 = initial void ratio
e_p = void ratio at the preconsolidation stress
f_p = pile side friction
f_s = measured cone sleeve friction
f_t = total cone sleeve friction
g = gravitation constant (= 9.8 m/s^2 = 32.2 ft/s^2)
g = exponent term in modified hyperbola for modulus reduction
h = depth to incompressible layer for shallow foundations
h_p = drainage path thickness (during consolidation)
h_s = height of penetrometer sleeve
k = hydraulic conductivity (cm/s); also coefficient of permeability
k_c = reduction factor from LCPT direct CPT method
k_E = $\Delta E_s/\Delta z$ = rate of soil modulus increase with depth
q = applied stress by shallow foundation
q_b = end bearing resistance for deep foundation
q_c = measured cone tip resistance
q_e = effective cone resistance = $q_t - u_2$
q_t = total cone resistance (correction per ASTM D 5778)
q_{t1} = stress-normalized cone tip resistance
q_{ult} = ultimate bearing stress for foundation system
r_d = stress reduction factor (for seismic ground analyses)
s = displacement of foundation
s_c = centerpoint displacement of foundation
s_u = c_u = undrained shear strength
t = time
t = foundation thickness
t_j = thickness of sleeve
t_{50} = time for dissipation to reach 50% completion
u_0 = hydrostatic (porewater) pressure
u_1 = porewater pressures measured midface of cone tip
u_2 = porewater pressures measured at shoulder position (behind the tip, or u_{bt})
u_3 = porewater pressures measured behind the sleeve
w_t = displacement at pile top
z = depth (below ground surface)
z_e = foundation embedment depth
z_w = depth to groundwater table
α = ratio of soil modulus to cone tip resistance: $\alpha = E_s/q_c$
α_c = ratio of constrained modulus to net cone resistance: $\alpha_c = D'/(q_t - \sigma_{vo})$
α_G = ratio of constrained modulus to small-strain shear modulus: $\alpha_c = D'/G_{max}$
β_G = $E_{so}/(k_E \cdot d)$ = dimensionless Gibson soil parameter
β_p = angle of plastification (for NTH piezocone method)
Δ_z = soil layer thickness
ϕ' = effective friction angle
γ_s = shear strain
γ_d = dry unit weight
γ_T = total unit weight
γ_{sat} = saturated unit weight
γ_w = unit weight of water (freshwater: γ_w = 9.8 kN/m^3 = 62.4 pcf; saltwater: γ_w = 10.0 kN/m^3 = 64 pcf)
ν = Poisson's ratio ($\nu' = 0.2$ for drained and $\nu_u = 0.5$ for undrained)
ρ_T = mass density = γ_T/g, where g = gravitational acceleration constant
Λ = $1 - C_s/C_c$ = plastic volumetric strain ratio
σ_{atm} = atmospheric pressure (1 atm = 1 bar = 100 kPa ≈ 1 tsf ≈ 14.7 psi)
σ_p' = effective preconsolidation stress (= P_c' = σ_{vmax}')
σ_v' = effective vertical stress
σ_{vo} = total vertical (overburden) stress
σ_{vo}' = effective vertical (overburden) stress
σ_h' = effective lateral stress
σ_{ho}' = effective geostatic lateral stress
τ = shear stress
τ_{cyc} = cyclic shear stress
τ_{max} = shear strength (maximum shear stress); for undrained conditions: $\tau_{max} = c_u = s_u$
A_b = area at pile foundation base
A_s = perimetric area on sides of pile foundation
A_F = area of shallow foundation base
B = width of foundation
B_q = normalized porewater pressure parameter
C_c = virgin compression index
C_s = swelling or rebound index
C_{se} = side friction coefficent (Unicone method)
C_{te} = tip coefficient (Unicone method)
C_K = modifier for pile installation (beta side friction)
C_M = modifier for pile material (beta side friction)
$C_{\alpha e}$ = coefficient of secondary compression
D' = constrained modulus = $E(1 - \nu)/[(1 + \nu)(1 - 2\nu)]$
D_R = relative density of sand
E_{fdn} = foundation Young's modulus
E_s = equivalent (Young's) soil modulus (E' for drained and E_u for undrained)

E_{s0} = equivalent (Young's) soil modulus just beneath foundation bearing elevation
E_u = undrained (Young's) modulus (Note: undrained is for no volume change: $\Delta V = 0$)
E' = drained (Young's) modulus (Note: drained is for no excess porewater pressure: $\Delta u = 0$)
F = normalized sleeve friction parameter
FR = R_f = friction ratio = f_s/q_t (%)
FS = factor of safety (also designated F_s)
G = shear modulus = $E/[2(1 + \nu)]$
$G_{\max}$ = $G_0 = \rho_T V_s^2$ = small-strain shear modulus
H_e = embedment depth of foundation
H_s = thickness of sand layer sandwiched between upper and lower clay layers
I_c = CPT soil classification index (based on Q and F)
$^*I_c$ = CPT soil classification index (based on Q, F, and B_q)
I_p = plasticity index (also PI)
I_E = footing displacement modifier for embedment
I_F = footing modifier for relative rigidity
I_{GH} = displacement influence factor for foundation on Gibson soil
I_H = displacement influence factor for shallow foundation on homogeneous soil
I_R = $G/\tau_{\max}$ = rigidity index of the soil = ratio of shear modulus to shear strength
I_0 = displacement influence factor for rigid pile
I_ρ = elastic displacement influence factor for pile foundation
K_c = fines correction factor for CPT in soil liquefaction analysis
K_F = foundation flexibility factor
K_H = modifier for correcting q_c for thin layer of sand
K_P = passive stress coefficient
K_0 = $\sigma_{ho}'/\sigma_{vo}'$ = lateral stress coefficient
L = length of pile foundation
M = $6\sin\phi'/(3 - \sin\phi')$ = critical state frictional parameter for strength envelope
N = penetration resistance or "blow counts" from SPT
N_c = bearing factor term for cohesion component
N_{kt} = cone bearing factor for evaluating undrained shear strength
N_m = $(q_t - \sigma_{vo})/(\sigma_{vo}' + a')$ = cone resistance number (For $a' = 0$: $N_m = Q$)
N_q = bearing factor for deep foundations
N_γ = bearing factor for drained shallow loading
PI = plasticity index
P_L = probability of liquefaction
Q = normalized cone tip resistance
Q = applied vertical force to foundation
Q_b = base capacity (at tip or toe of pile foundation)
Q_s = shaft capacity along sides of pile foundation
Q_t = applied top load on pile
Q_{ult} = ultimate axial capacity (force) of the foundation
R_k = bearing factor term for foundations on clay
RF = resistance factor
S_t = $s_{u\,(\text{peak})}/s_{u\,(\text{remolded})}$ = sensitivity (applies to fine-grained soils)
T_v = time factor for one-dimensional (vertical) consolidation
T^* = modified time factor for radial dissipation (for piezocone)
U_E = energy density from dynamic compaction operations
U' = $\Delta u/\sigma_{vo}'$ = normalized excess porewater pressure to effective overburden
U^* = $\Delta u/\Delta u_i$ = normalized excess porewater pressures for dissipation testing
V = volume
V_s = shear wave velocity
V_{s1} = stress-normalized shear wave velocity
W_p = weight of the foundation

APPENDIX A

Cone Penetration Testing Questionnaire

The survey questionnaire was prepared for this synthesis and reviewed initially by the panel members. It was distributed by TRB to a total of 64 departments of transportation (DOTs) (52 in the United States and 12 in Canada). A final return rate of 56 respondents was received (88%). A summary of the individual states that replied and their contact information is given in Table A1. An initial pre-test of the survey was conducted in February 2006 with five DOTs represented by panel members (California, Florida, Louisiana, Minnesota, and Missouri). Some slight adjustments were made to the questionnaire that was subsequently sent to the remaining DOT geotechnical groups.

The survey contained a total of 59 separate questions; however, only in one case did the respondent provide answers to all of these inquiries. On average, each responder provided answers to only about 10 to 25 questions. In addition, for some queries, multiple answers could be given by the respondent. Therefore, in the tally of responses, the number of respondents for each question is cited for reference. The results are presented in terms of either bar graphs or pie charts. For clarity, only the basic question and the graphical summary chart are provided. In some instances, a slight paraphrasing or modified version of the original question is presented to facilitate the presentation of the replies.

The questions are grouped into six broad categories: (1) Use of the cone penetrometer by each agency; (2) Maintenance and field operations of the CPT; (3) Geostratigraphy by cone penetration testing; (4) CPT evaluation of soil parameters and properties; (5) CPT utilization for deep foundations and pilings; and (6) Other aspects of cone penetration testing.

TABLE A1
LIST OF RESPONDENTS TO QUESTIONNAIRE FROM STATE AND PROVINCIAL DOTs

State/Province	Reply	Comments	DOT Contact
Alabama	Buddy Cox	a little with SES	coxb@dot.state.al.us
Arizona	John Lawson	None, ground hard, not familiar	jlawson@dot.state.az.us
Arkansas	Jonathan Annable	None	jon.annable@ahtd.state.ar.us
California*	Gem-Yeu Ma	20%	Gem-Yeu.Ma@dot.ca.gov
Colorado	Hsing-Cheng Liu	None	tim.aschenbrener@dot.state.co.us
Connecticut	Leo Fontaine	None, ground too hard	leo.fontaine@po.state.ct.us
District of Columbia	Wasi Khan	None	wasi.khan@dc.gov
Florida*	David Horhota	10%	david.horhota@dot.state.fl.us
Georgia	Tom Scrugges	10%	Thomas.Scruggs@dot.state.ga.us
Hawaii	Herbert Chu	None, ground too hard	herbert.chu@hawaii.gov
Idaho	Tri Buu	10%	tbuu@itd.state.id.us
Illinois	William M. Kramer	None	kramerwm@nt.dot.state.il.us
Indiana	Nayyar Siddiki	None but they just bought CPT rig	atkhan@indot.state.in.us
Iowa	Robert Stanley	10%	Robert.Stanley@dot.iowa.gov
Kansas	James J. Brennan	30%	brennan@ksdot.org
Kentucky	Darrin Beckett	2 projects in 10 years	bill.broyles@ky.gov
Louisiana*	Kim Garlington	30%	KimGarlington@dotd.louisiana.gov
Maine	Laura Krusinski	None	laura.krusinski@maine.gov
Maryland	Mark Wolcott	10%	mwolcott@sha.state.md.us
Massachusetts	Peter Connors	10%	peter.connors@state.ma.us
Michigan	Richard Endres	Not yet	endresr@michigan.gov
Minnesota*	Derrick Dasenbrock	80%	Derrick.Dasenbrock@dot.state.mn.us
Mississippi	Sean Ferguson	10%	sferguson@mdot.state.ms.us
Missouri*	Kevin W. McLain	20%	Kevin.McLain@modot.mo.gov
Montana	Rich Jackson	10%	ricjackson@mt.gov
Nebraska	Mark Lindemann	80%	marklindemann@dor.state.ne.us
Nevada	Jeff Palmer	4 times in 20 years; cobbles	pnoori@dot.state.nv.us
New Hampshire	Chuck Dusseault	None, ground too hard	fprior@dot.state.nh.us
New Jersey	Jack Mansfield	None	Jack.Mansfield@dot.state.nj.us
New Mexico	Bob Meyers	30%	robert.meyers@nmshtd.state.nm.us
New York	Bob Burnett	None	bburnett@dot.state.ny.us
North Carolina	Mohammed Mulla	10%	nwainaina@dot.state.nc.us
North Dakota	John Ketterling	None, not familiar	jketterl@state.nd.us
Ohio	Gene Geiger	Little	gene.geiger@dot.state.oh.us
Oregon	Jan Six	10%	jan.1.six@odot.state.or.us
Pennsylvania	Kerry Petrasic	10%	kpetrasic@state.pa.us
Puerto Rico	Ricardo Romero	None	edpagan@act.dtop.gov.pr
South Carolina	Jeff Sizemore	30%	sizemorejc@dot.state.sc.us
South Dakota	Dan Vockrodt	None	dan.vockrodt@state.sd.us
Tennessee	Len Oliver	0 to 10%, requires expertise	Len.Oliver@state.tn.us
Texas	Mark McClelland	None	MMCCLELL@gwia.dot.state.tx.us
Utah	Keith Brown	20%	kebrown@utah.gov
Vermont	Chad Allen	<10%	chris.benda@state.vt.us
Virginia	Ramesh Gupta, Ashton Lawler	20 to 30%	Ashton.Lawler@VDOT.Virginia.gov
Washington	Jim Cuthbertson	10%	cuthbej@wsdot.wa.gov
West Virginia	Jim Fisher	None, not familiar	jfisher@dot.state.wv.us
Wisconsin	Bruce Pfister	None	bruce.pfister@dot.state.wi.us
Wyoming	Mike Hager	1 project in 25 years !	mike.hager@dot.state.wy.us
Alberta	Roger Skirrow	10%	roger.skirrow@gov.ab.ca
British Columbia	Don Gillespie	20%	dirk.nyland@gov.bc.ca
Manitoba	Tony Ng	None	jhosang@gov.mb.ca
New Brunswick	Joe MacDonald	10%	Mike.Trites@gnb.ca
Newfoundland	Don Brennan	None, ground too hard	MercerCG@gov.nl.ca
Nova Scotia	Donald Piercey	None, too gravelly & rocky	stewartdo@gov.ns.ca
Ontario	Tae C. Kim	20%	gerry.chaput@mto.gov.on.ca
Quebec	Giles Grundin	40%	guy.richard@mtq.gouv.qc.ca

*DOTS used for pre-test.

QUESTIONS AND SUMMARY OF REPLIES

Part I—Use of Cone Penetration Testing by the DOT

1. On an annual basis in your state or province, what approximate percentage of geotechnical projects utilizes cone penetration testing (CPT)?

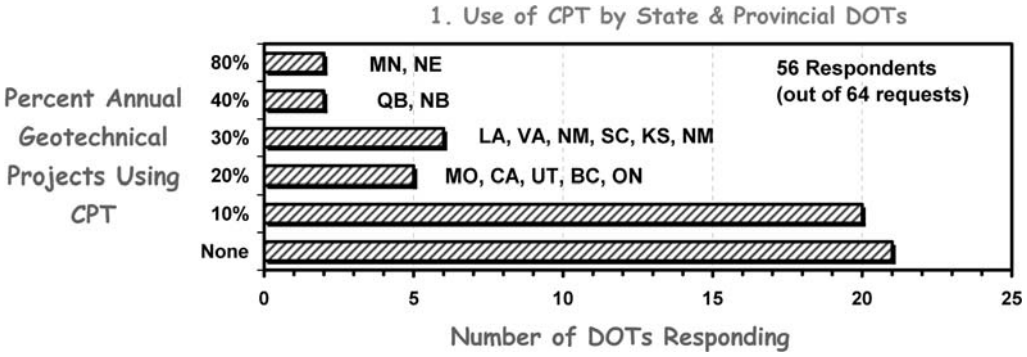

2. Who performs the CPTs on your projects?

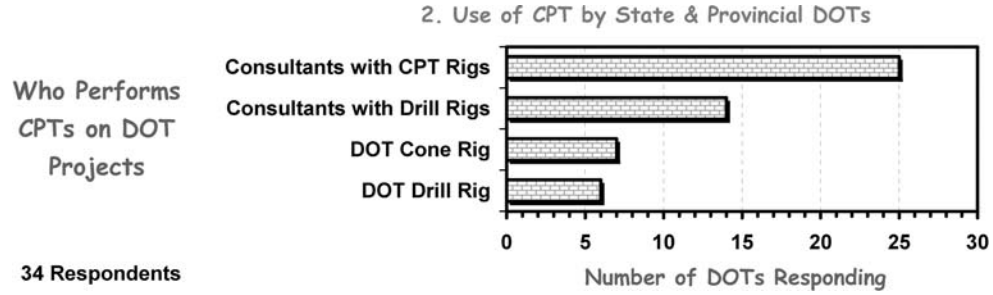

3. How many CPT systems are available and who runs them in-state?

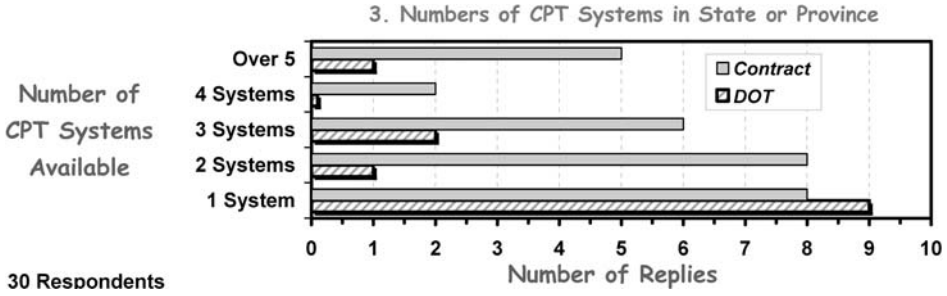

4. What types of penetrometer equipment are used?

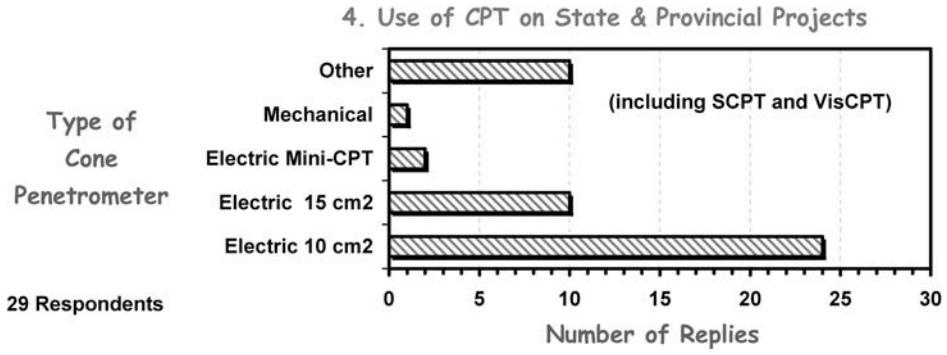

5. What is the brand or manufacturer of your penetrometer equipment?

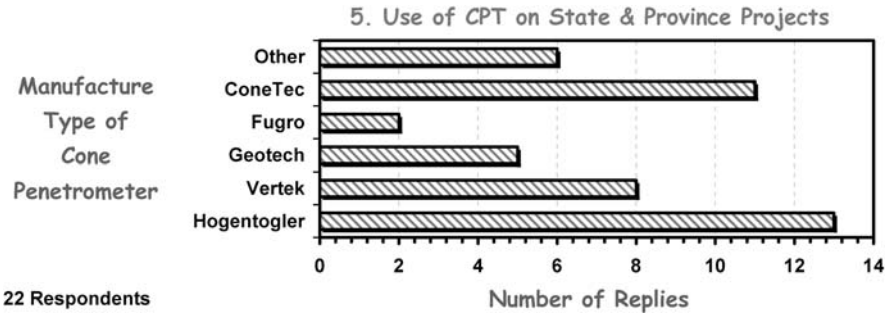

6. What is the brand or manufacturer of your hydraulic (pushing) system?

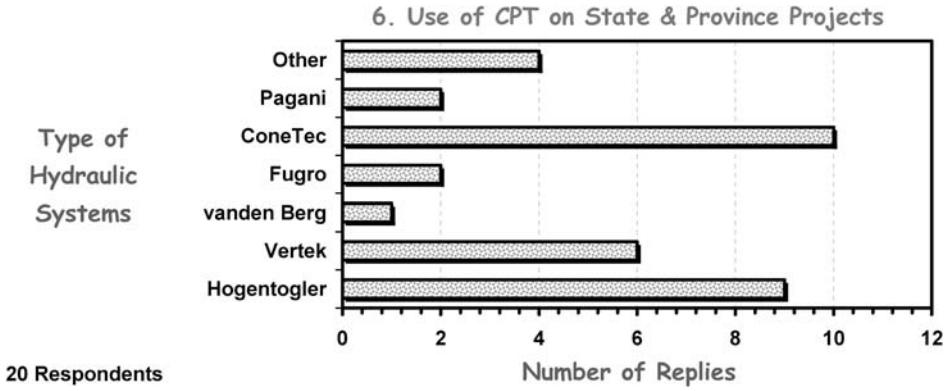

7. What soil types do you investigate by CPT? (Check all that apply.)

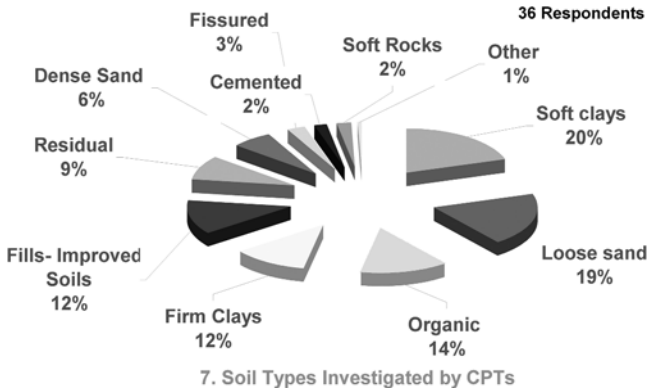

8. What types of projects is the CPT used on? (Check all that apply.)

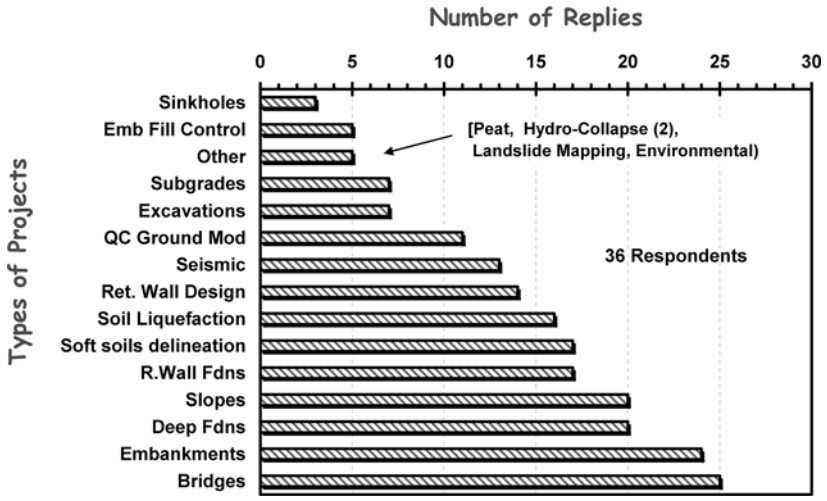

9. What average daily footage (metrical rate) of CPT is accomplished on your projects?

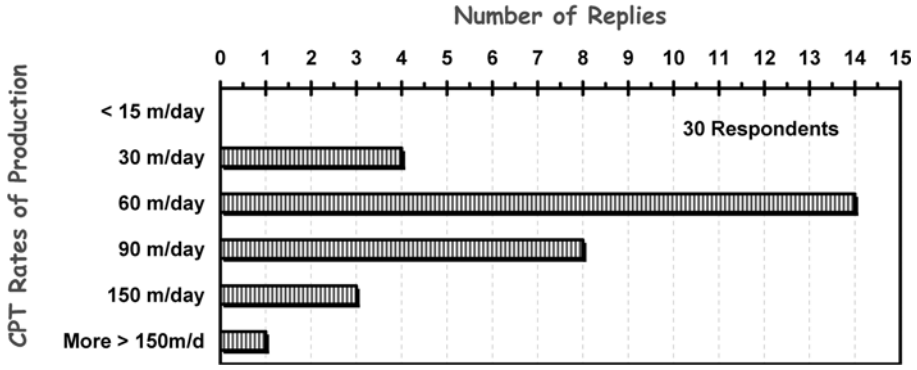

10. What circumstances prevent the use of CPT? (Check all that apply.)

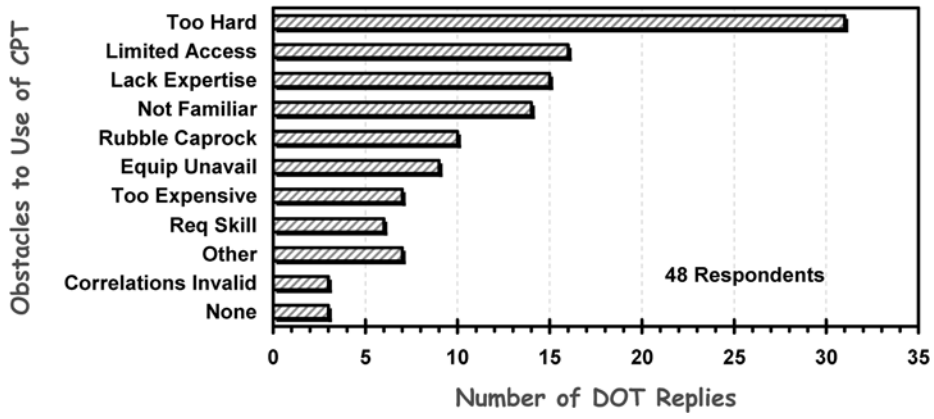

11. Have you had any unfavorable experiences with CPT on your projects?

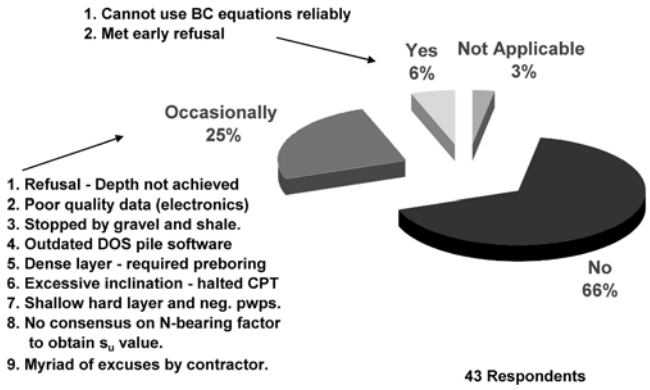

12. Over the next five years, how do you expect the projected use of CPT in your state or province?

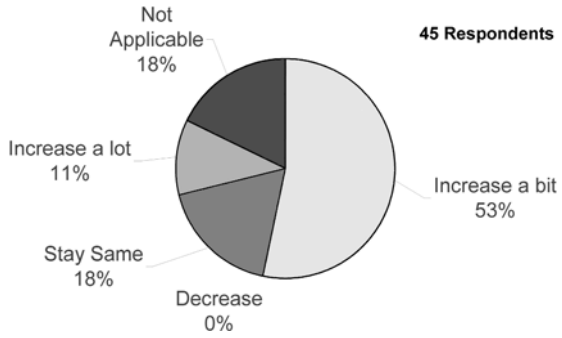

14. How often do you have your cone penetrometer systems calibrated?

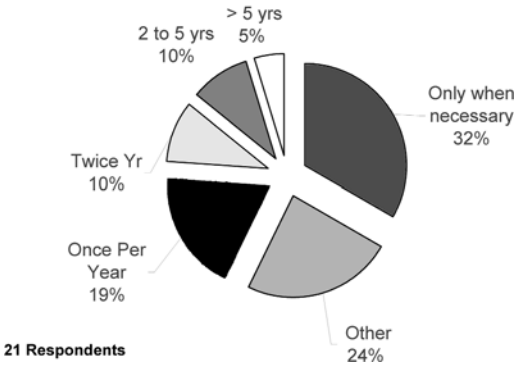

15. Specify the mounting platform and type of hydraulic pushing system.

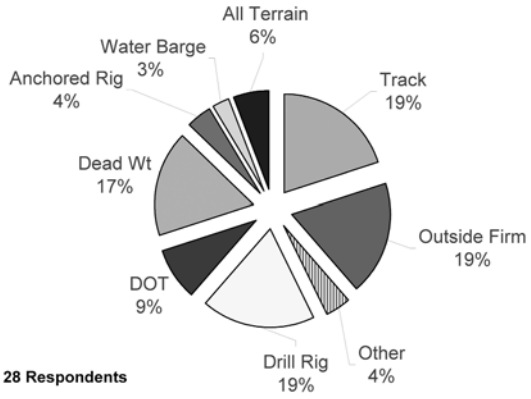

Part II—Maintenance and Field Operations

13. With regard to maintenance of equipment, how is this handled by your department?

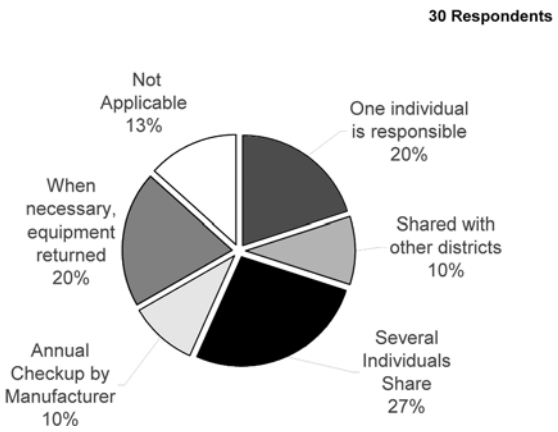

16. Give details regarding baseline readings (or "zero readings") for each sounding.

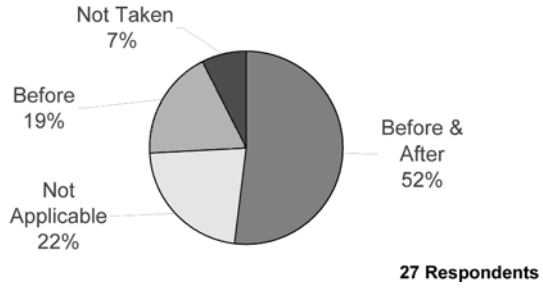

17. Provide details related to penetration porewater pressure readings. (Check all that apply.)

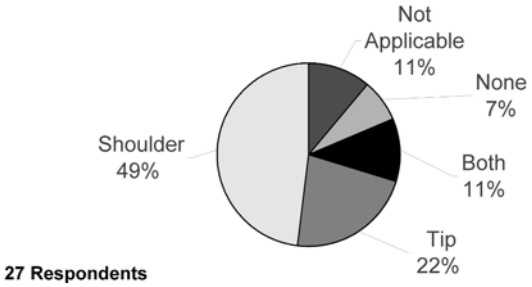

18. Give details related to the saturation of porous elements for porewater pressure readings.

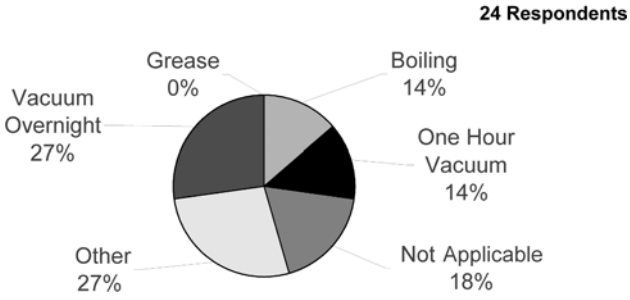

19. Specify the type of fluid used for saturating porous elements.

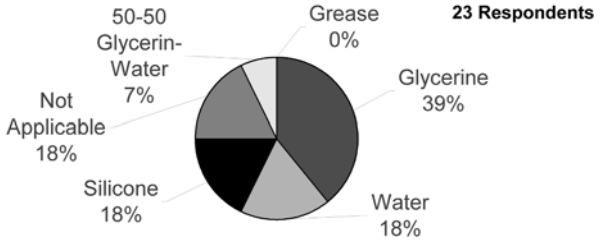

20. Give specifics on the saturation and assembly in the field.

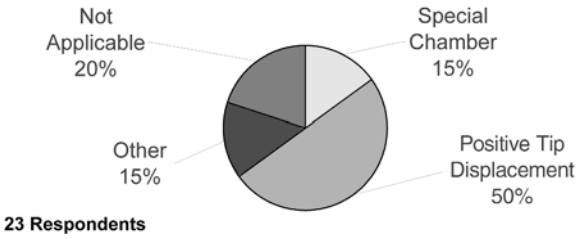

21. Provide details on the correction of tip resistance for porewater pressure effects.

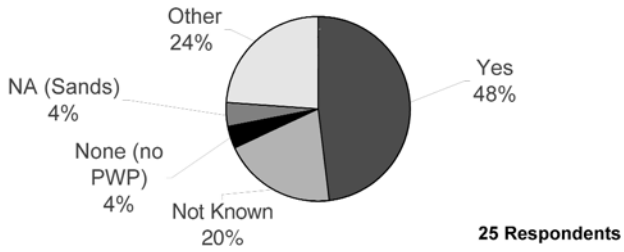

22. What standards and procedures do you follow?

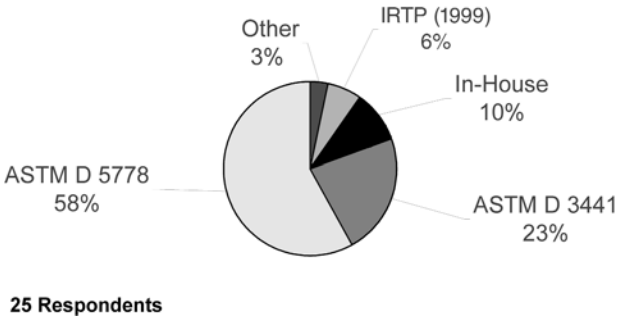

Part III—Geostratigraphy by Cone Penetration Testing

23. When using the CPT for delineation of geostratigraphy, the following apply:

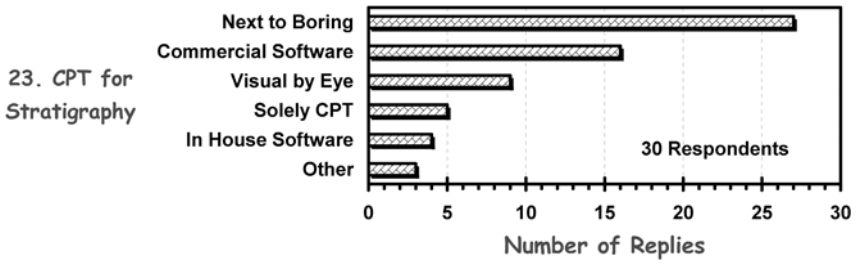

24. In presenting the CPT results for in-house use, we use (Check all that apply):

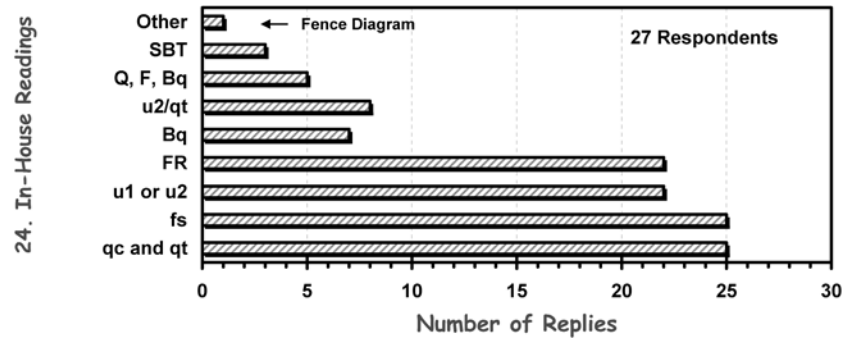

25. In presenting CPTs for bid documents, our department provides (Check all that apply):

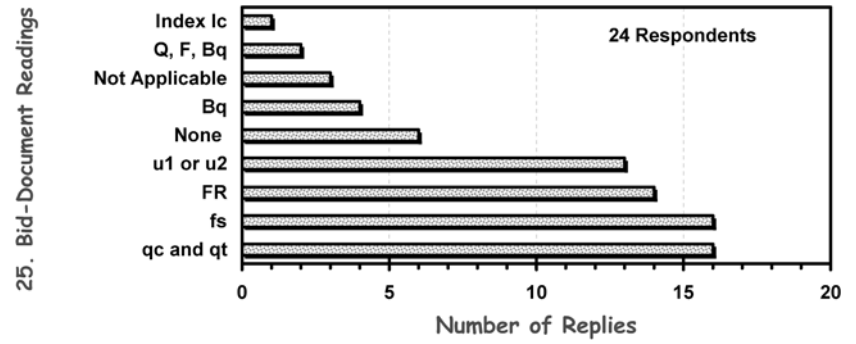

26. Our state uses the following CPT soil behavioral classification type (Check all that apply):

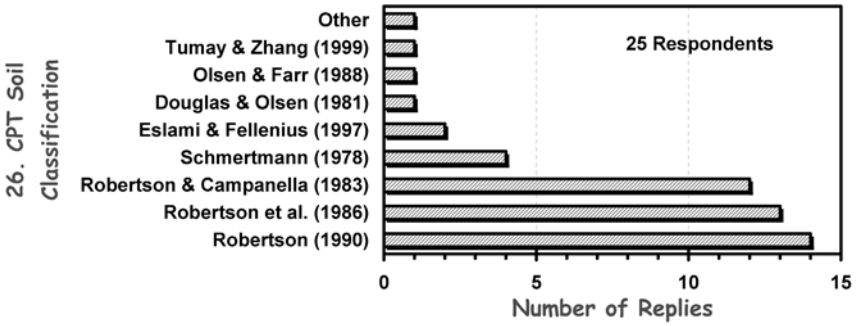

27. What soil types are not well reflected by the CPT classification methods?

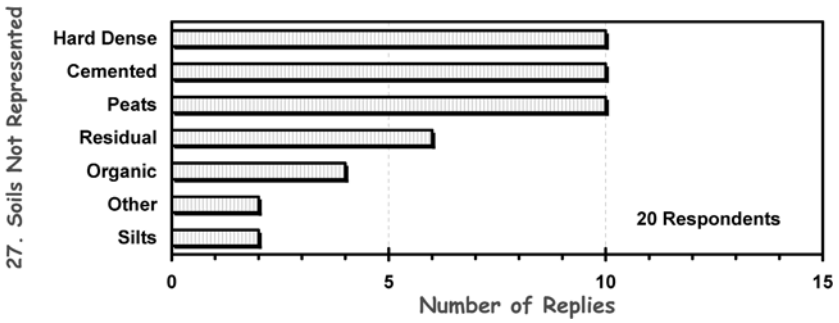

28. When CPTs are conducted, data provided to the state DOT engineer include:

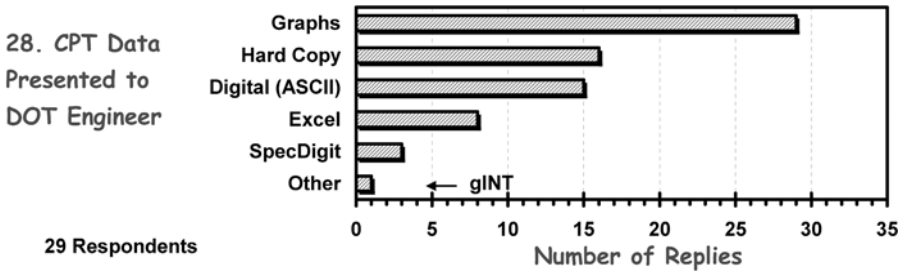

29. The selected CPT results that are presented as part of the plans package include:

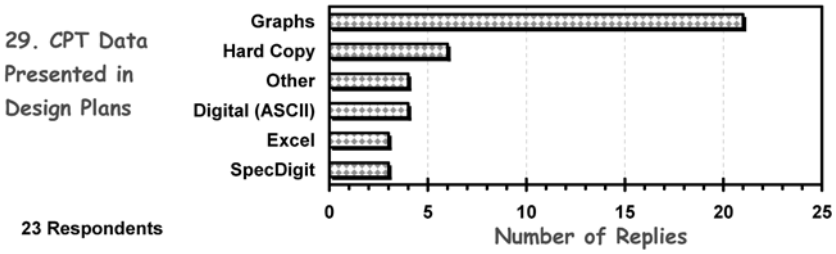

30. Are the CPT results used to estimate equivalent SPT *N*-values?

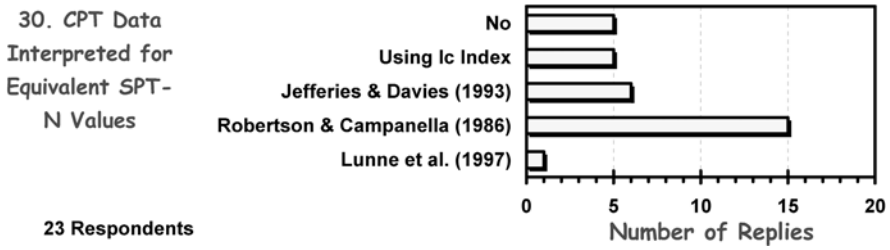

31. Have you used piezo-dissipation tests to determine hydrostatic porewater pressures?

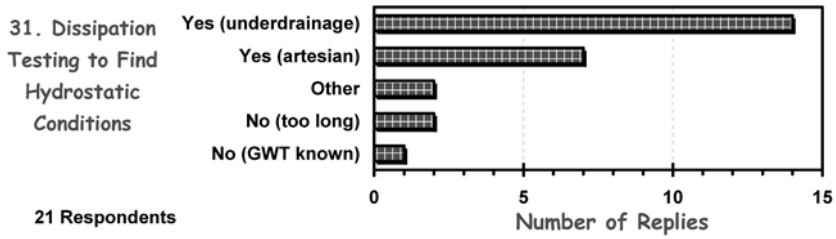

32. How often are the penetration readings taken during advancement?

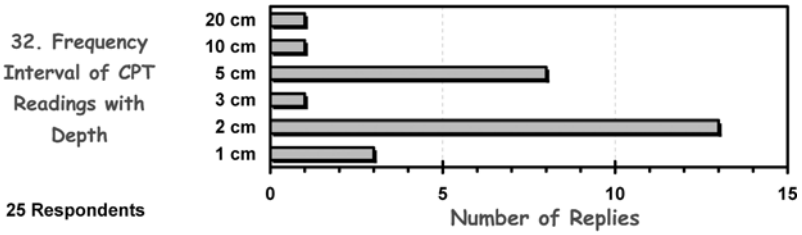

33. When the sounding has been completed and penetrometer is withdrawn, our field crew:

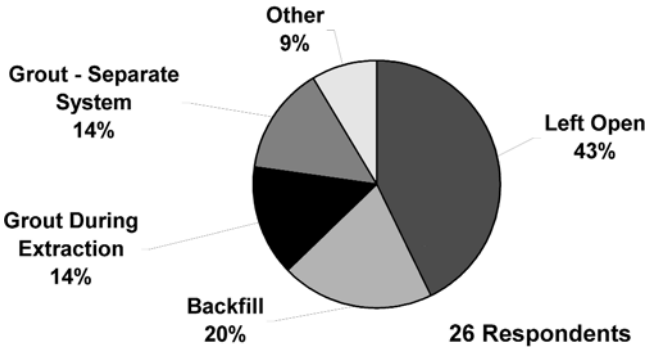

35. The total soil unit weight for calculating overburden stress is evaluated by:

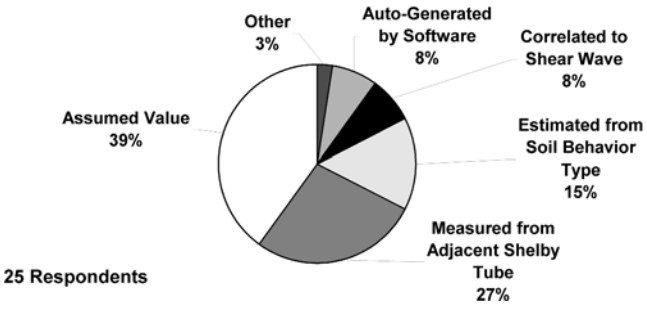

Part IV—CPT Evaluation of Soil Parameters and Properties

34. In the post-processing of CPT data, our group uses:

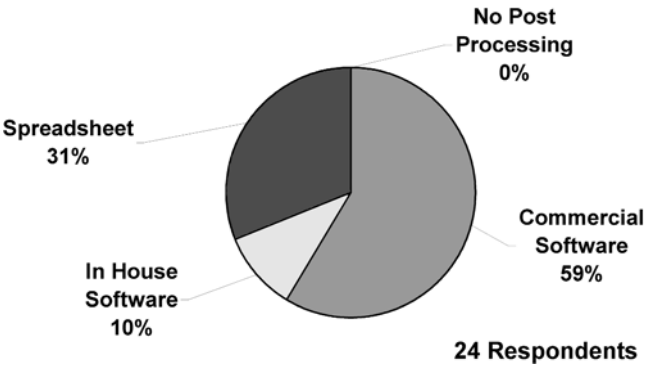

36. The groundwater depth for determining hydrostatic porewater pressures is obtained from:

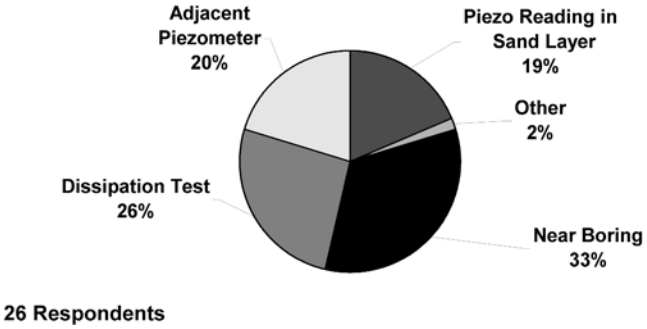

37. Our group uses the following reference documents (Check all that apply):

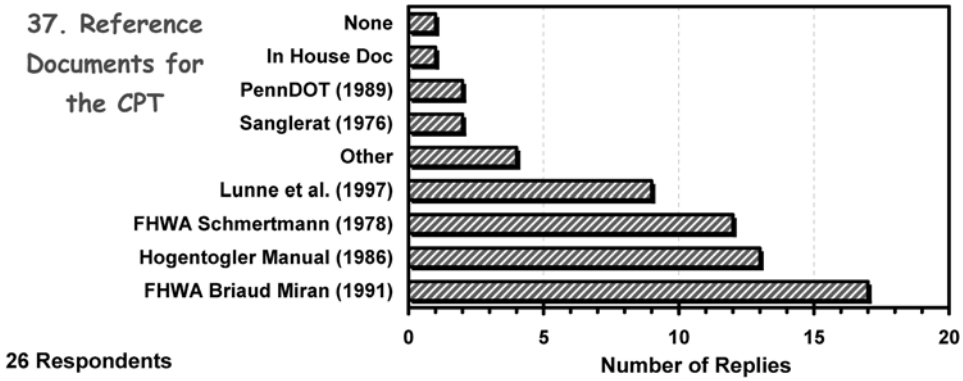

38. What soil parameters are evaluated from the CPT results? (Check all that apply):

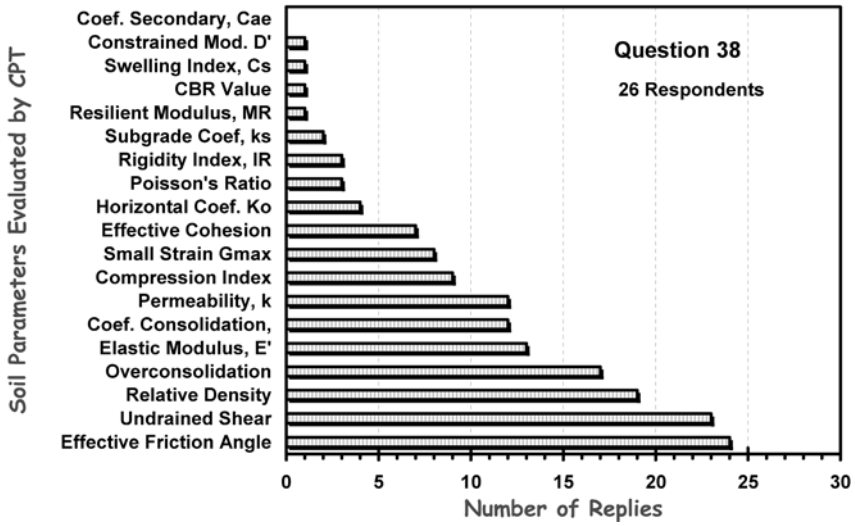

39. The aforementioned geotechnical parameters have been checked or verified by reference values.

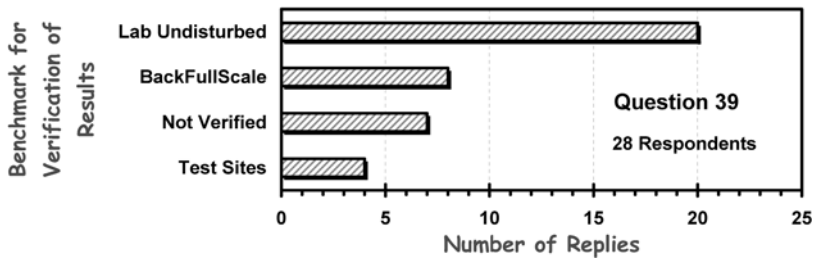

40. Regarding the undrained shear strength of a clay or silt, our group is most likely to calibrate the CPT results with the following mode:

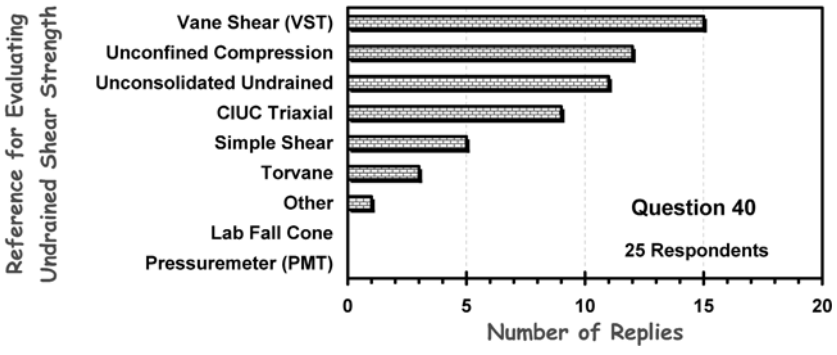

41. Regarding embankments constructed on soft ground, the CPT is useful for estimating:

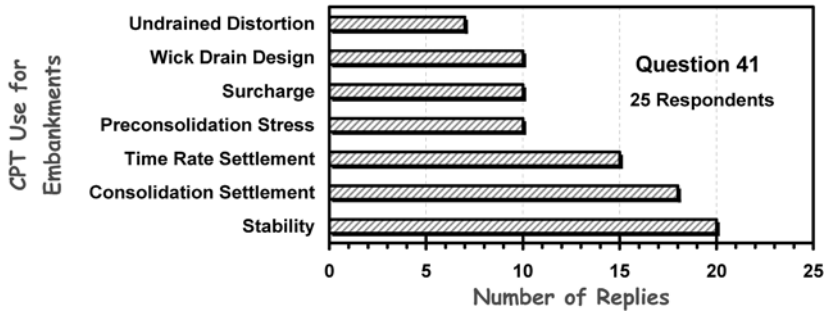

42. If you are concerned about seismic ground hazards, the CPT is useful for:

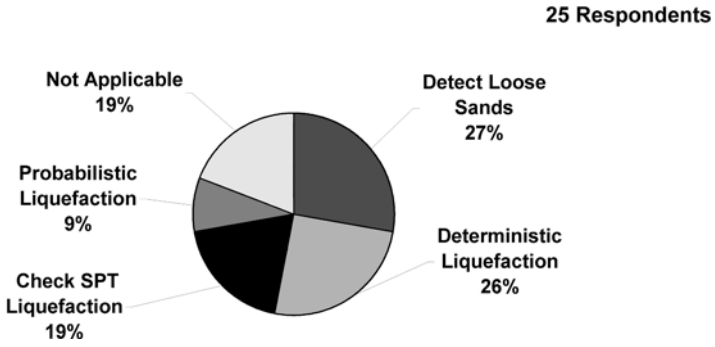

43. If you utilized seismic cone testing (SCPT), the results would apply to:

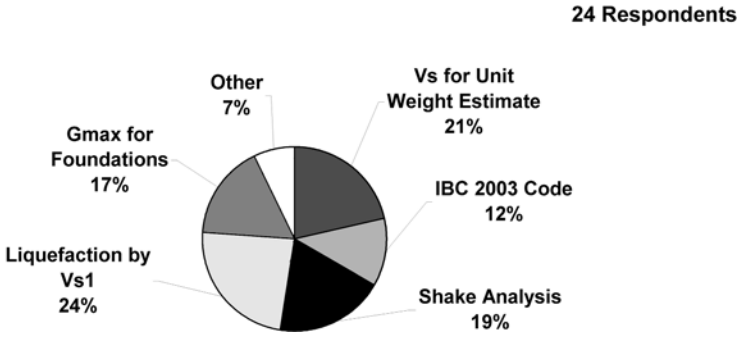

44. What methods are used to reduce dissipation data to obtain the coefficient of consolidation?

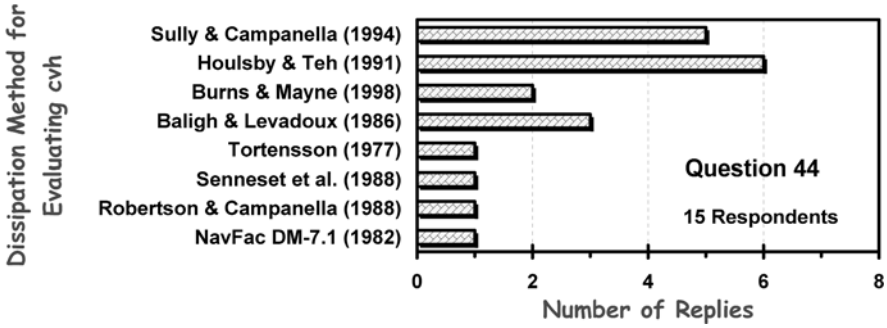

Part V—CPT Evaluation of Deep Foundations and Pilings

45. In the evaluation of axial pile capacity, our group uses the CPT data in the following approaches:

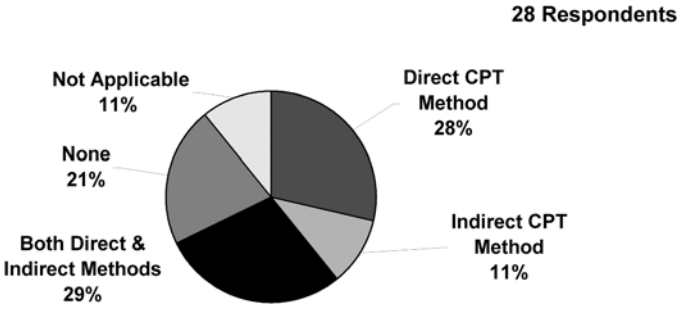

46. If direct CPT methods are used, the types of deep foundations considered include:

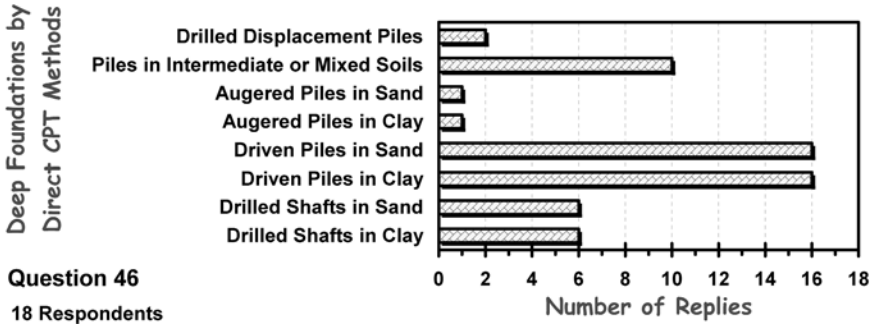

47. If using "indirect" CPT methods in clays, the alpha parameter is assessed by these methods:

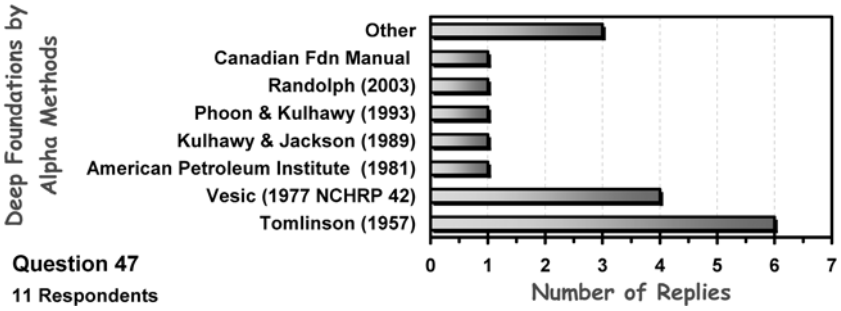

48. If using "indirect" CPT methods in sands or clays, the beta parameter is evaluated by these methods:

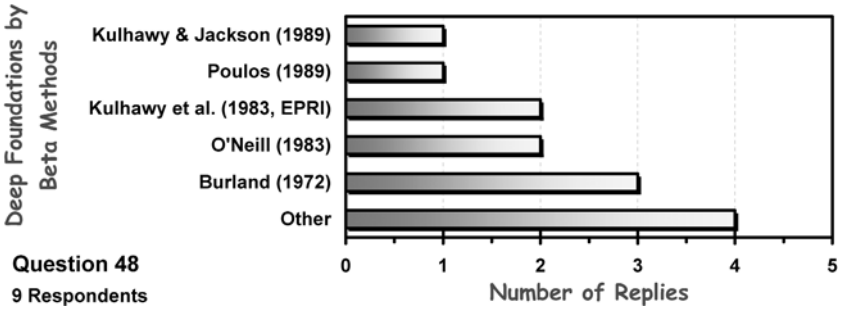

49. If using “direct” CPT methods for axial pile capacity, methods for assessing pile resistances include:

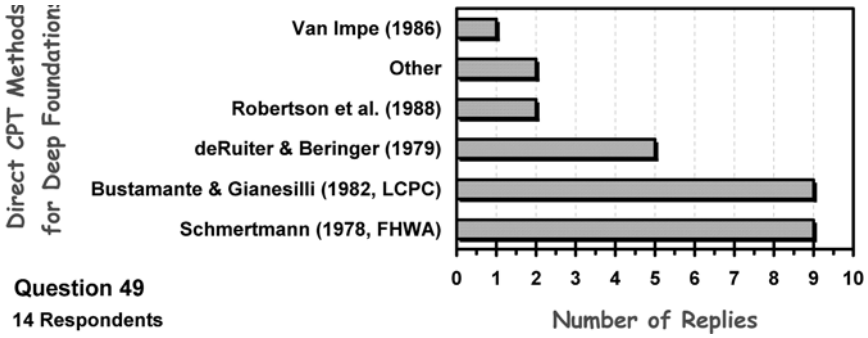

50. If using “direct” CPTu (piezocone) methods, the pile resistances are assessed by:

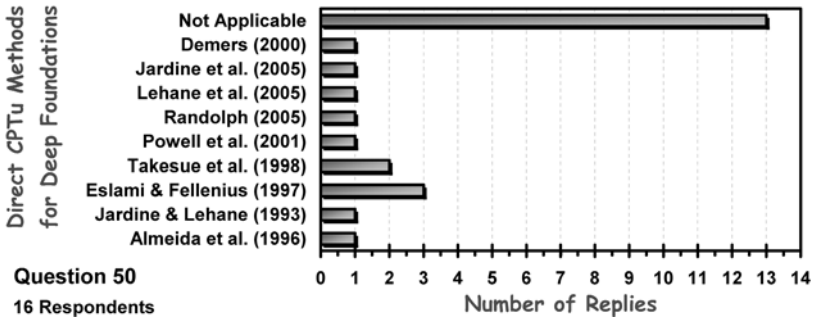

51. When evaluating axial pile response, our group uses CPT results for the following:

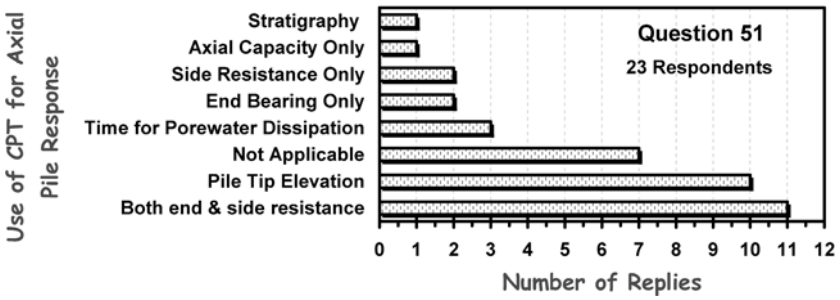

52. In the comparison of CPT methods with full-scale load tests, the axial capacity is defined by:

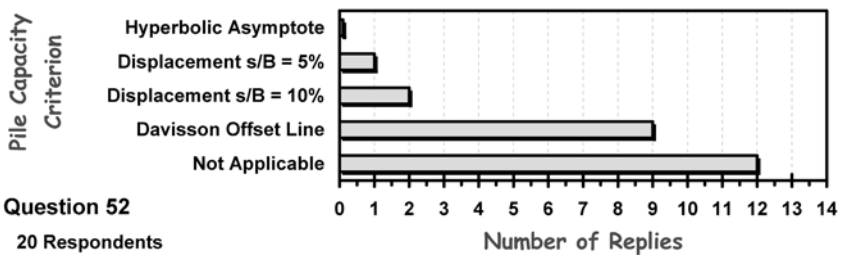

53. With regard to other pile loading modes, our group uses CPT for:

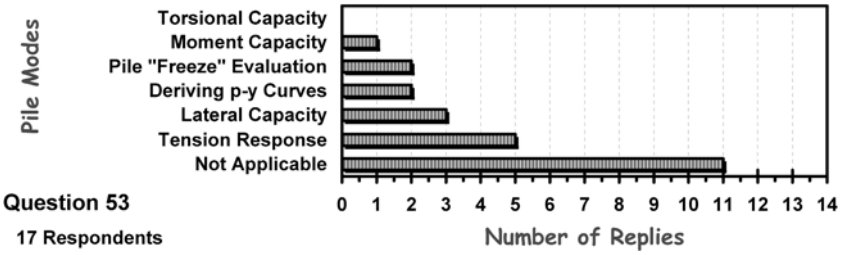

54. What additional CPT data reduction software would you like to see?

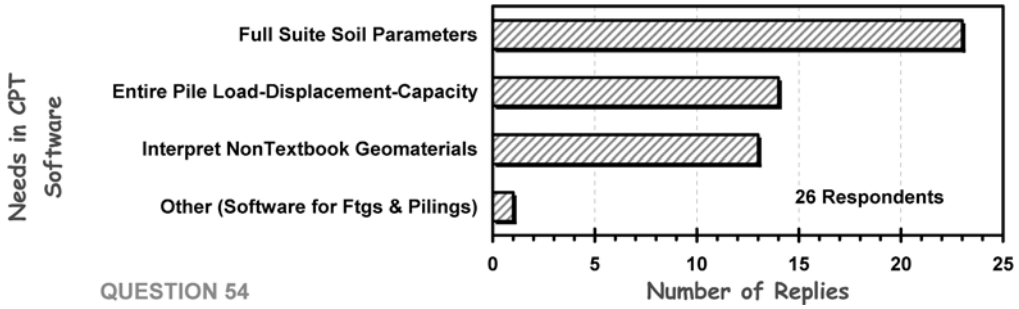

55. What is the biggest obstacle to increased use of CPT in your area?

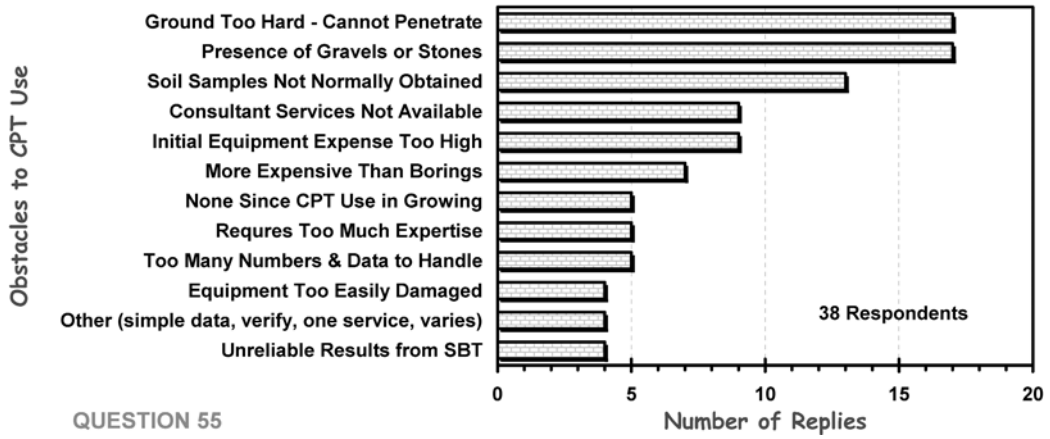

56. What research and development would increase use of CPT in your group?

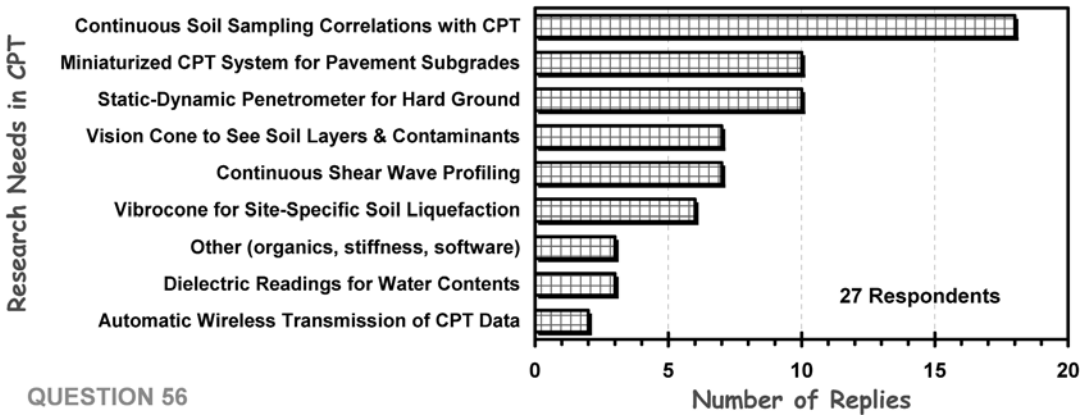

57. Do you have any case histories of successes or failure involving CPT that could be shared?

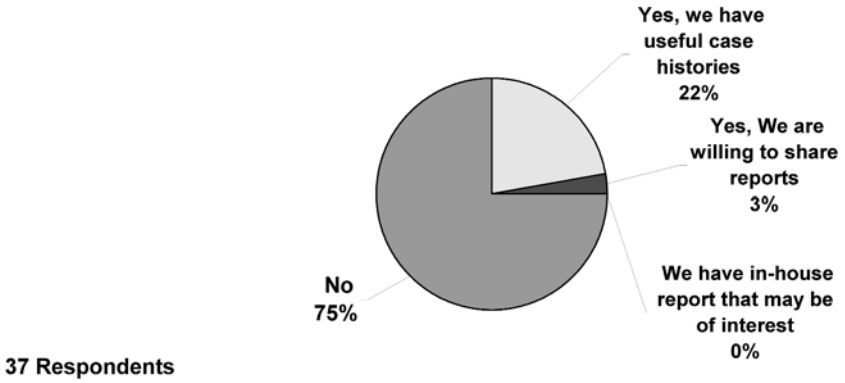

58. What measures are being undertaken to develop load resistance factored design (LRFD) factors with CPT results?

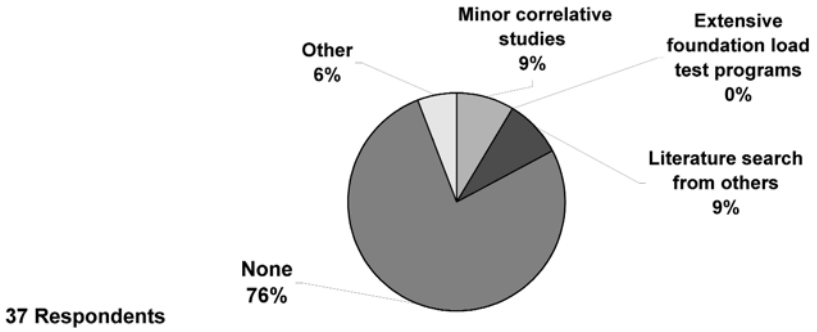

59. Have you initiated other research and/or implementation programs in your state or province related to CPT that would be of interest to others?

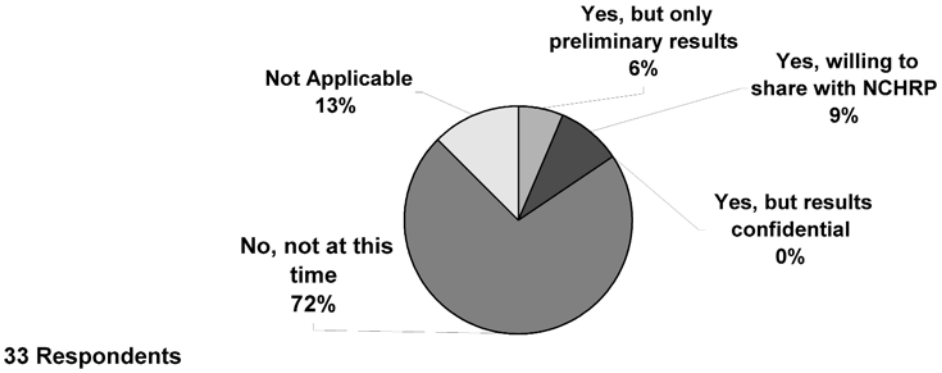

Abbreviations used without definitions in TRB publications:

AAAE	American Association of Airport Executives
AASHO	American Association of State Highway Officials
AASHTO	American Association of State Highway and Transportation Officials
ACI–NA	Airports Council International–North America
ACRP	Airport Cooperative Research Program
ADA	Americans with Disabilities Act
APTA	American Public Transportation Association
ASCE	American Society of Civil Engineers
ASME	American Society of Mechanical Engineers
ASTM	American Society for Testing and Materials
ATA	Air Transport Association
ATA	American Trucking Associations
CTAA	Community Transportation Association of America
CTBSSP	Commercial Truck and Bus Safety Synthesis Program
DHS	Department of Homeland Security
DOE	Department of Energy
EPA	Environmental Protection Agency
FAA	Federal Aviation Administration
FHWA	Federal Highway Administration
FMCSA	Federal Motor Carrier Safety Administration
FRA	Federal Railroad Administration
FTA	Federal Transit Administration
IEEE	Institute of Electrical and Electronics Engineers
ISTEA	Intermodal Surface Transportation Efficiency Act of 1991
ITE	Institute of Transportation Engineers
NASA	National Aeronautics and Space Administration
NASAO	National Association of State Aviation Officials
NCFRP	National Cooperative Freight Research Program
NCHRP	National Cooperative Highway Research Program
NHTSA	National Highway Traffic Safety Administration
NTSB	National Transportation Safety Board
SAE	Society of Automotive Engineers
SAFETEA-LU	Safe, Accountable, Flexible, Efficient Transportation Equity Act: A Legacy for Users (2005)
TCRP	Transit Cooperative Research Program
TEA-21	Transportation Equity Act for the 21st Century (1998)
TRB	Transportation Research Board
TSA	Transportation Security Administration
U.S.DOT	United States Department of Transportation